Heinrich Heine
Universität
Düsseldorf

Membrane translocation and chaperone-dependent folding of the lipase A of *Pseudomonas aeruginosa*

Inaugural-Dissertation

zur Erlangung des Doktorgrades

der Mathematisch-Naturwissenschaftlichen Fakultät

der Heinrich-Heine-Universität Düsseldorf

vorgelegt von

Athanasios Papadopoulos

aus Serres

Düsseldorf, September 2023

aus dem Institut für Biochemie

der Arbeitsgruppe Synthetische Membransysteme

der Heinrich-Heine-Universität Düsseldorf

Diese Arbeit wurde gefördert durch die Deutsche Forschungsgemeinschaft im Rahmen des Sonderforschungsbereichs 1208 „Identität und Dynamik von Membransystemen – von Molekülen bis zu zellulären Funktionen“.

Gedruckt mit der Genehmigung der Mathematisch-Naturwissenschaftlichen Fakultät der Heinrich-Heine-Universität Düsseldorf

Referent: Prof. Dr. Alexej Kedrov

Korreferent: Prof. Dr. Karl Erich Jaeger

Tag der mündlichen Prüfung: 05.12.2023

An meine Großeltern, welche meine Promotion nicht mehr erleben können.

«Δεν ελπίζω τίποτα, δε φοβούμαι τίποτα, είμαι λέφτερος»

- *Νίκος Καζαντζάκης*

Table of Contents

Abstract

The lipase A represents a virulence factor of the opportunistic human pathogen *Pseudomonas aeruginosa*. Upon lipase biogenesis, the protein is exported Sec-dependently to the periplasm where it obtains folding assistance for maturation by its cognate foldase LipH. The matured lipase is then secreted by the type II secretion system (T2SS) to the extracellular space. Elucidating the biogenesis of the lipase can may serve to reduce the pathogenicity of *P. aeruginosa*.

The synthesis and Sec-dependent translocation of the lipase A are important initial steps upon lipase biogenesis. To understand the transport process of the lipase A, the Sec system of *P. aeruginosa* PAO1 was reconstituted *in vitro*. This required the heterologous expression, purification, and characterization of the *Pseudomonas* Sec system (SecYEG, SecA and SecB), as well as the lipase A precursor (proLipA) as translocation substrate. The *Pseudomonas* Sec system manifested equal transport efficiency *in vitro* as the reference Sec system of *E. coli* when commonly utilized model substrate (proOmpA) was used with either proteoliposomes or inner membrane vesicles. However, the transport efficiency of proLipA remained low, likely due to partial folding and/or instant aggregation of the protein. Extensive efforts were made to improve the lipase transport efficiency, including optimization of targeting to Sec by various chaperones, creation of a more stable lipase variant, and a less specific variant of the translocon, but did not indicate comparable transport efficiency to proOmpA.

To obtain insights on the folding and maturation of the lipase A, its cognate chaperone, the full-length foldase ($LipH^{FL}$), was overexpressed and isolated from the membrane. $LipH^{FL}$ was purified and reconstituted in a model membrane system (proteoliposomes and nanodiscs), which were both capable of activating the lipase. Structural analysis of the soluble domain of LipH and LipA:LipH complex by small-angle X-ray scattering revealed a highly flexible foldase chaperone domain which interacts with the lipase in a 1:1 stoichiometry. To determine whether the foldase was able to capture the emerging substrate at early translocation steps, N- and C-terminal truncations of LipA were created and used for interaction studies. Binding of the foldase to the C-terminal but not to the N-terminal truncation of the lipase was observed, suggesting that the foldase recognizes the C-terminally truncated lipase that mimics a translocation intermediate, whereby the lack of the N-terminus corrupts the interactions. Additionally, the foldase $LipH^{FL}$ was co-expressed with the translocon SecYEG and native membrane vesicles were utilized for preliminary *in vitro* transport studies of proLipA to check if LipH is involved in lipase translocation.

Since the lipase A requires folding assistance and is highly prone to aggregation, the interactions with prominent periplasmic chaperones FkpA, SurA, Skp, YfgM and PpiD were investigated to check whether these proteins are involved in lipase biogenesis. The results indicated that the soluble periplasmic chaperone Skp prevents misfolding of the lipase *in vitro* and is crucial for lipase secretion as shown by *in vivo* analysis. The trimeric structure of *P. aeruginosa* Skp has been elucidated by small-angle X-ray scattering, identifying the open and closed conformation of the chaperone. Further interaction studies indicated two binding modes for LipA:Skp interactions with a 1:1 and 1:2 stoichiometry possessing binding affinities of 20 nM and 2 µM, respectively. Skp stabilizes the lipase via apolar interactions which are not affected by elevated ionic strengths. Therefore, Skp is a potent mediator upon lipase biogenesis that prevents aggregation, supports stabilization and the passage of unfolded LipA to LipH. Further structural investigations of the periplasmic chaperones were conducted and can further serve for more nuanced interaction studies with additional virulence factors.

The present work forms the basis for further investigations in aim to elucidate the biogenesis of secretory proteins serving as virulence factors of gram-negative bacterial pathogens.

Zusammenfassung

Die Lipase A ist ein Virulenzfaktor des opportunistischen Humanpathogens *Pseudomonas aeruginosa*. Die Biogenese der Lipase ist ein komplexer Prozess, bei dem das Protein mit vielen weiteren Protein interagiert, um in seine aktive Form gefaltet und in den extrazellulären Raum sekretiert zu werden. Die Aufklärung der Biogenese der Lipase kann dazu dienen, die Pathogenität von *P. aeruginosa* zu verringern.

Die Lipase A wird Sec-abhängig in das Periplasma exportiert, wo das Protein durch die Lipase-spezifische Foldase (LipH) in seinen aktiven Zustand gefaltet wird, bevor es durch das T2SS in den extrazellulären Raum sekretiert wird. Die Synthese und die Sec-abhängige Translokation der Lipase A sind wichtige und initiale Schritte der Lipase-Biogenese. Um den Transportprozess der Lipase A zu untersuchen, wurde das Sec-System von *P. aeruginosa* PAO1 *in vitro* rekonstituiert und die Lipase-Translokation analysiert. Dies erforderte die heterologe Expression, Reinigung und Charakterisierung des *Pseudomonas*-Sec-Systems (SecYEG, SecA und SecB) sowie des Translokationssubstrats (proLipA). Die Transporteffizienz des *Pseudomonas*-Sec-System ist ähnlich zum Sec-Referenzsystem von *E. coli*, sofern das Modellsubstrat proOmpA benutzt wurde. Der Transport der Lipase A (proLipA) ist gering, was wahrscheinlich auf intermediäre Faltung oder Aggregation des Proteins zurückzuführen ist. Es wurden vielfältige Versuche unternommen, um die Transporteffizienz der Lipase zu verbessern, u. a. durch den Einsatz verschiedener Chaperone, der Kreierung einer stabileren Lipase-Variante und einer weniger spezifische Translokonvariante, welche jedoch keine vergleichbare Transporteffizienz zu proOmpA ergaben.

Um Einblicke in die Faltung und Reifung der Lipase A zu erhalten, wurde die Lipase-spezifische Foldase in ihrer vollen Länge ($LipH^{FL}$) exprimiert und aus der Membran isoliert. Das gereinigte $LipH^{FL}$ wurde in Modellmembransystemen (Proteoliposomen und Nanodiscs) rekonstituiert, die in der Lage waren, die Lipase zu aktivieren. Darüber hinaus wurden die Interaktionen zwischen Lipase und Foldase mittels Strukturanalyse untersucht. Die Ergebnisse zeigen eine hochflexible Chaperon-Domäne der Foldase und einen Lipase:Foldase Komplex mit einer 1:1-Stöchiometrie. Um festzustellen, ob die Foldase an der Translokation der Lipase beteiligt ist bzw. frühe Translokationsintermediate der Lipase erkennt, wurden N- und C-terminal verkürzte Lipase-Varianten erzeugt und für Interaktionsstudien verwendet. Während die Foldase mit der C-terminal verkürzten Lipase interagiert, konnte keine Bindung zur N-terminal verkürzten Lipase-Variante festgestellt werden, was darauf hindeutet, dass die Foldase in der Lage ist frühe Translokationsintermediate der Lipase zu erkennen. Zusätzlich wurde die Co-Expression der foldase und des Translokons bewerkstelligt und isolierte IMVs für vorläufige *in-vitro*-Transportstudien verwendet.

Da die Lipase A stark zur Aggregation neigt und Faltungshilfe benötigt, wurden die Wechselwirkungen mit den weiteren prominenten periplasmatischen Chaperonen aus *P. aeruginosa* FkpA, SurA, Skp, YfgM und PpiD untersucht, um zu ermitteln, ob diese Proteine an der Lipase-Biogenese beteiligt sind. Das periplasmatische Chaperon Skp verhindert die Aggregation der ungefalteten Lipase *in vitro* und beeinflusst die Lipase-Sekretion *in vivo*. Die trimere Struktur von Skp aus *P. aeruginosa* PAO1 wurde mittels Röntgen-Kleinwinkelstreuung (SAXS) aufgeklärt, wobei die offene und die geschlossene Konformation des Chaperons identifiziert werden konnten. Weitere Interaktionsstudien ergaben zwei Bindungsmodi für LipA:Skp-Interaktionen mit einer Stöchiometrie von 1:1 bzw. 1:2, welche eine Bindungsaffinität von 20 nM und 2 µM haben. Skp stabilisiert die Lipase über apolare Wechselwirkungen, welche durch erhöhte Salzkonzentrationen nicht beeinträchtigt werden. Skp ist daher ein wirksamer Modulator bei der Lipase-Biogenese, der die Aggregation verhindert, die Stabilisierung unterstützt und den Übergang von LipA zu LipH fördert. Zusätzliche Strukturanalyse der periplasmatischen Chaperone wurden getätigt und können für weitere Arbeiten herangezogen werden.

Die vorliegende Arbeit bildet die Grundlage für weitere Untersuchungen zur Aufklärung der Biogenese von sekretorischen Proteinen, die als Virulenzfaktoren von bakteriellen Krankheitserregern dienen.

1. Introduction

1.1 *Pseudomonas aeruginosa* – An emerging and opportunistic bacterial pathogen

1.1.1 Microbiological profile of *P. aeruginosa*

Pseudomonas aeruginosa is an ubiquitous environmental gram-negative bacterial species that belongs to the genus *Pseudomonas* of class of the *Gammaproteobacteria* (Sneath, McGowan and Skerman, 1980; Diggle and Whiteley, 2020). The rod-shaped bacteria are motile, facultative aerobe and heterotrophic (Diggle and Whiteley, 2020). Several *P. aeruginosa* strains are identified and separated into 5 groups based on genome analysis which are further classified in environmental and clinical strains (Freschi *et al.*, 2019; Diggle and Whiteley, 2020). The strain *P. aeruginosa* PAO1 was initially isolated from human wound in the middle of the past century, and now serves as a reference laboratory strain (Diggle and Whiteley, 2020). *P. aeruginosa* grows in various environmental conditions, thriving in a broad range of temperatures, inhabiting dry and wet habitats as well as floral and faunal tissue sources (Diggle and Whiteley, 2020). The bacteria can undergo a lifestyle transition from planktonic motile state to biofilms which is especially important for chronical infection of the host (Valentini *et al.*, 2018). The biofilm lifestyle contributes to the high tolerance against commonly used antimicrobial therapeutic agents (Ciofu and Tolker-Nielsen, 2019). The vast variety of pathogenicity mediators enable *P. aeruginosa* to infect versatile hosts, while at the same time possessing a high antimicrobial resistance and secreting a plethora of virulence factors (Qin *et al.*, 2022). These traits and the ability to invade and to cause life-threatening infections on immunocompromised patients render *P. aeruginosa* as an opportunistic human pathogen (Sadikot *et al.*, 2005; Diggle and Whiteley, 2020). Especially upon pulmonary diseases, such as cystic fibrosis, *P. aeruginosa* represents the major microbe in the lungs and promotes severe inflammations of the host respiratory system (Sadikot *et al.*, 2005; Bhagirath *et al.*, 2016). Thus, *P. aeruginosa* has come into the spotlight of biomedical research and novel strategies in aim to fight these bacteria are required.

1.1.2 Pathogenicity of *P. aeruginosa*

Recently, the high occurrence of bacterial pathogens, such as *P. aeruginosa*, has turned into an emerging problem for the humankind (Driscoll, Brody and Kollef, 2007). With the ample usage of antibiotics in healthcare and food industry, the emergence of multi-resistant bacterial pathogens is promoted (Rice, 2008; Xu *et al.*, 2022). The representatives of the most medically relevant bacterial pathogens are gathered together in the "ESKAPE" group (*Enterococcus faecium*, *Staphylococcus aureus*, *Klebsiella pneumoniae*, *Acinetobacter baumannii*, *Pseudomonas aeruginosa*, *Enterobacter* species) (Rice, 2008; Morrison and Zembower, 2020). These bacteria commonly appear upon nosocomial infections and are capable to withstand most of antimicrobial treatments, raising the urgent requirement for novel therapeutics (Pendleton, Gorman and Gilmore, 2013). Among the ESKAPE group of bacterial pathogens, *P. aeruginosa* possess a high pathogenesis potential and is of critical priority for biomedical

research as listed by the World Health Organization (Driscoll, Brody and Kollef, 2007; Tacconelli *et al.*, 2018; Holmes *et al.*, 2021), and the pathways which convey its pathogenicity are of major interest for the assurance of public health (Rice, 2008; Tacconelli *et al.*, 2018). Besides the multidrug resistance, versatile pathogenic traits, such as the lifestyle transition from planktonic motile state to biofilms upon infection, as well as the secretion of pathogenicity mediators enable *P. aeruginosa* to act as an opportunistic pathogen (Strateva and Mitov, 2011; Rocha *et al.*, 2019; Jurado-Martín, Sainz-Mejías and McClean, 2021). Multiple studies, including genome analysis, extensive microbial network studies, investigations on the biofilm formation and the secretion of virulence factors were conducted in aim to understand the pathogenesis of *P. aeruginosa* (Cendra and Torrents, 2021; Jurado-Martín, Sainz-Mejías and McClean, 2021; Qin *et al.*, 2022). The genome of *P. aeruginosa* of 6.3 million base pairs (Mbp) is relatively large, in comparison to other gram-negative bacterial pathogens (Stover *et al.*, 2000). This vast genome encompasses a reservoir of genes which encode for various proteins that are involved in infection processes, thus forming the molecular basis of *P. aeruginosa* pathogenicity. Based on this molecular basis, multiple unique traits arise and represent inherent key functions which are important for adaptability and pathogenicity (Diggle and Whiteley, 2020; Liao *et al.*, 2022). Due to its peculiar resistance against common antimicrobial therapeutics *P. aeruginosa* is a frequently found in clinical environments, where it possesses one of the most emerging contaminants (Davane, 2014; Crone *et al.*, 2020). Especially, the high abundance in hospitals and the resulting nosocomial infections of immunocompromised patients paired with the ability to resist the host immune response set *P. aeruginosa* in the spotlight of biomedical research (Sadikot *et al.*, 2005; Driscoll, Brody and Kollef, 2007; Smith *et al.*, 2017; Filloux and Davies, 2019). Thus, the pathogenicity of *P. aeruginosa* refers to the ability to invade the host and to cause life-threatening infections, while possessing traits to refuse the host immune response and to resist common therapeutic treatments (Qin *et al.*, 2022).

Years of emphasized research revealed that *P. aeruginosa* possesses manifold secretion systems, that represent the so-called “wealth of pathogenic weapons”, which fulfill the export of its vast secretome and contribute to its high pathogenicity (Bleves *et al.*, 2010; Filloux, 2011). Here, various secretory proteins act as virulence factors upon infection and facilitate the rapid invasion of the host (Döring *et al.*, 1987; Strateva and Mitov, 2011; Qin *et al.*, 2022). Virulence factors contribute to various processes upon infection, supporting the attachment and colonization of the host, leading to the disruption of host tissues and allows for resistance against the host immune response (Diggle and Whiteley, 2020; Liao *et al.*, 2022). The vast majority of virulence factors enables for an increased adaptability of *P. aeruginosa* that in turn leads to its high pathogenicity potential (Jurado-Martín, Sainz-Mejías and McClean, 2021; Qin *et al.*, 2022). Understanding the mediators of pathogenicity of *P. aeruginosa* might help to develop novel therapeutic agents. In this frame, elucidating the processes which govern the secretion of virulence factors may serve to identify pathways that can be targeted by novel therapeutic treatments and help to fight bacterial infections and to prevent the rise of opportunistic bacterial pathogens (Rice, 2008; Qin *et al.*, 2022). In this frame, the secretory lipase A of *P. aeruginosa* PAO1 is an interesting target in aim to

elucidate the process of the biogenesis of a virulence factor, while investigating its transport and maturation.

1.2 Lipase A – a true bacterial lipase serving as a virulence factor

Lipases are ubiquitous lipolytic enzymes which can be found in all kingdoms of life, ranging from microorganisms to humans (Casas-Godoy *et al.*, 2018; Kovacic *et al.*, 2019). In bacteria, the group of lipolytic proteins are classified into 19 families, including the esterases (EC 3.1.1.1) and the "true" bacterial lipases (EC 3.1.1.3) (Casas-Godoy *et al.*, 2018; Kovacic *et al.*, 2019). The true lipases belong to family I of lipolytic enzymes, and are classified based on their sequence homology and physiological properties into eight subfamilies (I.1 – I.8) (Arpigny and Jaeger, 1999; Kovacic *et al.*, 2019). True bacterial lipases have versatile functions: They are involved in the lipid metabolism and signaling, they take a role in cell growth, and they can serve as virulence factors of many pathogenic bacteria, including of *P. aeruginosa* (Gilbert, 1993; Stehr *et al.*, 2003; Hausmann and Jaeger, 2010). Although the lipases between the various subfamilies possess low amino acid sequence similarity, they mostly comprise a common structural arrangement with the canonical α/β hydrolase fold (Ollis *et al.*, 1992; Kovacic *et al.*, 2019). The typical lipase fold enables structural flexibility and is important for the functional arrangement of the lipase as it allows for conformational changes of the protein (Kovacic *et al.*, 2019). A further common structural element is the lid domain which hides the active site in the closed conformation and moves away leading to an open state, where the catalytical center is accessible for substrates (Khan *et al.*, 2017). True bacterial lipases are capable to catalyze the hydrolysis as well as the synthesis reactions of various substrates (Jaeger and Reetz, 1998; Casas-Godoy *et al.*, 2018). They are of high biotechnological interest and utilized in manifold applications in broad industrial range (Jaeger and Reetz, 1998; Rios *et al.*, 2018). To fold into their active form, several secretory bacterial lipases require folding assistance by specific foldases which serve as steric chaperones (Frenken *et al.*, 1993; Hobson *et al.*, 1993; Rosenau, Tommassen and Jaeger, 2004; Pauwels *et al.*, 2007).

1.2.1 Structure of the lipase A

The major extracellular lipase of *P. aeruginosa* PAO1 is the lipase A (LipA), a true bacterial lipase, that is classified within family I and subfamily I.1 (Arpigny and Jaeger, 1999; Kovacic *et al.*, 2019). The mature form of the lipase A of *P. aeruginosa* PAO1 consists of 285 amino acids and has a molecular weight of ~29 kDa (Nardini *et al.*, 2000). The main substrates of lipases are long-chain acylglycerols (Jaeger *et al.*, 1994; Jaeger and Reetz, 1998). As a triacylglycerol hydrolase, LipA comprises the typical α/β hydrolase fold, whereby 5 hydrophobic β-sheets are surrounded by 5 α-helices (Figure 1.1) (Nardini *et al.*, 2000). Additionally, the active site of the lipase is covered by an α-helical lid domain which is important for its activity and stability (Khan *et al.*, 2017; Rashno *et al.*, 2018). The active site of the protein consists of a catalytic triad that composes of a nucleophilic serine (S82), an acidic aspartate (D229) and a basic histidine (H251) (Ollis *et al.*, 1992; Nardini *et al.*, 2000). In the open conformation the active site is accessible for the substrate, while in the closed conformation it is covered by the lid

domain (Nardini *et al.*, 2000). The underlying chemical mechanism of ester hydrolysis is based on nucleophilic substitutions on the substrate (Blow, Birktoft and Hartley, 1969; Ribeiro *et al.*, 2011). An additional structural feature of LipA is an intramolecular disulfide bridge between two cysteines (C183 and C235) that is formed upon maturation of the protein in the periplasm, a process assisted by proteins of the disulfide bond formation (Dsb) system (K. Liebeton, Zacharias and Jaeger, 2001). The disulfide bridge increases the lipase stability but it is not essential for the activity (Klaus Liebeton, Zacharias and Jaeger, 2001). Further, two aspartic acid residues (D209 and D253) form a calcium-binding pocket which stabilizes the active site of the protein (Nardini *et al.*, 2000).

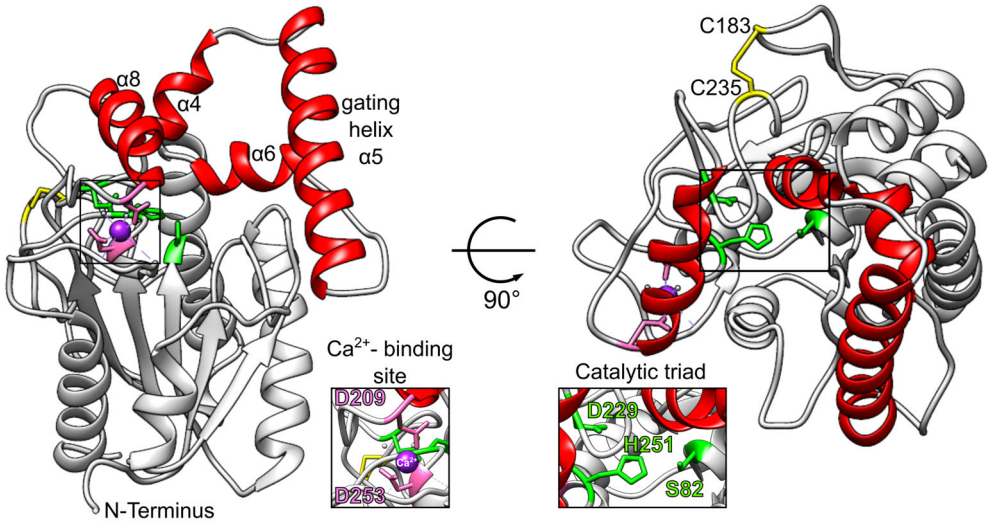

Figure 1. 1: The lipase A of *Pseudomonas aeruginosa* PAO1

The structure of the lipase A is shown in the open conformation (PDB: 1EX9, Nardini *et al.*, 2000). The lid domain (red) is comprised by α helices (α4 – 6 and α8), whereby the gating helix α5 is important for the stability and activity. The calcium-binding site (Ca^{2+}, purple) is important for the stability of the active site. The disulfide bridge between C183 and C235 (yellow) that stabilizes the protein. The catalytic triad (green) consists of S82, D229 and H251.

1.2.2 Function of the lipase A

Once the active LipA is secreted to the extracellular space, it fulfills a number of tasks that classify it as a virulence factor (Stehr *et al.*, 2003). LipA is capable to hydrolyze triacyl glycerol, thus possibly promoting growth and colonization of the host tissues upon infection cycle (Jaeger *et al.*, 1994; Stehr *et al.*, 2003). LipA accumulates and interacts with components of the biofilm matrix, such as alginate, that is formed upon infection cycle of *P. aeruginosa* (Tielen *et al.*, 2013). In an environment where lipids are the only carbon source, their hydrolysis enables the bacteria to use them for nutrient acquisition in aim to maintain bacterial growth (Stehr *et al.*, 2003). Biochemical characterizations of LipA indicated that the lipase is secreted together within lipopolysaccharide (LPS) micelles and this represents the native state of the enzyme as it is present upon *P. aeruginosa* infections (Jaeger, Kharazmi and Høiby, 1991). Early *in vitro* investigations revealed that LipA decreased the chemotactic mobility of monocytes, suggesting an inhibitory effect towards the host immune response (Jaeger, Kharazmi and Høiby, 1991;

Jaeger *et al.*, 1994). LipA received special attention for its role as a virulence factor after detecting the highly abundant anti-lipase antibodies in antisera obtained from cystic fibrosis patients (König, Jaeger and König, 1994). Further findings indicated that a synergistic action of LipA and the phospholipase C stimulates the release of inflammatory mediators from human platelets upon lung infections by *P. aeruginosa* (Jaeger *et al.*, 1994; König, Jaeger and König, 1994). Additionally, LipA plays a regulatory role in expression of the transcriptional sigma factor PvdS, that in turn controls the expression of further *P. aeruginosa* PAO1 major virulence factors, like pyoverdine (Potvin *et al.*, 2003; Funken *et al.*, 2011; Durán *et al.*, 2022).

1.2.3 Gene expression of the lipase A

LipA is expressed together with its cognate chaperone, the lipase-specific foldase (Lif) LipH, in a bicistronic operon (Wohlfarth and Winkler, 1988; Chihara-Siomi *et al.*, 1992). Early molecular analysis on the sequence of the operon were conducted in aim to elucidate the regulation of its expression, revealing the presence of two primers located upstream of the *lipA* gene, where the first one is dependent on an alternative transcriptional σ^{54}-factor (P1) and the second one which is of unknown function (P2) (Rosenau and Jaeger, 2000). Commonly, σ^{54}-dependent genes require an additional activator for transcription (Shingler, 1996). Thus, early mutational investigations aimed to identify the transcriptional activator for the lipase operon and revealed the presence of a two-component regulation system formed by a putative sensing kinase (LipQ) and a transcription factor (LipR) (Rosenau and Jaeger, 2000). LipR can bind to an activating sequence located upstream of P1 and enable transcription of the operon (Rosenau and Jaeger, 2000). The regulation of gene expression within the *lipA/H* operon depends on quorum sensing and further environmental signals (McKenney, Brown and Allison, 1995; Reimmann *et al.*, 1997; Jaeger, Dijkstra and Reetz, 1999; Rosenau and Jaeger, 2000; Swift *et al.*, 2001; Chadha, Harjai and Chhibber, 2022). A complex "quorum sensing cascade" includes multiple regulation levels that require involvement of general regulatory proteins as well as the stimulus of autoinducer compounds (Jaeger, Dijkstra and Reetz, 1999; Rosenau and Jaeger, 2000; Chadha, Harjai and Chhibber, 2022). In the initial phase, the regulation of gene expression is guided by a conserved general transcriptional activator termed GacA which globally regulates the expression of multiple virulence factors of *P. aeruginosa* (Reimmann *et al.*, 1997). Among others, GacA activates the quorum sensing-related factor termed RhlR that in turn mediates the activation of the two-component regulation system LipQ/R. The quorum sensing-mediated virulence is of major importance upon *P. aeruginosa* infections (Moradali, Ghods and Rehm, 2017; Chadha, Harjai and Chhibber, 2022). Additionally to the RhlR/I, the LasR and PqsR regulation pathways are also dependent on quorum sensing and in turn regulate the synthesis of multiple virulence factors, including the elastase, exotoxin A, pyocyanin, pyoverdine, lectin, several proteases as well as rhamnolipids and the type II secretion system (T2SS) (Chadha, Harjai and Chhibber, 2022). The signaling compounds for the mentioned quorum sensing regulated pathways in *Pseudomonas* are quinolones and lactones, including 2-heptyl-3-hydroxy-4-quinolone (PQS) for the

PqsR, *N*-3-oxo-dodecanyl-L-homoserine lactone (3-oxo-C12-HSL) for the LasR and *N*-butyryl-L-homoserine lactone (C4-HSL) for the RhlR dependent regulation (Chadha, Harjai and Chhibber, 2022). Recent studies revealed that an additional two-component system PmrA/PmrB is involved in the transcriptional and translational regulation of the lipase A (Liu *et al.*, 2018).

1.2.4 Biogenesis of the lipase A

The biogenesis of LipA involves multiple steps from synthesis to secretion of the protein, whereby LipA undergoes manifold interactions with other proteins (Figure 1.2). After its translation, the lipase A precursor (proLipA) is released from the ribosome into the cytoplasm. The precursor protein proLipA contains a N-terminal signal peptide which targets it for translocation through general secretory (Sec) pathway (Rosenau and Jaeger, 2000). Multiple cytoplasmic chaperones can be involved in targeting of secretory proteins to the Sec machinery, first of all the holdase SecB (Castanié-Cornet, Bruel and Genevaux, 2014). Once the lipase is translocated to the periplasm through the Sec translocon, the signal peptide is cleaved off by the signal peptidase I (SPase I, LepB), and the lipase is released for folding and maturation. The lipase-specific foldase LipH is essential for folding of the lipase (Hobson *et al.*, 1993). The foldase itself is anchored in the inner membrane, with its chaperoning domain facing the periplasm (Rosenau, Tommassen and Jaeger, 2004). LipH acts hereby as a so-called steric chaperone, an "intermolecular folding catalyst", providing conformational information to the lipase A which allows it to overcome its thermodynamic folding barrier (Ellis, 1998; Rosenau, Tommassen and Jaeger, 2004; Pauwels *et al.*, 2007). After folding assistance by the foldase, the lipase is trapped in native state that possesses a rather high unfolding energy barrier (Pauwels *et al.*, 2007). The prominent periplasmic chaperone Skp prevents off-pathway aggregation and misfolding of the unfolded lipase and is important for LipA secretion (Papadopoulos *et al.*, 2022). Additionally, further prominent periplasmic proteins could be involved in lipase maturation processes, as indicated for proteins of the disulfide bond formation (Dsb) system which support the formation of the intermolecular disulfide bridge of LipA and contribute to its stabilization (K. Liebeton, Zacharias and Jaeger, 2001). Thus, these observations suggest that there might be multiple protein:protein interactions between LipA and further periplasmic proteins which are occurring and required upon the lipase biogenesis. Secretion of the mature lipase to the extracellular space is conducted by T2SS (Filloux, 2011). In *P. aeruginosa*, T2SS responsible for LipA secretion is termed the Xcp machinery which represents a supercomplex of 12 proteins spanning the inner and outer membrane. How the folded LipA transferred to the Xcp system remains widely elusive, although previous interaction studies were conducted to elucidate putative workwise of the system (Douzi *et al.*, 2011).

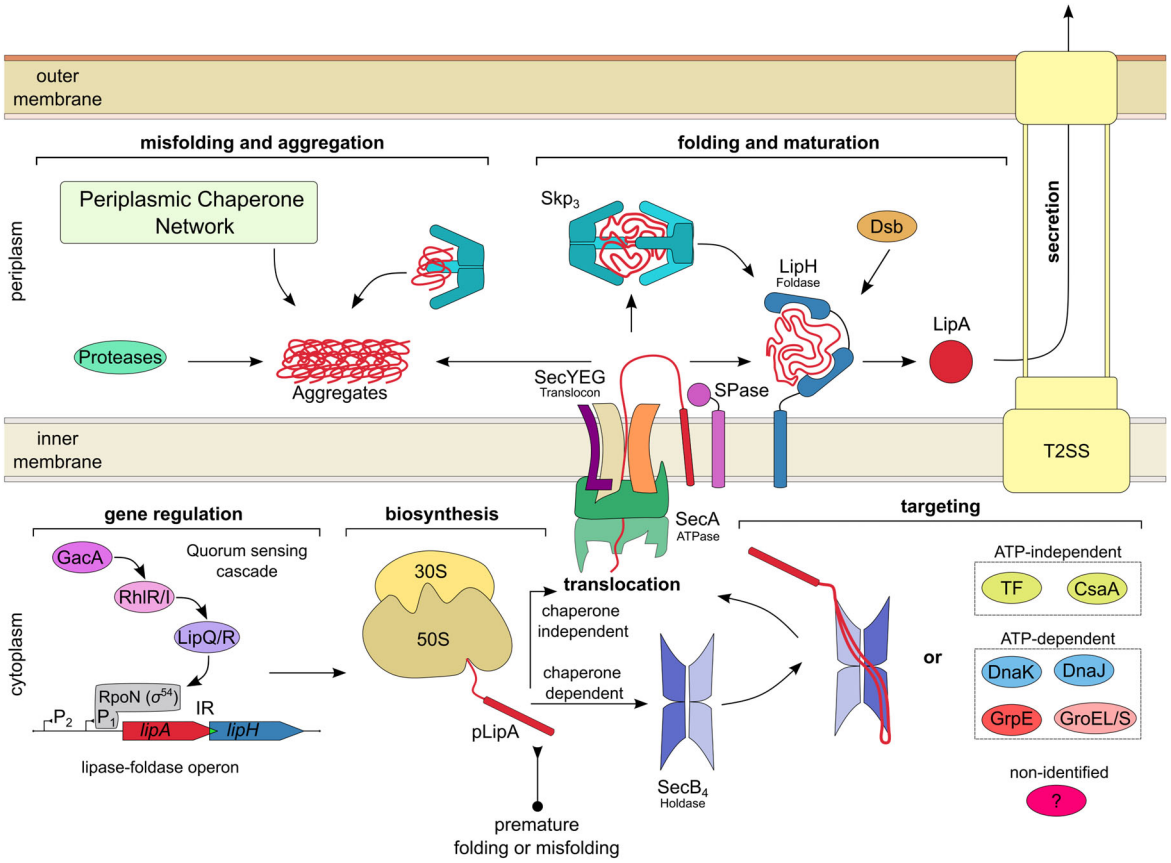

Figure 1. 2: Schematic representation of the biogenesis of lipase A in *Pseudomonas aeruginosa* PAO1

Comprehensive overview of the biogenesis of the lipase A, including current knowledge and hypothetical steps of that pathway. A bicistronic operon (*lipA/H*) encodes for LipA and its cognate foldase (LipH). The gene expression of the lipase operon is regulated by a quorum sensing dependent cascade (GacA, RhlR/I), including the two-component system (LipQ/R) and the alternative sigma factor (RpoN (σ^{54})). Upstream of the operon there are two promotors present which one is of unknown function (P2) and the other one is dependent on σ^{54}-transcription factor. The genes for the lipase A (*lipA*) and the foldase (*lipH*) share an intergenic region (IR, green). Upon biosynthesis the lipase precursor (pLipA) is released from the ribosome into the cytoplasm, containing an N-terminal signal peptide (red bar) that dedicates its Sec-dependent translocation. pLipA is most likely targeted for translocation in a chaperone-dependent manner, whereby the holdase SecB or other adenosine triphosphate (ATP)-independent (Trigger Factor “TF”, CsaA) or ATP-dependent (DnaK/J, GrpE, GroEL/S) as well as non-identified chaperones can be involved. In addition, a chaperone-independent targeting by SecA or in a co-translational fashion are worth to be mentioned since an immediate aggregation of the preprotein pLipA after release is very likely, due to its high intrinsic aggregation propensity. Once pLipA reaches the translocon, it is translocated through SecYEG by ATPase action of SecA. The translocated pLipA emerges to the periplasmic site, where its signal peptide is cleaved by the signal peptidase (SPase I, LepB). The mature domain of LipA is folded to its active and secretion competent form by the lipase-specific foldase LipH. The intramolecular disulfide bond is formed upon assistance of Dsb system. To prevent off-pathway routes of the aggregation-prone unfolded mature domain of LipA, the periplasmic chaperone network with the prominent chaperone Skp is involved in preventing misfolding of the lipase. Off-pathway aggregates are likely degraded by periplasmic proteases, to not become toxic for the cell. The folded LipA is secreted through the type II secretion system (T2SS) to the extracellular space.

1.3 Protein export via the general secretory pathway

Biological membranes serve as dynamic borders for the cell, and the transport of biomolecules across the membrane is an essential process that must be tightly regulated. In this frame multiple transport mechanisms are required. In bacteria, a plethora of mechanisms for protein transport across the cell envelope evolved (Papanikou, Karamanou and Economou, 2007) (Figure 1.3). As for other biomolecules, the transport of proteins across the cell membrane is considered essential to maintain protein homeostasis (Tsirigotaki *et al.*, 2017; Oswald *et al.*, 2021). The transport processes of proteins are evolutionary related among eukaryotes and prokaryotes, and the general secretory (Sec) pathway is universally conserved (Bolhuis, 2004; Yuan *et al.*, 2010; Beckwith, 2013; Denks *et al.*, 2014; Oswald *et al.*, 2021). Other transport systems, besides the Sec, include the twin arginine translocation pathway (Tat) which transports folded proteins across the cytoplasmic membrane, as well as multiple secretion systems which allow protein export across the bacterial cell envelope (Economou *et al.*, 2006; Papanikou, Karamanou and Economou, 2007; Palmer and Berks, 2012). The requirement for a general secretory pathway employed for bacterial protein export is obvious, as about 20 – 30 % of the proteome represents proteins that act outside of the cytoplasm (Holland, 2004). Thus, for bacteria the protein export through the Sec pathway is of major importance as it contributes to the biogenesis of the cell envelope and further to the secretion of proteins which facilitate the adaptation of the bacteria in the environments they inhabit (Holland, 2004; Oswald *et al.*, 2021). Two primary routes for protein export through Sec are recognized: The co-translational protein insertion into the membrane and the post-translational protein translocation across the membrane (Tsirigotaki *et al.*, 2017; Oswald *et al.*, 2021). The hydrophobicity of the export protein plays a critical role for the selection of the route it takes through the Sec pathway. Commonly, the decisive step towards the Sec is determined by the properties of the signal peptide (SP) of the secretory client protein (Rusch and Kendall, 2007). Proteins with highly hydrophobic signal peptides are directed to co-translational insertion, while less hydrophobic signal peptides determine the direction towards post-translational translocation (Rusch and Kendall, 2007; Owji *et al.*, 2018). The co-translational protein insertion is facilitated by the signal recognition particle (SRP) and its receptor FtsY (Steinberg *et al.*, 2018). The ribosome-bound nascent polypeptide chain (RNC) is recognized at early translational stage by the SRP, forming the SRP-RNC complex that is targeted to the SRP receptor FtsY (Angelini, Deitermann and Koch, 2005; Steinberg *et al.*, 2018). Thus, a ternary SRP-RNC-FtsY complex is formed and further targeted to the translocon SecYEG or the insertase YidC (Steinberg *et al.*, 2018). Both SecYEG and YidC can function as independent insertases (Dalbey *et al.*, 2014; Steinberg *et al.*, 2018; Kater *et al.*, 2019). The formation of a quaternary complex of SRP-RNC-FtsY with SecYEG causes conformational changes within the translocon which facilitate the protein insertion into the membrane (Jomaa *et al.*, 2017). The route of a protein upon insertion is determined by its intrinsic properties (Rusch and Kendall, 2007). Multiple membrane proteins are known to utilize YidC for insertion (Dalbey *et al.*, 2014). Although, membrane protein insertion can be conducted independently of YidC, many proteins are inserted via a cooperative mechanism utilizing

SecYEG and YidC together (Dalbey *et al.*, 2014; Petriman *et al.*, 2018; Steinberg *et al.*, 2018). In this cooperative mechanism, conformational changes cause the lateral opening of the translocon which provides a gateway for insertion of hydrophobic transmembrane helices (TMH) of the membrane protein, while YidC serves as a guide for the correct release and topology of them (Dalbey *et al.*, 2014; Steinberg *et al.*, 2018). In rare cases, small membrane proteins can also undergo post-translational insertion mediated by SRP (Steinberg *et al.*, 2020). Commonly, the post-translational Sec pathway is utilized for secretory proteins, whereby in bacteria the translocation of unfolded preproteins across the plasma membrane is aimed (Arkowitz, Joly and Wickner, 1993; Schneewind and Missiakas, 2014; Tsirigotaki *et al.*, 2017). While the translocon SecYEG builds the core channel of the protein export machinery, additional Sec proteins are involved in post-translational transport, including the ATPase SecA, the holdase SecB and other cytoplasmic chaperones, as well as the membrane protein complex SecDFYajC and the outward-facing membrane-bound chaperones YfgM and PpiD (Denks *et al.*, 2014; Götzke *et al.*, 2014; Tsirigotaki *et al.*, 2017; Tsukazaki, 2018; Oswald *et al.*, 2021; Miyazaki *et al.*, 2022). The majority of secretory proteins in bacteria follows the post-translational and SecA-mediated targeting to the translocon (Driessen and Nouwen, 2008; Chatzi *et al.*, 2014; Oswald *et al.*, 2021). Here, the released preproteins can be kept unfolded and in a translocation-competent state by the holdase SecB or other cytoplasmic chaperones, prior being recognized by SecA and targeted for translocation through the translocon SecYEG. The protein transport through SecYEG can be facilitated by proton motive force which is enabled by the heterodimeric membrane protein complex SecDF. Hereby, SecDF is embedded in the cytoplasmic membrane near SecYEG. SecDF is believed to function as a proton-conducting channel, which lets protons to pass from the periplasm to the cytoplasm, while the periplasmic domain undergoes conformational transitions that are involved in the enhancement of protein translocation through the Sec system (Tsukazaki, 2018). This movement catches emerging preproteins coming through SecYEG and enhances their directional movement from the cytoplasmic to the periplasmic site. Upon translocation, the signal peptide is inserted into the membrane, while the rest of the protein is transported across the membrane. To cleave the “anchored” mature domain of the protein the signal peptidase I (SPase I, LepB), a membrane-bound protein, recognizes a specific cleavage motif located at the C-terminal end of the signal peptide and cleaves the mature domain of the inserted signal peptide (Auclair, Bhanu and Kendall, 2012; Furukawa *et al.*, 2017; Tsukazaki, 2018). Once the protein is translocated, several periplasmic proteins take over the passage of translocated proteins (Stull, Betton and Bardwell, 2018). Here, periplasmic chaperones influence on the correct assembly and/or folding of their client proteins (Missiakas and Raina, 1997; Goemans, Denoncin and Collet, 2014; Stull, Betton and Bardwell, 2018). The presence of the periplasmic chaperone network further facilitates several procedures, including the biogenesis of outer membrane proteins and prevention of off-pathway routes and/or protein aggregation (Stull, Betton and Bardwell, 2018). The successful and efficient secretion of extracytosolic proteins is a fundamental process that is crucial for bacteria, such as *P. aeruginosa*. Virulence factors, like the lipase A of *P. aeruginosa*, are secreted to the extracellular space where they

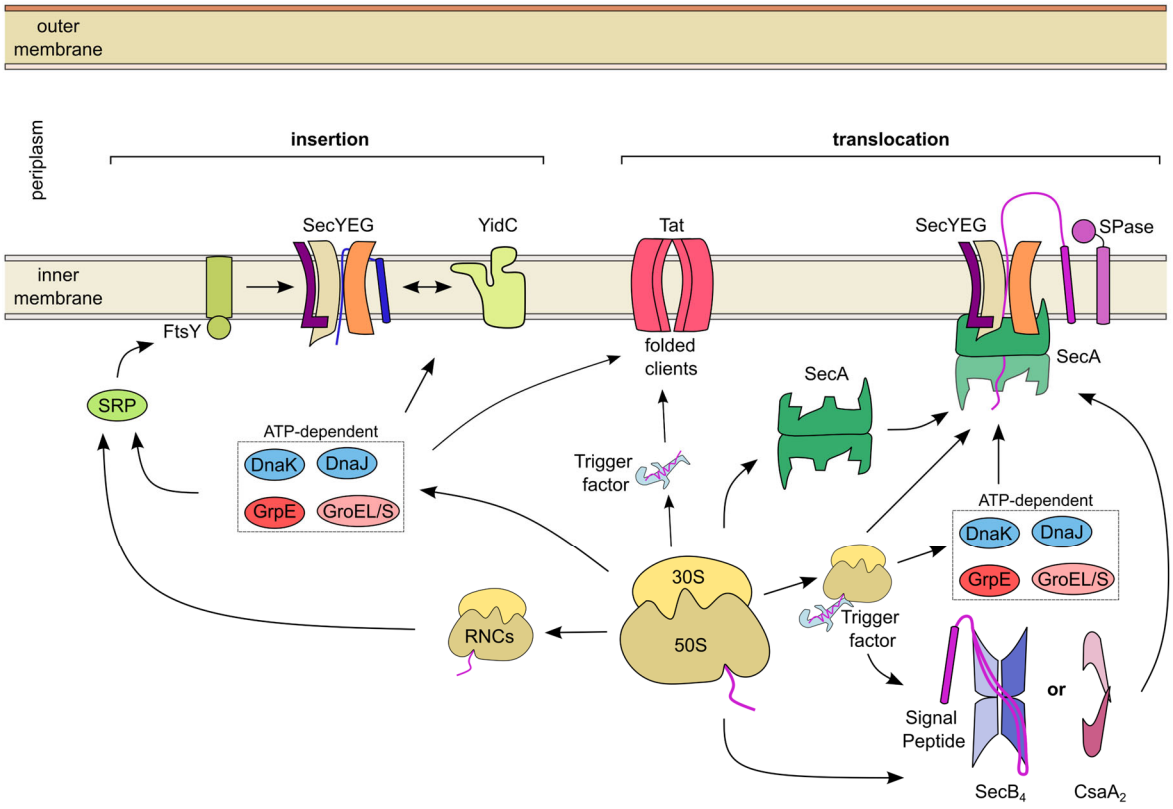

Figure 1. 3: Protein export across the cytoplasmic membrane in gram-negative bacteria

The export of proteins is schematically depicted for gram-negative bacteria. Unfolded secretory proteins can be translocated across the cytoplasmic membrane (inner membrane) via the Sec translocon, whereby targeting can occur due to multiple interactions with ATP-dependent and independent chaperones and/or via SecA. Folded client proteins can be exported by the Tat pathway. Membrane proteins can be inserted to the inner membrane by SecYEG and YidC.

are mostly acting on the border between the host and the pathogen. The successful release of virulence factors is thus directly related to a successful protein export.

1.3.1 The translocon SecYEG

The central component of the Sec pathway is the translocon SecYEG which is built of membrane proteins itself (Figure 1.4). The Sec translocon is a heterotrimeric membrane protein complex which is located in the cytoplasmic membrane of bacteria (Denks *et al.*, 2014). In bacteria, the translocon forms a protein-conducting channel that allows for protein insertion into and protein translocation across the cytoplasmic membrane (Veenendaal, Van Der Does and Driessen, 2004; Du Plessis, Nouwen and Driessen, 2011; Lycklama a Nijeholt and Driessen, 2012; Kater *et al.*, 2019). The central subunit SecY is surrounded by SecE and flanked by SecG (Van Den Berg *et al.*, 2004). Furthermore, SecY represents the major protein of the translocon and contains 10 TMHs which arrange pseudo-symmetrically in two halves formed by TMH 1 to 5 and 6 to 10, reminding the shape of an hour glass (Van Den Berg *et al.*, 2004; Tanaka *et al.*, 2015). Here, TMH 5 and 6 are connected by a loop termed the hinge region, indicating a calm-shell arrangement (Oswald *et al.*, 2021). On structural level, SecY forms a conduit for

protein export and is stabilized by SecE, whereas the flanking SecG is not essential for protein translocation (Belin *et al.*, 2015). The internal hourglass-like architecture of SecY is formed by a central pore with an inner ring of hydrophobic and bulky amino acid residues which are important for the integrity of the translocon and modulation of the impermeable resting state (Park and Rapoport, 2011). On the other side of SecY, a flexible region between TMHs 2 and 7/8 termed the "lateral gate" allows for polypeptide insertion into the lipid phase of the membrane (Kater *et al.*, 2019). On the periplasmic side a helical plug-domain serves to seal the membrane channel in its resting state (Van Den Berg *et al.*, 2004; Lycklama a Nijeholt, Wu and Driessen, 2011; Tanaka *et al.*, 2015). The cytosolic loops C4 and C5 of SecY represent the essential binding sites for SecA, the signal recognition particle (SRP) receptor FtsY and the ribosome (Mori and Ito, 2006; Das and Oliver, 2011; Kuhn *et al.*, 2011; Oswald *et al.*, 2021). Upon protein translocation, interactions with the preprotein as well as SecA cause conformational rearrangements which allow the translocon to obtain a stable open state (Van Den Berg *et al.*, 2004; Kusters and Driessen, 2011; Ma *et al.*, 2019). Those conformational changes include opening of the lateral gate and the displacement of the plug-sealing, allowing the preprotein to exit the translocon (Ma *et al.*, 2019; Dong *et al.*, 2023). The required power for the protein translocation is provided by the essential motor ATPase SecA. The translocons of *E. coli* and *P. aeruginosa* possess high structural homology, although the amino acid sequences represent moderate identity, as pairwise alignments of the constituting subunits indicate ~ 65 % identity for SecY, ~ 46 % for SecE and ~ 49 % for SecG (Waterhouse *et al.*, 2009). The structural model of *P. aeruginosa* translocon shows a heterotrimeric membrane protein complex of similar fashion as observed for *E. coli*.

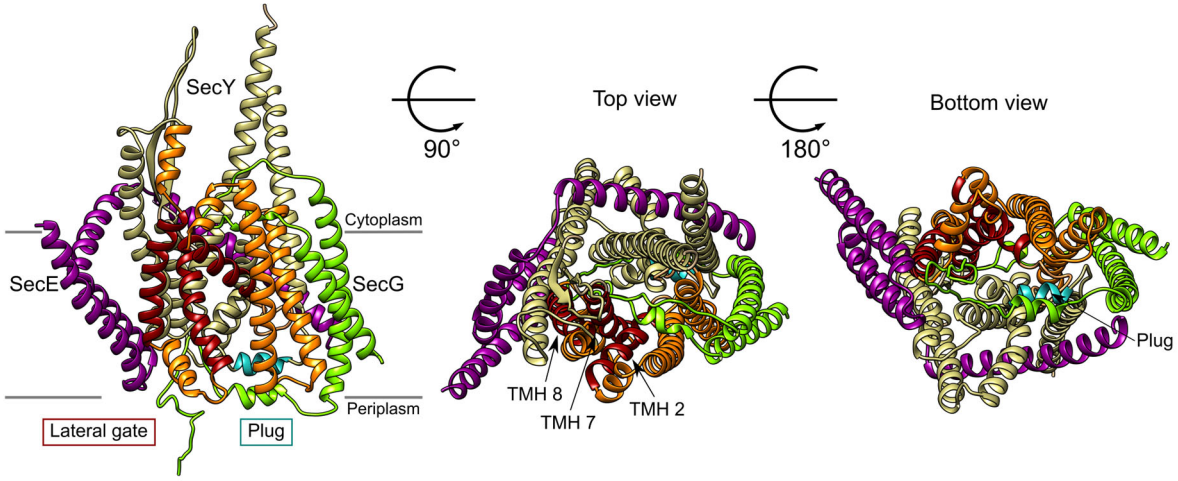

Figure 1. 4: The translocon SecYEG of *Pseudomonas aeruginosa* PAO1

The AlphaFold model of the translocon SecYEG is shown. The heterotrimeric membrane protein consists of the SecY core protein (khaki and orange) which is surrounded by SecE (violet) and flanked by SecG (green). The translocon subunits are indicated in the figure. The transmembrane helices (TMH 2, 7 and 8) which form the lateral gate are colored separately (dark red) as well as the plug domain (cyan). The translocon is further depicted in the top and bottom view.

1.3.2 The motor protein SecA

In the bacterial Sec system, SecA is a multidomain protein functioning as an essential nanomotor for the protein translocation process. SecA assembles with the translocon SecYEG upon protein translocation, and it can recognize the unfolded secretory clients delivered by the cytoplasmic holdase chaperone SecB (Kusters and Driessen, 2011; Grady, Michtavy and Oliver, 2012). Upon Sec-dependent protein transport, SecA hydrolyses ATP and provides the required power-strokes for post-translational protein translocation (Vrontou and Economou, 2004; Catipovic *et al.*, 2019). Structurally, SecA is divided into multiple subdomains which are of functional diversity (Figure 1.5). On one side, the N-terminal helix of SecA is important for interaction with the lipids of the cytoplasmic membrane (Kamel *et al.*, 2022). At the same side, the preprotein cross-linking domain (PPXD) is important for binding of preproteins. The PPXD is flanked by a helical wing domain (HWD) which is also involved in preprotein binding (Kusters and Driessen, 2011; Bhanu, Zhao and Kendall, 2013). Further, the so-called two helix finger (2HF) is important upon translocation process, where it interacts with the preprotein and pushes it into the translocon (Erlandson *et al.*, 2008). A helical scaffold domain (HSD) connects the N-terminal site to the C-terminal site of SecA. On the other side, two nucleotide biding domains (NBD1 and NBD2) are located which are required for the ATPase activity of the protein (Kusters and Driessen, 2011). NBD1 and NBD2 possess the conserved Walker A and B motifs involved in the nucleotide binding (Lycklama a Nijeholt and Driessen, 2012). Further, SecA contains a C-terminal metal-binding site which coordinates a zinc ion. This so-called zinc finger is important for interactions with the holdase chaperone SecB (Fekkes *et al.*, 1999).

The preprotein recognition step is essential for protein translocation, as recognition and binding of preproteins cause conformational changes in SecA, which link preprotein binding to the hydrolytic activity of SecA (Zimmer and Rapoport, 2009; Kusters and Driessen, 2011; Gouridis *et al.*, 2013; Catipovic *et al.*, 2019). It is shown that SecA undergoes conformational changes upon preprotein translocation, switching from a dimeric receptor state to a monomeric state functioning as nanomotor driven by ATP hydrolysis (Sardis and Economou, 2010; Gouridis *et al.*, 2013). Upon the translocation process, SecA interacts with high affinity with the cytoplasmic domains of the translocon and with the surrounding lipid environment of the cytoplasmic membrane (Kuhn *et al.*, 2011; Kamel *et al.*, 2022). Putative mechanisms of the processive protein translocation by SecA are discussed in literature (Collinson, Corey and Allen, 2015; Allen *et al.*, 2016), and several functional models have been proposed. The power-stroke mechanism of SecA suggests that conformational rearrangement of SecA upon ATP-binding causes a movement of the 2HF domain that pushes the bound preprotein into the Sec translocon, while a so-called “clamp domain” formed by PPXD and NBD2 (Zimmer, Nam and Rapoport, 2008) traps the preprotein to avoid backsliding and to ensure the directional transport through Sec translocon (Erlandson *et al.*, 2008; Catipovic *et al.*, 2019). Alternatively, a Brownian ratchet mechanism is proposed for SecA-mediated translocation, whereby free diffusion of the preprotein through the Sec translocon is biased in a directional fashion by the binding and hydrolysis of ATP (Allen

et al., 2016). In brief, this model considers a "two-way communication" between SecA and SecYEG where ATP-binding and hydrolysis regulate the opening of the translocon, while the conformational state of the translocon (open or closed/resting) regulates the nucleotide exchange on SecA (Allen *et al.*, 2016). It is important to mention that the properties of the preprotein, like the size and secondary structural elements or partial folding, tremendously affect the translocation efficiency, as the dynamic diffusion of the preprotein in the translocon triggers both the opening of SecYEG and the nucleotide exchange on SecA (Allen *et al.*, 2016). Recent findings suggested a further catch-and-release mechanism, where the intrinsic properties of the preprotein can have an impact on translocation mediated by SecA (Krishnamurthy *et al.*, 2022). Hereby, segmental parts of the preproteins, including the signal peptide and the mature domain, link the independent functional domains of SecA (clamp and ATPase domain) and influence the conformational dynamics of the motor ATPase, thus directly impacting on the SecA-mediated translocation process. Upon hydrolysis of ATP, SecA undergoes conformational movements in the clamp domain which in turn cause versatile interactions with the preprotein segments and allow for the "catch-and-release" modulation (Krishnamurthy *et al.*, 2022). All mechanisms for the SecA mode of action have in common, that in the absence of ATP (or ADP-bound state) SecA is quiescent, and the translocation is prohibited, and only the formation of translocase complexes and the presence of ATP favor translocation of preproteins (Allen *et al.*, 2016; Catipovic *et al.*, 2019; Krishnamurthy *et al.*, 2022).

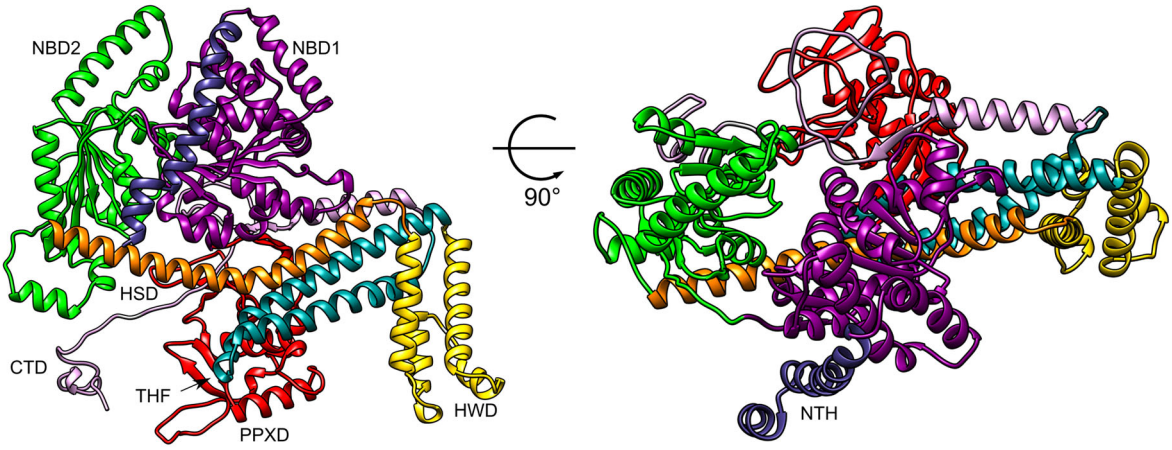

Figure 1. 5: The motor ATPase SecA of *Pseudomonas aeruginosa* PAO1

The AlphaFold model of the motor ATPase SecA is shown. The various colors indicate the different domains of SecA: helical scaffold domain (HSD, orange), peptide cross linking domain (PPXD, red), two helix finger (2HF, cyan), helical wing domain (HWD, yellow), nucleotide binding domain 1 (NBD1, violet), nucleotide binding domain 2 (NBD2, green), N-terminal helix (NTH, dark blue), the C-terminal domain (CTD, plum).

1.3.3 Targeting of preproteins for translocation via the Sec system

Efficient preprotein targeting to the general secretory (Sec) system is an important process to enable the Sec-dependent protein export. The secretory proteins are synthesized by the ribosome and release into the cytoplasm prior they are targeted for export to the Sec machinery. SecA alone can interact with preproteins and target those for post-translational translocation to SecYEG (Chatzi *et al.*, 2014). Additionally and most commonly, preprotein targeting can be assisted by molecular chaperones, including the ATP-independent cytoplasmic chaperones which serve as so-called holdases keeping the preprotein in an unfolded translocation-competent state, including SecB, trigger factor (TF) or CsaA (Müller *et al.*, 2000; Bechtluft *et al.*, 2010; Sharma, Rani and Goel, 2018; De Geyter *et al.*, 2020). The targeting to the Sec machinery is dependent on the properties of the preprotein. The recognition and binding of preproteins to molecular chaperones or further targeting partners is determined by their amino acid composition (primary structure), partial folding events (secondary structure), and intrinsic signals (signal peptides or mature domain targeting domains) of the preprotein as well as the translation machinery itself (Castanié-Cornet, Bruel and Genevaux, 2014; Tsirigotaki *et al.*, 2017, 2018; Kaushik, He and Dalbey, 2022). The signal peptide (SP) determines the protein path to the Sec and is governed by its hydrophobicity (Rusch and Kendall, 2007; Owji *et al.*, 2018; Kaushik, He and Dalbey, 2022). A SP of post-translationally targeted preproteins typically contains a positively charged N-terminal region, followed by a prolonged hydrophobic core region, and flanked by a less hydrophobic C-terminal region which contains an signal peptidase I (SPase I, LepB) cleavage motif (A-X-A, where X is varying residue) (Kaushik, He and Dalbey, 2022). The functions of the SP are manifold: It promotes binding to chaperones, delays the premature folding, and influences the translocation process (Owji *et al.*, 2018; Kaushik, He and Dalbey, 2022).

Targeting of preproteins to the Sec machinery is commonly mediated by cytoplasmic chaperones which have distinct modes of action and together they constitute a broad interactional network in the cytoplasm (Castanié-Cornet, Bruel and Genevaux, 2014; De Geyter *et al.*, 2020). Chaperones may serve as holdases which avoid compacting and/or aggregation of the preproteins, and they can play a role as targeting mediators for the preprotein to SecA:SecYEG machinery(Bechtluft *et al.*, 2010; Sharma, Rani and Goel, 2018; Jiang, Wynne and Huber, 2021). The most well-studied holdase is SecB, a stable homotetrameric protein that recognizes and hydrophobically grabs the freshly released preproteins in the cytoplasm, while they remain competent for translocation through the Sec machinery (Fekkes *et al.*, 1998; Dekker, De Kruijff and Gros, 2003; Bechtluft *et al.*, 2010). Upon formation of the SecB tetramer, a hydrophobic groove is formed on each side of the protein oligomer which functions as a binding site for hydrophobic patches of the preprotein mature domain. Thus, a preprotein binds by winding around SecB, while at the same time it is kept from occasional misfolding (Huang *et al.*, 2016). SecB interacts with SecA, and binding affinity is enhanced upon preprotein recognition (Hartl *et al.*, 1990; Randall and Henzl, 2010). In addition to SecB, a functional homolog named CsaA is found in gram-positive bacteria, archaea and also in gram-negative *P. aeruginosa* PAO1, but not in *Escherichia coli* (Linde *et al.*, 2003;

Sharma, Rani and Goel, 2018; Sharma, Kumari and Goel, 2021). It is shown that CsaA acts in SecB-like fashion upon preprotein targeting and SecA:SecYEG-mediated translocation (Müller *et al.*, 2000; Sharma, Rani and Goel, 2018). In contrast to the holdases SecB and CsaA, the cytoplasmic chaperone trigger factor (TF) directly interacts with the emerging preproteins on the ribosome exit tunnel, while being able to complex with SecB and/or SecA, prohibiting aggregation of the preprotein and facilitating targeting to the Sec machinery (Maier *et al.*, 2005; Hoffmann, Bukau and Kramer, 2010; De Geyter *et al.*, 2020). Furthermore, TF is involved in multiple processes with ATP-dependent chaperones which help to maintain protein homeostasis in bacteria (Mogk, Huber and Bukau, 2011; Castanié-Cornet, Bruel and Genevaux, 2014). Additionally, ATP-dependent molecular chaperones might be involved in protein targeting to the Sec machinery, since TF and DnaK share a common substrate pool (Deuerling *et al.*, 2003; Castanié-Cornet, Bruel and Genevaux, 2014). Early studies indicated that DnaK and DnaJ participate in protein export, while substituting for SecB when it is not present (Wild *et al.*, 1992). While it is suggested that TF slows down folding of nascent preproteins, it is shown that DnaK and TF are cooperating in folding of newly synthesized proteins (Deuerling *et al.*, 1999). Furthermore, conformational dynamics of preproteins are crucial for efficient targeting and translocation (Sardis *et al.*, 2017). Especially the relationship of the signal peptide and the mature domain is delicate and functions in a "rheostatic" manner that delays folding and maintain preproteins in their translocation-competent state (Sardis *et al.*, 2017; Smets *et al.*, 2022). In addition, the mature domain of the preprotein plays a crucial role for translocation, as it possesses loosely packed folding intermediates which serve as targeting signals to Sec machinery (Tsirigotaki *et al.*, 2018). In conclusion, multiple factors are potentially involved in targeting of preproteins to the Sec machinery, whereby the molecular chaperones and the intrinsic targeting signals contribute to the translocation-competent secretome.

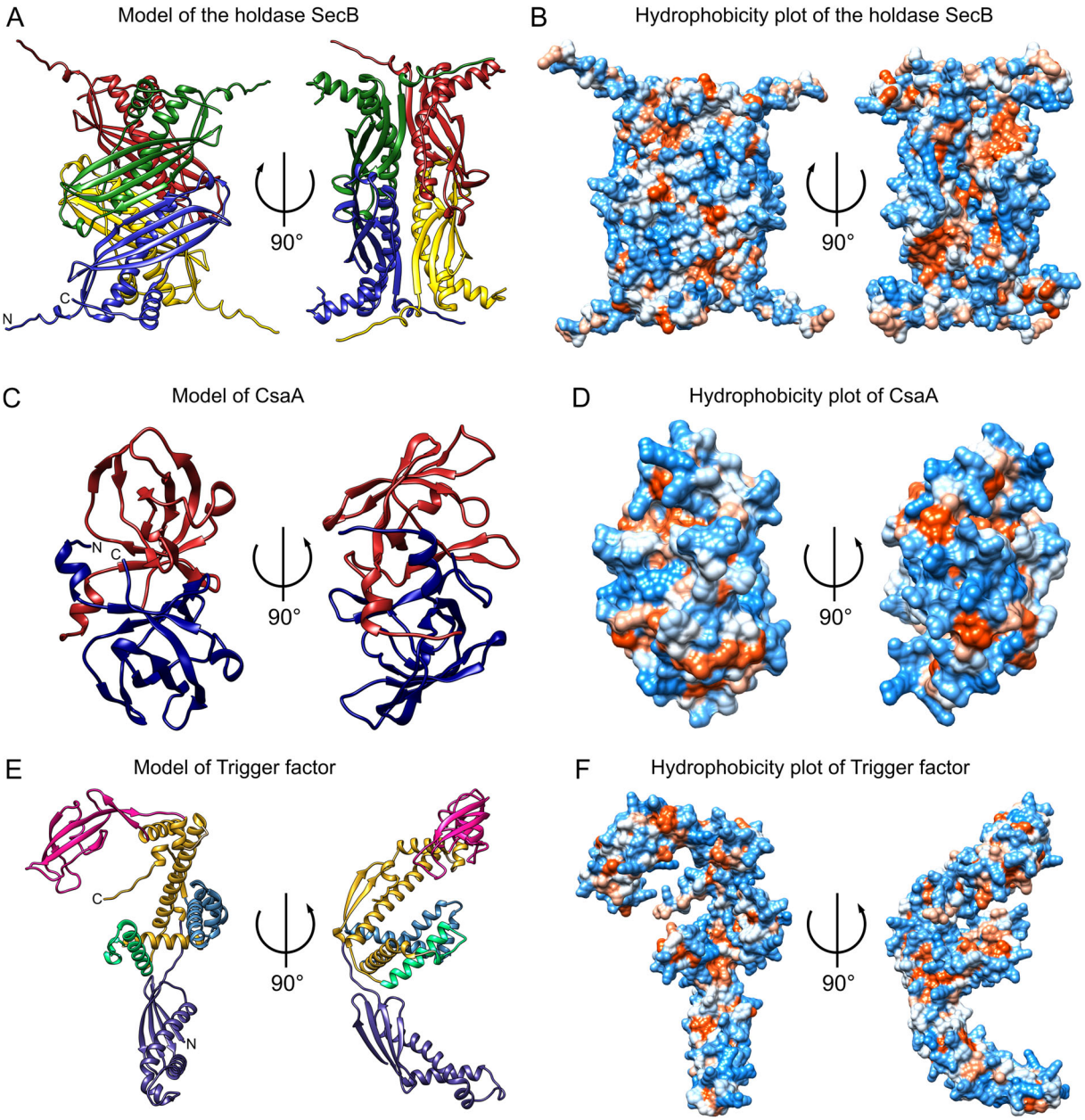

Figure 1. 6: ATP-independent cytoplasmic chaperones potentially involved in preprotein targeting to the Sec system of *Pseudomonas aeruginosa* PAO1

The AlphaFold models of the cytoplasmic chaperones are shown (A, C and E). The hydrophobicity analysis indicates the hydrophobic (red) and hydrophilic (blue) areas of the chaperones (B, D and F). **A**: The holdase SecB is formed by a dimer of dimers. Each protomer is colored separately (green, blue, red and yellow). **B**: Hydrophobicity analysis of SecB indicates the hydrophobic groove which is involved in holdase function allowing the unfolded preprotein to wind around the chaperone. **C**: CsaA is a functional homolog of SecB. **D**: Hydrophobicity analysis of CsaA indicates hydrophobic spots of CsaA which could be involved in client interactions. **E**: Trigger factor, a chaperone that can directly interact with the ribosome and grab the emerging client substrate. **F**: Hydrophobicity analysis of Trigger factor indicates a partially hydrophobic interior, thus reflecting putative interaction sites for the unfolded client. The N- and C-termini for the monomers are indicated in the figure (N and C).

1.4 Type II secretion system of *Pseudomonas aeruginosa*

The secretion of manifold bacterial proteins requires versatile and efficient export systems which allow for successful transport of folded and unfolded clients to the extracellular space. Therefore, bacteria have developed multiple secretion systems, to achieve transport over one or two bacterial membranes (Chagnot *et al.*, 2013). Up to nine secretion systems are described, which vary by their mechanisms and substrate specificity (Economou *et al.*, 2006; Chagnot *et al.*, 2013; Costa *et al.*, 2015; Green and Mecsas, 2016; Tsirigotaki *et al.*, 2017; Filloux, 2022). With emphasis on *P. aeruginosa*, multiple secretion systems are characterized and represent factors which support its pathogenicity by creating a so-called "wealth of pathogenic weapons" (Bleves *et al.*, 2010; Filloux, 2022). Here, the Sec-dependent secretion is an essential step in functioning of type II, V and VIII secretion systems (T2SS, T5SS and T8SS) (Bleves *et al.*, 2010; Filloux, 2022). T2SS of *P. aeruginosa* is termed Xcp and is ortholog to the Gsp system of *E. coli* (Filloux, 1998). Additionally, two homolog systems to Xcp are present in *P. aeruginosa*, termed the Hxc and Txc systems (Ball *et al.*, 2002; Bleves *et al.*, 2010; Cadoret *et al.*, 2014). T2SS is based on two-step mechanism whereby the secretory client proteins are initially transported to the periplasm by utilizing the Sec or Tat pathway, before they are recognized and secreted via T2SS to the extracellular space (Filloux, 1998; Sandkvist, 2001). While multiple secretory clients for the Xcp system are identified, only few clients are known for the homologous Txc and Hxc systems (Ball *et al.*, 2002; Douzi *et al.*, 2011; Filloux, 2011; Cadoret *et al.*, 2014). In *P. aeruginosa*, T2SS consists of 12 proteins, XcpA and XcpP to XcpZ (Filloux, 1998). Structurally, T2SS forms a molecular supercomplex that spans through the inner and outer membrane of *P. aeruginosa*, and comprises four sub-complexes (Tommassen *et al.*, 1992; Filloux, 2004; Thomassin *et al.*, 2017). An inner membrane platform is formed by XcpPSYZ, and is associated with the cytoplasmic ATPase sub-complex XcpR (Douzi *et al.*, 2011). The interactions of the Inner membrane platform and the ATPase are crucial for the assembly of the central pseudopilus, a further sub-complex which is mainly composed of XcpT and is primed by XcpUVWX (Douzi *et al.*, 2011; Thomassin *et al.*, 2017). The pseudopilus is important for the secretion through T2SS, as it pushes the substrate through the secretin in a "piston-like" manner (Filloux, 2004; Douzi *et al.*, 2011; Korotkov and Sandkvist, 2019). On the periplasmic side, XcpP is protruding and contacting the secretin. The secretin is built by XcpQ which oligomerizes and forms a sub-complex that spans through the outer membrane, allowing for the exit of secretory clients to the extracellular space. Furthermore, it is suggested that XcpP plays a role in the recognition of the client proteins (Douzi *et al.*, 2011). Early studies indicated that the major extracellular lipase (LipA) of *P. aeruginosa* PAO1, is secreted into the extracellular space by T2SS (Jaeger *et al.*, 1994; Sandkvist, 2001). Upon secretion, the LipA is initially transported to the periplasm in unfolded state, and after maturation and folding it employs the T2SS for secretion to the extracellular space (Jaeger *et al.*, 1994; Filloux, 1998, 2011). Like LipA, multiple secretory proteins connected to pathogenicity of *P. aeruginosa* were identified as T2SS substrates, including the additional lipase LipC, the exotoxin ToxA, the phospholipases PlcB and PlcH and the elastases LasA and LasB (Filloux, 2011). It remains

to be elucidated how the recognition between LipA and T2SS occurs, although XcpP might be involved (Douzi *et al.*, 2011). Potentially, further periplasmic interaction partners are involved in the lipase secretion process. It is sound, that especially for the secretion of pathogenicity mediators, such as virulence factors and/or toxins, the export processes require efficient secretion machineries. Bacterial secretion systems of opportunistic pathogens increase their pathogenicity, being often essential for infection processes (Liao *et al.*, 2022). In this frame, T2SS forms an important part which is crucial for the export virulence factors of *P. aeruginosa*.

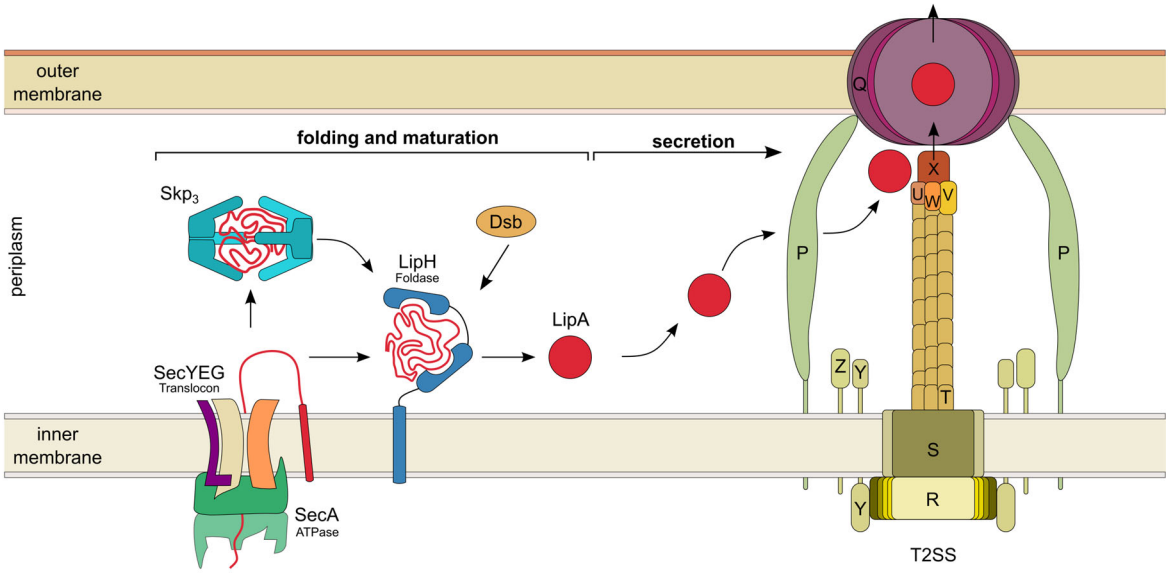

Figure 1. 7: Folding and secretion of the lipase A of *Pseudomonas aeruginosa* PAO1

After successful translocation of the lipase precursor (red) through the SecYEG translocon and the subsequent folding and maturation of lipase LipA, the protein is released for secretion. The subunits of the type II secretion system (T2SS) are indicated corresponding to the nomenclature of Xcp machinery of *P. aeruginosa*. The present illustration depicts the overall architecture of the Xcp machinery upon secretion of LipA. The molecular supercomplex spans both the inner and the outer membrane. The Xcp machinery consists of 12 proteins. The inner membrane platform is built by XcpPSYZ. The cytoplasmic ATPase XcpR is linked to the inner membrane platform and is crucial for the assembly of the pseudopilus XcpTUVWX. For the secretion through the T2SS, LipA is most likely initially recognized by XcpP, before it is pushed by a “piston-like” movement of the pseudopilus structures XcpTUVWX through the secretin XcpQ which spans through the outer membrane.

1.5 Protein folding and the role of chaperones

1.5.1 The theory of protein folding, misfolding and aggregation

Proteins are an essential group of biomolecules with manifold functions for biological systems. Independently of the place where they act, their polypeptide chains must undergo folding reactions to achieve their functional state. Protein folding is the process which nascent polypeptide chains undergo to acquire their defined functional conformation. The process of protein folding is driven by various forces that govern the folding pathways, including intra- and intermolecular interactions which are determined by the amino acid sequence (Dods, 2019). Furthermore, the overall thermodynamics govern the whole folding process of proteins and impact on the molecules as well as on their surroundings (Dobson, 2003). Early studies suggested that the primary structure of a protein solely guides the folding of a protein into its native state and is driven by physical properties of its constituent amino acid residues. This theory is the so-called thermodynamic hypothesis or "Anfinsen Dogma", and describes that proteins fold stepwise on a track along an energetic landscape in aim to reach their native conformation at which the free Gibbs energy is on its minimum (Anfinsen *et al.*, 1961; Anfinsen, 1973). Along the folding pathway a protein explores various intermediate states until reaching its native conformation (Dinner *et al.*, 2000; Plotkin and Onuchic, 2002; Dobson, 2003; Dill and MacCallum, 2012; Dods, 2019). The thermodynamic hypothesis was further disputed, as the so-called "Levinthal paradox" arose. Based on the Levinthal paradox, a protein cannot fold spontaneously into its native state by encountering stepwise all possible conformations (Levinthal, 1969). A stepwise folding through all possible conformations of a polypeptide into its native conformation would require way too much time for folding. It is also sound that based on the polypeptide properties, a polypeptide would possess many more opportunities to misfold occasionally rather than to fold correctly into its native state. Protein folding can follow multiple pathways depending on the amino acid sequence which forms the interaction spots of the polypeptide with itself and its surroundings. Upon folding process, proteins repeatedly fold and unfold in a rapid time scale (Bieri and Kiefhaber, 1999; Englander and Mayne, 2014). Short-ranging intramolecular interactions lead to the fast formation of secondary structures, while long-range contacts of secondary structural elements are required for the formation of tertiary structure (Fersht, 2000). In general, the folded structural elements of a protein are stabilized by versatile non-covalent interactions, including electrostatic interactions and hydrogen bonds which contribute to the stable maintenance of the protein fold**.** The energetic landscape of protein folding can be envisioned as a "funnel" which depicts the free energy level of the processes a protein undergoes upon folding, and the transition of the unfolded conformation to the native folded conformation is associated with the drop of free energy. An early and nearly initial step upon protein folding is a so-called hydrophobic collapse which drives the polypeptide to fold from the unfolded state to a compact folding intermediate state, which is guided by interactions of the hydrophobic amino acid residues striving to escape the exposure to the polar aqueous solvent (Lapidus *et al.*, 2007). A prominent intermediate conformation upon protein folding is the molten globule state in which secondary structural elements are present and form a compact

conformation but lacking the tertiary fold (Kuwajima, 1989; Judy and Kishore, 2019). The fate of that intermediate folding state is not locked, but after the molten globule state the folding funnel conically narrows, leading to conformational transitions which approach the energetic minimum. That in turn forces the proper transition of the protein into the stable and native conformational fold.

The native conformation of a protein reflects a state that has a certain degree of flexibility which is required to fulfill its biological functions and can be challenged by the surrounding conditions (Houben, Rousseau and Schymkowitz, 2022). Such conditions are determined by the solvent, temperature, or co-solutes and can promote misfolding that results in protein aggregation. Thus, when the protein fold is disturbed, the misfolding and aggregation are promoted. There is no general mechanism of aggregation, but rather a favored hypothesis postulating that folding intermediates can either follow the track towards folding or misfolding in dependency to various causes. Upon correct protein folding, the hydrophobic amino acid residues are buried into the protein core while the hydrophilic residues are exposed to the aqueous solvent. Due to this order, a tight packing of the protein occurs and pushes the polypeptide towards the correct folding track in aim to obtain its native fold. It is sound that on the one side the intrinsic properties of a protein guide its folding processes and must be determinative for its proper fold, but on the other side they could as well impact on the protein's aggregation propensity when challenged (Houben, Rousseau and Schymkowitz, 2022). In addition to that, external factors, including the environmental temperature, pH, spatial confinements, as well as molecular crowding can have a severe impact on protein folding and/or promote misfolding. The accumulation of misfolded proteins can in turn be toxic for the cell and promote further protein misfolding, aggregation and malfunctioning (Houben, Rousseau and Schymkowitz, 2022).

As mentioned beforehand, when the conformational stability of a protein is challenged, the protein can misfold and aggregate, thus protein aggregation occurs upon folding into a non-native protein fold. That non-native protein fold is of major importance and determinative for protein aggregation. In addition, current research refers to the existence of aggregation prone regions (APRs) in nearly every known protein (Houben, Rousseau and Schymkowitz, 2022). Taken together, these properties imply that every protein has an intrinsic tendency to aggregate. Upon aggregation process the misfolded proteins cluster together and form nucleation points which can serve as further aggregation seeds and form larger protein aggregates. Here, the hydrophobic segments of a protein manifest APRs that interact with each other, resulting in the formation of insoluble unstructured or structured protein aggregates which appear to be of amorphous or fibrillar arrangements. Those protein aggregates are seemingly enriched in β-sheets, that possess high stability (Houben, Rousseau and Schymkowitz, 2022). In this frame, it seems like a contradiction that the precious native fold of a protein is less stable than the unwanted protein aggregates. Notably, the occurrence of misfolded proteins and the formation of protein aggregates is associated with a vast pool of partially lethal diseases, including Alzheimer's diseases, Parkinson's diseases, and Huntington's disease (Irvine *et al.*, 2008; Jarosińska and Rüdiger, 2021). Among multiple cellular mechanisms that have evolved to support protein folding, to prevent misfolding and to avoid

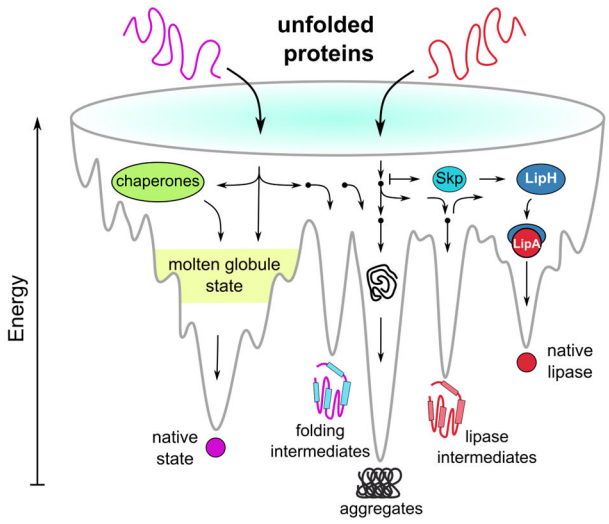

Figure 1. 8: The folding landscape of the lipase A

The folding landscape is depicted for common proteins (magenta) and in more detail for the lipase A (red). Proteins fold from the high energetic unfolded state to their native conformation which manifests a local energetic minimum. The folding landscape of proteins can therefore be depicted as a funnel, where the protein folds based on its intrinsic properties (amino acid sequence and intramolecular interactions) and environmental properties (solvent and intermolecular interactions). The molten globule state represents prominent intermediate folding states where secondary structural elements are compactly arranged, but the tertiary fold is not present. Molecular chaperones participate in the folding landscape of a protein, they can prevent misfolding and aggregation or directly assist protein folding. Multiple chaperones (green) work in a promiscuous manner, binding rather unspecific to non-proper folded client proteins. The lipase A of *Pseudomonas aeruginosa* requires a specific foldase chaperone (LipH) to fold into its native state. The unfolded protein is highly prone to aggregation, therefore the prominent periplasmic chaperone Skp serves as a potent folding mediator by preventing off-pathway routes of the lipase. The figure was inspired by (Englander and Mayne, 2014).

protein aggregation, the universal existence of molecular chaperones plays a crucial role (Hartl, Bracher and Hayer-Hartl, 2011; Horowitz *et al.*, 2018).

1.5.2 Molecular chaperones as saviors of the protein fold

The propensity of the protein to fold into its native conformation depends on multiple intrinsic and extrinsic factors, including the physicochemical properties determined by the amino acid sequence, the surrounding conditions, as well as intermolecular interactions. Seeking to fold into its native conformation, a protein acquires multiple intermediate conformations. Those intermediate states cause exposure of hydrophobic patches which can pursue intermolecular interactions and promote misfolding. Here, off-pathway folding routes endanger the proper folding of a protein. A guiding help for many proteins is offered by molecular chaperones. Those molecular chaperones are defined as "a functional class of unrelated families of protein that assist the correct non-covalent assembly of other polypeptide-containing structures *in vivo*, but are not components of these assembled structures when they are performing their normal biological functions" (Ellis, 1993). Thus, besides the intrinsic polypeptide

properties which govern protein folding pathways, molecular chaperones can function as folding mediators which largely mediate protein homeostasis (Hartl, Bracher and Hayer-Hartl, 2011; Mogk, Huber and Bukau, 2011; Horowitz *et al.*, 2018; Buchner, 2019). Typically, molecular chaperones in the cytoplasm promiscuously interact with multiple clients and thus play a key role in manifold cellular procedures associated with protein processing (Hartl, Bracher and Hayer-Hartl, 2011; Castanié-Cornet, Bruel and Genevaux, 2014). Their main tasks are the assistance of protein folding, the prevention of misfolding and aggregation, the disaggregation as well as targeting of proteins to certain destination in the cell (Hartl and Hayer-Hartl, 2002; Saibil, 2013). Several ATP-dependent and independent systems of molecular chaperones are known in bacteria, and prominent examples include the heat shock proteins (Hsp), such as the DnaJK (Hsp70 and Hsp40), GrpE (Hsp90), the GroEL/ES system, the Clp disaggregase system, and the cytoplasmic holdases (Saibil, 2013; Castanié-Cornet, Bruel and Genevaux, 2014; Bascos and Landry, 2019; Kawagoe, Ishimori and Saio, 2022; Kim *et al.*, 2022). A common feature among the different classes of chaperones is that most of them undergo promiscuous transient binding to exposed hydrophobic residues of a client protein, thus acting directly against the triggers of misfolding and aggregation while at the same time promoting intramolecular interactions that are important for the proper protein folding (Balchin, Hayer-Hartl and Hartl, 2020). Thus, molecular chaperones prevent off-pathway aggregation and facilitate protein folding by recognizing and interacting with folding intermediates (Hartl and Hayer-Hartl, 2002). To fulfill their tasks, molecular chaperones need to meet certain requirements to perform versatile functions on various clients. In this frame, molecular chaperones possess high plasticity allowing their interactive domains to adoptively interact with putative clients (Saibil, 2013; Chum *et al.*, 2019; Hiller, 2019). Further, this general plasticity allows the chaperones to be resistant against common environmental stress conditions, including heat and chemical and/or oxidative stress (Voth and Jakob, 2017). These peculiar properties are typical for cytoplasmic molecular chaperones, allowing them to be crucial players in proteostasis.

In addition to the cytoplasmic chaperones, a highly abundant periplasmic chaperone network is present in gram-negative bacteria (Stull, Betton and Bardwell, 2018). The periplasm is a well-separated space that is distinct of the cytoplasm, but mostly reflects the milieu of the extracellular space. The periplasmic chaperones need to fulfill similar tasks as their cytoplasmic counterparts, by preventing off-pathway routes and providing folding assistance to unfolded and/or partially folded proteins. At the same time, the periplasmic chaperones have to be very stable by themselves in aim to resist the relatively harsh periplasmic environment (Liu *et al.*, 2004; Stull, Betton and Bardwell, 2018). In the periplasm there is no ATP present, thus periplasmic chaperones rely on mechanisms, others than driven by ATP hydrolysis (Stull, Betton and Bardwell, 2018). The expression of periplasmic chaperones is regulated by various mechanisms, whereby many of those are induced by environmental stress which can correlate with protein unfolding (Stull, Betton and Bardwell, 2018). It is sound that some periplasmic chaperones must be stress-specific on the one side and on the other share their client substrates. While there are chaperones attributed to certain denaturing conditions, but being less specific for their clients, like HdeA

and HdeB at acidic stress, other chaperones, like Spy, act in more specific manner for client proteins and function as holdases and/or foldases helping to resist aggregation and promoting proper folding (Hong *et al.*, 2012; Koldewey *et al.*, 2016; Voth and Jakob, 2017; Kim, Wu and Lee, 2021; Mitra *et al.*, 2021). There are prominent periplasmic chaperones, such as FkpA, SurA, and Skp which contribute to biogenesis of outer membrane proteins (OMPs) and mediate the transit of secretory client proteins through the periplasm (De Geyter *et al.*, 2016; Stull, Betton and Bardwell, 2018). Upon OMP biogenesis periplasmic chaperones interact with the β-barrel assembly machinery (BAM). While Skp functions as an anti-aggregase for OMPs, SurA is also involved in BAM-mediated folding by accelerating the folding rate of OMPs (Chum *et al.*, 2019; Schiffrin *et al.*, 2022). Further interactions with other outer membrane complexes that are involved in OMP biogenesis, including the TamA of *E. coli* are also indicated (De Geyter *et al.*, 2016). Other periplasmic chaperones, including YfgM and PpiD are integrated in the outer leaflet of the inner membrane where they act as ancillary subunits of the Sec pathway and attribute to the translocation process (Götzke *et al.*, 2014; De Geyter *et al.*, 2016; Jauss *et al.*, 2019). Together the different periplasmic chaperones form an interactive network that is indispensable for gram-negative bacteria (Stull, Betton and Bardwell, 2018).

To fulfill their tasks, periplasmic chaperones require to be tolerant to stress conditions (chemicals, temperature and pH) but also need to possess high plasticity and to bind transiently to their clients (Chum *et al.*, 2019). Furthermore, the highly abundant network of periplasmic chaperones constitutes potential interaction partners for secretory clients and suggests their putative involvement in the biogenesis of virulence factors that are of major interest for biomedical research. The role of prominent periplasmic chaperones of *P. aeruginosa* upon the lipase biogenesis remains widely elusive, although recent investigations suggest that Skp is a potent folding mediator for the lipase by preventing off-pathway aggregation, supporting carry-over to the foldase LipH, and the secretion of LipA (Papadopoulos *et al.*, 2022). These observations are in line with the main role attributed to the periplasmic chaperones which is to maintain the solubility of the client proteins. Thus, the client proteins will not aggregate and cannot become toxic for the cell. Additional investigations suggested that the periplasmic chaperones SurA and Skp are contributing to the virulence of gram-negative bacteria (Figaj *et al.*, 2022). Further investigations indicate that the loss of SurA in *P. aeruginosa* causes a reduction of virulence and antibiotic resistance (Klein *et al.*, 2019). By being involved in manifold interactions with secretory clients, it is sound that periplasmic chaperones could impact on the path of secretory proteins, and influence the protein folding, maturation, and secretion.

1.5.3 Steric foldases – molecular chaperones acting as folding catalysts

The steric foldases are intermolecular chaperones which serve as “folding catalysts”, as they provide the missing steric information to the client protein to fold into the native conformation (Hobson *et al.*, 1993; Rosenau, Tommassen and Jaeger, 2004). In comparison to the unspecific molecular chaperones in the bacterial cytoplasm and periplasm, the intermolecular steric chaperones assist in folding of a protein in

a steric fashion rather than preventing its off-pathway routes (Rosenau, Tommassen and Jaeger, 2004). Prominent examples of intermolecular steric chaperones include the soluble periplasmic chaperone FimC that assists folding of FimH adhesin in *Escherichia coli*, and the membrane-anchored chaperone CpaB that is required by its cognate secretory protease CpaA from *Acinetobacter baumannii* (Vetsch *et al.*, 2004; Nishiyama *et al.*, 2005; Nagradova, 2007; Pauwels *et al.*, 2007; Urusova *et al.*, 2019). In the known structure, CpaA surrounds its chaperone CpaB (Urusova *et al.*, 2019), so the client clamps the relatively small chaperone domain suggesting a peculiar mode of action of the chaperone, therefore preventing the autoproteolytic activation of the protease beyond stabilizing it prior secretion (Urusova *et al.*, 2019). Furthermore, intramolecular steric chaperones are also known and should be mentioned, such as the prodomains of bacterial proteases which support the folding and protect autodigestion of the protein, e.g. the α-lytic protease from *Lysobacter* enzymogenes, the subtilisins from *Bacillus subtilis*, and the elastase from *Pseudomonas aeruginosa* (Ellis, 1998; Sohl, Jaswal and Agard, 1998; Pauwels *et al.*, 2007).

The lipase-specific foldases (Lifs) are a peculiar class of steric chaperones acting as membrane-bound folding modulators that are essential for the folding pathways of their cognate lipases (Frenken *et al.*, 1993; Rosenau, Tommassen and Jaeger, 2004). Several lipase:foldase systems are known in bacteria, including the genera *Pseudomonas*, *Burkholderia*, *Acinetobacter*, and *Vibrio* (Rosenau, Tommassen and Jaeger, 2004). The Lifs are classified into four different families based on sequence homology, whereby family I comprises the *Pseudomonas* Lifs, family II comprises mostly the *Burkholderia* Lifs, family III comprises the *Acinetobacter* Lifs and family IV comprises mostly the *Vibrio* Lifs (Rosenau, Tommassen and Jaeger, 2004). All Lifs predictively share a similar overall architecture which is mainly α-helical, whereby two globular mini domains (MDs) on both termini are connected by an extended helical domain (EHD) (Rosenau, Tommassen and Jaeger, 2004; Pauwels *et al.*, 2006). Early cross-linking studies suggested a 1:1 stoichiometry of the foldase:lipase complex which was also validated by structural investigations (Shibata, Kato and Oda, 1998a; Pauwels *et al.*, 2006). The structural data of *Burkholderia glumae* and the recently acquired homology model of *P. aeruginosa* PAO1 foldase:lipase complex (Figure, 1.9) suggests a α-helical scaffold of the foldase that wraps around the lipase reminding of headphones clamping around the head (Pauwels *et al.*, 2006), that differs greatly from CpaA:CpaB system described above. A highly conserved sequence motif (Rx_1x_2FDY (F/C)L (S/T)A) is present on MD1 within the Lifs of families I and II and is considered important for its folding activity as it has been shown in previous mutagenesis studies (Shibata, Kato and Oda, 1998b, 1998c; Rosenau, Tommassen and Jaeger, 2004). Moreover, structural dynamics within MD1 of *P. aeruginosa* Lif mediate the activation of the lipase, although the mechanism of folding catalysis is likely depended on more complex multi-domain interactions (Viegas *et al.*, 2020). Lifs are capable of decreasing the energetic folding barriers of their client lipases by transferring steric information to the lipase which is required for folding into the native and enzymatically active conformation (Rosenau, Tommassen and Jaeger, 2004; Pauwels *et al.*, 2007). It is suggested that upon foldase:lipase interactions, not only the lipase undergoes

conformational changes pushing it towards its native fold, but also the foldase experiences conformational rearrangements which enable a tight compaction of the complex leading to overcome the energetic folding barrier (Pauwels *et al.*, 2006). Notably, the high energetic barrier which needs to be trespassed to allow folding of the lipase into its native conformation, manifests at the same time a "kinetic trap" for the native conformation in terms of unfolding which would require to overcome the same energetic barrier to unfold (Rosenau, Tommassen and Jaeger, 2004; Pauwels *et al.*, 2007).

A "multi-turnover catalysis" of the foldase-mediated lipase folding was proposed, since the foldase is expressed to way lower levels in comparison to its cognate lipase (El Khattabi *et al.*, 1999; Rosenau, Tommassen and Jaeger, 2004). Furthermore, Lifs are anchored by an N-terminal membrane domain to the inner membrane, while the chaperone domain faces the periplasm. The suggested conservation of Lif architecture might be indicative for a conserved mode of action, although mutagenesis studies and cross-species folding and activation investigations indicated a high specificity of the Lif by selectively activating solely their cognate lipase (El Khattabi *et al.*, 1999). Molecular studies of "hybrid" Lifs containing parts of closely related bacterial species indicated that the C-terminus of the foldase is determinative for its specificity towards the lipase (El Khattabi *et al.*, 1999). Further investigations indicated that the N-terminal membrane domain (TMD) is not essential for the interactions with the lipase but rather prevents the secretion of the Lif itself, since a truncated version lacking that region facilitated the active lipase (Shibata, Kato and Oda, 1998b; El Khattabi *et al.*, 1999, 2000). An additional, but rather unstructured proline- and alanine-rich domain located close to the N-terminal TMD termed the variable domain (VD) is widely present in Lifs and is supposed to space the chaperoning domain from the membrane interface (Rosenau, Tommassen and Jaeger, 2004).

In *P. aeruginosa* the lipase:foldase system is formed by two proteins, the lipase A (LipA) and the foldase LipH which are encoded in a bicistronic operon (Rosenau and Jaeger, 2000), and their expression is regulated via quorum sensing (Rosenau and Jaeger, 2000). Further studies identified a second extracellular lipase in *P. aeruginosa*, termed LipC, that also requires the foldase LipH for folding into the native conformation (Martinez, Ostrovsky and Nunn, 1999). Recent molecular dynamic simulations suggest that the foldase structurally stabilizes the lipase, facilitating the opening of the enzyme and thus leading to the active conformation of the lipase (Verma *et al.*, 2020). Taken together, the previous observations indicate that the Lifs are essential for the proper folding of enzymatically active lipase.

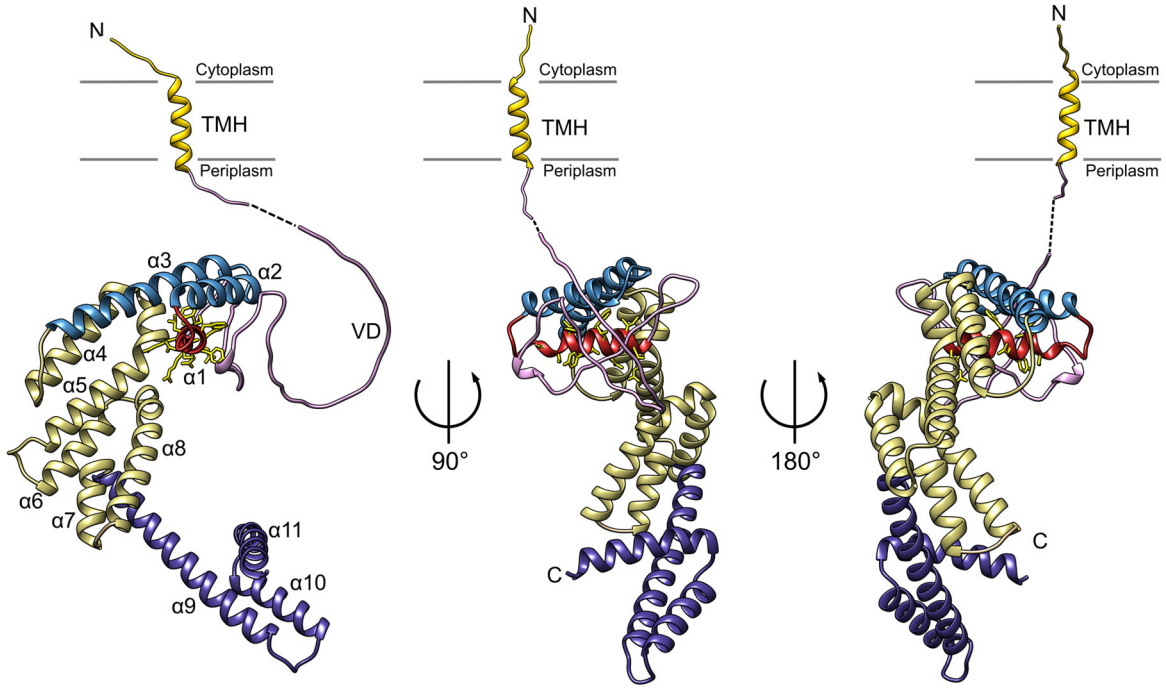

Figure 1. 9: The foldase LipH of *Pseudomonas aeruginosa* PAO1

The AlphaFold model of the foldase LipH is shown. The various colors indicate the different domains of LipH. The N-terminal trans membrane helix (TMH, gold) was manually modeled into that orientation, and the very flexible variable domain (VD, plum) is partially truncated (dashed line, black). The membrane is indicated (solid line, grey) and the cytoplasmic and periplasmic sites are indicated. The mini domain 1 (light blue) is indicated and the α-helix containing the foldase consensus motif (Rx_1x_2FDY (F/C)L (S/T)A) is colored separately (red) and the side chains of the corresponding amino acid residues are shown (yellow). The extended helical domain (khaki) connects the MD1 to the C-terminal mini domain 2 (MD2, dark blue). The protein is mostly α-helical and the helices are indicated in the figure (α1 – 10).

2 Aims and objectives

Pseudomonas aeruginosa is an opportunistic human pathogen with high adaptability and intrinsic as well as gained antibiotic resistance which comprises a huge arsenal of pathogenicity mediators, such as manifold virulence factors and diverse systems for protein secretion (Bleves *et al.*, 2010; Qin *et al.*, 2022). Due to these traits, *P. aeruginosa* is difficult to treat and it represents a frequent cause of life-threatening infections in medically relevant environments (Diggle and Whiteley, 2020; Qin *et al.*, 2022). The rising demand for novel therapeutic treatments against bacterial pathogens also enhances the requirement to elucidate the processes which convey the pathogenicity of *P. aeruginosa* (Qin *et al.*, 2022). The major secretory lipase of *P.* aeruginosa is LipA, and it is classified as a virulence factor that is involved in various processes upon infection (Jaeger *et al.*, 1994; Stehr *et al.*, 2003; Liao *et al.*, 2022). The lipase A is translocated by the general secretory (Sec) system across the inner membrane to the periplasm where it gets folded by its cognate foldase LipH, and is further secreted across the outer membrane through the type II secretion system (T2SS) to the extracellular space in its active form (Rosenau and Jaeger, 2000; Bleves *et al.*, 2010; Filloux, 2022). The present thesis aims to elucidate the processes which guide the biogenesis of the virulence factor lipase A of *P. aeruginosa.* One of the key steps upon lipase biogenesis is its translocation across the inner membrane through the Sec system. The Sec system of *P. aeruginosa* constitutes primarily of the membrane-embedded translocon SecYEG as well as the cytoplasmic motor ATPase SecA and the holdase chaperone SecB (Crane and Randall, 2017). To study the Sec-dependent translocation of proLipA, first (1) it was necessary to establish the minimal Sec system of *P. aeruginosa* PAO1 *in vitro* and to characterize the individual Sec components. Once the lipase is translocated to the periplasm, the lipase-specific foldase LipH mediates the folding of the lipase to its mature and active form (Rosenau, Tommassen and Jaeger, 2004). Although it had been already shown that the soluble domain of LipH facilitates folding of the lipase, minor is known about the role of the full-length foldase and the contributions of the membrane to the lipase maturation and secretion (Frenken *et al.*, 1993; Hobson *et al.*, 1993; Rosenau, Tommassen and Jaeger, 2004). Thus, secondly (2) in aim to elucidate the putative role of LipH upon translocation of proLipA and folding of the mature LipA the interactions of both proteins on membrane interface were investigated. It remains to be elucidated if further interactions of the foldase with the translocon or further periplasmic proteins occur during lipase biogenesis. A highly abundant periplasmic chaperone network represents additional putative interaction partners for LipA, that could be involved in lipase maturation and secretion as well (Stull, Betton and Bardwell, 2018). Thus, thirdly (3) in aim to examine whether additional periplasmic proteins are involved in lipase maturation and secretion, prominent periplasmic chaperones were selected and investigated. This group of proteins includes the ubiquitous periplasmic chaperones Skp, FkpA, SurA, YfgM and PpiD. The conducted research attributes to an enriched understanding of the processes ongoing upon transport, maturation, and secretion of the virulence factor lipase A of *P. aeruginosa*.

3 The Sec system of *P. aeruginosa* and the lipase transport

3.1 Introduction to the Sec system of *P. aeruginosa* and the lipase A biogenesis

The general secretory pathway (Sec) constitutes the ubiquitous major machinery for protein export within all domains of life (Bolhuis, 2004; Denks *et al.*, 2014; Dudek *et al.*, 2015; Tsirigotaki *et al.*, 2017). The bacterial Sec system has been a matter of investigations for decades, revealing its outstanding role for the insertion into and export of proteins across the membrane (Pugsley and Schwartz, 1985; Pugsley, 1993; Dalbey and Kuhn, 2012; Beckwith, 2013; Crane and Randall, 2017; Tsirigotaki *et al.*, 2017; Oswald *et al.*, 2021). The export of proteins is essential for bacteria as it is involved in adaptation to challenging environmental conditions, acquisition of nutrients, and it mediates the pathogenicity by secreted virulence factors (Stathopoulos *et al.*, 2000; Lee and Schneewind, 2001; Tsirigotaki *et al.*, 2017). The core unit of the Sec system is the translocon SecYEG forming the protein conductive channel, thus enabling protein export through the cytoplasmic bacterial membrane (Lycklama a Nijeholt and Driessen, 2012). The transport process of secretory proteins through the Sec system is enabled by the ATPase action of SecA which is the motor protein of the system that provides the required power for the translocation process (Kusters and Driessen, 2011). SecA complexes with the translocon SecYEG and recognizes SecB and the preprotein (Tsirigotaki *et al.*, 2017). Upon translocation process, complexing of the Sec components and ATP hydrolysis by SecA cause conformational rearrangements of the Sec system which lead to opening of the translocon and enable the passage of the preprotein for export (Lycklama a Nijeholt and Driessen, 2012; Crane and Randall, 2017; Oswald *et al.*, 2021). In turn, the preprotein itself influences the translocation process as it possess inherent interactions between its signal peptide and mature domain which serve as targeting and secretion signals (Chatzi *et al.*, 2017; Sardis *et al.*, 2017; Tsirigotaki *et al.*, 2017). Once the secretory protein is transported across the cytoplasmic membrane, the signal peptide is cleaved, and the protein is liberated for maturation and secretion.

The export of various virulence factors through the Sec system contributes to the pathogenicity of gram-negative bacterial pathogens, such as *Pseudomonas aeruginosa* (Stathopoulos *et al.*, 2000). The enhanced pathogenicity of *P. aeruginosa* is attributed to an enormous adaptational potential against commonly utilized therapeutic agents and the secretion of versatile pathogenicity mediators, such as virulence factors, that allow it to evade the host immune response and promote the infection of the host tissues (Moradali, Ghods and Rehm, 2017; Qin *et al.*, 2022). Upon infection cycle, *P. aeruginosa* secretes multiple virulence factors, including exotoxins, proteases, and lipases which can facilitate the invasion and colonization of the host by damaging the inhabited tissues or stimulating the inflammation processes (Stehr *et al.*, 2003; Bleves *et al.*, 2010; Filloux, 2011; Strateva and Mitov, 2011; Rocha *et al.*, 2019; Jurado-Martín, Sainz-Mejías and McClean, 2021; Liao *et al.*, 2022; Qin *et al.*, 2022). Among those virulence factors, the lipase A (LipA) is a prominent secretory protein of *P. aeruginosa* which is of biomedical and biotechnological interest (Jaeger and Reetz, 1998; Nardini *et al.*, 2000). As an ester-

hydrolase (EC 3.1.1.3) it breaks down triacylglycerols into their constituent acyl chains and glycerol and can hydrolyze or synthesize a wide range of further substrates (Jaeger and Reetz, 1998). Although, the concrete role of LipA upon *P. aeruginosa* infection remains still widely elusive, it had been shown that the lipase is involved in manifold processes that can contribute to the infection cycle (Jaeger *et al.*, 1994; Stehr *et al.*, 2003). Once secreted, LipA accumulates in the biofilm matrix, where it interacts with the exopolysaccharide alginate (Tielen *et al.*, 2013). The biofilm mode of *P. aeruginosa* reflects a persistent life style which mediates the infection process and contributes to the pathogenicity of these bacteria (Tuon *et al.*, 2022). Furthermore, LipA acts together with the phospholipase C upon *P. aeruginosa* infections, causing inhibitory effects on the host immune response and stimulating the release of inflammatory mediators that in turn can cause tissue damages to the host lung (Jaeger, Kharazmi and Høiby, 1991; Jaeger *et al.*, 1994; König, Jaeger and König, 1994). LipA can have regulatory roles on the expression of further virulence factors, including pyoverdine (Potvin *et al.*, 2003; Funken *et al.*, 2011; Durán *et al.*, 2022). Taken together, the lipase A contributes to the infection and pathogenicity of *P. aeruginosa*.

LipA needs to be transported to the periplasm, where it receives folding assistance by the lipase-specific foldase chaperone LipH before it completely maturates prior to its secretion to the extracellular space. The lipase precursor (proLipA) is synthesized and released to the cytoplasm, containing an N-terminal signal peptide that targets it to the Sec-dependent translocation pathway. In aim to elucidate the Sec-dependent transport process of the lipase A of *P. aeruginosa* PAO1, the establishment of the Sec system of *Pseudomonas* as well as transport substrates are needed. In the presented investigations, the functional expression, reconstitution, and characterization of the major Sec components, as well as the expression and purification of transport substrates were achieved, and the Sec-dependent transport was reconstituted *in vitro*. To characterize the functionality of the individual Sec components, protein:protein interactions were investigated by biochemical and biophysical approaches, indicating binding of SecA:SecYEG and holdase action of SecB. The Sec system of *Escherichia coli* served initially as a well-studied reference system. The precursor of the outer membrane protein A (proOmpA) from *E. coli*, that is commonly used as a model substrate for transport studies, served as a reference for an efficiently translocated Sec-substrate. Although the established Sec system of *P. aeruginosa* manifests the same degree of functionality in comparison to the well-studied Sec system of *E. coli* in the applied *in vitro* approach, the transport efficiency of the proLipA remained low. Extensive efforts were made to improve the lipase transport but did not result in increased transport efficiency. The transport of proLipA and additional transport substrates originating from *P. aeruginosa* PAO1 remained low and far off to be in a comparable range with the model substrate proOmpA from *E. coli*. The present investigations resulted in the successful *in vitro* reconstitution of the Sec system of *P. aeruginosa* PAO1 and allowed to track protein translocation through that system as well as protein:protein interactions.

3.2 Experimental procedures

3.2.1 Molecular cloning

For the establishment of suitable expression vectors of the Sec system of *P. aeruginosa* PAO1, multiple constructs were generated and used. The following section focuses on the main working constructs used for heterologous expression of *Pseudomonas* Sec system in *E. coli*. A tabular overview is listed in the appendix section.

The genes of *P. aeruginosa* PAO1 strain were acquired from the *Pseudomonas* Genome database (www.pseudomonas.com) (Winsor *et al.*, 2016). Those included PA4243 (*secY*), PA4276 (*secE*), PA4747 (*secG*), PA4403 (*secA*), PA5128 (*secB*), PA1800 (*tig*), PA3221 (*csaA*), PA2862 (*lipA*), PA2863 (*lipH*), PA4813 (*lipC*), PA4067 (*oprG*), PA1954 (*fapC*), PA3647 (*skp/OmpH/hlpA*). The genomic DNA from *P. aeruginosa* PAO1 served as a template for the amplification of the genes of interest via PCR using the KOD Xtreme polymerase (Novagen/Merck) or the Phusion High-Fidelity DNA Polymerase (Ultra DNA Polymerase, Jena Bioscience) as well as cloning primers containing the restriction sites for classical cloning, overlaps for Gibson assembly or constructed to suit for site-directed mutagenesis (Eurofins Genomics). After PCR, the amplified products were analyzed by agarose gel electrophoresis and isolated from the Gel using the NucleoSpin Gel and PCR Clean-up kit (Macherey-Nagel). The DNA concentrations were determined spectrophotometrically by measuring the absorbance at 260 nm via NanoDrop (Thermo Fisher Scientific). Further, standard molecular cloning approaches were applied to insert the genes of interest into the target vectors by either classical restriction nuclease-based cloning or by utilization of the Gibson assembly (New England Biolabs). The generated constructs were further used as templates for PCR serving for site-directed mutagenesis. The site-directed mutagenesis procedures included the enzymatic digest of methylated DNA by DpnI treatment (New England Biolabs) to avoid false positive cloning results due to the persistence of the template DNA. Additionally, phosphorylation of the acquired PCR products by polynucleotide kinase (PNK, New England Biolabs) was conducted to allow for subsequent blunt end ligation. Treatment with PNK and DpnI followed the supplier protocols (New England Biolabs). After ligation, the constructs were used to transform *E. coli* DH5α (Thermo Fisher Scientific), a recipient strain for cloning and plasmid multiplication. For the isolation of plasmid DNA, the NucleoSpin Plasmid kit (Macherey-Nagel) was used. The isolated plasmids were further analyzed by Sanger sequencing (Eurofins Genomics).

For constructing a suitable expression vector of the Sec translocon of *P. aeruginosa*, a pTrc99a-based plasmid (Amann, Ochs and Abel, 1988) containing the Sec translocon genes of *E. coli* (pEK20, generous gift from Arnold Driessen) served as a template. Following a consecutive replacement of the corresponding *E. coli* genes with those of *P. aeruginosa* using Gibson assembly resulted in the plasmid harboring the genes encoding for the target translocon. This initial construct (pAT3) encodes for an N-terminal deca-histidine tag followed by a flexible linker and an HRV-3C protease cleavage motif prior the SecY gene. In course of further optimizations for functionality, the existing vector (pAT3) was

shortened in the N-terminal region. The resulting construct contains a shorter hexa-histidine tag which is directly connected to an enterokinase cleavage site (pAT90). In aim to increase the transport of substrates through the Sec translocon, a double mutant of $SecY_{F281Y, I403N}$ (pAT113) was created by site-directed mutagenesis of the recent construct. It is known for the SecY homolog of *E. coli*, that this double mutant, termed *prlA4*, has a decreased specificity for client proteins, allowing for translocation of substrates with defective signal peptide (Van Der Wolk *et al.*, 1998; de Keyzer *et al.*, 2002). Furthermore, a single-cysteine variant of SecYEG was created by site-directed mutagenesis by Alexej Kedrov. Therefore, a construct encoding for single-cysteine on $SecE_{S118C}$ was used and the N-terminal tag was shortened by site-directed mutagenesis. The resulting construct encodes for His_6-EK-$SecYE_{S118C}G$ (pAT109) which was utilized for functional studies.

The amplified *secA* gene of *P. aeruginosa* PAO1 was initially inserted into pET21a vector using the *NdeI/HindIII* restriction sites. The resulting construct features the expression of SecA with a flexible C-terminal hexa-histidine tag after a linker region. This construct was further modified by site-directed mutagenesis to introduce an HRV-3C protease cleavage motif prior the histidine tag and resulted to the final expression plasmid (pAT76) utilized for the present studies. Additionally, a similar pET21a-based construct encoding for SecA of *E. coli* was used for the expression and served as a reference in early trials (Kamel *et al.*, 2022).

The amplified SecB gene of *P. aeruginosa* PAO1 was cloned into a pRSFDuet-1 vector (Novagen/Merck) using *NotI/NheI* restriction sites. The resulting construct (pAT7) features the expression of SecB with an N-terminal octa-histidine tag followed by a flexible linker and an HRV-3C protease cleavage motif.

The genes encoding for trigger factor (TF) and CsaA of *P. aeruginosa* PAO1 were cloned into suitable expression vectors. The gene encoding for TF PA1800 (*tig*) was inserted into pET21a using *NdeI/XhoI* restriction sites and featuring the expression of a C-terminal hexa-histidine tag (pAT62). For insertion of CsaA-encoding gene PA3221 (*csaA*) into a suitable expression vector, a pBAD-based expression vector was used with *KpnI/HindIII* as restriction sites (Guzman *et al.*, 1995). The resulting construct (pAT102) allows for the expression of the chaperone CsaA with an N-terminal octa-histidine tag followed by a flexible linker and an HRV-3C protease cleavage motif.

As a reference substrate, the precursor of the outer membrane protein A (proOmpA) was used in the present study. proOmpA represents a substrate that is commonly used for *in vitro* transport studies through Sec system. A pTrc99a-based plasmid encoding for a single-cysteine mutant ($proOmpA_{C302S}$) was used for its expression (van der Does *et al.*, 2000). In aim to create suitable expression vectors for Sec transport substrates which originate from *P. aeruginosa*, multiple constructs were generated. For the creation of a suitable expression vector of proLipA, the codon optimized sequence of the gene PA2862 (*lipA*) (Integrated DNA Technologies) encoding for the precursor form of the lipase A (proLipA), was inserted into pET21a by using the restriction sites *BamHI/HindIII* (pAT35). Later, the

N-terminal T7 tag was removed by site-directed mutagenesis (pAT80, proLipA-His_6) as well as the C-terminal hexa-histidine tag (pAT83, proLipA). Additionally, in aim to enhance the transport efficiency, constructs encoding for a less aggregating mutant of $proLipA_{F144E}$ (Papadopoulos *et al.*, 2022) were created, either with C-terminal hexa-histidine tag (pAT84, $proLipA_{F144E}$-His_6) or without that (pAT85, $proLipA_{F144E}$). Constructs encoding for single-cysteine (C183S) variants of proLipA (pAT98) and $proLipA_{F144E}$ (pAT99) were created by site-directed mutagenesis. In aim to increase the potential for periplasmic localization of the lipase, the gene encoding for $LipA_{F144E}$ were inserted into pET22b (Novagen/Merck) by using *NcoI/BamHI* restriction sites (pAT117). The vector pET22b was chosen, because it harbors the signal peptide of pectate lyase B (SP_{PelB}) of *Erwinia carotovora* which is commonly used for efficient periplasmic secretion of fused proteins.

Genes encoding for further substrates for translocation were cloned. Those included the precursor forms of PA4813 (*lipC*) for the second extracellular lipase C of *P. aeruginosa* PAO1, PA4067 (*oprG*) for the outer membrane protein G (OprG), PA1777 (*oprF*) for the outer membrane protein F (OprF) and PA1954 (*fapC*) for the functional amyloid-forming protein FapC. During the experimental procedures it turned out that the subset of the chosen *Pseudomonas* preproteins did not express sufficiently. To solve that issue the DNA sequences in the gene region encoding for the signal peptides (SP) were codon optimized by site-directed mutagenesis. Therefore, the SP positions were identified via SignalP-5.0 algorithm (Petersen *et al.*, 2011), the corresponding gene sequence was analyzed and codon-optimized by utilization of codon optimization tool (Integrated DNA Technologies, IDT). Primers containing the codon-optimized gene region were designed and used for extensional PCR.

To assemble a plasmid of proLipC expression, the gene was inserted into pET21a via *BamHI/HindIII* sites following the same approach as for proLipA cloning. The final pET21a-based construct lacks the N-terminal T7 tag and encodes for proLipC (pAT86). A construct encoding for a single-cysteine variant (pAT100, C183S) of proLipC was created by site-directed mutagenesis. For proOprG, the gene was initially cloned into the same pTrc-based expression vector as proOmpA. Unfortunately, that construct did not express. In a further step, SP-encoding gene region was codon-optimized by site-directed mutagenesis. Still, the expression did not lead to a sufficient result, thus the target gene of proOprG with codon optimized SP (CO-SP) was subcloned into pET21a-based vector by Gibson Assembly. The final construct lacks the N-terminal T7 tag and encodes for proOprG with a C-terminal cysteine residue (F232C) allowing for fluorescent labeling (pAT88). For proOprF, the gene of interest was inserted into pET21a-based vector lacking the N-terminal T7 tag via *EcoRI/HindIII* restriction sites. The resulting construct encodes for proOprF (pAT133). For proFapC, a pET28b-based construct was initially created by using *NcoI/HindIII* restriction sites to insert the gene of interest (pAT119), later the SP region was partially codon-optimized by site-directed mutagenesis to increase expression levels. Both constructs encode for proFapC with an additional glycine (G2) after the start methionine (pAT121). A further mutation occurred during cloning procedures being A253T but was not considered critical for the purpose of the project which was primary the transport through Sec system.

3.2.2 Expression and purification procedures

The heterologous expression of Sec components of *P. aeruginosa* PAO1 was conducted in *E. coli* . The success of the expressions was determined by sodium dodecyl sulfate poly acrylamide gel electrophoresis (SDS-PAGE) stained with colloidal chemical Coomassie solution (Quick Coomassie stain, Serva). The samples were mixed with 5 x sample loading buffer (0.25 M Tris/HCl pH 6.8, 0.5 M DTT, 10 % SDS, 60 % glycerol, 0.02 % (w/v) bromophenol blue). The protein concentration was determined spectrophotometrically by measuring the absorbance (A) at 280 nm and further calculations based on the molar extinction coefficient given by ProtParam tool (Gasteiger *et al.*, 2005).

3.2.2.1 Expression and purification of *P. aeruginosa* PAO1 SecYEG translocon

The constructs encoding for SecYEG variants of *P. aeruginosa* PAO1 were heterologously expressed in *E. coli* C41(DE3). The protocol is oriented on recent research (Kamel *et al.*, 2022). Overnight cultures were grown at 37°C upon shaking at 180 rpm and used for inoculation of pre-warmed LB medium (Luria-Bertani medium or lysogeny broth, yeast extract 5 g/l, tryptone 10 g/l, NaCl 10 g/l). Bacterial cells were kept for growing at 37°C upon shaking at 180 rpm while the OD of the culture was measured in several time points. At OD_{600} of 0.6 overexpression was induced upon addition of 0.5 mM isopropyl-β-D-thiogalactopyranoside (IPTG; Merck/Sigma-Aldrich) and carried out for 2 h at the same conditions. The cells were harvested by centrifugation at 6000 *g* for 15 min at 4°C (rotor SLC-6000, Sorvall/Thermo Fisher) and subsequently resuspended in 20 mM 4-(2-hydroxyethyl)-1-piperazineethanesulfonic acid (Hepes)/KOH pH 7.4, 50 mM KOAc, 5 mM $Mg(OAc)_2$, 1 mM DTT, cOmplete protease inhibitor (Roche), 5 % glycerol. Cells were lysed by mechanical disruption (M-110P cell disruptor Microfluidics Inc.). The cell debris was removed by centrifugation at 10000 *g* for 10 min at 4°C (rotor SS34, Sorvall/Thermo Fisher). To pellet the crude membranes, ultracentrifugation at 205000 *g* for 1 h at 4°C (rotor 45 Ti, Beckman Coulter) was conducted. The membranes were resuspended in 20 mM Hepes/KOH pH 7.4, 50 mM KOAc, 5 mM $Mg(OAc)_2$, 1 mM DTT, cOmplete protease inhibitor, 5 % glycerol. Isolated membranes were flash-frozen with liquid nitrogen and stored at -80°C until further utilization. For solubilization the membranes were put to 50 mM Hepes/KOH pH 7.4, 500 mM KCl, 0.2 mM tris-(2-carboxymehtyl)-phosphine (TCEP; Thermo Fisher), cOmplete protease inhibitor, 5 % glycerol, n-dodecyl-β-D-maltopyranoside (DDM) and incubated for 1 h at 6°C on a rolling table. The samples were applied for centrifugation at 20000 *g* for 10 min at 4°C (Hermle Z216 M) to remove the non-soluble material. After solubilization, the translocons were purified by immobilized metal ion affinity chromatography (IMAC). His-tagged translocons were immobilized on nickel-nitrilotriacetic acid agarose resin (Ni^{2+}-NTA resin; Qiagen) equilibrated with wash buffer (50 mM Hepes/KOH pH 7.4, 500 mM KCl, 0.2 mM TCEP, 20 mM imidazole, 5 % glycerol, 0.1 % (w/v) DDM). The translocons were incubated for binding on the Ni^{2+}-NTA resin for 1 h at 6°C on a rolling table. Afterwards, the SecYEG-loaded resin was washed extensively with the wash buffer to remove non-specifically and weakly-bound impurities, and the protein was eluted with elution buffer (50 mM Hepes/KOH pH 7.4,

150 mM KCl, 0.2 mM TCEP, 300 mM imidazole, 5 % glycerol, 0.1 % (w/v) DDM) in several fractions. Alternatively, the translocons were purified in different buffering systems, including tris (hydroxymethyl)aminoethane (Tris) as buffering agent. The expression and purification procedures remain very similar, utilizing the following buffers, cell resuspension buffer (20 mM Tris/HCl pH 7.5, 150 mM KOAc, 5 mM $Mg(OAc)_2$, 5 % glycerol, 0.2 mM phenylmethylsulfonyl fluoride (PMSF: Roche), solubilization buffer (20 mM Tris/HCl pH 7.5, 150 mM KOAc, 0.2 mM TCEP, 5 % glycerol, 1 % (w/v) DDM), wash buffer (20 mM Tris/HCl pH 7.5, 500 mM KOAc, 0.2 mM TCEP, 10 mM imidazole, 0.1 % (w/v) DDM) and elution buffer (20 mM Tris/HCl pH 7.5, 150 mM KOAc, 0.2 mM TCEP, 300 mM imidazole, 5 % glycerol, 0.1 % (w/v) DDM). The different buffer composition did not affect the purity of the sample. To remove the imidazole, the eluted protein fractions were applied to PD-10 desalting column (Cytiva) and transferred to desired buffer composition suitable for downstream analysis. Optionally, the protein subjected to size exclusion chromatography (SEC) using a Superdex 200 Increase 10/300 GL column (Cytiva) in desired buffer compositions (e.g., 20 mM Tris/HCl pH 7.5, 150 mM KOAc, 0.2 mM TCEP, 5 % glycerol, 0.05 % (w/v) DDM) unless otherwise stated. The success of the purification was further evaluated by SDS-PAGE. Samples were flash-frozen in liquid nitrogen and stored at -80°C until further usage.

3.2.2.2 Polymer-based extraction and fluorescent labeling of SecYEG

In aim to isolate SecYEG within near-native nanodiscs (NDs), 200 µl membranes containing overexpressed single-cysteine variant $SecYE_{S118C}G$ (pAT109), were applied for solubilization with 2.5 % (w/v) diisobutylene-maleic acid (DIBMA) polymers for 1 h at 37°C in 50 mM Tris/HCl pH 8.0, 100 mM NaCl, 10 % glycerol, 0.2 mM TCEP, cOmplete protease inhibitor in a total volume of 2 ml. Meanwhile, 400 µl of Ni^{2+}-NTA agarose resin (Qiagen) was washed extensively with MQ and equilibrated with 2 ml of 50 mM Tris/HCl pH 8.0, 100 mM NaCl, 10 % glycerol, 0.2 mM TCEP, 5 mM imidazole, cOmplete protease inhibitor cocktail. After solubilization, the samples were centrifuged at 100000 *g* for 30 min at 4°C to remove non-solubilized material. Subsequently, each sample was applied for binding to Ni^{2+}-NTA resin for 17 h (overnight) at 4°C, rotating on a vertical rotational mixer at moderate rpm to avoid the generation of foam. The next day, the flow-through was collected and the loaded Ni^{2+}-NTA beads were washed with 5 ml of 50 mM Tris/HCl pH 8.0, 100 mM NaCl, 10 % glycerol, 0.2 mM TCEP, 10 mM imidazole, cOmplete protease inhibitor cocktail. For fluorescent labeling, the sample was incubated for 2 h at 4°C rolling with 1 ml 50 mM Tris/HCl pH 8.0, 100 mM NaCl, 10 % glycerol, 5 mM imidazole, 40 µM Alexa Fluor 488-maleimide (Thermo Fisher). After incubation, the sample was slowly washed with 2 ml of 50 mM Tris/HCl pH 8.0, 100 mM NaCl, 10 % glycerol, 5 mM imidazole by gravity flow. The elution was conducted in three fractions of 400 µl with 50 mM Tris/HCl pH 8.0, 100 mM NaCl, 10 % glycerol, 300 mM imidazole. The sample was analyzed by SDS-PAGE to control the purification efficiency and labeling specificity. Prior staining with colloidal chemical Coomassie solution (Quick Coomassie stain, Serva), the gel was fluorescently imaged. To

remove the imidazole and for measuring, the sample was diluted 10 – 20 x times with 50 mM Tris/HCl pH 8.0, 100 mM NaCl, 10 % glycerol and applied to 30 kDa cut-off concentrating devices (Amicon; Merck/Millipore). After several dilution and re-concentration cycles, the final imidazole concentration in the sample reached approximately 1.8 µM which allowed to use the sample for further biochemical and biophysical investigations. As the translocon represents the major compound in the polymer-based near-native ND, the concentration of translocons was estimated spectrophotometrically.

3.2.2.3 Expression and purification of soluble Sec components

Overexpression of *P. aeruginosa* SecA and SecB was carried out heterologously in *E. coli* BL21(DE3) using pAT76 and pAT7 constructs. In brief, overnight cultures were grown at 37°C upon shaking at 180 rpm and used to inoculate pre-warmed LB medium. As soon as the cultures reached OD_{600} of 0.6, the overexpression was induced upon addition of 0.5 mM IPTG and carried out for 2 h at 37°C shaking at 180 rpm. Cells were harvested by centrifugation at 5000 *g* for 15 min at 4°C (rotor SLC-6000, Sorvall/Thermo Fisher) and subsequently resuspended in 20 mM Tris/HCl pH 7.5, 50 mM KOAc, 10 mM $Mg(OAc)_2$, 1 mM 1,4-dithiothreitol (DTT; Merck/Sigma-Aldrich), 20 % glycerol, cOmplete protease inhibitor cocktail for SecA and 20 mM Tris/HCl pH 7.5, 50 mM KOAc, 5 mM $Mg(OAc)_2$, 1 mM DTT, 5 % glycerol, 0.2 mM PMSF for SecB. Cells were lysed by mechanical cell disruption (M-110P cell disruptor Microfluidics Inc.) and the debris as well as the crude membranes were removed by ultracentrifugation at 205000 *g* for 45 min at 4°C (rotor 45 Ti, Beckman Coulter). For the subsequent purification of SecA by IMAC, a 1 ml HisTrap FF column (Cytiva) was utilized based on the supplier protocol. The column was rinsed with 5 column volume (CV) of deionized water (MQ) and further equilibrated with 5 CV of buffer (20 mM Tris/HCl pH 7.5, 250 mM KOAc, 5 mM $Mg(OAc)_2$, 1 mM DTT, 20 % glycerol, cOmplete protease inhibitor cocktail, 5 mM imidazole). The clarified lysate was loaded to the column by utilization of a peristaltic pump with a flow-rate of 1 ml/min at 4°C. Afterwards, the column was connected to a chromatography apparatus (ÄKTA pure, Cytiva/GE Life Sciences). Two buffers were prepared to contain no (Buffer A) and 300 mM imidazole (Buffer B) in 20 mM Tris/HCl pH 7.5, 250 mM KOAc, 5 mM $Mg(OAc)_2$, 1 mM DTT, 20 % glycerol, cOmplete protease inhibitor cocktail, and were connected to different pumps of the system. Application of a gradient flow between Buffer A and B allowed to conduct various wash steps of the column prior elution, including a 10 ml wash with 10 mM imidazole and a further 20 ml with 20 mM imidazole to remove possible non-specifically bound impurities from the column matrix. The elution step was conducted by application of 300 mM imidazole (100 % Buffer B) for 10 ml and collected in 1 ml fractions. The main peak fractions were analyzed by SDS-PAGE stained with colloidal chemical Coomassie solution (Quick Coomassie stain, Serva). Afterwards the sample was applied for SEC on Superose 6 Increase 10/300 GL column (Cytiva) in 20 mM Tris/HCl pH 7.5, 50 mM KOAc, 5 mM $Mg(OAc)_2$, 1 mM DTT, 20 % glycerol. SecB was purified by manual IMAC utilizing Ni^{2+}-NTA agarose resin (Qiagen). In brief, the Ni^{2+}-NTA resin was rinsed extensively with MQ and equilibrated with wash buffer (20 mM Tris/HCl

pH 7.5, 500 mM KOAc, 5 mM $Mg(OAc)_2$, 1 mM DTT, 5 % glycerol, 20 mM imidazole). SecB was applied for binding to the resin for 1 h at 6°C on a rolling table. Afterwards, the loaded Ni^{2+}-NTA resin was extensively washed with wash buffer. The elution of SecB from the Ni^{2+}-NTA beads was conducted in 0.5 ml fractions upon addition of elution buffer (20 mM Tris/HCl pH 7.5, 150 mM KOAc, 5 mM $Mg(OAc)_2$, 1 mM DTT, 5 % glycerol, 300 mM imidazole, 0.2 mM PMSF). The sample was applied to SEC on Superdex 200 Increase 10/300 GL column (Cytiva) in 20 mM Tris/HCl pH 7.5, 50 mM KOAc, 5 mM $Mg(OAc)_2$, 1 mM DTT, 5 % glycerol for further purification to homogeneity. When needed for further experiments, the protein was buffer exchanged by usage of desalting column (PD10, Cytiva) to match the desired buffer or purified in other buffering conditions. The protein samples were analyzed by SDS-PAGE and stained with colloidal chemical Coomassie solution (Quick Coomassie stain, Serva). The concentration of the purified proteins was determined spectrophotometrically.

For the heterologous overexpression of trigger factor (TF), the strain *E. coli* BL21(DE3) harboring pAT62 plasmid was utilized. This construct encodes for trigger factor of *P. aeruginosa* PAO1 with a fused hexa-histidine tag on the C-terminus (TF-His_6). A single colony was used for growing a pre-culture in LB supplied with 100 µg/ml ampicillin at 37°C overnight shaking at 180 rpm. These growth conditions were kept throughout the whole expression procedure. The pre-culture used to inoculate pre-warmed LB media with supplied with ampicillin. The cells were grown until reaching OD_{600} ~ 0.6 and overexpression was induced for 2 h upon addition of 0.5 mM IPTG. Afterwards the cells were harvested by centrifugation at 5000 *g* for 15 min at 4°C. After harvesting, the cell pellet was suspended in 20 ml cell resuspension buffer (20 mM Tris/HCl pH 7.5, 50 mM KCl, 1 mM DTT, 0.2 mM phenylmethylsulfonyl fluoride (PMSF), 5 % glycerol) and flash-frozen in liquid nitrogen and stored at -80°C until further usage. For purification, the cells were thawed in water at room temperature upon occasional vortexing. The cells were lysed by mechanical disruption (M-110P cell disruptor, Microfluidics Inc.). The cell lysate applied for ultracentrifugation on 205000 g for 1 h at 4°C to pellet the cell debris and membranes, while the soluble proteins remain in the supernatant. For binding, 20 ml of clarified supernatant were applied for IMAC on 0.5 ml Ni^{2+}-NTA beads (Qiagen). Therefore, the Ni^{2+}-NTA resin was prior rinsed with 60 ml MQ and subsequently equilibrated with 10 ml wash buffer (20 mM Tris/HCl pH 7.5, 500 mM KCl, 1 mM DTT, 0.2 mM PMSF, 10 mM imidazole, 5 % glycerol). The incubation for binding was conducted at 6°C for 1 h rolling. Afterwards, the flow-through was collected and the TIG-loaded Ni^{2+}-NTA resin was rinsed with 20 ml wash buffer for 3 times. The first wash fraction was collected. The captured protein was eluted from the Ni^{2+}-NTA beads in several fractions, by adding of 800 µl elution buffer (20 mM Tris/HCl pH 7.5, 500 mM KCl, 1 mM DTT, 0.2 mM PMSF, 300 mM imidazole, 5 % glycerol) per fraction. The fractions were analyzed by SDS-PAGE. Further, purified TIG was applied for SEC on Superdex 200 Increase 10/300 GL (Cytiva) in 20 mM Tris/HCl pH 7.5, 50 mM KOAc, 5 mM $Mg(OAc)_2$, 1 mM DTT, 5 % glycerol. Prior SEC, the IMAC fractions were centrifuged at 100000 *g* for 1 h at 4°C to remove occasional aggregates.

For the heterologous expression of CsaA, the strain *E. coli* BL21(DE3) harboring the construct pAT102 encoding for His_8-3C-CsaA was used. As described above, a single colony was used to grow a pre-culture overnight which served to inoculate pre-warmed LB media supplied with 100 µg/ml ampicillin. The growth conditions were set at 37°C upon 180 rpm shaking and kept throughout the whole cultivation. The overexpression was induced at OD_{600} ~ 0.6 by addition of 0.2 % (w/v) L-arabinose to the culture. The cells were harvested and purified as described above for TIG. In brief, the cells were resuspended in 20 mM Tris/HCl pH 7.5, 100 mM NaCl, 10 % glycerol, 0.2 mM PMSF. For IMAC, the wash buffer contained 20 mM Tris/HCl pH 7.5, 500 mM NaCl, 10 % glycerol, 10 mM imidazole. The elution buffer contained 20 mM Tris/HCl pH 7.5, 100 mM NaCl, 10 % glycerol, 300 mM imidazole. After IMAC the samples were applied for SEC on Superdex 200 Increase 10/300 GL column (Cytiva) in 20 mM Tris/HCl pH 7.5, 100 mM NaCl, 10 % glycerol, and the peak fractions of CsaA were analyzed by SDS-PAGE. The samples were flash-frozen with liquid nitrogen and stored at -80°C until further usage.

3.2.2.4 Expression, purification, and fluorescent labeling of Sec substrates

Pseudomonas preproteins were expressed in *E. coli* BL21(DE3) for proLipA variants and *E. coli* Rosetta™ (DE3) pLysS (Novagen/Merck) for proLipC and proLipC variants, proOprG, proOprF and proFapC. In aim to accumulate the precursor form of the protein in the cytoplasm and to avoid signal peptide cleavage, the following protocol was applied which is oriented on previous research (Oliver *et al.*, 1990). Briefly, pre-cultures were grown overnight at 37°C upon shaking at 180 rpm and used for inoculation of LB media with appropriate antibiotics. The inoculated cell cultures were grown at same conditions until reaching OD_{600} ~ 0.6, and 4 mM sodium azide (NaN_3) were added to the culture from a freshly prepared 0.5 M stock solution. The addition of sodium azide inhibits protein secretion to the periplasm (Oliver *et al.*, 1990). The cultures were let 10 min for incubation with NaN_3 in the same conditions, prior inducing the overexpression by addition of 0.5 mM IPTG to the media. The cultivation for overexpression last for 2 h at 37°C upon shaking at 180 rpm. The cells were harvested by centrifugation at 4000 *g* for 20 min at 4°C. The overexpressed protein accumulated in the cytoplasm resulting in the formation of inclusion bodies. For the isolation of the inclusion bodies, the protocol is oriented on previous studies (Hausmann, 2008; Dollinger, 2018). The harvested cells were suspended in buffer IB (50 mM Tris/HCl pH 7.0, 5 mM EDTA, 1 mM TCEP, 10 µg/ml DNase I and 50 µg/ml lysozyme) with 1 ml per 0.1 g of cells, transferred to 2 ml reaction tubes (Sarstedt) and incubated 15 min at RT with slight agitation on a rolling bench. The cells were lysed by sonication utilizing the following pulses: 30 seconds at 50 % amplitude and 0.8 cycles, 30 seconds at 60 % amplitude and 0.8 cycles, 30 seconds at 80 % amplitude and 0.8 cycles (Ultrasonic homogenizer UP100H (100W) equipped with an M3 sonotrode/ultrasonic horn (Hielscher Ultrasonics). During the sonication procedure the samples were kept on ice. After cell lysis, the solution was centrifuged at 15000 *g* for 10 min at 4°C utilizing a bench top centrifuge. After centrifugation, the supernatant (SN) was removed,

and the pellet was suspended in 0.5 – 1 ml of buffer IB and put again for centrifugation at 15000 *g* for 10 min at 4°C. This step was repeated for two times. Afterwards, the pellet was suspended only in 50 mM Tris/HCl pH 7.0 to remove residual amounts of previous buffering agents and put again for centrifugation at the same parameters. After centrifugation the SN was removed, and the pellet was suspended in buffer with urea (20 mM Tris/HCl pH 7.25, 8 M urea) to cause chaotropically induced unfolding of the protein. The resulting solution put for centrifugation at 21380 *g* for 10 min at 4°C to remove residual impurities and transferred to reaction tubes for storage (Low Protein Binding, Sarstedt). Optionally, the chaotropically unfolded proteins were purified by ion exchange chromatography based on the supplier's protocol (HiTrap Q HP column, Cytiva).

For the overexpression of substrates originating from *E. coli*, being the precursor of the outer membrane protein A (proOmpA) already pre-existing plasmids were used. For proOmpA, the plasmid pET502 encoding for single-cysteine mutated proOmpA$_{C302S}$ was used. For the overexpression the *E. coli* MM52 strain was utilized (Oliver and Beckwith, 1981). In brief, a preculture grown overnight at 30°C upon shaking at 180 rpm was used to inoculate LB media supplied with 100 µg/ml ampicillin. The culture was grown at the same conditions until $OD_{600} \sim 0.6$ and 4 mM NaN_3 were add to the culture and let grow at 37°C upon shaking at 180 rpm for 10 min. The overexpression was induced by addition of 0.5 mM IPTG, and cells were cultivated for expression for 2 hs at 37°C upon 180 rpm shaking.

The isolated substrates were also applied for fluorescent labeling with fluorescein-5-maleimide (Thermo Fisher Scientific). 10 – 20-fold molar excess of the dye was added to the urea-denatured proteins. The sample was filled with urea buffer to 300 – 500 µl final volume to ensure proper mixing in the tube. Then the sample was put on a rolling table in dark conditions and incubated at 6°C overnight. The next day, the sample was precipitated with 20 % (w/v) trichloroacetic acid (TCA) for 30 – 60 min on ice. After incubation, centrifugation at 21380 *g* for 15 min at 4°C was conducted to pellet the aggregated protein. The supernatant was removed, and 1 ml of ice-cold acetone was added to the sample for washing by vortexing. The sample was put for centrifugation at 21380 *g* for 15 min at 4°C again and the SN was removed afterwards. Optionally, the acetone-wash can be repeated to remove free dye. A subsequent drying step at 37°C was utilized for 15 min to enable evaporation of remained acetone. The pellet was suspended with 20 mM Tris/HCl pH 7.25, 8 M Urea. Finally, the substrate proteins were aliquoted, flash-frozen with liquid nitrogen and stored at -80°C until further usage.

3.2.3 Isolation of bacterial inner membranes vesicles

To separate inner and outer membrane fractions, 20 and 70 % (w/v) sucrose solutions were prepared in 20 mM Tris/HCl pH 7.5, 150 mM KOAc, 5 mM $Mg(OAc)_2$ and applied to centrifuge tubes (Open-Top Thinwall Ultraclear, Beckman Coulter) on a Gradient Station (BioComp Instruments) to generate a continuous density gradient. Crude bacterial membranes were applied on top and centrifuged for 16 h at 110000 *g* at 4°C (SW40 rotor, Beckman Coulter) (Kanonenberg *et al.*, 2019). After centrifugation, the gradient was harvested in fractions of 1 ml utilizing the Gradient Station. When the last fraction #12

was incompletely collected, calculation based on the piston position were used to complete the fraction for the figures. Spectral profiling of the gradients during fractionation procedure was conducted by UV measurement at 280 nm through the equipped Triax Flow Cell (BioComp Instruments). Collected fractions were further analyzed by SDS-PAGE. For this, 5 µl of fraction were mixed with 5 µl of 5 x sample loading buffer (SB) and run on 15 % acrylamide gel, then stained with colloidal chemical Coomassie solution (Quick Coomassie stain, Serva). The fractions containing inner membrane vesicles (IMVs) were pulled together and diluted at least 5-fold, to fill the maximal volume of the ultracentrifugation tube, with 20 mM Tris/HCl, 150 mM KOAc, 5 mM $Mg(OAc)_2$ to decrease the sucrose concentration. The solution was mixed by vortexing and applied for ultracentrifugation at 205000 *g* (Ti 60, Beckman Coulter) for 1 h at 4°C to pellet the IMVs. Afterwards, the supernatant was removed and the IMVs were suspended in 20 mM Tris/HCl pH 7.5, 50 mM KOAc, 5 mM $Mg(OAc)_2$, 5 % glycerol, optionally with or without 0.2 mM PMSF. The density of the membranes was estimated spectrophotometrically by absorbance. The IMVs were aliquoted, and flash-frozen with liquid nitrogen for storage at -80°C. Optionally, in aim to isolate larger amounts of IMVs, the SW32 rotor was utilized.

3.2.4 Liposome preparation and reconstitution of SecYEG

For the creation of liposomes with tailored lipid composition, synthetic lipids (Avanti Polar Lipids, Inc.) were used from chloroform stocks of known concentrations. For liposome formation 10 µmol of lipids were used. The lipid composition of the liposomes is indicated in the results section. Mixing of the lipids in defined ratios and subsequent application for evaporation under vacuum conditions let to removal of chloroform and formation of lipid film on the surface of the glass reaction tube. Therefore, the tube was connected to a rotary evaporator (IKA) with 140 rpm and put on heating at 40°C for at least 15 min. The pressure applied by the vacuum pump was regulated by a valve and kept below 200 mbar. Afterwards, the lipid film was carefully resuspended 2 ml buffer (50 mM Hepes/KOH pH 7.4, 50 or 150 mM KCl) to obtain a concentration of 5 mM liposomes. The liposomes were extruded using the Mini-Extruder set (Avanti Polar Lipids, Inc.) and porous polycarbonate membranes (Nuclepore, Whatman). In this procedure, the crude liposomes were extruded initially by eleven passes through 400 nm and subsequently by another round of eleven passes through 200 nm pore size membranes. The protocol is oriented on previous research (Kamel *et al.*, 2022). For the reconstitution of purified SecYEG, the liposomes were destabilized with 0.2 % (w/v) DDM or 0.5 % (w/v) Triton X-100 at 40°C for 10 min. 1 nmol of the protein was reconstituted in 1:1000 protein to lipid ratio, thus 200 µl of liposomes from 5 mM stock were used for the procedure. The translocons were diluted with 50 mM Hepes/KOH pH 7.4, 50 or 150 mM KCl, 0.2 mM TCEP, 5 % glycerol, 0.1 % (w/v) DDM to obtain 1 nmol of the protein in 400 µl. After destabilization, the liposomes were added to the protein and kept on ice for 30 min. To remove the detergent, 100 mg/ml Bio-Beads SM-2 were prepared based on the manufacturer guidelines (Bio-Rad). After incubation on ice, the sample solution was transferred to 70 mg of Bio-Beads and incubated at 6°C rolling over night. The next day, the solution was transferred

for ultracentrifugation at 166300 *g* for 45 min at 4°C to pellet the proteoliposomes. As 200 µl of the liposomes were utilized for reconstitution, the resulting proteoliposomes were resuspended in the same volume in buffer (50 mM Hepes/KOH pH 7.4, 50 or 150 mM KCl). To check the orientation of the reconstituted translocons, the N-terminal tag of SecY was proteolytically digested by enterokinase (EK). For correctly oriented translocons, the N-terminus of SecY is exposed outside of the proteoliposomes, thus the integrated enterokinase cleavage motif becomes accessible for cleavage by the protease. The resulting change of the molecular weight between cleaved and non-cleaved samples is detectable by SDS-PAGE. 5 µl proteoliposomes were added to a 1.5 ml reaction tube with or without 1 µl enterokinase light chain (New England Biolabs) and filled total volume of 20 µl with 20 mM Tris/HCl pH 8.0, 50 mM NaCl. The samples were incubated overnight at 25°C with slight agitation. Afterwards, 10 µl of the samples were withdrawn and mixed with 10 µl of 5 x SDS Sample Buffer and subsequently applied for SDS-PAGE. The cleavage efficiency was determined by comparing the band intensities of cleaved and non-cleaved samples after staining (ImageQuant TL, Cytiva/GE Life Sciences). Detergent-purified translocons were used as a reference indicating the maximal cleavage. The subtraction of the background signal was conducted by using the implemented Local average algorithm.

3.2.5 Size exclusion chromatography combined with multi angle light scattering

SEC – MALS was conducted to determine the oligomeric state of the Sec components. Purified proteins of 0.25 – 0.3 mg/ml concentration were centrifuged at 100000 *g* for 1 h at 4°C to remove occasional aggregates. After centrifugation, 450 – 500 µl of SecYEG were injected for SEC on Superdex 200 Increase 10/300 GL column (Cytiva). The column was connected to a miniDAWN TREOS II light scattering device and Optilab-TrEX Ri-detector (Wyatt Technology Corp.). The buffer for SecYEG was 20 mM Tris/HCl pH 7.5, 100 mM KOAc, 0.2 mM TCEP upon addition of 0.05 and 0.1 % (w/v) DDM. For analysis of the data, the software ASTRA 7.3.2was employed (Wyatt Technology Corp.). The measurements were performed in collaboration with Eymen Hachani.

3.2.6 Small-angle X-ray scattering

For the data acquisition of SecA, SecB and CsaA of *P. aeruginosa* PAO1 a batch mode of measurements was conducted and the beamline BM29 at the ESRF Grenoble was utilized which was equipped with a PILATUS 2M detector (Dectris) at a fixed distance of 2.827 m for SecA and SecB and with 2.812 m for CsaA (Pernot *et al.*, 2010, 2013). The measurements were performed with concentrations ranging, for SecA from 0.47 – 2.40 mg/ml at 10°C, for SecB with 0.75 – 4.57 mg/ml at 20°C and for CsaA 1.21 – 4.43 mg/ml at 10°C. The corresponding buffer for SecA and SecB consisted of 20 mM Tris/HCl pH 7.5, 50 mM KOAc, 5 mM $Mg(OAc)_2$, 1 mM DTT, 5 % glycerol, while for CsaA the buffer contained only 20 mM Tris/HCl pH 7.5, 100 mM NaCl, 5 % glycerol. For SecA and CsaA, one frame collected per second and the data scaled to absolute intensity against water.

The SAXS measurement for TIG was conducted at the Center for Structural Studies of the Heinrich Heine University Düsseldorf. The data was collected in-house at Xeuss 2.0 Q-Xoom system from Xenocs which was equipped with a PILATUS 3 R 300K detector (Dectris) and a GENIX 3D CU Ultra Low Divergency x-ray beam delivery system. The sample-to-detector distance was set at 0.55 m for this experiment and resulted in an achievable q-range of 0.1 – 6 nm^{-1}. The sample concentration was 1.3 mg/ml in 20 mM Tris/HCl pH 7.5, 50 mM KOAc, 5 mM $Mg(OAc)_2$, 1 mM DTT, 5 % glycerol and the measurements were conducted at 15°C . The sample was injected via an autosampler into the Low Noise Flow Cell (Xenocs). For that sample, 24 frames with an exposure time of ten min were collected. The data was scaled to the absolute intensity of water.

All used programs for data processing were part of the ATSAS Software package (version 3.0.3) (Manalastas-Cantos *et al.*, 2021). Primary data reduction was performed with the program PRIMUS (Konarev *et al.*, 2003). With the Guinier approximation, the forward scattering I (0) and the radius of gyration (Rg) were determined (Guinier, 1939). The GNOM software was used to estimate the maximum particle dimension (Dmax) with the pair-distribution function p (r) (Svergun, 1992). Low resolution models were calculated with GASBORMX (Svergun, Petoukhov and Koch, 2001; Petoukhov *et al.*, 2012). SASREFMX was employed for the reconstruction of the calculated dimers (SecA and TIG) (Petoukhov and Svergun, 2005; Petoukhov *et al.*, 2012). For CsaA, the missing N-terminus containing the purification tag was added with the software CORAL (Petoukhov *et al.*, 2012). The superimpositions of the predicted models were enabled by the software SUPCOMB (Kozin and Svergun, 2001). All SAXS measurements and analysis were conducted in tight collaboration with Jens Reiners from the Center for Structural Studies at the Heinrich Heine University of Düsseldorf.

3.2.7 Microscale Thermophoresis

MST was used to check on interactions between the SecYEG and SecA from *P. aeruginosa*. A single-cysteine variant of the translocon $SecYE_{S118C}G$ (pAT109) was isolated by polymer-based extraction via DIBMA and fluorescently labeled as described above (Chapter 3.2.2.2). The sample was applied for ultracentrifugation at 100000 *g* for 30 min at 4°C to remove occasional aggregates. The concentration of the sample was determined by UV/Vis and the sample was diluted to 200 nM in 20 mM Tris/HCl pH 7.5, 50 mM KOAc, 0.5 mg/ml BSA, 5 % glycerol and protected from light. For the measurement 10 µl of the diluted sample were mixed with SecA ranging from 0.23 nM to 7.5 µM to a final volume of 20 µl in a 0.5 ml reaction tube (Sarstedt). SecYEG:SecA samples were incubated for 15 min at RT in the dark, then loaded into glass capillaries and applied for analysis by Monolith NT.115 instrument (NanoTemper Technologies, Munich, Germany). The MST power was set to 80 % as well as the LED power in the blue channel. The thermophoresis was detected over time by normalized fluorescence traces for 30 seconds with 5 seconds set for delay and recovery. The aggregation of the samples was monitored by a capillary profile scan. The data was evaluated by NT Analysis software (NanoTemepr Technologies, Munich, Germany).

3.2.8 Sedimentation analysis

The aggregation of the lipase precursor was investigated in various KOAc concentrations in presence or absence of SecB. The previously described protocol to track lipase sedimentation was utilized with minor modifications (Papadopoulos *et al.*, 2022). For the reaction, 0.5 µM fluorescently labeled and urea-denatured lipase precursor were diluted in 5 mM Tris, 5 mM glycine, 1 mM $CaCl_2$, 5 % glycerol to generate the master mix. 5 µM SecB was applied to 1.5 ml reaction tubes (Sarstedt) containing 20 mM Tris/HCl pH 7.5 and varying KOAc concentrations in aim to achieve the indicated ionic strength. The master mix was applied to the tube, and the reaction was run and evaluated as described previously (Papadopoulos *et al.*, 2022).

3.2.9 *In vitro* protein translocation through Sec system

The translocation through the Sec system was investigated *in vitro* using various fluorescently labeled substrates for transport. The protocol is oriented on previous research and contains only minor modifications (de Keyzer, van der Does and Driessen, 2002). In brief, for the transport reaction with inverted inner membrane vesicles (IMVs), a total reaction volume of 50 µl with IMVs of 0.5-1 optical density, 1 µM SecA and 0.5-1 or 2.5 µM $SecB^4$ as well as 0.5-1 µM substrate were added per reaction. The reaction buffer contains 20 mM Tris/HCl pH 7.5, 50 mM KOAc, 5 mM $Mg(OAc)_2$, 10 mM DTT, 50 µg/ml phosphocreatine kinase and 10 mM phosphocreatine. Alternatively, KCl and $MgCl_2$ were utilized instead of KOAc and $Mg(OAc)_2$ but did not affect the performance of the assay. For the *in vitro* transport reaction into proteoliposomes, a total reaction volume of 50 µl, including 10 µl proteoliposomes, 1 µM SecA and 1 µM $SecB^4$ as well as 1 µM substrate were added per reaction. The reaction buffer contains 50 mM Hepes/KOH pH 7.4, 50 mM KCl, 5 mM $MgCl_2$, 10 mM DTT, 50 µg/ml phosphocreatine kinase and 10 mM phosphocreatine. The samples were incubated for 5 min at 37°C, and the transport reaction was started upon addition of 6 mM ATP. The same reaction lacking ATP was used as negative control. After starting the transport reaction, all samples were incubated for 15 min at 37°C. Afterwards, 10 % of the reaction volume were taken and served later as reference for the preprotein input. 0.2 mg/ml proteinase K (Thermo Fisher Scientific) was added to each reaction and mixed by modest vortexing. The samples were incubated at RT for 15 min, afterwards 20 % (w/v) TCA was added to the samples, and they were moved to ice for 15 min incubation. After the incubation, the samples were centrifuged for at 21380 *g* for 15 min at 4°C to pellet the precipitated sample. TCA was removed, and 1 ml of ice-cold acetone was added to the samples. After a brief vortexing, the samples were centrifuged again at 21380 *g* for 5 min at 4°C. The acetone was removed, and the samples were put for drying at 37°C for 10-15 min, until the residual acetone evaporated. The dried precipitates were resuspended from the tube walls by 2 x SDS-PAGE sample buffer, following subsequent incubation at 95°C for 5 min prior loading for SDS-PAGE. Successful translocation of the transport substrates resulted in the prevention of proteolytic digest by the protease, allowing to detect and quantify their in-gel fluorescence signal (ImageQuant TL, Cytiva/GE Life

Sciences). The subtraction of the background signal was conducted via Local average algorithm. Based on the signal of the preprotein input, the amount of the transported substrate was determined.

3.3 Results

3.3.1 Establishment of the Sec system of *P. aeruginosa* PAO1

The first step to establish the Sec system of *P. aeruginosa* PAO1 was the successful overexpression of the primary Sec components. The translocon SecYEG, the motor ATPase SecA and the holdase SecB were individually expressed and purified. The overexpression was conducted heterologously in *E.* coli expression strains (Figure 3.1). The histidine-tagged proteins were further purified by immobilized metal ion affinity chromatography (IMAC). In further downstream processing, size exclusion chromatography (SEC) was utilized to achieve highly homogeneous protein samples that were suitable for further investigations (Figure 3.1). The overexpressed his-tagged SecYEG solubilized well in commonly used detergent DDM. The purified protein complex indicates three main bands when analyzed by SDS-PAGE, with a molecular weight (MW) for His_6- SecY at ~ 38 kDa, for SecE at ~ 15 kDa and for SecG at ~ 17 kDa (Figure 3.1, A). When applied for SEC in 0.05 % (w/v) DDM, His_6-EK-SecYEG eluted at ~ 11.2 ml with a homogenous peak on Superdex 200 Increase 10/300 GL (Cytiva) (Figure 31, A). Furthermore, SecA and SecB also purified well, and were further analyzed by SDS-PAGE, with SecA migrating at ~ 105 kDa and SecB at ~ 20 kDa which matches for both the MW of the monomers. When applied for SEC, SecA eluted at ~16.3 ml on Superose 6 Increase 10/300 GL and SecB eluted at ~ 13.5 ml on Superdex 200 Increase 10/300 GL (Cytiva) indicating the MW of the SecA dimer (~ 210 kDa) and SecB tetramer (~ 80 kDa) based on the observed elution volumes and in respect to the column specifications (Figure 31, B and C). In aim to characterize the Sec translocon, the oligomeric state of SecYEG in detergent micelles of two different DDM concentrations, 0.05 and 0.1 % (w/v), was analyzed by SEC coupled to multi angle light scattering (MALS) (Figure 3.1, D). As described in literature, increasing detergent concentration could promote the monomerization of the translocon and could support protein transport (Bessonneau, 2002). Nearly no difference was observed in the elution volume of the translocon at ~11.2 ml between the two applied DDM concentrations (Figure 3.1, D). The determined molecular weights of both samples were very similar, when comparing the 0.05 % (w/v) DDM with MW of 229.2 ± 2.1 kDa to the 0.1 % (w/v) DDM with 228.5 ± 8.8 kDa, suggesting that in both cases there are two translocons within one DDM micelle. Thus, increasing the detergent concentration from 0.05 % to 0.1 % (w/v) DDM did not lead to monomerization of translocons in the micelles, suggesting that indeed the dimeric state could be preferred. Since the usage of DDM allows for purification of delipidated translocons (van der Does *et al.*, 2000), and resulted in homogenously purified SecYEG (Figure 3.1, A and D), this detergent was kept for further experimental procedures. Additionally, structural analysis of SecA and SecB were conducted in aim to characterize the soluble Sec components. The homology models of the proteins were generated by phyre2 (Kelley *et al.*, 2015). The proteins were applied for small angle X-ray scattering (SAXS). The solved surface envelopes of SecA and SecB matched the homology models and indicated that SecA was dimeric and SecB tetrameric in solution (Figure 3.1, E).

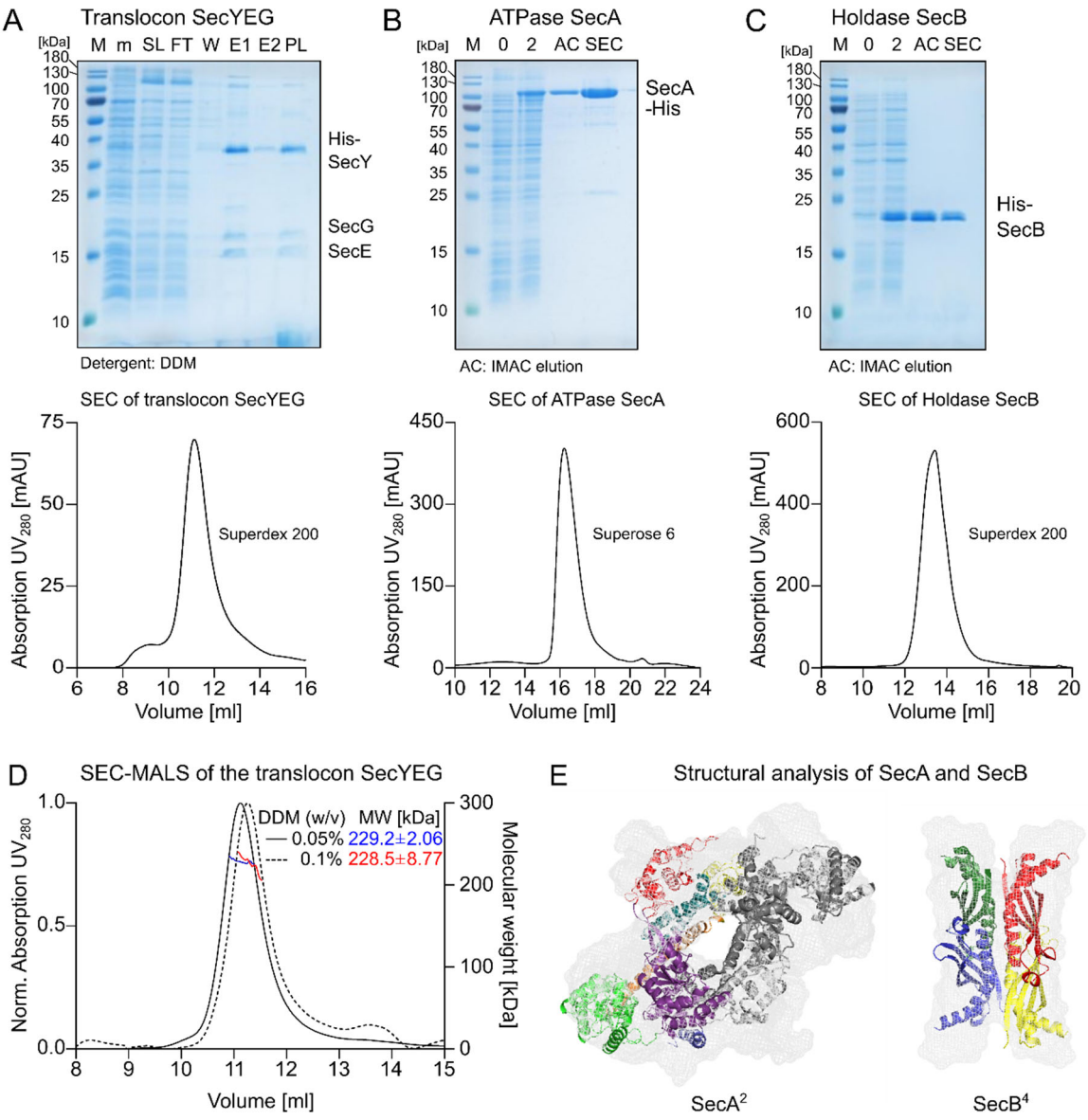

Figure 3. 1: Characterization of the major Sec components from *P. aeruginosa* PAO1

SDS-PAGE of translocon SecYEG **(A)**, the ATPase SecA **(B)** and the holdase SecB **(C)**. M: Prestained Molecular Weight Marker,10-180 kDa (PageRuler^{TM}, Thermo Fisher Scientific). Crude membranes (m) after overexpression of membrane proteins (SecYEG) and detergent solubilization (SL) as well as cells prior induction (0) and after harvesting (2) for soluble proteins (SecA and SecB) were checked. Clarified cell lysates for SecA and SecB or detergent-solubilized membranes for SecYEG were applied for affinity chromatography (IMAC), and stepwise analysis after binding to the NiNTA resin of the flow-through fraction (FT), the wash fraction (W), the elution fractions (E1/2 or AC), and for SecYEG reconstituted in proteoliposomes (PL), are depicted. The bands of the proteins of interest are annotated. SEC profiles are shown below SDS-PAGE images. Used columns are indicated in the figure. SEC-MALS analysis of SecYEG (**D**) to determine the oligomeric state in DDM detergent micelles of varying detergent concentration was conducted. (**E**) Structural analysis of soluble Sec components indicates the SAXS envelopes depicted in grey mesh. SecA as dimer and SecB as tetramer. The homology models are colored inside the envelopes. The various colors indicate the different domains of SecA: helical scaffold domain (orange), peptide cross linking domain (red), two helix finger (cyan), helical wing domain (yellow), nucleotide binding domain 2 (green), nucleotide binding domain 1 (violet), N-terminal helix (blue). The homology model of SecB tetramer is colored, with each monomer in a different color (green, red, blue, and yellow).

The results are in line with observations made by SEC upon purification procedures, and the protein elution volumes match the expected MW of the oligomers (Figure 3.1, B and C). The homology model of SecA resembles the known arrangement of SecA in other bacterial species, possessing multiple domains (Figure 3.1, E) (Lycklama a Nijeholt and Driessen, 2012; Lindič *et al.*, 2020). The dimer of SecA forms a "donut-like" shape and is in line with observations made for SecA of other bacterial species (Hunt *et al.*, 2002; Ding *et al.*, 2003; Sharma *et al.*, 2003). The homology model of SecB indicates the tetrameric state of the holdase and reflects also its functional form (Figure 3.1, E) (Xu, Knafels and Yoshino, 2000; Huang *et al.*, 2016).

The second step to establish the functional *P. aeruginosa* Sec system was the overexpression and purification of substrates for translocation. Here, the focus lay on the lipase A precursor (proLipA). Initial attempts indicated that the heterologous overexpression of proLipA is challenging, being likely hindered by rare codons in the wild-type gene sequence (Zalucki, Beacham and Jennings, 2009). A codon-optimized version of the proLipA gene led to elevated expression in form of inclusion bodies, but further optimization was required as the protein accumulated as a mixture of its precursor and mature form. Apparently, the expression of preproteins is in general a challenging task, since the preproteins need to be accumulated in the cytoplasm. During this cytoplasmic enrichment, the preproteins need to be protected from proteolytic digest to maintain the precursor form, so cleavage of the mature domain from the N-terminal signal peptide (SP) is avoided. In respect to that, the inhibition of protein export through the Sec machinery was achieved by addition of sodium azide (NaN_3) to the cell culture (Figure 3.2) (Oliver *et al.*, 1990). The incubation with sodium azide upon heterologous overexpression in *E. coli* led to accumulation of proLipA in form of inclusion bodies in the cytoplasm (Figure 3.2, A). Furthermore, in aim to characterize the Sec system of *P. aeruginosa* PAO1, other substrates for the Sec-dependent transport were expressed and purified as described above (Figure 3.2, B). Those include the precursor forms of the lipase C, the outer membrane proteins OprG and OprF, and the functional amyloid-forming protein FapC. The expression of most of the preproteins required either the partial or complete codon optimization of the gene sequence encoding for SP or the utilization of a suitable expression strain, capable of the transcription and translation of rare codons, such as *E. coli* Rosetta™ (DE3) pLysS (Novagen/Merck). The preproteins were fluorescently labeled to allow for their in-gel detection in later transport experiments. The precursor of the outer membrane protein OmpA of *E. coli* was used as a reference, as it is commonly used as a substrate in translocation studies through the well-studied *E. coli* Sec System (de Keyzer, van der Does and Driessen, 2002).

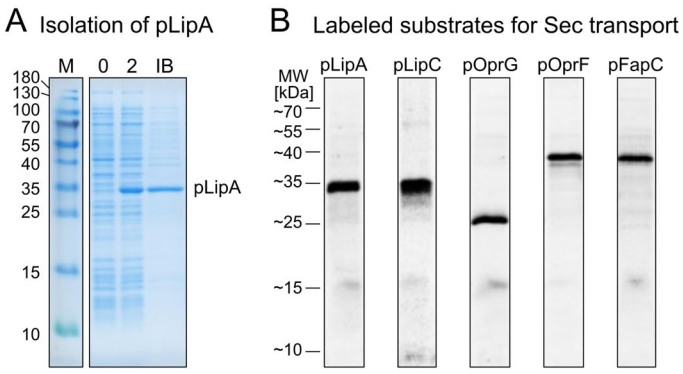

Figure 3. 2: Sec transport substrates of *P. aeruginosa* PAO1

A: Expression and purification of proLipA. M: Prestained Molecular Weight (MW) Marker,10-180 kDa. The cells are shown prior induction (0) and after harvesting (2). Treatment with NaN_3 successfully led to accumulation of preprotein in the cytoplasm. The protein purifies in form of inclusion bodies (IB). **B**: Fluorescently labeled substrates to use in Sec transport.

3.3.2 *In vitro* reconstitution of protein transport by the *P. aeruginosa* Sec system

To investigate the Sec-dependent lipase translocation, the Sec system of *P. aeruginosa* PAO1 was reconstituted *in vitro*. Since protein transport through the Sec pathway had been an object of research for decades (Beckwith, 2013), multiple approaches have been developed to reconstitute the Sec system of *E. coli* and track protein translocation *in vitro* in a well-defined experimental setup. Therefore, the translocon SecYEG requires to be in its functional membrane-embedded state. A suitable approach to obtain the translocon in its functional state is the isolation of inverted inner membrane vesicles (IMVs), e.g. by density gradient centrifugation. The advantage of the IMVs is that the topology and functionality of the protein will likely not be disturbed upon isolation procedures since no detergent-based solubilization or reconstitution step is required. An additional advantage of the IMVs is that they endogenously contain components which can contribute to efficient protein transport, including SecDF that utilizes the proton gradient across the membrane to pull out the emerging preprotein of the translocon SecYEG (Arkowitz and Wickner, 1994; Tsukazaki and Nureki, 2011; Tsukazaki, 2018). In this approach, crude *E. coli* membranes harboring heterologously overexpressed SecYEG were applied for ultracentrifugation on a continuous sucrose density gradient (Figure 3.3). The utilization of the density gradient separates the soluble components from macromolecular complexes, first of all the ribosomes, and further allows separation of IMVs from the outer membrane vesicles (Figure 3.3, A). The SecYEG-containing gradient fractions were identified by SDS-PAGE (Figure 3.3, A). The isolated vesicles were further utilized for *in vitro* transport experiments through the Sec machinery.

Besides the isolation of the translocon-harboring IMVs, the reconstitution of the translocons in model liposomes of tailored lipid composition was also conducted (Figure 3.3, B). The orientation of the reconstituted translocons was determined by proteolytic cleavage of the N-terminal histidine tag via

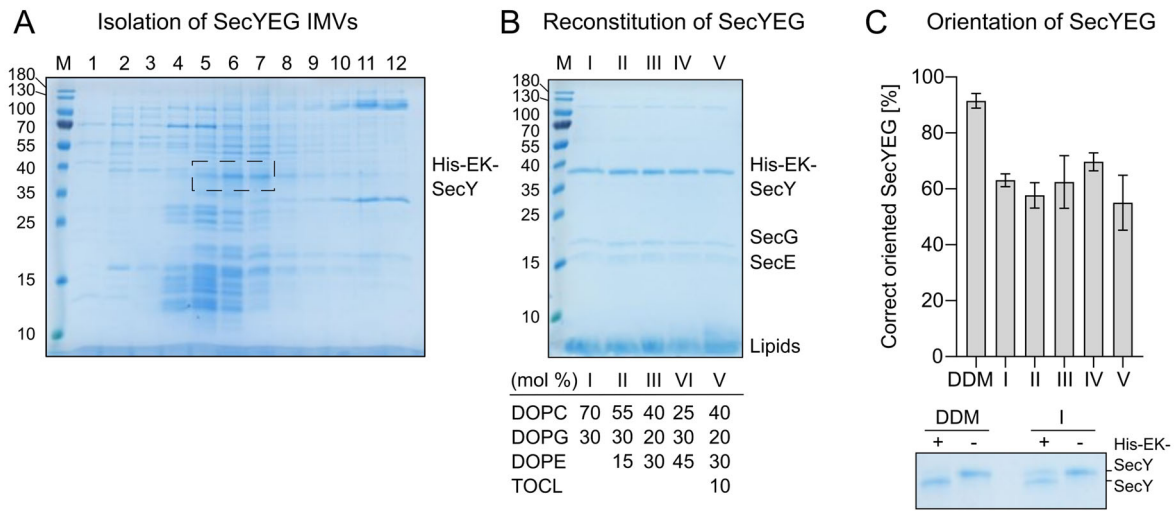

Figure 3. 3: Isolation and reconstitution of SecYEG

A: The collection of continuous sucrose gradient (20 – 70 %) upon fractionation of crude membranes was analyzed by SDS-PAGE. The fractions containing IMVs (5, 6 and 7) were selected, and SecY-band is indicated in dashed quadric. **B**: SecYEG translocons were reconstituted in liposomes of tailored lipid composition (I – V, indicated in the table), and analyzed by SDS-PAGE. The corresponding bands of proteoliposomes (PL) are indicated. M: Prestained Molecular Weight Marker,10-180 kDa. **C**: The orientation of the translocons was estimated by enterokinase cleavage of the poly-histidine tag. Only correctly oriented translocons are suitable for cleavage after reconstitution. The cleavage results in a shift to lower molecular weight that was used for quantification. SecYEG in detergent (DDM) served as reference for maximal cleavage upon utilized conditions. The cleavage efficiency is shown in the bar plot and an exemplary SDS-PAGE for DDM and PL with lipid composition I (70 % DOPC/ 30 % DOPG) is shown below. Similar observations made for PL with other lipid compositions (II – V). Bands are indicated for tagged-SecY (His-EK-SecY) and digested SecY (SecY). +: Treated with EK, -: no protease added. The cleavage conducted at least in technical duplicates, the mean values and standard deviation (SD) are shown.

enterokinase (EK) and subsequent analysis by SDS-PAGE (Figure 3.3, C). When the N-terminus is exposed outwards and accessible for cleavage, the translocons are reconstituted in the functionally relevant orientation, as the conductive channel is oriented towards the vesicular lumen. The results indicated that approximately 50 – 70 % of the translocons were in the correct orientation after the reconstitution (Figure 3.3, C), which was in line with results observed for SecYEG of *E. coli* (Kamel *et al.*, 2022).

Although protein translocation utilizes SecYEG as the conductive channel through the membrane, the transport procedure is only enabled through interactions with the motor ATPase SecA which provides the required energy. Upon protein translocation, interactions of SecA with SecYEG are essential. To examine the binding between SecYEG and SecA, microscale thermophoresis experiments (MST) were conducted. Membranes harboring the overexpressed single-cysteine variant of the translocon $SecYE_{S118C}G$ were utilized for isolation by polymer-based extraction with DIBMA forming directly near-native nanodiscs (near-native NDs), and were further fluorescently labeled (Figure 3.4, A). The obtained near-native NDs were tested for binding to SecA, revealing K_D of 75 ± 10 nM (Figure 3.4, B).

These results indicate that isolated SecA and SecYEG are capable to interact. The SecA:SecYEG interaction is crucial for reconstitution of the Sec-dependent protein translocation *in vitro*. Additionally, the holdase action of SecB was investigated by conducting sedimentation analysis with the lipase precursor (proLipA) in presence or absence of the holdase chaperone and varying ionic strength. The preprotein proLipA is sensitive to salt and it sediments already up to ~ 50 % at moderate KOAc concentration of 50 mM (Figure 3.4, C). The sedimentation is likely caused by instant aggregation of the lipase precursor and is partially in line with observations made for the mature LipA (Papadopoulos *et al.*, 2022). When SecB is added to the sedimentation reaction, proLipA remains in the soluble fraction, indicating the holdase action of SecB (Figure 3.4, C). SecB can hold ~ 40 – 70 % of proLipA in solution with respect to the ionic strength in the reaction conditions (Figure 3.4, C).

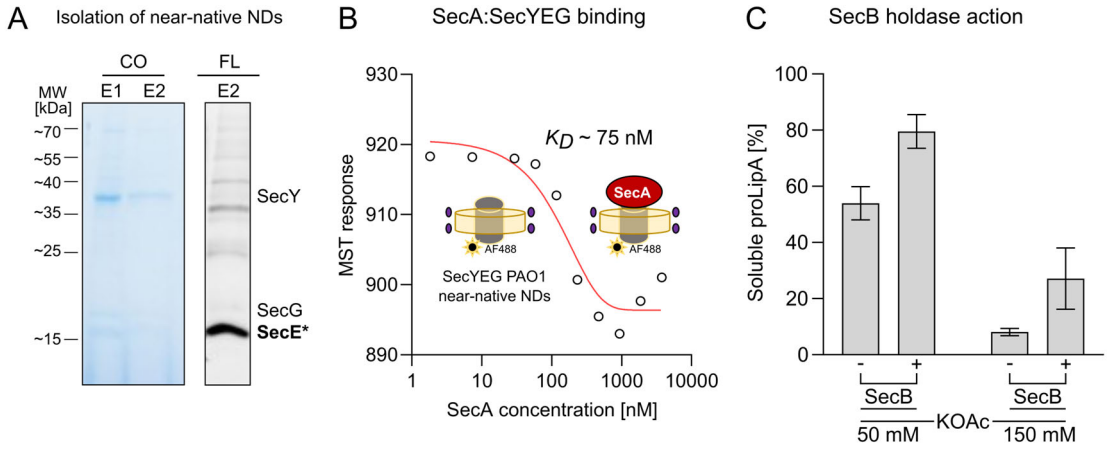

Figure 3. 4: Interactions of Sec components of *P. aeruginosa* PAO1

A: Polymer extracted (DIBMA) and fluorescently labeled (star: Alexa Fluor 488) $SecYE_{S118C}G$ near-natives nanodiscs (NDs). Coomassie-stained and fluorescence images of corresponding SDS-PAGE of the elution fractions (E1 and E2) are shown and protein bands are indicated. MW: Molecular weight indicated in kDa. **B**: Microscale thermophoresis (MST) disclose strong binding of SecA to SecYEG (K_D ~ 75 nM). The scheme represents near-native NDs harboring labeled SecYEG alone or when bound to SecA. **C**: Sedimentation analysis of lipase precursor (proLipA) indicates holdase action of SecB. The soluble fraction of proLipA in presence (+ SecB) or absence (- SecB) is depicted upon application of varying ionic strength (50 and 150 mM KOAc). The assay was performed in technical triplicates, the mean values and standard deviation (SD) are shown.

Combining the individual Sec components together results in the creation of minimal transport system *in vitro* which should be sufficient to facilitate protein transport through the isolated IMVs and proteoliposomes. Focused on the Sec system of *P. aeruginosa,* the homologous *E. coli* Sec system and the model transport substrate proOmpA were used as well-established references. When IMVs containing SecYEG of either bacteria were employed, the translocation assays resulted in equal transport efficiencies of proOmpA (~ 30 %) for both Sec systems (Figure 3.5, A). These results indicated the successful *in vitro* reconstitution of the Sec system of *P. aeruginosa* PAO1, being capable of protein translocation up to the same degree as the well-studied *E. coli* Sec system. Efforts were made to accomplish the Sec-mediated transport of proLipA, but the transport efficiency was very low (< 1 %),

below the reliable detection level. Recent investigations have revealed that the hindered transport might correlate with the high aggregation propensity of the lipase (Papadopoulos *et al.*, 2022) or suggest that the inefficient transport might arise from hindered lipase targeting to the SecA:SecYEG machinery. Additionally, intrinsic features of the secretory protein, including kinetically unstable folding intermediates, are determinative for preprotein transport (Tsirigotaki *et al.*, 2018). In aim to avoid instant aggregation of the lipase, the acquired stabilizing mutation F144E (Papadopoulos *et al.*, 2022) was introduced (proLipA$_{F144E}$). Unfortunately, the transport efficiency remained low with up to ~ 1.7 % (Figure 3.5, A).

To probe the functionality of the Sec system of *P. aeruginosa* PAO1 in a well-defined membrane system, proteoliposomes of tailored lipid composition were utilized. Previous observations indicated decreased transport efficiency when proteoliposomes were utilized for the transport reaction. The transport efficiency indicates to be dependent on the lipid composition of the proteoliposomes. To enhance transport in proteoliposomes, optimization procedures were required leading to the addition of tetraoleoyl cardiolipin (TOCL) upon formation of model membranes, as it manifests stimulatory effects on the Sec-mediated protein transport (Gold *et al.*, 2010). The resulting proteoliposomes indicated a transport efficiency for proOmpA of ~ 15 % (Figure 3.5, B). Further translocation substrates (depicted in Figure 3.2, B) were tested for Sec-dependent transport in IMVs, but the transport efficiency remained very low (< 5 %). Only proFapC indicated an immediate relatively increased transport efficiency with (> 3 – 5 %), that was later confirmed in further ongoing investigations reaching up to 10 % (in collaboration with Max Busch).

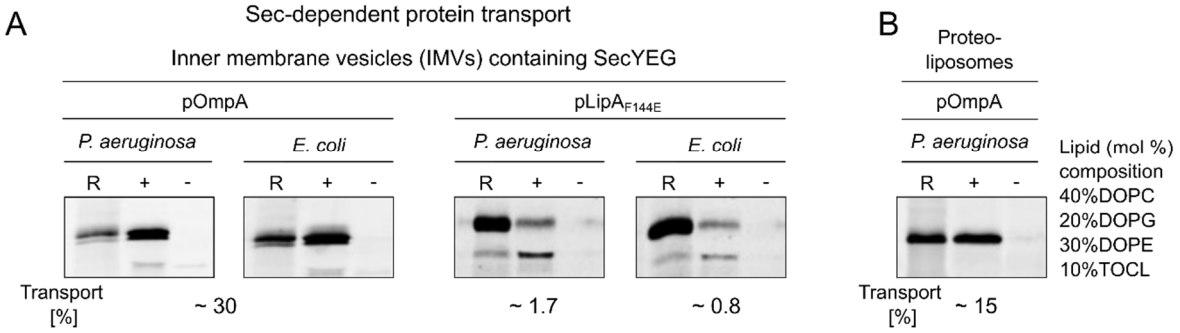

Figure 3. 5: Sec-dependent protein transport and lipase translocation of *P. aeruginosa* PAO1

A: The *in vitro* protein transport of the fluorescently labeled lipase A (pLipA$_{F144E}$) and proOmpA (pOmpA) into inner membrane vesicles (IMVs) is shown for IMVs containing overexpressed SecYEG translocons of *P. aeruginosa* or *E. coli*. The buffer of the transport reaction for pOmpA into IMVs with *P. aeruginosa* SecYEG was 20 mM Tris/HCl pH 7.5, 150 mM KOAc, 5 mM Mg(OAc)$_2$, 5 % glycerol and for the other reactions as described in the method section. **B:** *In vitro* protein transport in proteoliposomes containing *P. aeruginosa* SecYEG is shown for the model substrate pOmpA. The lipid composition is depicted in the figure. R: 10 % of total substrate input. +/-: transport with and without ATP. Transport indicated in %.

3.3.3 Investigations made to improve the transport of the lipase A

Since the Sec system of *P. aeruginosa* PAO1 was successfully reconstituted and applied to track protein transport *in vitro*, multiple approaches were taken to enhance the Sec-dependent transport efficiency of the lipase A. To rule out the possibility that the intramolecular disulfide bond formation causes spatial hindrance upon translocation of the lipase or that the used fluorescent labeling agent jams the translocon, a single-cysteine variant (C183S) of the proLipA$_{F144E}$ was generated. Additionally, this lipase variant was labeled with the smaller fluorescent dye BODIPY-maleimide. The relative transport efficiency of the single-cysteine variant of proLipA$_{F144E}$ remained low. It is important to mention that no hindrance upon transport was observed for F5M-labeled proOmpA, where the transport through Sec is highly efficient (Figure R5, A). Further, a truncation of 34 amino acid residues was introduced at the C-terminal end of proLipA in aim to overcome possible and/or partial misfolding of the lipase, but here also the transport remained low and far off a comparable range which is commonly observed in transport studies with proOmpA. Further factors that could possibly enhance the Sec-mediated lipase transport were investigated. The SecYEG translocon of *P. aeruginosa* PAO1 was modified to become less specific for the transported substrates, including point mutations found in the *prlA4* mutant of *E. coli* being less selective and allowing for enhanced transport of proteins (Van Der Wolk *et al.*, 1998; de Keyzer *et al.*, 2002). Therefore, a double mutant of the *Pseudomonas* translocon (SecY$_{F218Y,I403N}$EG) was created. Indeed, the transport efficiency of proOmpA increased up to ~ 40 % (Figure 3.6, A), indicating the expected effect of the mutations. Although the transport efficiency for proLipA$_{F144E}$ slightly increased to ~ 2 % upon utilization of the *prlA4* mutant in comparison to non-mutated SecYEG with ~ 0.6 % (Figure 3.6, A), the transport remained low and not in comparable range to proOmpA.

Repeatedly poor translocation of proLipA raised the question, whether the targeting of the lipase precursor to the Sec machinery is forming a bottleneck for translocation. This pointed the focus on the signal peptide (SP) of the lipase. Since several studies reported that bioengineered signal peptides and/or those from other bacterial origin may be suitable for enabling the targeting and secretion of fusion protein (Sockolosky and Szoka, 2013; Freudl, 2018; Kaushik, He and Dalbey, 2022), commonly used SP of the well-studied proOmpA from *E. coli* and the commercially available SP of the periplasmic pectate lyase (PelB) from *Erwinia carotovora* were fused to LipA. Exchanging the SP of LipA did not lead to increase of transport of the lipase (Figure 3.6, A). Further mutual stabilizing effects of the SP and the mature domain were not observed. Also, the combination of the several approaches was not leading to an increased transport efficiency. Taken together, these observations indicate that the transport efficiency of the lipase through the Sec machinery is not only determined by the Sec system itself but might be strictly dependent on the unique properties of the preprotein. Additionally, based on these observations, the question raised, whether there are further proteins involved in lipase targeting to the Sec system. To answer this question, two ATP-independent cytoplasmic chaperones, trigger factor (TF) and CsaA, were investigated besides SecB in aim to prevent proLipA aggregation and support its targeting to SecA:SecYEG. While CsaA supports the protein export in absence of SecB , TF directly

contacts the ribosome and grabs the nascent polypeptide and is further able to interact with SecB (Sharma, Rani and Goel, 2018; De Geyter *et al.*, 2020). Both chaperones, TF and CsaA, were cloned, overexpressed, purified, and characterized. Structural analysis of the cytoplasmic chaperones was conducted by small X-ray scattering (SAXS) experiments, revealing the surface envelope of the proteins (Figure 3.6, B). The data indicates that TF is present as a monomer, while CsaA is dimeric in solution. The homology models of the proteins were generated by Phyre2 (Kelley *et al.*, 2015), and fit into the SAXS envelope (Figure 3.6, B). Both chaperones did not lead to an increased transport efficiency of proLipA. Thus, since multiple ATP-dependent chaperones are widely present in the cytoplasm and possess manifold effects on protein homeostasis, DnaK (Hsp70), DnaJ (Hsp40) and HtpG (Hsp90) were applied in further attempts to facilitate the lipase translocation. ATP-dependent chaperones play a crucial role in various protein-maintaining processes and can assist to prevent aggregation (Castanié-Cornet, Bruel and Genevaux, 2014). Preliminary results indicate only moderate effects of the utilized chaperones on the lipase stabilization and translocation (Busch, 2021).

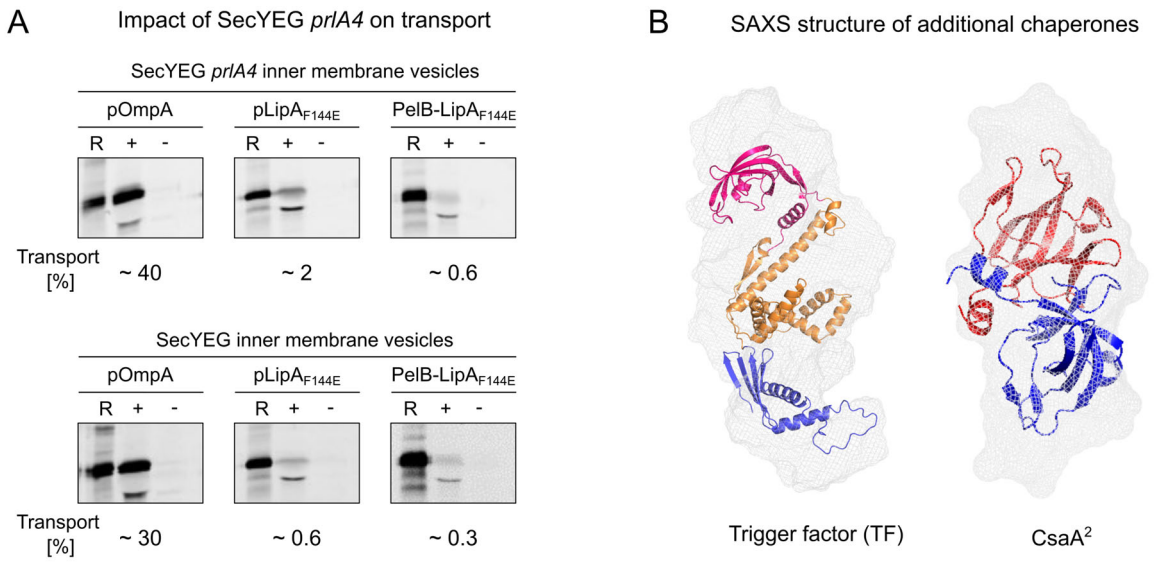

Figure 3. 6: Factors investigated in aim to improve the Sec-dependent lipase transport

A: The impact of SecYEG *prlA4* mutant on *in vitro* protein transport of the lipase A (pLipA$_{F144E}$) and the model substrate proOmpA (pOmpA) as well as signal peptide exchanged LipA (PelB-LipA$_{F144E}$) is shown in comparison to non-mutated SecYEG. Substrates are fluorescently labeled. R: 10 % of total substrate input. +/: transport with and without ATP. Transport indicated in %. The buffer of the transport reaction was 50 mM Hepes/KOH pH 7.4, 20 mM KCl. **B:** The SAXS envelope for the ATP-independent cytoplasmic chaperones is shown (grey mesh). The homology models are fitted inside. Trigger factor (TF) monomer is colored based on its domains (pink: head domain (Peptidyl-Prolyl Isomerase, orange: body and arms for folding and holding, blue: tail for interacting with ribosome). CsaA dimer is colored for each monomer (red and blue).

3.4 Discussion

The Sec system represents a general pathway for protein export among all domains of life. In bacteria approximately 30 % of the proteome are destined for functioning beyond the cytoplasm, including proteins which act in the cell envelope as well as in the extracellular space. The lipase A, the major extracellular lipase of the opportunistic human pathogen *Pseudomonas aeruginosa*, serves as a virulence factor secreted upon the infection cycle (Jaeger *et al.*, 1994; Stehr *et al.*, 2003). Establishing the Sec system of *P. aeruginosa* PAO1 *in vitro* imposes the first step to study the lipase translocation and can help to elucidate processes ongoing upon the lipase biogenesis. The expression, purification, and characterization of the Sec system of *P. aeruginosa* PAO1 was achieved progressively, and the soluble Sec components were structurally characterized. SAXS structure and homology modeling of SecB indicated the tetrameric assembly, in agreement with the previous reports on SecB of *E. coli* and *Haemophilus influenzae* which is described as "dimer of dimers", indicating its functional state (Huang *et al.*, 2016). For the motor ATPase SecA, SAXS revealed a dimer in solution which resembles a "donut-like" shape observed in crystal structures of SecA from *Mycobacterium tuberculosis* (Sharma *et al.*, 2003) and *Bacillus subtilis* (Hunt *et al.*, 2002), but not *E. coli* (Papanikolau *et al.*, 2007). The ATPase SecA was capable of binding to the translocon SecYEG, which is crucial for protein translocation.

The isolation of the translocon SecYEG from the membrane was conducted by detergent-based solubilization. Therefore, SecYEG was solubilized by DDM, that was also used in previous studies for the translocon of *E. coli* (van der Does *et al.*, 2000). Although previous studies suggested that the oligomeric state of the *E.coli* translocon can be modified by increased detergent concentration (Bessonneau, 2002), increasing the concentration of DDM in the present experiments did not lead to monomerization of SecYEG of *P. aeruginosa* PAO1. The oligomeric state of the translocon in the detergent micelles was analyzed by SEC-MALS, suggesting that the dimeric state could be preferred upon the applied experimental conditions. It is valid to question whether these results indicate a tendency of the translocon to form preferably the dimeric state in detergent micelles or whether the observed occurrence of two copies of SecYEG is just due to the micelle size itself. On the one hand, nearly no difference was observed upon SEC-MALS in the elution volume and the molecular weight of the translocon in both analyzed DDM concentrations, 0.05 and 0.1 % (w/v). On the other hand, if the dimeric state is not a preferred state of the translocon, then decreased detergent concentration or detergents with smaller micelle size would probably promote the occurrence of a single copy of the translocon inside the smaller micelle. The oligomeric state of the detergent-solubilized translocons cannot be directly compared to its membrane-reconstituted state due to the absence of the lipid environment. Thus, the dimeric state of the translocon might be an inherent feature of the protein which is influenced by a combination of the environmental factors and interaction partners, both in detergent and the membrane environment. Previous research indicated that for the translocon of *E. coli* the dimeric state is partially supported in the lipid bilayer and can vary in dependence to its binding partners (Koch *et al.*, 2021). It is also possible, that the stable and/or oligomeric state of the translocon is influenced by the remaining

lipids, which are not removed upon solubilization with mild detergents. The delipidation of the translocon could affect its functional state, since already previous studies of reconstituted translocons of *E. coli* indicated a strict dependence of transport activity on identity of the surrounding phospholipids (van der Does *et al.*, 2000). Nonetheless of the origin of SecYEG dimerization, the completed biochemical and partially structural characterization indicated the functional states of the individual Sec components and provided the required information in aim to reconstitute the Sec system *in vitro*.

The Sec translocon of *P. aeruginosa* PAO1 was isolated in inverted inner membrane vesicles (IMVs) or reconstituted in proteoliposomes of tailored lipid composition. The application of the primary Sec components allowed to track protein translocation *in vitro*. To improve the translocation efficiency *in vitro*, IMVs harboring the overexpressed translocon of *P. aeruginosa* PAO1 were utilized. The IMVs represent a near-native environment for the translocon and allow to overcome the otherwise necessary reconstitution step of the membrane protein. Furthermore, IMVs contain additional facilitative factors, like endogenous SecDF which facilitates the release of secretory proteins from the translocon at late translocation stage, thus promoting the translocation efficiency (Tsukazaki, 2018). The well-known model substrate, proOmpA of *E. coli*, was utilized to estimate the functionality of the *Pseudomonas* Sec system in comparison to the Sec system from *E. coli*. The Sec system of *Pseudomonas* indicates a comparable transport efficiency for proOmpA when protein translocation was analyzed into IMVs. In contrast, the application of the minimal Sec system containing the soluble proteins SecA and SecB as well as the translocon SecYEG reconstituted in proteoliposomes required an optimized lipid composition, and thus indicated a lipid-dependent translocation efficiency different to that of *E. coli*. The presence of tetraoleoyl cardiolipin (TOCL) in the tailored proteoliposomes increased transport efficiency for proOmpA through the *Pseudomonas* Sec system and confirmed the previously observed stimulatory effect of cardiolipin on the Sec-mediated protein transport (Gold *et al.*, 2010). Cardiolipin (CL) is closely associated with SecYEG where it is suggested to possess stabilization effects of the dimeric state of the translocon (Gold *et al.*, 2010). Furthermore, CL supports tight binding of the ATPase SecA to the membrane and thus enhances the hydrolysis of ATP (Gold *et al.*, 2010; Collinson, 2019). The low translocation efficiency and the lipid dependency possibly correlated due to the individual requirements of SecA to bind peripherally to the membrane. As indicated for *E. coli*, cardiolipin and phosphatidyl-glycerol (PG) are crucial for SecA membrane binding (Collinson, 2019; Kamel *et al.*, 2022). The N-terminal helix of SecA, which differs in between of *P. aeruginosa* and *E. coli*, was shown to mediate the binding of SecA to the membrane, thus affecting the SecA:SecYEG assembly and determining the translocation efficiency (Kamel *et al.*, 2022). Further investigations on SecA:lipid interactions are required to elucidate the membrane-binding properties of SecA from *P. aeruginosa* PAO1.

Although, the reconstitution of the functional Sec system of *P. aeruginosa* PAO1 *in vitro* represented a challenging task it was finally accomplished. The *Pseudomonas* Sec system indicated the same degree of functionality as observed for the reference Sec system of *E. coli*. The functional reconstitution of the

Pseudomonas Sec system is the first step to study the lipase translocation. Another essential task was to obtain the translocation-competent lipase precursor (proLipA). The expression and purification of the precursor proteins appeared to constitute a challenging process, including multiple pitfalls, like the low or no detectable expression levels, lack of accumulation in the cytoplasm possibly due to degradation and/or export of preproteins, difficulties in purification of the preproteins in form of inclusion bodies and unfolding by chaotropic salts (urea and GdnHCl). Thus, the expression and purification of proLipA, as well as further substrates required extensive optimizations, and successful expression of the preproteins could be achieved after codon optimization. The occurrence of "non-optimal" codons in secretory proteins of *E. coli* could slow down the translational rates (Power *et al.*, 2004; Tsirigotaki *et al.*, 2017), and corresponding codon analysis of *P. aeruginosa* preproteins suggest that rare codons are also present which could inhibit heterologous expression. Especially the codon usage in the gene sequence encoding for the signal peptide (SP) of the Sec-dependent preproteins plays a role in protein export, by containing non-optimal codons which are important for a balanced gene expression, folding and export *in vivo* (Zalucki, Beacham and Jennings, 2009). In turn, the presence of non-optimal codons might be unbeneficial for the heterologous overexpression of preproteins. For multiple tested substrates the partial or complete codon optimization of the gene sequence encoding for the SP led to successful overexpression of the preprotein. The accumulation of the preprotein was achieved by inhibition of protein export via sodium azide treatment upon the overexpression. Sodium azide is a potent inhibitor of SecA interfering with the metal-binding properties of the protein (Cranford-Smith *et al.*, 2020). Inactivation of the primary export machinery might be deleterious for the cell over time, but the approach seems to be suitable to accumulate preproteins in the cytoplasm over the short time of overexpression.

The isolated preproteins originating from *P. aeruginosa* PAO1 were applied for *in vitro* translocation through the Sec system. None of the *Pseudomonas* preproteins was transported with high efficiency in comparison to the model substrate proOmpA from *E. coli*. Only proFapC indicated a slightly increased transport efficiency in comparison to the other *P. aeruginosa* preproteins. The low transport efficiency of the preproteins could be due to various causes. The hindered transport could be related to instant aggregation of the preprotein, although the presence of the N-terminal SP should keep the preprotein more soluble. SP may not only affect the rate of translation of the protein, but it has also an impact on targeting, as it slows down the folding of the preprotein, thus reserving time for protein:chaperone interactions which support secretory processes (Zalucki, Beacham and Jennings, 2009; Freudl, 2018; Smets *et al.*, 2022). Additionally, the delicate relationship of SP and the mature domain of secretory proteins has been proposed to function in a "rheostatic" manner, therefore signal peptides can finely tune the disorder of the mature domains and are essential for targeting and secretion (Sardis *et al.*, 2017). It is also proposed that the disorder of the mature domains of preproteins results in folding intermediates which predominate the targeting-competence of secretory proteins (Chatzi *et al.*, 2017). In addition, cytoplasmic chaperones are important targeting mediators. The requirement for targeting to the Sec machinery might be varying for the different preproteins. It is discussed that, although the majority of

secretory proteins are targeted via SecB to the SecA:SecYEG machinery for translocation, some preproteins can be recognized by SecA alone or require the interaction of further chaperones (Chatzi *et al.*, 2014). Furthermore, additional ATP-independent chaperones could be involved in preprotein targeting to the Sec, including trigger factor (TF) that can directly capture the preprotein at the ribosome *in vivo*, and CsaA that is a functional homolog of SecB which is present in *P. aeruginosa* PAO1 but not in *E. coli* (Sharma, Rani and Goel, 2018; De Geyter *et al.*, 2020). Since SecB indicated to prevent the aggregation of proLipA, it was utilized upon *in vitro* translocation analysis, but did not enhance the transport efficiency. In addition to SecB, TF and CsaA were tested in *in vitro* transport of proLipA, but also did not indicate an increased transport efficiency.

It is possible that the translocation of proLipA could be hindered not only due to inefficient targeting, but rather the formation of folding intermediates which are not competent for translocation. Folding intermediates are not necessarily protein aggregates, but also not unfolded states of the preprotein which would support its translocation-competence. Furthermore, the disulfide oxidation *in vitro* could pose a major barrier for translocation, as the lipase contains an intramolecular disulfide bridge formed in its mature domain. The cytoplasm is a reducing environment where the formation of a disulfide bridge is not promoted. Single-cysteine proLipA variant was checked upon *in vitro* translocation in aim to rule out the formation of disulfide bond, but did not indicate sufficient translocation efficiency, thus pointing away from the hypothesis that the disulfide bond formation prohibits sufficient translocation. In turn, these observations stress that the preprotein might fold into intermediate folding state not competent for translocation *in vitro*. An additional concern is that the foldase LipH might be involved upon translocation process. Possibly, the foldase recognizes and interacts with the emerging proLipA at an early translocation step, thereby creating a pull force which is important to fulfill translocation through the translocon. This argument finds its parallel thoughts when, considering the role of SecDF upon translocation process. SecDF facilitates the release of the emerging preprotein from the translocon when most of the protein is already translocated. The effect of SecDF is dependent on the preprotein itself. Considering on what is known about proOmpA, the action of SecDF might be sufficient to support proOmpA transport, but not for other translocation substrates. Thus, for proLipA a similar requirement could be the case, that LipH is needed to pull on the emerging preprotein and facilitate its transport. Additionally, a less specific mutant of the *Pseudomonas* translocon SecYEG was created, following the previous mutations introduced for the *E. coli* translocon (Van Der Wolk *et al.*, 1998; de Keyzer *et al.*, 2002). Although the mutant translocon indicated increased transport efficiency for proFapC upon initial screenings (in collaboration with M. Busch), the proLipA transport efficiency was not increased, pointing again on the substrate being not competent for translocation *in vitro*.

It remains to be clarified, why proLipA is not translocation-competent *in vitro*, and whether the limitations originate from inherent features of the substrate or are based on technical and methodical aspects. Thinking of the methodical limitations, the purified substrate for translocation is expressed in inclusion bodies and then unfolded by the usage of high molar concentrations of chaotropic agents, such

as urea or guanidinium chloride. The working principle of those chaotropic agents is to structure the water molecules in the surrounding aqueous environment allowing the protein to expose its hydrophobic regions and enabling it to unfold and to not suffer hydrophobic collapse (Salvi, De Los Rios and Vendruscolo, 2005). But it remains elusive which intermolecular protein:protein interactions can still occur (Singh *et al.*, 2015). Although the effect of the chaotropic agent might not favor translocation of proLipA *in vitro*, the same procedure works for the model substrate proOmpA, an outer membrane protein with a distinct distribution of polar and apolar amino acids. When proLipA is added to the *in vitro* transport reaction and thus transferred into the aqueous solution, it may undergo fast folding into intermediates that are not competent for transport. Furthermore, this rapid dilution could also promote aggregation of proLipA. Stunningly, only proOmpA which is widely used for translocation studies, could be transported with an increased efficiency of approximately 20 – 30 %. Not many other substrates for translocation, besides proOmpA, are that frequently used or indicate such efficient transport levels, and examples include proPhoA, proMBP and proLamB (van der Does *et al.*, 2000; de Keyzer, van der Does and Driessen, 2002; Bariya and Randall, 2019). Sticking only to proOmpA, the best and most established Sec-substrate, might not be sufficient in aim to characterize the Sec system of further bacterial species. Therefore, more nuanced models for studying Sec-mediated protein translocation are needed, especially when comparing the newly established Sec system of *P. aeruginosa* PAO1 upon highly challenging translocation of the pathogenicity-mediating lipase to the well-studied Sec system of *E. coli* with proOmpA. Furthermore, elaboration on the *in vitro* Sec-transport of various substrates originating from *P. aeruginosa* that are involved in pathogenicity of this bacterial species will be valuable.

Taken together, the results indicate that the activity of the newly established Sec system of *P. aeruginosa* PAO1 is comparable to the model Sec system of *E. coli.* However, the translocation process of proLipA and further substrates of *P. aeruginosa* PAO1 is a highly challenging venture, at least under *in vitro* conditions. Approaches to solve the aggregation, intermediate folding and targeting of proLipA to the Sec system improved the transportation slightly, but not to the desired degree. Using proFapC as a virulence-associated factor could serve to elucidate transport and secretion of factors involved in pathogenicity of bacterial pathogens and represent a further suitable approach.

4 Chaperone-dependent folding and maturation of the lipase A

4.1 Introduction to the chaperone-dependent folding and maturation of the lipase A

The biogenesis of the lipase A of *P. aeruginosa* is a procedure that includes different steps, starting from synthesis to translocation of the preprotein into the periplasm, followed by the maturation and secretion of the active virulence factor. During these processes LipA undergoes multiple interactions with its molecular environment. Although the initial release from the ribosome and subsequent protein translocation from the cytoplasm to the periplasm manifest the primary steps upon lipase biogenesis, the essential folded state is acquired afterwards on the periplasmic site (Rosenau, Tommassen and Jaeger, 2004). Once LipA is translocated, its maturation is promoted by the specific folding mediator LipH (Rosenau, Tommassen and Jaeger, 2004). The foldase LipH is a membrane-bound chaperone which provides the required steric information specifically to its client lipases and enables them to overcome the energetic folding barrier (Pauwels *et al.*, 2007). The chaperone domain of LipH protrudes into the periplasm, being distantly spaced from the membrane interface and the anchoring transmembrane helix by an unstructured proline- and alanine-rich variable domain (Rosenau, Tommassen and Jaeger, 2004). It is suggested that the anchoring of the foldase evolved in aim to avoid co-secretion with the lipase, as the lipase-specific foldase and the lipase are tightly interacting with each other upon folding. Structural information on the lipase:foldase complex of *Burkholderia glumae* indicates a large interaction interface between two proteins, supporting tight binding (Pauwels *et al.*, 2006). The peculiar structure of LipH suggests a high degree of plasticity which might be important for its mode of action (Pauwels *et al.*, 2006; Dittrich *et al.*, 2023). The exact folding mechanism remains widely elusive, although manifold investigations were conducted and a foldase consensus motif was identified (Rosenau, Tommassen and Jaeger, 2004). In addition, tight lipase:foldase binding suggest a challenge for the release of the lipase, which might require interaction with a further protein of the secretory machinery (Pauwels *et al.*, 2006).

The acquired information on LipA:LipH interactions originates solely from investigations utilizing the soluble foldase domain. How the folding of the lipase by the foldase could be affected at the membrane interface remains elusive. In aim to elucidate the folding and maturation the lipase A of *P. aeruginosa* PAO1, the foldase LipH was characterized. Here, for the first time, the successful expression, purification, and biochemical characterization of the full-length foldase LipH in the membrane environment were conducted. In addition, the soluble chaperone domain of LipH as well as the lipase:foldase complex were used for structural analysis which allowed to obtain low-resolution structural information.

4.2 Experimental Procedures

4.2.1 Molecular cloning

The following section focuses on the main working constructs used for heterologous expression of foldase LipH and the lipase A. A tabular overview is listed in the appendix section. The genes of *P. aeruginosa* PAO1 strain were selected using *Pseudomonas* Genome database (www.pseudomonas.com) (Winsor *et al.*, 2016). Those included PA2862 (*lipA*), PA4813 (*lipC*), PA2863 (*lipH*) as well as genes PA4243 (*secY*), PA4276 (*secE*), PA4747 (*secG*) encoding for the translocon SecYEG that were mentioned in beforehand (Chapter 3.2.1). The genomic DNA of *P. aeruginosa* PAO1 served as a template for gene amplification via PCR, using the KOD Xtreme polymerase (Novagen/Merck) or the Phusion High-Fidelity DNA Polymerase (Ultra DNA Polymerase, Jena Bioscience) as well as cloning primers containing the restriction sites for classical cloning, overlaps for Gibson assembly or constructed to suit for site-directed mutagenesis unless otherwise stated. The DNA concentrations were determined spectrophotometrically by measuring the absorbance at 260 nm via NanoDrop (Thermo Fisher Scientific). The target genes were inserted into the cloning vectors by restriction-based cloning procedures or Gibson assembly based on the supplier protocols (New England Biolabs). Further, site-directed mutagenesis served for modification of the created constructs. The enzymes and chemicals required for molecular cloning were used based on the supplier protocols (New England Biolabs).

The construct encoding for the mature LipA (pAT72) was created by inserting PA2862 (*lipA*) gene into pET22b plasmid by *NdeI/BamHI* oriented on previous research (Hausmann *et al.*, 2008). Site-directed mutagenesis of this construct allow to generate a further plasmid encoding for the mutant $LipA_{F144E}$ (pAT81) (Papadopoulos *et al.*, 2022). Truncations at the C-terminal (pAT149, lacking 81 amino acids) and N-terminal (pAT152, lacking 7 amino acids) ends of the lipase A were generated by site-directed mutagenesis using the construct encoding for $LipA_{F144E}$ (pAT81) as a template.

The construct encoding for the soluble domain of the foldase LipH (pAT9 and pEHTHis19) was used as for previous research (Hausmann *et al.*, 2008). To create suitable expression vectors for the full-length foldase ($LipH^{FL}$), the gene of interest PA2863 (*lipH*) was initially inserted into pTrc99a-based plasmid encoding of His_{10}-3C $LipH^{FL}$ (pAT8) with prolonged N-terminus. Furthermore, to promote expression levels, pRSFDuet-1-based plasmid encoding for His_8-3C $LipH^{FL}$ was created by insertion of *lipH* gene via *NotI/NheI* restriction sites (pAT56) featuring the expression in kanamycin selective media. The resulting constructs were utilized for further experiments. Initially, in aim to generate a construct which is suitable for the co-expression of LipH/SecYEG the fragment encoding for His_{10}-3C-LipH (from pAT8) was inserted into pTrc-based construct that encodes for His_{10}-3C-SecYEG via Gibson assembly (pAT66). As the prolonged tag on SecYEG inhibited *in vitro* transport, the N-terminal tag was shortened via site-directed mutagenesis (pAT108). The final construct (pAT108) encodes for His_6-EK-SecYEG/His_{10}-3C-LipH.

4.2.2 Expression and purification

The lipases (LipA and $LipA_{F144E}$), C- and N-terminal truncations, as well as soluble foldase variants were expressed and isolated according to existing protocols (Papadopoulos *et al.*, 2022), unless otherwise stated. To express and purify the full-length foldase LipH, the developed constructs were heterologously overexpressed in *E. coli* expression strains. Multiple common detergents have been screened in aim to solubilize $LipH^{FL}$ from the membrane as well as polymer-based extraction was conducted. Furthermore, the proteins have been purified by immobilized metal ion affinity chromatography (IMAC) and subsequent size exclusion chromatography (SEC). The concentration of purified proteins was determined spectrophotometrically by the absorbance (A) at 280 nm and the molar extinction coefficient obtained by ProtParam tool (Gasteiger *et al.*, 2005). The purification efficiency was further evaluated by SDS-PAGE stained with colloidal chemical Coomassie solution (Quick Coomassie stain, Serva). To enable loading for SDS-PAGE, the protein samples were mixed with 5 x sample loading buffer (0.25 M Tris/HCl pH 6.8, 0.5 M DTT, 10 % SDS, 60 % glycerol, 0.02 % (w/v) bromophenol blue, modified from Jena Biosciences).

4.2.2.1 Expression and purification of the full-length foldase LipH

The full-length foldase ($LipH^{FL}$) was heterologously expressed in *E. coli* BL21(DE3). Pre-cultures were grown overnight at 37°C upon shaking at 180 rpm and used for inoculation of pre-warmed LB medium (Luria-Bertani medium or lysogeny broth, yeast extract 5 g/l, tryptone 10 g/l, NaCl 10 g/l). Cells were grown at 37°C upon shaking at 180 rpm while the OD of the culture was monitored. At OD_{600} of ~ 0.6, overexpression was induced upon addition of 0.5 mM isopropyl-β-D-thiogalactopyranoside (IPTG; Merck/Sigma-Aldrich) and carried out for 2 h keeping constantly the same growth conditions. The cells were harvested by centrifugation at 6000 *g* for 20 min at 4°C (rotor SLC-6000, Sorvall/Thermo Fisher) and subsequently resuspended in 20 mM Tris (hydroxymethyl)aminoethane/HCl pH 8.0, 100 mM NaCl, 1 mM DTT (Merck/Sigma-Aldrich), 5 % glycerol and cOmplete protease inhibitor cocktail (1 pill/50 ml; Roche), unless otherwise mentioned. Cells were lysed by shear force (M-110P cell disruptor Microfluidics Inc.). The cell debris was removed by centrifugation at 10000 *g* for 10 min at 4°C (rotor SS34, Sorvall/Thermo Fisher). To pellet the crude membranes, including the inner membranes harboring the overexpressed foldases, ultracentrifugation at 205000 *g* for 1 h at 4°C (rotor 45 Ti, Beckman Coulter) was conducted. The membranes were resuspended in the same buffer (20 mM Tris/HCl pH 8.0, 100 mM NaCl, 1 mM DTT, 5 % glycerol, and cOmplete protease inhibitor cocktail) unless otherwise mentioned and stored at -80°C until further usage. In aim to solubilize the full-length foldase, n-dodecyl-β-D-maltopyranoside (DDM) and n-decyl-β-D-maltopyranoside (DM) were utilized. The screened solubilization conditions included either 2 % (w/v) DDM or 3 % (w/v) DM (Anatrace) in 50 mM Tris/HCl pH 8.0, 100 mM NaCl, 0.2 mM TCEP, 10 % glycerol, and cOmplete protease inhibitor cocktail for 1 h at 6°C on a rolling table. After solubilization, the samples were centrifuged at 20000 *g* for 10 min at 4°C (Hermle Z216 M) to remove non-soluble material and then applied for purification by immobilized metal ion affinity chromatography (IMAC). His-tagged foldases were immobilized on

nickel-nitrilotriacetic acid agarose resin (Ni^{2+}-NTA resin; Qiagen) equilibrated with wash buffer (50 mM Tris/HCl pH 8.0, 100 mM NaCl, 0.2 mM TCEP, 20 mM imidazole, cOmplete protease inhibitor cocktail, including the detergent of choice). The detergent concentrations for the washing and elution steps were set to be ~5-fold above the specific critical micelle concentrations (CMC) resulting in 0.05 % (w/v) for DDM and 0.45 % (w/v) for DM. The samples were applied to the Ni^{2+}-NTA resin for binding for 1 h at 6°C on a rolling table. Afterwards, the resin was washed extensively with wash buffer to remove weakly bound impurities, and the protein was eluted with elution buffer (50 mM Tris/HCl pH 8.0, 100 mM NaCl, 0.2 mM TCEP, 300 mM imidazole, 10 % glycerol, cOmplete protease inhibitor cocktail) in several fractions. When indicated, the protein was applied for size-exclusion on Superdex 200 Increase 10/300 GL column (Cytiva) in the desired buffer compositions (e.g., 50 mM Tris/HCl pH 8.0, 100 mM NaCl, 0.2 mM TCEP, 10 % glycerol, 0.5 % DM) unless otherwise stated. The concentration of the purified $LipH^{FL}$ was determined spectrophotometrically and the purification yield was further analyzed SDS-PAGE stained with colloidal chemical solution (Quick Coomassie stain, Serva).

4.2.2.2 Co-expression and purification of the SecYEG/LipH

The construct encoding for SecYEG/$LipH^{FL}$ of *P. aeruginosa* PAO1 was heterologously expressed in *E. coli* C41(DE3). Pre-cultures were grown overnight at 37°C upon shaking at 180 rpm and used for inoculation of pre-warmed LB medium. Bacterial cells were kept for growing at 37°C upon shaking at 180 rpm while the OD of the culture was measured in several time points. At OD_{600} of ~ 0.6, overexpression was induced upon addition of 0.5 mM IPTG (Merck/Sigma-Aldrich) and carried out for 2 h at the same conditions. The cells were harvested by centrifugation at 6000 *g* for 20 min at 4°C (rotor SLC-6000, Sorvall/Thermo Fisher) and subsequently resuspended in 20 mM Tri/HCl pH 7.5, 150 mM KOAc, 5 mM $Mg(OAc)_2$, 5 % glycerol, 0.2 mM PMSF (Roche). Cells were lysed by shear force (M-110P cell disruptor Microfluidics Inc.). The cell debris was removed by centrifugation at 10000 *g* for 10 min at 4°C (rotor SS34, Sorvall/Thermo Fisher). To pellet the crude membranes an ultracentrifugation at 205000 *g* for 1 h at 4°C (rotor 45 Ti, Beckman Coulter) was conducted. The membranes were resuspended in 20 mM Tris/HCl pH 7.5, 150 mM KOAc, 5 mM $Mg(OAc)_2$, 5 % glycerol, 0.2 mM PMSF. Isolated membranes were flash-frozen by liquid nitrogen and stored at -80 °C until further application. Co-expressed proteins were detected by affinity purification. For purification via IMAC, the membranes were applied for solubilization in 50 mM Tris/HCl pH 8.0, 100 mM NaCl, 0.2 mM TCEP, 10 % glycerol, 1 % (w/v) DDM, cOmplete protease inhibitor (Roche) for 1 h at 6°C on a rolling table. After solubilization, the sample was applied for centrifugation at 21380 *g* for 5 min at 4°C to remove insolubilized material. His-tagged proteins were immobilized on Ni^{2+}-NTA resin (Qiagen) equilibrated with wash buffer (50 mM Tris/HCl pH 8.0, 100 mM NaCl, 0.2 mM TCEP, 20 mM imidazole, 10 % glycerol, 0.1 % (w/v) DDM). The solubilized proteins were incubated to bind to the Ni^{2+}-NTA resin for 1 h at 6°C on a rolling table. Afterwards, the resin was

washed extensively with wash buffer to remove non-specific weakly-bound impurities, and the protein was eluted with elution buffer (20 mM Tris/HCl pH 8.0, 100 mM NaCl, 0.2 mM TCEP, 300 mM imidazole, 10 % glycerol, 0.1 % (w/v) DDM, cOmplete protease inhibitor) in several fractions. The concentration of the detergent-purified protein content was determined spectrophotometrically. The yield of the purification was further analyzed by SDS-PAGE stained with colloidal chemical Coomassie solution (Quick Coomassie stain, Serva).

4.2.2.3 Immunodetection of purified proteins

For immunoblotting, the crude isolated membranes harboring the overexpressed proteins and the purified proteins were suspended in SDS-PAGE loading buffer and loaded on SDS-PAGE. The gel was used for transfer of the proteins to PVDF membrane (Cytiva) for 1 h at 4°C using the tank-blot system (Bio-Rad Laboratories). The transfer from the gel to the membrane was evaluated by visual detection of the prestained marker bands on the membrane. The PVDF membrane was washed three times with TBS buffer (20 mM Tris-HCl pH 8.0, 250 mM NaCl) upon slight agitation at ambient temperature for 5 min. The membrane put for blocking in TBS-T buffer (20 mM Tris-HCl pH 8.0, 250 mM NaCl, 0.1 % Tween-20) supplemented with 5 % skimmed milk for 1 h at ambient temperature. After incubation, the membrane was rinsed with TBS-T buffer and subsequently washed with it for two times 10 min and one time for 10 min with TBS. The primary antibodies were diluted (1:2000 for anti-His (Qiagen) and 1:4000 for anti-LipH, a generous gift from Karl-Erich Jäger) in TBS-T with 2 % (w/v) BSA (bovine serum albumin, Fraction V, Sigma-Aldrich) and incubated overnight at 4°C rolling in a 50 ml falcon. After overnight incubation, the membrane was rinsed with TBS-T buffer and subsequently washed with it two times for 10 min and one time for 10 min with TBS. The secondary antibodies conjugated to horseradish peroxidase (anti-mouse for anti-His and anti-rabbit for anti-LipH, Dianova/Sigma-Aldrich) were diluted in TBS-T with 2 % (w/v) BSA and applied to the membrane for 1 h upon slight shaking at ambient temperature. Again, the membrane was rinsed after incubation with TBS-T buffer and subsequently washed with it two times for 10 min and one time for 10 min with TBS. The blot was developed with Westar C Ultra 2.0 chemiluminescent substrate (Cyanagen) and imaged on Amersham Imager 680RGB (Cytiva).

4.2.2.4 Isolation of inner membrane vesicles

To separate inner and outer membrane fractions of lysed bacterial cells, the protocol described previously (Chapter 3.2.3) was utilized. In brief, a continuous sucrose density gradient from 20 to 70 % (w/v) was generated. Here, for LipH the buffer contained 20 mM Tris/HCl pH 8.0, 100 mM NaCl and for co-expressed SecYEG/LipH the buffer contained 20 mM Tris/HCl pH 7.5, 150 mM KOAc. The crude membranes were loaded over the gradient (200 – 300 µl) and centrifuged for 16 h at 110000 *g* at 4°C in either SW40 or SW32 rotor (Beckman Coulter). Afterwards, the gradient was harvested in fractions utilizing the Gradient Station (BioComp Instruments). The fractions were analyzed by SDS-PAGE, and IMV-containing fractions were pulled together. The samples were diluted with sucrose-free

buffer and applied for ultracentrifugation to pellet the inner membrane vesicles (IMVs). Afterwards, the membranes were resuspended in buffer (for LipH-IMVs in 20 mM Tris/HCl pH 8.0, 100 mM NaCl, 10 % glycerol or for SecYEG/LipH-IMVs in 20 mM Tris/HCl pH 7.5, 150 mM KOAc, 5 mM $Mg(OAc)_2$, 5 % glycerol). The IMV aliquots were flash-frozen and stored at -80°C until further usage.

4.2.2.5 Polymer-based extraction LipH and LipH/SecYEG

The isolation of the full-length foldase and co-expressed SecYEG/ $LipH^{FL}$ was achieved by utilizing the previously described protocol for the translocon isolation with minor modifications. In brief, 200 µl membranes containing overexpressed $LipH^{FL}$ or SecYEG/$LipH^{FL}$ were solubilized with 2.5 % (w/v) diisobutylene-maleic acid (DIBMA) polymers for 1 h at 37°C upon shaking at 650 rpm in 50 mM Tris/HCl pH 8.0, 100 mM NaCl, 10 % glycerol, 0.2 mM TCEP, cOmplete protease inhibitor in a total volume of 2 ml. Each sample was applied to 400 µl Ni^{2+}-NTA agarose resin (Qiagen) which was washed extensively with MQ and equilibrated with wash buffer (2 ml of 50 mM Tris/HCl pH 8.0, 100 mM NaCl, 10 % glycerol, 0.2 mM TCEP, 5 mM imidazole, cOmplete protease inhibitor) beforehand. After solubilization, a subsequent centrifugation step at 100000 *g* for 30 min at 4°C was conducted to remove the non-soluble material. The samples were applied for binding to Ni^{2+}-NTA resin overnight at 6°C, rotating on a vertical rotational mixer at moderate rpm to avoid the generation of foam. The next day, the beads were washed with 2.5 ml of 50 mM Tris/HCl pH 8.0, 100 mM NaCl, 10 % glycerol, 0.2 mM TCEP, 10 mM imidazole, cOmplete protease inhibitor. The samples were eluted with 50 mM Tris/HCl pH 8.0, 100 mM NaCl, 10 % glycerol, 300 mM imidazole in multiple fractions.

4.2.2.6 Liposome preparation and reconstitution of full-length LipH

For preparing liposomes with tailored lipid composition, the protocols were followed as described previously (Chapter 3.2.4). In brief, synthetic lipids (Avanti Polar Lipids, Inc.) were used from chloroform stocks of known concentrations. Mixing of the lipids in defined ratios and evaporation under vacuum (below 200 mbar) conditions at 40°C for at least 15 min with 140 rpm rotation (Rotary evaporator, IKA) led to removal of chloroform and formation of lipid film on the surface of the glass reaction tube. The lipid film was carefully resuspended in 1.2 – 2 ml of the buffer (20 mM Tris/HCl pH 8.0, 100 mM NaCl) in aim to obtain liposomes. The liposomes were extruded by the Mini-Extruder set (Avanti Polar Lipids, Inc.) and porous polycarbonate membranes (Nuclepore, Whatman). The crude liposomes were extruded initially for eleven passes through 400 nm and subsequently for another round of eleven passes through 200 nm pore size membranes. The protocol is oriented on previous research (Kamel *et al.*, 2022).

For the reconstitution of the purified $LipH^{FL}$, the liposomes were destabilized with 0.2 % (w/v) DDM at 40°C for 10 min. 1 nmol of the protein was reconstituted at 1:1000 protein to lipid ratio, thus 200 µl of liposomes were used for the procedure. $LipH^{FL}$ was diluted to a volume of 300 µl with 20 mM Tris/HCl

pH 8.0, 100 mM NaCl, 10 % glycerol, 0.1 % (w/v) DDM and kept on ice. After destabilization, the liposomes were added to the protein solution and the reaction incubated on ice for 30 min. To remove the detergent the solution was added to 70 mg of Bio-Beads SM-2 and incubated at 6°C rolling over night. Afterwards the solution was transferred for ultracentrifugation at 100000 *g* for 1 h at 4°C to pellet the proteoliposomes. The resulting proteoliposomes were resuspended in 20 µl buffer (20 mM Tris/HCl pH 8.0, 100 mM NaCl). To check the orientation of the reconstituted foldase, proteolytic cleavage of the N-terminal affinity tag was conduct by 3C HRV protease. Therefore, 0.5 µl of protease were added to 10 µl of proteoliposomes and incubated at ambient temperature for 1.5 h. Afterwards, 10 µl of the samples were withdrawn and mixed with 10 µl of 5 x SDS-PAGE sample buffer and subsequently applied for SDS-PAGE.

For the reconstitution of $LipH^{FL}$ in nanodiscs (NDs), a ratio of 1:2:100 of protein:MSP:lipid was utilized. 100 µl of liposomes (5 mM stock) were destabilized for 10 min with 0.5 % Triton X-100 at 40°C. The protein was diluted in buffer (20 mM Tris pH 8.0, 100 mM NaCl, 0.1 % (w/v) DDM) to 500 µl and kept on ice. After destabilization, $LipH^{FL}$ and MSP1D1 were pipetted simultaneously to the liposomes and incubated for 30 min on ice. After the incubation the sample was supplied to 70 mg of Bio-Beads to remove the detergent at 6°C rolling overnight. The next day, the sample was centrifuged at 30000 g for 30 min at 4°C. The supernatant was applied for size-exclusion chromatography on Superdex 200 Increase 10/300 GL column (Cytiva). The resulting peak fractions were analyzed by SDS-PAGE which allowed to distinguish between LipH-containing and empty NDs.

4.2.3 *In vitro* activity of LipA

The hydrolytic activity of the lipase was measured *in vitro* upon the hydrolysis of para-nitrophenyl butyrate (*p*NPB) as described elsewhere (Papadopoulos *et al.*, 2022). For the measurement, 1 µM of urea-denatured LipA was mixed with inner membrane vesicles (IMVs), proteoliposomes (PL) or nanodiscs (NDs) containing $LipH^{FL}$ in a total volume of 40 µl with TGCG buffer (5 mM Tris, 5 mM glycine, 1 mM $CaCl_2$, 5 % glycerol, pH 9.0). $LipH^{FL}$ -PL were tested for the lipase activation by addition 12 µl of the suspension to the activation reaction. For the NDs, $LipH^{FL}$ concentration was estimated by SDS-PAGE band intensity roughly at 0.2 µM. IMVs were add to 1 OD based on absorption (A280) measurement. The samples were incubated for 15 min at 37°C for complex formation. Afterwards, 10 µl sample were transferred into a 96-well plate containing 100 µl TGCG. *p*NPB was diluted to 10 mM by adding 1.76 µl to 1 ml acetonitrile. Briefly before the measurement, the *p*NPB solution was again 10-fold diluted with 50 mM triethanolamine pH 7.4 and 100 µl were pipetted to each well for measurement. The absorbance of the p-nitrophenolate was monitored at 410 nm over 3.5 h at 37°C on a plate reader (Infinite 200 pro, TECAN). LipA alone served as negative control, and the autohydrolysis of *p*NPB was monitored in the same buffering condition lacking the protein. The measurements were conducted in technical triplicates.

4.2.4 Microscale Thermophoresis

MST was utilized to track binding of the foldase and the lipase A of *P. aeruginosa* PAO1. LipA and the soluble domain of LipH were purified as described previously (Papadopoulos *et al.*, 2022). Isolated urea-denatured lipase variants ($LipA_{F144E}$, $LipA^{\Delta N7aa}$ and $LipA^{\Delta C81aa}$) were fluorescently labeled with AlexaFluor 488-maleimide (Thermo Fisher Scientific). In brief, 10 to 20-fold molar excess of the dye was added to the protein. The sample was filled with 20 mM Tris/HCl pH 7.25, 8 M urea to 300 – 500 µl final volume in the tube and put on a rolling table under darkened conditions and incubated at 6°C overnight. The next day, the sample was precipitated with 20 % (w/v) trichloroacetic acid (TCA) for 30 – 60 min on ice. After incubation, centrifugation at 21380 *g* for 15 min at 4°C was conducted to pellet the precipitated protein. The supernatant (SN) was removed, and 1 ml of ice-cold acetone was added to the sample for washing by vortexing. The sample was put for centrifugation at 21380 *g* for 15 min at 4°C again and the SN was removed afterwards. After subsequent drying step (37°C for 15 min) the pellet was suspended with 20 mM Tris/HCl pH 7.25, 8 M urea. The concentrations of the proteins were determined spectrophotometrically by measuring the absorbance (A) at 280 nm. For the MST measurement, the foldase ($LipH^{\Delta TMD}$) was transferred into MST buffer (5 mM Tris, 5 mM glycine, 1 mM $CaCl_2$, 5 % glycerol, 0.5 mg/ml BSA, 0.05 % (w/v) Tween-20, pH 9.0). Further, the fluorescently labeled lipase variants were diluted to 100 nM in MST buffer, and 10 µl of the lipase were mixed with the foldase soluble domain ranging from 0.23 nM to 7.5 µM in a 0.5 ml reaction tube (Sarstedt). The lipase:foldase samples were incubated for 15 min at ambient temperature in the dark, then loaded into premium capillaries and applied for analysis by Monolith NT.115 instrument (NanoTemper Technologies, Munich, Germany). The MST power was set to 80 % and the LED power to 40 % in the blue channel. The thermophoresis was detected over time by normalized fluorescence traces for 30 seconds with 5 seconds set for delay and recovery. The aggregation of the samples was monitored by a capillary profile scan prior the experiment. The data was evaluated by NT Analysis software (NanoTemper Technologies, Munich, Germany) allowing to remove the disturbances occurred likely due to aggregation. The K_D fit was conducted by GraphPad Prism (Version 9.2.0, GraphPad Software, LLC 1994 - 2021) based on one-site total binding model.

4.2.5 Size exclusion chromatography combined with multi angle light scattering

To determine the oligomeric state of the detergent-solubilized full-length foldase (His_8-$LipH^{FL}$), the purified protein was applied for SEC-MALS analysis on Superdex 200 Increase 10/300 GL column (Cytiva) in 50 mM Tris/HCl pH 8.0, 100 mM NaCl, 0.2 mM TCEP, supplied with either 0.5 % (w/v) DM or 0.1 % (w/v) DDM. The samples were applied to ultracentrifugation at 100000 *g* for 30 min at 4°C to remove occasional aggregates. 500 µl of the DDM-solubilized sample with a concentration of 0.16 mg/ml and 230 µl of the DM-solubilized sample with a concentration of 0.2 mg/ml were injected. SEC-MALS was also performed to determine the molecular weight and oligomeric state of LipH soluble domain ($LipH^{\Delta TMD}$), as well as the molecular weight and stoichiometry of LipA:$LipH^{\Delta TMD}$ complex. For $LipH^{\Delta TMD}$ the concentration was 56 µM (~ 2 mg/ml), and 150 µl were

injected for analysis. To analyze the complex, 25 µM of urea-denatured LipA were incubated with equimolar amount of $LipH^{\Delta TMD}$ for 1 h at 4°C. To remove occasional aggregates the samples were centrifuged at 100000 *g* for 1 h at 4°C. After centrifugation, 100 µl of the complex were injected for analysis. The SEC-MALS runs were conducted on Superdex 200 Increase 10/300 GL column (Cytiva). The buffer was 50 mM Tris/HCl pH 8.0, 100 mM NaCl, 0.2 mM TCEP. The column was connected to a miniDAWN TREOS II light scattering device and Optilab-TrEX Ri-detector (Wyatt Technology Corp.). For analysis of the data, the software ASTRA 7.3.2 was employed (Wyatt Technology Corp.).

4.2.6 Small-angle X-ray scattering

SAXS measurement for $LipH^{\Delta TMD}$ was conducted at the Center for Structural Studies of the Heinrich Heine University of Düsseldorf. The data was collected at Xeuss 2.0 Q-Xoom system from Xenocs, which was equipped with a PILATUS 3 R 300K detector (Dectris) and a GENIX 3D CU Ultra Low Divergency X-ray beam delivery system. The sample to detector distance was set at 0.55 m for this experiment and resulted in an achievable q-range of 0.1 – 6 nm^{-1}. The sample concentration was 11.82 mg/ml in 50 mM Tris/HCl pH 8.0, 100 mM NaCl, 0.2 mM TCEP, 5 % glycerol, cOmplete protease inhibitor, and the measurements was conducted at 15°C. The sample was injected via an autosampler into the Low Noise Flow Cell (Xenocs). For that sample, 24 frames with an exposure time of ten min were collected. The data was scaled to the absolute intensity of water.

To conduct structural analysis of the lipase:foldase complex, 100 µl of the isolated and urea-denatured $LipA_{F144E}$ (40 mg/ml in 20 mM Tris/HCl pH 7.25, 8 M urea) was mixed with 400 µl of $LipH^{\Delta TMD}$ (1 mg/ml in 5 mM Tris, 5 mM glycine, 1 mM $CaCl_2$, 5 % glycerol, pH 9.0). The sample incubated for 30 min at 37°C for complex formation and subsequently centrifuged at 21380 g for 10 min at 4°C. For the data acquisition of LipH:LipA of *P. aeruginosa* PAO1, SEC-SAXS was conducted on the P12 beamline (PETRA III, DESY Hamburg) (Blanchet *et al.*, 2015). The sample-to-detector distance of the P12 beamline was 3.00 m, results in an achievable q-range of 0.03 – 7.0 nm. The SEC-SAXS runs were performed at 10°C with a Superdex 200 increase 10/300 GL column (Cytiva) (100 µl inject, Buffer: 5 mM Tris, 5 mM glycine,1 mM $CaCl_2$, 5 % glycerol) with a flow-rate of 0.6 ml/min. We collected 2400 frames with an exposer time of 0.995 sec/frame. Data were scaled to absolute intensity against water. All used programs for data processing were part of the ATSAS Software package (Version 3.0.3) (Manalastas-Cantos *et al.*, 2021). Primary data reduction was performed with the program PRIMUS and CHROMIXS (Konarev *et al.*, 2003; Panjkovich and Svergun, 2018). With the Guinier approximation, the forward scattering I (0) and the radius of gyration (Rg) were determined (Guinier, 1939). The GNOM software was used to estimate the maximum particle dimension (Dmax) with the pair-distribution function p (r) (Svergun, 1992). Homology model of $LipH^{\Delta TMD}$ were created with Phyre2 (Kelley *et al.*, 2015). Additionally, we created an AlphaFold model of the LipA:LipH, complex and used CORAL for the modeling of the N-terminal part of LipH (amino acid residues 1 – 70) which was not modeled with high confidence by AlphaFold (Jumper *et al.*, 2021) (Petoukhov *et al.*, 2012).

Additionally, we calculate an *ab-initio* model of the LipA:LipH complex using GASBOR and superimposed the models with SUPCOMB (Kozin and Svergun, 2001) (Svergun, Petoukhov and Koch, 2001). All SAXS measurements and analysis were conducted in close collaboration with Jens Reiners from the Center for Structural Studies at the Heinrich Heine University of Düsseldorf.

4.3 Results

4.3.1 Isolation and characterization of the full-length foldase LipH

Investigating the lipase A folding and maturation process constitutes a major challenge. First, LipA is highly prone to aggregation, which makes it very difficult to work with. Thus, a substantially more stable lipase mutant was identified and generated within the project (Papadopoulos *et al.*, 2022). Second, as demonstrated by previous research, the lipase A requires folding-assistance by a membrane-bound lipase-specific foldase (Lif) chaperone named LipH (Frenken *et al.*, 1993; Hobson *et al.*, 1993; Rosenau, Tommassen and Jaeger, 2004). How the recognition between the lipase and its chaperone occurs is still not completely understood. While previous studies focused solely on the folding and maturation of the lipase mediated by the soluble LipH domain (El Khattabi *et al.*, 1999, 2000; Dollinger, 2018) the current research aimed to investigate the processes mediated by the full-length foldase ($LipH^{FL}$) upon the lipase biogenesis at the membrane environment. This required the expression and isolation of the full-length LipH as well as its functional reconstitution. Further investigations were conducted to check the possible involvement of the foldase upon LipA translocation, therefore $LipH^{FL}$ and the translocon SecYEG were co-expressed.

The first step to characterize the action of $LipH^{FL}$ was the successful expression and purification of the protein. Therefore, $LipH^{FL}$ was heterologously expressed in *E.* coli which resulted in reasonable yields when utilizing constructs which encode for N-terminally histidine-tagged foldase. To boost the expression level and avoid degradation of the overexpressed protein, two constructs encoding for $LipH^{FL}$ with difference in the length of the N-terminal tag (His_{10}-$LipH^{FL}$ and His_8-$LipH^{FL}$) were created and tested for expression and purification. The successful solubilization of $LipH^{FL}$ from the membrane was achieved with the detergents DM and DDM (Figure 4.1, A). Initial metal ion affinity purification (IMAC) of the full-length LipH resulted in a prominent band on SDS-PAGE at ~ 41 kDa matching the expected molecular weight of the protein, and certain degradation products of lower molecular weights (Figure 4.1, A). Size-exclusion chromatography (SEC) of DM-solubilized His_8-$LipH^{FL}$ showed homogenously purified protein and less intense pattern of degradation products as indicated by SDS-PAGE analysis (Figure 4.1, B). Purified His_8-$LipH^{FL}$ and the cognate degradation bands were observed by immunoblotting (Figure 4.1, C), confirming the purified foldase as well as the observed degradation products. The employed detergents possess different micelle sizes (~ 70 kDa for DDM and ~ 40 kDa for DM) which may have an impact on the oligomeric state of the protein (Stetsenko and Guskov, 2017). Combined SEC with multi-angle light scattering (MALS) allowed the determination of oligomeric state of the detergent-purified full-length foldase (Figure 4.1, D and E). For DDM-solubilized $LipH^{FL}$, two close peaks were observed at 10.9 and 11.6 ml on Superdex 200 Increase 10/300 GL column (Cytiva), and further analysis of these peaks revealed molecular weights of 201.9 ± 3.3 kDa for the first peak and 129.1 ± 2.9 kDa for the later eluting peak. The molecular weight determined for the first peak matched the trimeric state of $LipH^{FL}$ while the second peak possibly resembled dimeric foldases in the DDM micelles (Figure 4.1, D). SEC-MALS analysis conducted for DM-solubilized $LipH^{FL}$ reveals a major

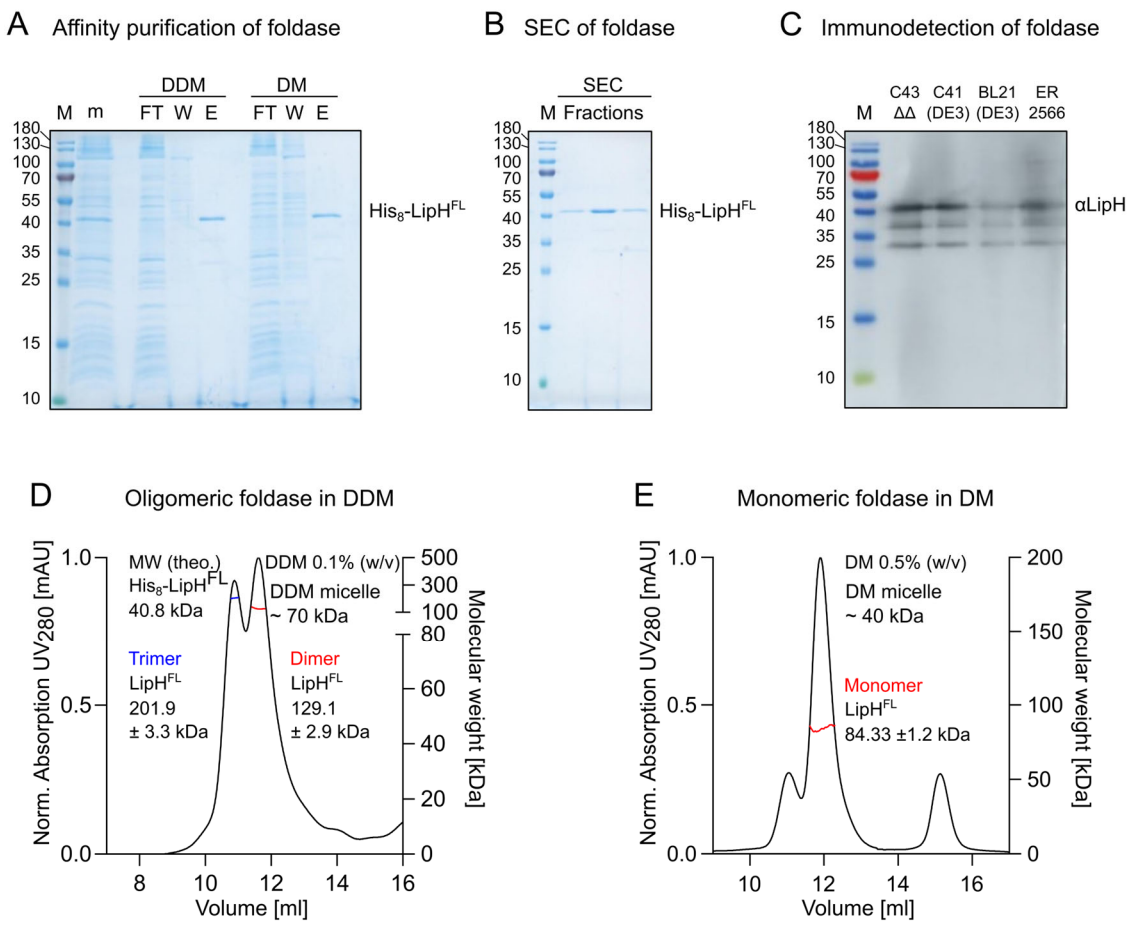

Figure 4. 1: Purification and characterization of the full-length foldase of *P. aeruginosa* PAO1

A: The full-length foldase (His-LipH^{FL}) was solubilized by in 2 % (w/v) DDM or 3 % (w/v) DM and purified by IMAC. m: crude membranes, FT: flow-through fraction, W: wash fraction, E: elution fraction. **B**: LipH^{FL} purified by SEC. Fractions analyzed by SDS-PAGE. **C**: Immunodetection of SEC-purified LipH^{FL} expressed in different *E. coli* strains by αLipH antibodies. M: Prestained Molecular Weight Marker,10-180 kDa (PageRuler^{TM}, Thermo Fisher Scientific), depicted on the SDS-PAGE and Immunodetection images. **D**: SEC-MALS of His$_8$-LipH^{FL} in DDM indicates two peaks, possibly representing trimeric (blue) and dimeric (red) foldases in DDM micelles. **E**: SEC-MALS of His$_8$-LipH^{FL} in DM indicates a major peak, likely representing the monomeric His$_8$-LipH^{FL} in the DM micelle. The molecular weight (MW) of LipH^{FL} was determined in 0.1 % (w/v) DDM and 0.5 % (w/v) DM micelles. The MW of the detergent micelles for each detergent as well as for reconstituted LipH^{FL} is indicated in the figure (Stetsenko and Guskov, 2017).

peak eluting at ~ 11.9 ml indicating molecular weight of 84.3 ± 1.2 kDa, likely reflecting the monomeric LipH^{FL} in DM micelles (Figure 4.1, E).

To investigate whether the foldase is involved in the Sec-dependent translocation of LipA, LipH^{FL} was co-expressed with the translocon SecYEG (His$_{10}$-LipH^{FL}/His$_6$-SecYEG). After heterologous expression in *E. coli* and isolation of the crude membranes, the co-expressed proteins were solubilized by detergent and purified by immobilized metal ion affinity chromatography (IMAC) resulting in prominent SDS-PAGE bands for LipH^{FL} at ~ 41 kDa and SecY at ~ 38 kDa as well as SecE at ~ 15 kDa and SecG at

~ 17 kDa, in the elution fraction (Figure 4.2, A). The detergent-based purification of co-expressed SecYEG/LipH^{FL} resulted in different levels of the proteins, as the band for LipH^{FL} on SDS-PAGE was substantially weaker than those of the translocon (Figure 4.2, A). Speculations are possible here, as it is not known whether the histidine-tags are equally accessible for affinity purification or whether the solubilization efficiency was equal for both proteins. In turn, comparing the solubilization of LipH^{FL} alone (Figure 4.1, A) to the solubilization when co-expressed with SecYEG (Figure 4.2, A) the solubilization levels are similar as indicated by band intensity on SDS-PAGE. It is also possible, that the proteins are expressed to different expression levels. To prove that the proteins are indeed co-expressed, the immunodetection of the translocon SecYEG by anti-His antibodies and of the foldase LipH by anti-LipH antibodies was conducted (Figure 4.2, B). While the immunoblot against the histidine tag presented a strong and clear signal of a MW of ~ 38 kDa, there was no band detected at ~ 41 kDa with the anti-His antibodies, suggesting that the histidine-tag of SecYEG is accessible, while the tag of LipH is not. The immunodetection conducted with anti-LipH antibodies confirmed the presence of the foldase in the co-expressed sample by indicating a prominent band at ~ 41 kDa (Figure 4.2, B).

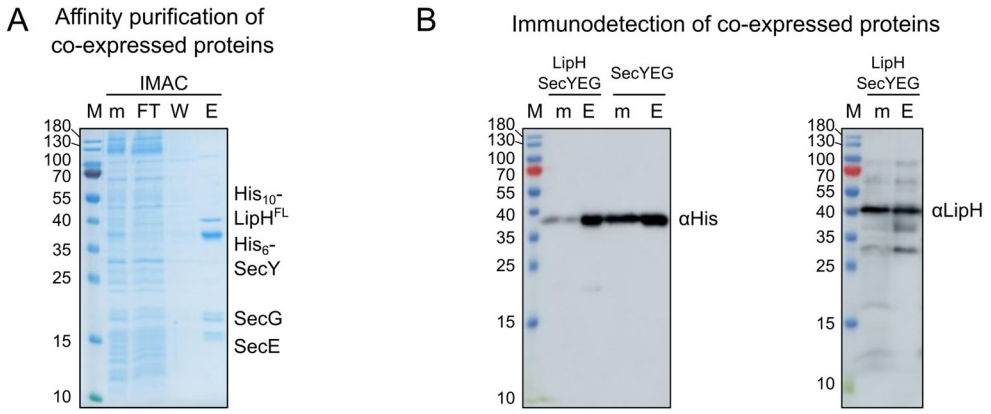

Figure 4. 2: Co-expression of the foldase and the translocon of *P. aeruginosa* PAO1

The full-length foldase (His_{10}-LipH^{FL}) and the translocon (His_6-SecYEG) were co-expressed by utilizing a plasmid encoding for both products. **A**: SDS-PAGE of co-expressed, detergent-solubilized, and IMAC-purified SecYEG/LipH^{FL}. **B**: Immunodetection of the histidine-tagged translocon (αHis, left) and the foldase (αLipH, right). The histidine-tag of the foldase did not indicate signal when blotted against anti-His antibodies, suggesting limited accessibility of the tag. M: Prestained Molecular Weight Marker,10-180 kDa (PageRuler^{TM}, Thermo Fisher Scientific), m: crude membranes, FT: flow-through fraction, W: wash fraction, E: elution fraction.

To check the functionality of the membrane-bound foldase, inner membrane vesicles (IMVs) harboring either LipH^{FL} or co-expressed SecYEG/LipH^{FL} were isolated by density gradient centrifugation (Figure 4.3, A and B). The isolated IMVs were employed to study the foldase-mediated maturation of LipA. Furthermore, IMVs containing co-expressed LipH^{FL}/SecYEG were utilized for *in vitro* LipA translocation experiments but did not indicate any enhancing effect of the foldase by improving the transport efficiency. In addition, the full-length LipH and the co-expressed SecYEG/LipH^{FL} were

extracted by detergent-free polymers, resulting in the formation of near-native nanodiscs (NDs) (Figure 4.3, C and D). The isolated near-native NDs could be further used in biophysical assays to study the binding of the lipase to the membrane-bound LipH^{FL}. The isolated IMVs and the polymer-extracted NDs represent near-native membrane systems which contain additional endogenous *E. coli* proteins. Although they allow to study the foldase action in the membrane environment, they are not tunable on their lipid as well as protein composition.

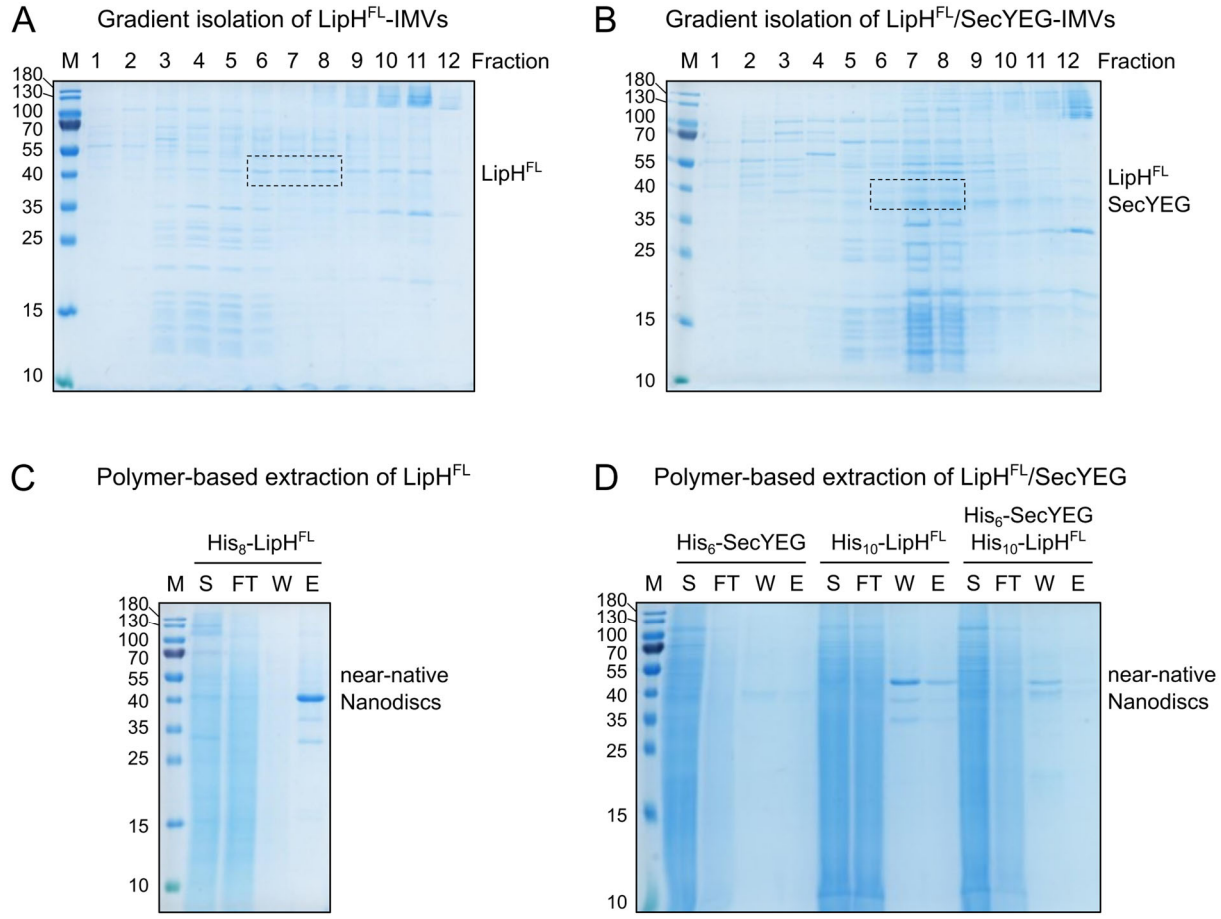

Figure 4. 3: Isolation of the foldase in near-native membranes

The full-length foldase LipH was overexpressed in *E. coli* and membranes harboring the protein were isolated. The crude membranes were separated by density gradient centrifugation. The collection of continuous sucrose gradient (20 – 70 %) upon fractionation was analyzed by SDS-PAGE. The fractions containing the LipH^{FL} and thus the inner membrane vesicles (IMVs) are 6, 7 and 8. LipH^{FL} bands are indicated by dashed quadric. **A**: IMVs harboring the foldase LipH^{FL}. **B**: IMVs harboring co-expressed LipH^{FL}/SecYEG. **C**: Polymer-based extraction and IMAC purification of His$_8$-LipH^{FL}. **D**: Polymer-based extraction and IMAC purification of His$_6$-SecYEG, His$_{10}$-LipH^{FL} and co-expressed His$_6$-SecYEG/His$_{10}$-LipH^{FL}. The proteins were extracted from the crude membranes by DIBMA polymer. M: Prestained Molecular Weight Marker,10-180 kDa (PageRuler^{TM}, Thermo Fisher Scientific), S: DIBMA-solubilized, FT: flow-through fraction, W: wash fraction, E: elution fraction.

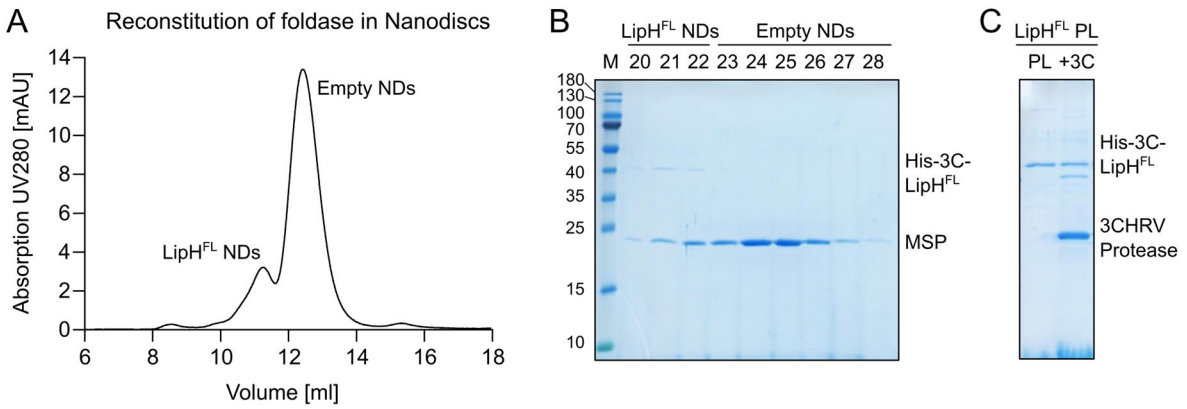

Figure 4. 4: Reconstitution of full-length foldase in model membranes

A: Size-exclusion chromatography (SEC) indicates LipH^{FL} reconstituted in nanodiscs (NDs). Separation between LipH^{FL} NDs and empty NDs is given by two peaks. SEC on Superdex 200 Increase 10/300 GL (Cytiva). **B**: SDS-PAGE of SEC fractions of ND-reconstitution of LipH^{FL}. Foldase (His-3C-LipH^{FL}) and membrane scaffold protein (MSP) are indicated. M: Prestained Molecular Weight Marker,10-180 kDa. **C**: Proteoliposomes (PL) containing foldase (His-3C-LipH^{FL}. Samples treated with 3C HRV Protease (+3C) to check the orientation of the foldase after reconstitution.

Thus, synthetic lipids were utilized to obtain defined membrane composition for reconstitution of LipH^{FL}. The reconstitution of the full-length foldase in model membrane systems was achieved in proteoliposomes and nanodiscs (NDs) (Figure 4.4). The proteolytic cleavage of the histidine tag indicates that most of the foldases are oriented outwards of the liposomal lumen (~ 63 %) (Figure 4.4, C).

Upon the presented investigations it was possible to isolate and reconstitute for the first time the full-length foldase LipH of *P. aeruginosa* PAO1. The successful isolation, reconstitution, and further characterization of the full-length foldase are key steps in aim to elucidate the processes upon lipase biogenesis. All membrane-associated foldase samples were further used for functional investigations. Furthermore, the presented isolation and reconstitution approaches can serve in later investigations to study possible foldase:lipase interactions on the membrane interface, forming the basis for biochemical and biophysical analysis with the full-length chaperone in near-native and model membrane environment.

4.3.2 Functional investigations of the full-length foldase

The functional investigation of the full-length foldase LipH is of major importance in aim to elucidate its mode of action upon the lipase biogenesis. After successful isolation and reconstitution of LipH^{FL}, the focus was set on the folding action of LipH^{FL} towards the lipase A. Thus, the acquired samples were utilized for biochemical investigations. The ability of LipH^{FL} to assist in folding of LipA was tracked by the lipase activation analysis. To check the functionality of foldase in near-native membranes, inner membrane vesicles (IMVs) harboring either LipH^{FL} or co-expressed SecYEG/LipH^{FL} were applied for

activation of the lipase A. The resulting lipolytic activity of the lipase towards *p*-nitrophenol butyrate (pNPB) served as an indication for the natively folded protein, that in turn indicated that LipH in IMVs possessed folding activity, and thus was in its functional state (Figure 4.5, A). When comparing the IMVs harboring LipH^{FL} with those containing co-expressed SecYEG/LipH^{FL}, the hydrolytic activity of LipA was reduced when it was activated by the co-expressed foldase (Figure 4.5, A). This could be due to lower expression level of the foldase when it was co-expressed with the translocon. Although the folding action of LipH^{FL} towards LipA was decreased when it was co-expressed with SecYEG, the results indicated that the foldase was still functional in this type of IMVs. Co-expression of SecYEG/LipH^{FL} allowed for further experimental approaches to investigate possible effects of LipH upon the lipase transport. To investigate the putative role of LipH upon Sec-mediated translocation of the lipase, the same IMVs were utilized. Although the LipH^{FL} appeared functional upon the lipase folding, the results of *in vitro* transport did not indicate any increase in transport efficiency of the lipase when the foldase was present. Thus, the low translocation efficiency could be due to instant aggregation and/or inefficient targeting of the lipase precursor to the Sec system (chapter 3.1.1). Further, LipH^{FL} was reconstituted in proteoliposomes, as well as in nanodiscs (NDs), and the chaperone was able to fold LipA into its active form, as validated by the resulting hydrolytic activity of the lipase (Figure 4.5, B). Here, the hydrolytic activity of the lipase folded by LipH^{FL}-NDs was increased in comparison to LipH^{FL} proteoliposomes. This can be due to the accessibility of the foldase chaperone domain in the NDs. While after reconstitution in proteoliposomes, not all foldase chaperone domains are oriented outward of the vesicles, thus not being accessible for folding of the lipase.

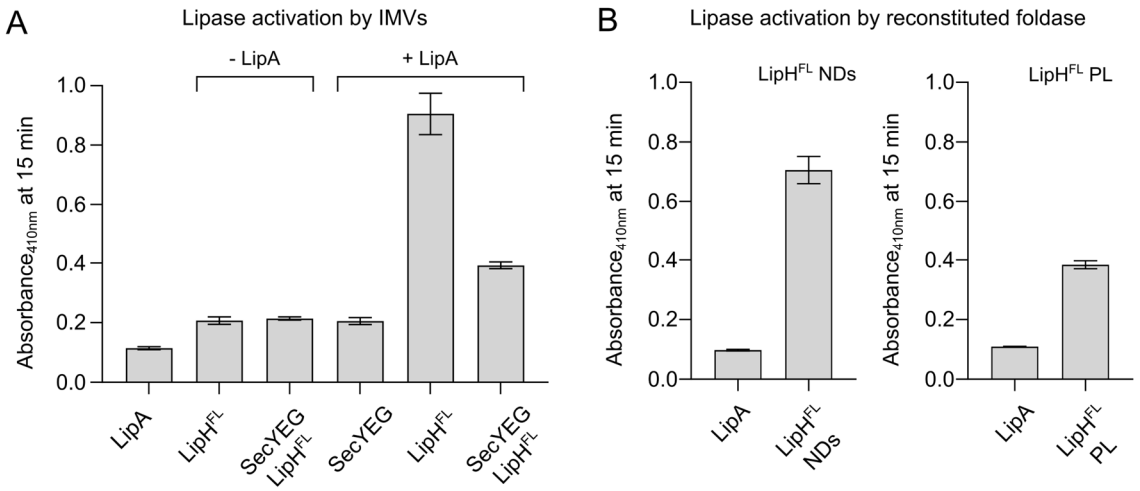

Figure 4. 5: Functional analysis of the full-length foldase in membrane systems

A: Lipase activation by IMVs with LipH^{FL} or co-expressed LipH^{FL}/SecYEG. LipA: no foldase added (inactive), -/+LipA: in presence or absence of lipase A. LipH^{FL}: IMVs with foldase, SecYEG: IMVs with the translocon, SecYEG/LipH^{FL}: IMVs with co-expressed translocon and foldase. **B**: Lipase activation by LipH in membrane mimetics. NDs: nanodiscs, PL: proteoliposomes. Lipolytic activity of LipA against *p*NPB, measured via the absorbance caused by *p*NPB hydrolysis after 15 min. The mean values and the standard deviation are shown.

4.3.3 Binding and recognition of the lipase A by the foldase

Recognition and binding of the lipase by its cognate foldase manifest key steps of the lipase biogenesis. Early studies demonstrated a very specific interaction of the lipase with the foldase leading to a tight binding of the proteins (El Khattabi *et al.*, 1999). Indeed, tight binding of the lipase to the foldase soluble domain was observed, but the mechanism of recognition remains still unclear (Viegas *et al.*, 2020). The first step to characterize the lipase:foldase complexing was the determination of the complex stoichiometry as well as further structural analysis. SEC-MALS as well as structural analysis by SAXS were conducted (Figure 4.6).

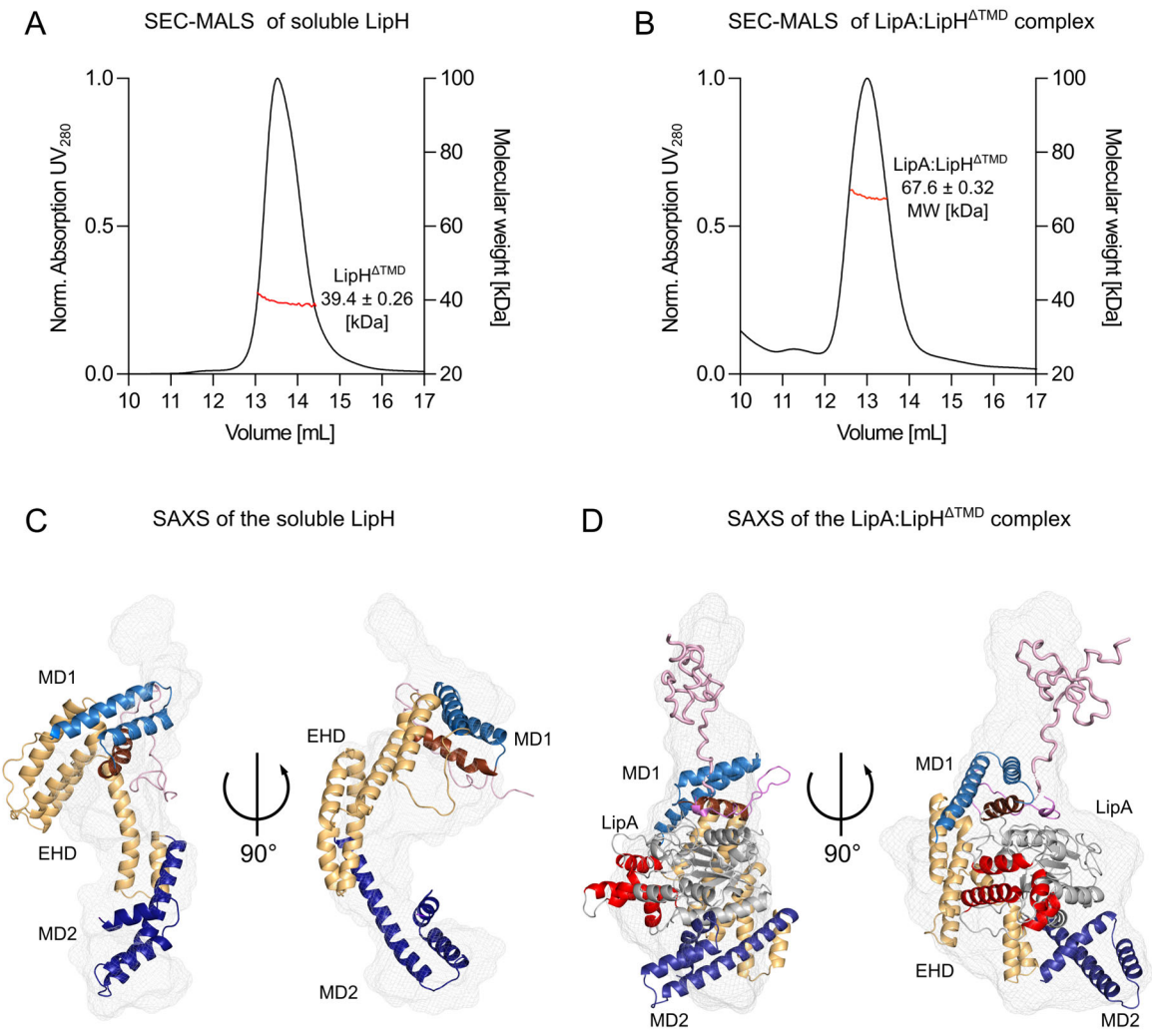

Figure 4. 6: Characterization of LipH soluble domain and in complex with LipA

Analysis were conducted for the soluble foldase domain (LipH$^{\Delta TMD}$) and the lipase:foldase complex (LipA:LipH$^{\Delta TMD}$). SEC-MALS analysis of (**A**) LipH$^{\Delta TMD}$ and (**B**) LipA:LipH$^{\Delta TMD}$. Molecular weight (MW, red line). SAXS envelope (grey mesh) of (**C**) LipH$^{\Delta TMD}$ and (**D**) LipA:LipH$^{\Delta TMD}$ complex. The homology models of the LipH$^{\Delta TMD}$ and LipA:LipH$^{\Delta TMD}$ complex are depicted inside the envelope. MD1: mini domain 1 (light blue), EHD: extended helical domain (khaki-orange), MD2: mini domain 2 (dark blue). The α-helix containing the foldase consensus motif (Rx$_1$x$_2$FDY (F/C)L (S/T)A) is colored separately (dark red). LipA: dark grey with the α-helices of the Lid-domain (red).

Analysis of the lipase:foldase complex by both approaches indicate a 1:1 stoichiometry, indicating an intact formation of the protein complex. The calculated molecular weights of LipA is 30.18 kDa and of $LipH^{\Delta TMD}$ 38.32 kDa. The molecular weight of the lipase:foldase complex determined by SEC-MALS was 67.6 ± 0.32 kDa, while the soluble domain of the foldase ($LipH^{\Delta TMD}$) 39.4 ± 0.32 kDa (Figure 4.6, A) (Papadopoulos *et al.*, 2022), thus matching the values calculated for 1:1 stoichiometry. The lack of structural information of the lipase:foldase complex of *P. aeruginosa* PAO1 hampers further characterization of the binding and recognition process and can only be complemented with previous observations made for *Burkholderia glumae* (Pauwels *et al.*, 2006). The putative structure of the foldase and in complex with the lipase was obtained by the homology modeling and small-angle X-ray scattering (SAXS) analysis. The resulting SAXS envelope represents important low-resolution structural data of the *P. aeruginosa* foldase LipH and the LipH:LipA complex (Figure 4.6, C and D). The data indicates a "C-like" shape for the envelope of the foldase and fits to the homology model (Figure 4.6, B). When the foldase binds the lipase, an increased density is detected in the SAXS envelope, forming a bulky shape, where the homology model of the complex fits well (Figure 4.6, D). Taken together, the structural data confirms an equimolar complex formation of LipH:LipA.

To elucidate the recognition of the lipase by its dedicated foldase, the LipH soluble domain was utilized to track the binding of fluorescently labeled lipase. The binding of the denatured lipase A was monitored by microscale thermophoresis (MST). The recently created stable mutant of LipA ($LipA_{F144E}$) was utilized for these experiments, in aim to avoid the fast aggregation of the protein (Papadopoulos *et al.*, 2022), and allowing for the successful recognition by the foldase. The results reveal a strong binding interaction between LipA and LipH soluble domain, with a dissociation constant (K_D) in the low nanomolar range (~ 8.8 nM) (Figure 4.7, A), being in the similar range to that which was reported for lipase:foldase interactions before (Pauwels *et al.*, 2006; Viegas *et al.*, 2020).

Since the lipase follows the Sec-dependent translocation to the periplasm in unfolded state, it must emerge out of the translocon first by its N-terminus. Once at the periplasmic side, the lipase requires folding assistance by the membrane-bound LipH. It is tempting to speculate that the foldase recognizes the emerging lipase at an early translocation stage, whereby the N-terminus of LipA might be of major importance for recognition by LipH. To test this hypothesis, an N-terminally truncated LipA variant lacking the first seven amino acids ($LipA^{\Delta N7}$) of the mature lipase domain was generated and employed for MST experiments. The results did not indicate any clear binding to the foldase (Figure 4.7, B), suggesting that the N-terminus of the lipase is essential for the recognition by the foldase. In case of an N-terminally governed lipase translocation event, these results underline that the N-terminus of LipA constitutes the part which is initially recognized by the foldase. Oppositely, the recognition of the lipase by the foldase should not be hindered in absence of C-terminally located residues. To check that, a C-terminal LipA truncation lacking 81 amino acids was analyzed for binding to the foldase. Oppositely to the N-terminal truncation, the results indicate binding of the C-terminal LipA truncation by the foldase (Figure 4.7, C). The resulting K_D (~ 10.8 nM) is in the same range as for full-length LipA. These results

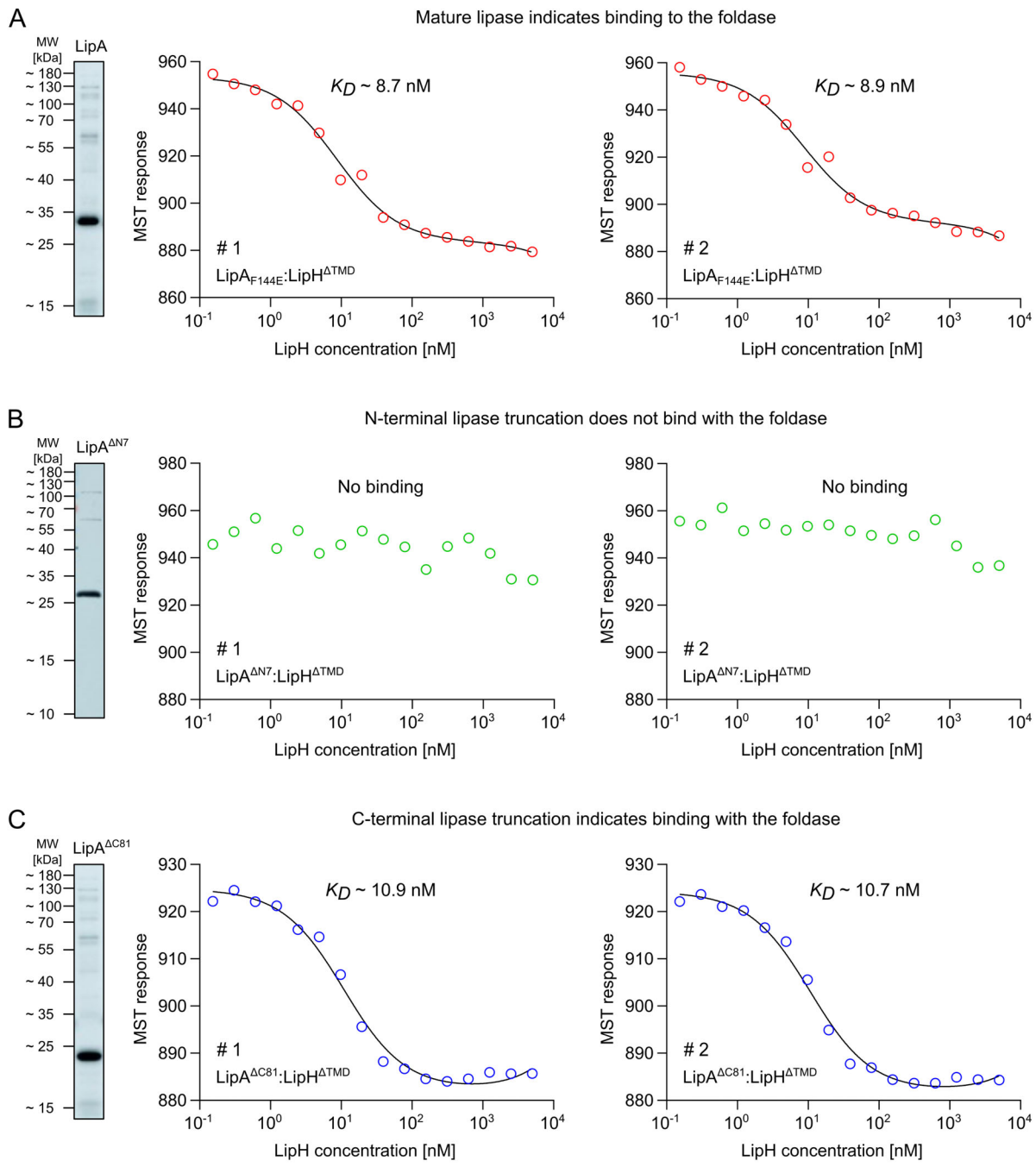

Figure 4. 7*:* Binding of the lipase to the foldase monitored by MST

The binding of the soluble foldase domain (LipH$^{\Delta TMD}$) to fluorescently labeled LipA was detected via microscale thermophoresis (MST). The full-length lipase (LipA$_{F144E}$) as well as N- and C-terminal truncations (LipA$^{\Delta N7}$ and LipA$^{\Delta C81}$) are shown by in-gel fluorescence. **A**: Binding indicated for LipA (LipA$_{F144E}$) by LipH soluble domain (LipH$^{\Delta TMD}$). **B**: No clear binding determined for LipA N-terminal truncation (LipA$^{\Delta N7}$) lacking the first seven amino acids by LipH$^{\Delta TMD}$. **C**: Binding detected for LipA C-terminal truncation (LipA$^{\Delta C81}$) lacking 81 aa from the C-terminus. First and second technical replicates are depicted for each measurement. K_Ds are indicated in the figure (A and C).

underline that the initial recognition events likely occur between the N-terminus of LipA and the foldase, whereby the C-terminus is later recognized by the foldase.

4.4 Discussion

The major secretory lipase LipA of *P. aeruginosa* is a virulence factor. Upon its targeting within the cytoplasm, transport across the inner membrane by the Sec machinery and secretion to the extracellular space by the type II secretion system (T2SS), the lipase interacts with multiple proteins. In the periplasm the lipase is folded by the lipase-specific foldase LipH which is important for LipA to maturate and reach its secretion-competent form (El Khattabi *et al.*, 2000; Rosenau, Tommassen and Jaeger, 2004). So far, investigations on the lipase:foldase system were primarily conducted with the soluble domain of the chaperone, and structural information of the system was achieved for homologous lipase:foldase complex of *Burkholderia glumae,* representing the initial information on that system (El Khattabi *et al.*, 2000; Pauwels *et al.*, 2006). The lack of information on the full-length foldase $LipH^{FL}$ is a barrier on track to elucidate the folding and maturation processes of the lipase A. It is unclear how the membrane environment affects the folding and maturation of the lipase. It is also not clarified if and how the presence of the membrane and/or other membrane-associated proteins, including the Sec translocon, impact the folding and release of the mature lipase. Therefore, the functionality and dynamics of the full-length foldase within the membrane is of substantial interest.

Limited insights on the full-length foldase derived from a homologous lipase:foldase system of *P. aeruginosa* TE3285 point to the essential properties of the foldase chaperone domain upon lipase folding, but also indicate aggregation of the full-length foldase which had very low ability to activate the lipase (Shibata, Kato and Oda, 1998b). Within the investigations of the present thesis, expression, and isolation of the full-length foldase LipH of *P. aeruginosa* PAO1 was achieved for the first time. $LipH^{FL}$ was characterized in detergent and within the lipid environment. The comparison of $LipH^{FL}$ solubilized by the different detergents (DDM and DM) indicated varying degree of the protein oligomerization in dependence to the detergent micelle size. While SEC-MALS analysis in DDM indicated two equally intense fractions likely representing trimeric and dimeric $LipH^{FL}$ in the detergent micelles, the smaller DM micelles harbored mostly monomeric $LipH^{FL}$. The oligomeric state of membrane proteins can be altered by the detergent (Reading *et al.*, 2015). Although each protein interacts in a peculiar and highly individual manner with the detergent, the oligomerization of $LipH^{FL}$ might be spatially promoted due to the left non-occupied space in the larger DDM micelles, thus forcing oligomerization of up to three foldases in a single micelle. Additionally, the preference of the rather small and single transmembrane domain (TMD) of $LipH^{FL}$ possibly tends to approach the other TMDs of the further foldase copies. These inter-helical interactions might shield the TMDs from the aqueous environment and stabilize the protein. Since no data were available until yet to compare the purified full-length foldase, further investigations are required to confirm the actual oligomeric state in the membrane environment. Furthermore, the foldase could interact with the translocon SecYEG upon the lipase translocation. Assumingly, on the one hand putative *in vivo* interactions of the foldase and the translocon could influence the oligomeric state of the foldase, while on the other hand the protruding substrate would require one copy of the foldase to pursue folding and maturation.

The successful co-expression and isolation of the full-length foldase together with the translocon is crucial to study the interaction between both proteins *in vitro*. The data indicate that both proteins were co-expressed. The immunodetection suggested that the histidine tag used for affinity purification of both proteins could not be accessed for the full-length LipH although the protein is purifiable, and LipH was detected when the protein-specific antibodies were used. Taken together, the immunodetection of co-expressed proteins indicates the successful expression and purification of them. An additional, but necessary step in terms of characterizing the full-length foldase was the validation of its functional state. Both, IMVs containing $LipH^{FL}$ and co-expressed $LipH^{FL}$/SecYEG were utilized for LipA activation and indicated the functionality of the foldase. The comparison of both datasets indicates lower LipA activation for the co-expressed sample which could be due to varying expression levels of the foldase. To enable investigations in more defined membrane systems, the functional reconstitution of the foldase into proteoliposomes ($LipH^{FL}$-PL) and MSP-based nanodiscs ($LipH^{FL}$-NDs) with tailored lipid composition were utilized. Functional reconstitution of the foldase was achieved for both membrane mimetics, whereby the $LipH^{FL}$-NDs indicated higher LipA activation values.

The foldase supports the lipase folding upon providing steric information and enabling the protein to overcome its folding barrier (El Khattabi *et al.*, 2000; Pauwels *et al.*, 2007). The high folding barrier of the lipase might be also related to the increased aggregation propensity of the protein. Efforts to create stable lipase variants were conducted leading to more stable lipase mutants in comparison to the wild type (Rashno *et al.*, 2018; Papadopoulos *et al.*, 2022). Additionally, a single point mutation of a lipase from *Pseudomonas* sp. strain KFCC 10818 indicated activity of that variant without requiring folding assistance by its cognate foldase (Kim *et al.*, 2001). These insights on the lipase properties to aggregate or in turn to be stabilized by mutations might help to elucidate the folding procedure of the enzyme and the working mechanism of the cognate foldase. In fact, the foldase as a steric chaperone acts differently in comparison to further periplasmic chaperones that serve as holdases and/or antiaggregases. While the foldase binds tightly and specific to the lipase and helps its client to overcome the folding barrier, it also stabilizes the lipase in a way that it is less aggregating when complexed to the foldase (Pauwels *et al.*, 2007; Papadopoulos *et al.*, 2022). In contrast, the seventeen kilodalton protein (Skp/HlpA/OmpH) of *P. aeruginosa*, a chaperone which majorly possess antiaggregase function, binds to the lipase, and thus prevents it from aggregation but does not provide steric information required for folding of the lipase into its active form (Papadopoulos *et al.*, 2022). Prevention of the lipase aggregation might be a crucial aspect upon further investigations to get insights about the lipase biogenesis.

The current results indicate the most efficient activation of the lipase by the soluble domain of the foldase in comparison to the membrane-based systems. The accessibility of the foldase chaperon domain is likely a key factor for the efficient folding of the lipase. Firstly, LipH-NDs manifested higher lipase activation in comparison to the proteoliposomes, as the chaperone domain is accessible on either side of the nanodiscs, while in proteoliposomes the reconstituted foldases can be oriented in two ways, where only the outward-facing chaperone domain was accessible for the lipase. Secondly, the membrane-

anchored LipH may experience spatial restrictions at the interface which hamper the complexing with the lipase. The presence of a proline- and alanine-rich variable domain (VD) after the N-terminal transmembrane domain (TMD) in the full-length foldase is suggested to function as a flexible linker that bridges the space between the membrane-interface and the chaperone domain of the foldase (Rosenau, Tommassen and Jaeger, 2004). The mutation or deletion of the VD led to reduced secretion levels of LipA (Aboubi, 2008). Therefore, the spatial distancing might be critical for the lipase:foldase interactions, to maintain a certain degree of flexibility of the chaperone domain which is important for the interaction with the lipase. Data obtained for the *in vitro* formed lipase:foldase complex indicates 1:1 stoichiometry, and the SAXS analysis of the soluble domain suggests that the chaperone domain is highly flexible. The obtained structural data on the foldase and lipase:foldase complex of *P. aeruginosa* PAO1 resembles the data derived from previous studies on the homolog system of *B. glumae* (Pauwels *et al.*, 2006). The high degree of flexibility of LipH, and the spatial limitations at the same time might be beneficial for the release of the maturated lipase from the chaperone. Accordingly, it would make sense that the foldase recognizes the protruding lipase at an early translocation step and begins to interact with the lipase in spatial proximity to the translocon. As indicated by binding analysis via MST conducted with N- and C-terminal truncations of the lipase, the recognition of the lipase by the foldase in not corrupted and binding occurs when a large C-terminal part of the protein is truncated, while already the deletion of seven amino acids on the N-terminus results in no clear binding. The results indicate that LipH can recognize shortened, but N-terminally intact variants of LipA that mimic translocation intermediates of the protein, suggesting a possible recognition of the protruding lipase upon the translocation process. Furthermore, preliminary interaction studies by surface plasmon resonance (SPR, conducted in collaboration with M. Busch) of the detergent-solubilized foldase and the reconstituted foldase in proteoliposomes indicated a decreased binding affinity shifting from nM to µM range, suggesting that the binding and release of the lipase might be dependent on the environmental conditions and/or spatial restrictions. Spatial restrictions could affect the accessibility and conformational dynamics of the foldase itself. The reduced binding affinity of the lipase to the reconstituted full-length foldase might be considered as an approximation to the processes that govern foldase:lipase interaction *in vivo*, whereby a less tight association of the proteins would be beneficial for the release of the mature lipase and thus probably being supportive for its secretion. The current observations support that the release of the lipase might not be only conducted by contacts to the secretion machinery. One may speculate that the release of mature LipA from the foldase is promoted by the recognition of protruding unfolded lipase emerging from the translocon and thus displacing the already folded protein. LipH is not upregulated upon gene expression of *lipAH* operon, pointing to the foldase as an "multi-turnover" catalyst upon the lipase folding (El Khattabi *et al.*, 1999; Rosenau, Tommassen and Jaeger, 2004) which would support an repetitive process whereby LipH recognizes freshly translocated LipA. Early studies postulated that periplasmic interactions are determinative on

the ratio of folded and unfolded lipase, and may provide a regulatory feedback that in turn can affect the lipase gene expression and export (Rosenau and Jaeger, 2000).

However, the isolation of the co-expressed LipH/SecYEG in near-native membranes (IMVs/NDs) can be used as a powerful tool for further analysis of the translocation system, hence the proteins should be in their functional state and do not require reconstitution. Recent results support the translocation capability of the proposed LipH/SecYEG IMVs, and point to the limitations of the experiment due to the properties of the lipase precursor as described above. It remains to be elucidated whether the foldase is truly involved in lipase translocation, e.g. by catching the emerging lipase at the translocon exit. So far, the high aggregation propensity and the probable intermediate folding of the lipase precursor in the tested *in vitro* translocation experimental set up did not indicate enhanced high transport.

In conclusion, an overall symphony of protein interactions is required upon the lipase biogenesis. The results indicate that the reconstitution of the foldase into model membranes was conducted successfully. This opens a wide field of application towards understanding the processes which guide the chaperone-dependent folding of bacterial proteins and can be utilized to enrich the knowledge on the maturation of secretory virulence factors, with the lipase:foldase system serving as an peculiar system of these processes. Taken together, the presented investigations on the lipase:foldase system build the fundamental basis for further research to elucidate essential processes upon biogenesis of the lipase A of *P. aeruginosa* PAO1.

5 Novel players upon lipase biogenesis

5.1 Introduction to the periplasmic chaperone network of *P. aeruginosa* PAO1

The periplasm represents a challenging environment for secretory proteins. The conditions in the periplasm reflect mostly those of the extracellular space, thus being oxidizing and chemically relatively harsh. In aim to reach their destination and to fulfill their task the secretory clients need to trespass the periplasmic space in a secured manner. A periplasmic chaperone network escorts the secretory client proteins by assisting protein folding and preventing off-pathway routes (Figure 5.1). The proteins which constitute the periplasmic network are relatively small and versatile but share similar functions. The mode of action of the periplasmic chaperones is ATP-independent. The lack of ATP in the periplasm, the common energy source for the vast cellular metabolism, represents an additional challenge to the workwise for those helper proteins. The periplasmic chaperones can serve as anti-aggregases or peptidyl-prolyl isomerases accelerating the folding rates of their clients (Stull, Betton and Bardwell, 2018). One main task of the periplasmic chaperones is their contribution to the biogenesis of outer membrane proteins (OMPs) (Stull, Betton and Bardwell, 2018). Upon OMP biogenesis, the periplasmic chaperones interact with the protruding client OMP which is transported through the Sec pathway in unfolded state (Gao, Nakajima An and Skolnick, 2022). The periplasmic chaperones can either assist the protein translocation through the Sec system, as the ancillary Sec subunits YfgM and PpiD, or enable safe passage of the client OMP through the periplasm, as exemplified by Skp, SurA and FkpA. These manifold modes of action of the periplasmic chaperones put them to the spotlight, as they carry all the traits to be putative interaction partners for the secretory lipase A of *Pseudomonas aeruginosa* PAO1.

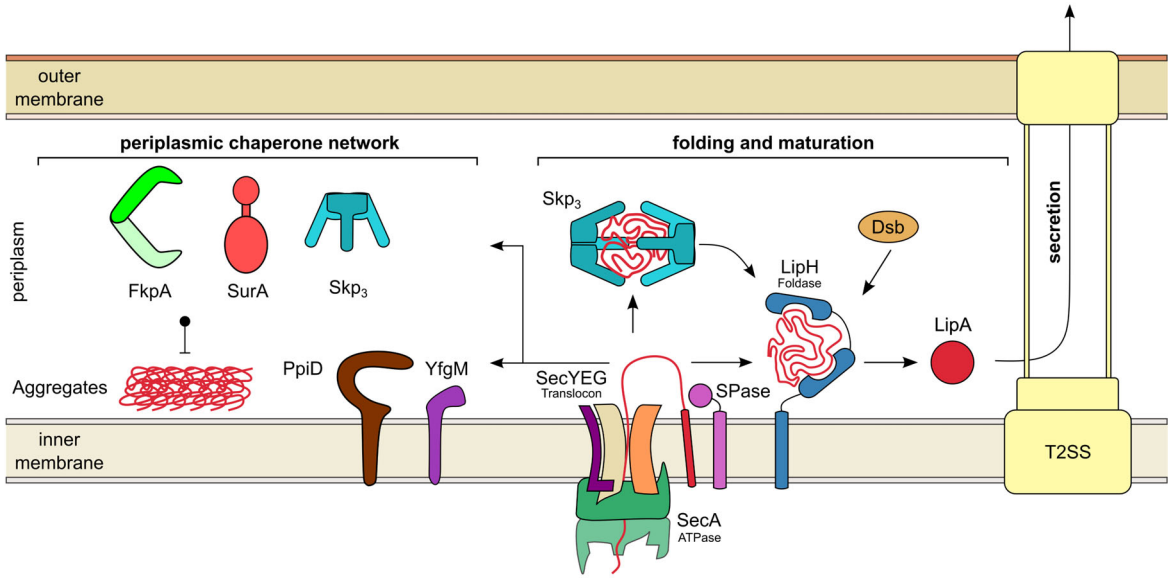

Figure 5. 1: The putative role of the periplasmic chaperone network upon lipase biogenesis

The soluble (FkpA, SurA and Skp) as well as the membrane-bound (YfgM and PpiD) periplasmic chaperones represent putative interaction partners for the lipase. Skp indicated to prevent off-pathway routes and being important for the secretion of LipA. All proteins are indicated by name in the scheme.

5.2 Experimental procedures

5.2.1 Molecular cloning

For the investigation of the periplasmic chaperones of *P. aeruginosa* PAO1, the molecular cloning, purification and characterization were conducted as described beforehand (Papadopoulos *et al.*, 2022). For structural analysis of Skp, a construct encoding for the protein with a N-terminal hexa-histidine tag and a thrombin cleavage site was created by insertion into pET28b-based plasmid via Gibson assembly (pAT115 His_6-TK-Skp-SS).

5.2.2 Expression and purification

The periplasmic chaperones FkpA, SurA, Skp, and the soluble domains of YfgM ($YfgM^{\Delta TMD}$) and PpiD ($PpiD^{\Delta TMD}$) were expressed and purified as described recently (Papadopoulos *et al.*, 2022). N-terminal tagged Skp used for further structural analysis was expressed from pAT115 in *E. coli* Rosetta^{TM} (DE3) pLysS. The transformed cells were streaked and put for cultivation overnight at 37°C on LB (Luria-Bertani medium or lysogeny broth, yeast extract 5 g/l, tryptone 10 g/l, NaCl 10 g/l) agar supplemented with 50 µg/ml kanamycin and 25 µg/ml chloramphenicol. For expression, a single colony picked from the plate was used to inoculate a pre-culture that was put for cultivation overnight at 37°C 180 rpm in LB media containing 50 µg/ml kanamycin and 25 µg/ml chloramphenicol. The pre-culture was used to inoculate fresh LB media containing 50 µg/ml kanamycin and 25 µg/ml chloramphenicol. The cells were grown at 37°C to an OD_{600} of ~ 0.6 and expression was induced by addition of 1 mM IPTG. The expression was conducted for 2 h at 37°C and afterwards the cells were harvested by centrifugation at 5000 *g* at 4°C for 20 min. The cell pellets were resuspended in 20 mM Tris/HCl pH 8.0, 100 mM NaCl, 10 % glycerol. The cells were flash-frozen in liquid nitrogen and stored at -80°C until further processing. For purification, the cells were lysed by cell disruption (M-110P cell disruptor, Microfluidics Inc.) and put for centrifugation at 205100 *g* for 1 h at 4°C. The clarified lysate was utilized for immobilized metal ion affinity chromatography (IMAC) of histidine-tagged proteins using Ni^{2+}-NTA agarose resin (Qiagen). The resin was equilibrated with buffer (20 mM Tris/HCl pH 8.0, 100 mM NaCl, 10 mM imidazole, 10 % glycerol) and the lysate applied for binding to the beads for 1 h at 6°C rolling. Afterwards the flow-through was removed by gravity flow and the Ni^{2+}-NTA resin was washed with wash buffer (20 mM Tris/HCl pH 8.0, 250 mM NaCl, 20 mM imidazole, 10 % glycerol). The purified protein was eluted from the Ni^{2+}-NTA resin in several fractions with elution buffer (20 mM Tris/HCl pH 8.0, 100 mM NaCl, 1 mM DTT, 300 mM imidazole, 10 % glycerol). The samples were applied for size exclusion chromatography (SEC) on Superdex 200 Increase 10/300 GL column (Cytiva) in aim to purify the protein to homogeneity. The protease cleavage of the affinity tag was conducted by using the thrombin cleavage kit (Thrombin CleanCleave^{TM} Kit, Sigma-Aldrich) based on the manufacturer's protocols. The samples were analyzed by SDS-PAGE and flash-frozen by liquid nitrogen and stored at -80°C until further usage.

5.2.3 Structural investigations

The homology modeling of periplasmic chaperones was conducted by utilization of phyrre2 tool (Kelley *et al.*, 2015). For Skp of *P. aeruginosa* PAO1 the homology modeling was conducted as described recently (Papadopoulos *et al.*, 2022). The structural model of Skp was generated by AlphaFold (Jumper *et al.*, 2021). X-ray crystallography was conducted in collaboration with Prof. Albert Guskov (University of Groningen, Netherlands). For crystallization, the affinity tag of purified Skp (pAT115) was removed by thrombin cleavage, as described in the previous section (Chapter 5.2.2). The protein was concentrated until precipitation occur and at this concentration the sample was pipetted for crystallization using the MemGold^{TM} (Molecular Dimensions). The best conditions for crystallization were 100 mM Tris/HCl pH 8.0, 300 mM Magnesium nitrate hexahydrate, 23 % (w/v) PEG2000. The crystal resolution at synchrotron energy was 2.7 Å.

For the small angle X-ray scattering (SAXS) analysis of Skp, the protocols and data derives from recent research (Papadopoulos *et al.*, 2022). For SAXS of the periplasmic chaperones FkpA, SurA and the soluble domains of YfgM and PpiD of *P. aeruginosa* PAO1 the proteins were expressed and purified by affinity purification and subsequent SEC on Superdex 200 Increase 10/300 GL column (Cytiva) in 20 mM Hepes/KOH pH 7.4, 50 mM KCl, 5 mM $MgCl_2$, 10 % glycerol as described recently (Papadopoulos *et al.*, 2022). The protein concentrations were, 5.03 mg/ml for FkpA, 3.66 mg/ml for SurA as well as for 11.68 mg/ml YfgM$^{\Delta TMD}$ and 3.05 mg/ml for PpiD$^{\Delta TMD}$. The data was collected in-house at Xeuss 2.0 Q-Xoom system from Xenocs which was equipped with a PILATUS 3 R 300K detector (Dectris) and a GENIX 3D CU Ultra Low Divergency x-ray beam delivery system. The sample-to-detector distance was set at 0.55 m for this experiment and resulted in an achievable q-range of 0.1 – 6 nm^{-1}.

All used programs for data processing were part of the ATSAS Software package (Version 3.0.3) (Manalastas-Cantos *et al.*, 2021). Primary data reduction was performed with the program PRIMUS (Konarev *et al.*, 2003). With the Guinier approximation, the forward scattering I (0) and the radius of gyration (Rg) were determined (Guinier, 1939). The GNOM software was used to estimate the maximum particle dimension (Dmax) with the pair-distribution function p(r) (Svergun, 1992). Low resolution models were calculated with GASBOR and GASBORMX (Svergun, Petoukhov and Koch, 2001; Petoukhov *et al.*, 2012). SASREFMX was employed for the reconstruction of the calculated dimers (FkpA). The superimpositions of the predicted models were enabled by the software SUPCOMB (Kozin and Svergun, 2001). All SAXS measurements and analysis were conducted in tight collaboration with Jens Reiners from the Center for Structural Studies at the Heinrich Heine University of Düsseldorf.

5.3 Results

5.3.1 The periplasmic chaperone Skp prevents misfolding of the secretory lipase A from *Pseudomonas aeruginosa*

Authors:	Athanasios Papadopoulos, Max Busch, Jens Reiners, Eymen Hachani, Miriam Baeumers, Julia Berger, Lutz Schmitt, Karl-Erich Jaeger, Filip Kovacic, Sander H.J. Smits and Alexej Kedrov
Type:	Original Research Article
Published in:	Frontiers in Molecular Biosciences
Impact factor:	6.113 (2022)
Date of Publication:	24. October 2022
Contribution:	70 % own contribution, the list of author contributions is included in the publication P.19. The detailed list of contributions: Molecular cloning Expression and purification of the proteins Biochemical and biophysical investigations *In vivo* experiments Manuscript writing

frontiers | Frontiers in Molecular Biosciences

TYPE Original Research
PUBLISHED 24 October 2022
DOI 10.3389/fmolb.2022.1026724

OPEN ACCESS

EDITED BY
David A Dougan,
La Trobe University, Australia

REVIEWED BY
Björn Burmann,
University of Gothenburg, Sweden
Axel Mogk,
Heidelberg University, Germany

*CORRESPONDENCE
Alexej Kedrov,
Kedrov@hhu.de

SPECIALTY SECTION
This article was submitted to Protein Folding, Misfolding and Degradation, a section of the journal Frontiers in Molecular Biosciences

RECEIVED 24 August 2022
ACCEPTED 26 September 2022
PUBLISHED 24 October 2022

CITATION
Papadopoulos A, Busch M, Reiners J, Hachani E, Baeumers M, Berger J, Schmitt L, Jaeger K-E, Kovacic F, Smits SHJ and Kedrov A (2022), The periplasmic chaperone Skp prevents misfolding of the secretory lipase A from Pseudomonas aeruginosa. *Front. Mol. Biosci.* 9:1026724. doi: 10.3389/fmolb.2022.1026724

The periplasmic chaperone Skp prevents misfolding of the secretory lipase A from *Pseudomonas aeruginosa*

Athanasios Papadopoulos[1], Max Busch[1], Jens Reiners[2], Eymen Hachani[3], Miriam Baeumers[4], Julia Berger[5], Lutz Schmitt[3], Karl-Erich Jaeger[5], Filip Kovacic[5], Sander H. J. Smits[2,3] and Alexej Kedrov[1]*

[1]Synthetic Membrane Systems, Institute of Biochemistry, Heinrich Heine University Düsseldorf, Düsseldorf, Germany, [2]Center for Structural Studies, Heinrich Heine University Düsseldorf, Düsseldorf, Germany, [3]Institute of Biochemistry, Heinrich Heine University Düsseldorf, Düsseldorf, Germany, [4]Center for Advanced Imaging, Heinrich Heine University Düsseldorf, Düsseldorf, Germany, [5]Institute of Molecular Enzyme Technology, Jülich Research Center, Jülich, Germany

Pseudomonas aeruginosa is a wide-spread opportunistic human pathogen and a high-risk factor for immunodeficient people and patients with cystic fibrosis. The extracellular lipase A belongs to the virulence factors of *P. aeruginosa*. Prior to the secretion, the lipase undergoes folding and activation by the periplasmic foldase LipH. At this stage, the enzyme is highly prone to aggregation in mild and high salt concentrations typical for the sputum of cystic fibrosis patients. Here, we demonstrate that the periplasmic chaperone Skp of *P. aeruginosa* efficiently prevents misfolding of the lipase A *in vitro*. *In vivo* experiments in *P. aeruginosa* show that the lipase secretion is nearly abolished in absence of the endogenous Skp. Small-angle X-ray scattering elucidates the trimeric architecture of *P. aeruginosa* Skp and identifies two primary conformations of the chaperone, a compact and a widely open. We describe two binding modes of Skp to the lipase, with affinities of 20 nM and 2 μM, which correspond to 1:1 and 1:2 stoichiometry of the lipase:Skp complex. Two Skp trimers are required to stabilize the lipase via the apolar interactions, which are not affected by elevated salt concentrations. We propose that Skp is a crucial chaperone along the lipase maturation and secretion pathway that ensures stabilization and carry-over of the client to LipH.

KEYWORDS

protein secretion, folding, aggregation, LipA, SurA, FkpA, PpiD, YfgM

Introduction

The Gram-negative bacterium *Pseudomonas aeruginosa* is a widespread opportunistic human pathogen of the highest biomedical importance, as indicated by the World Health Organization (Sadikot et al., 2005; Driscoll et al., 2007). The pathogenic potential of *P. aeruginosa* is associated with multiple secreted virulence

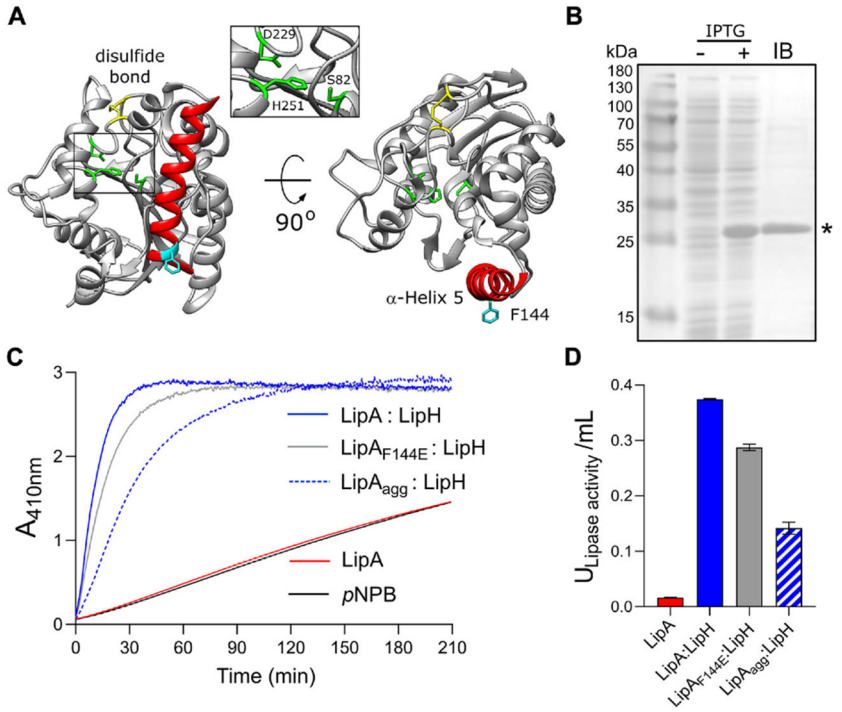

FIGURE 1
Lipase A from *Pseudomonas aeruginosa* PAO1. **(A)** Structure of the lipase LipA (PDB ID: 1EX9). The catalytic triad of Ser-82, Asp-229 and His-251 is shown in green, the disulfide bridge between Cys-183 and Cys-235 is shown in yellow. The α-helix 5 forming the lid domain is shown in red, with the residue F144 in cyan. **(B)** LipA expression and purification visualized on SDS-PAGE. Cell lysates prior to adding IPTG ("-") and after 2 h of expression ("+") are shown. Lane "IB": isolated inclusion bodies. LipA band is indicated with an asterisk. **(C)** Lipase activity *in vitro* mediated by the foldase LipH. Change in absorbance at 410 nm is associated with hydrolysis of the substrate, para-nitrophenyl butyrate (*p*NPB). Once folded in presence of LipH, the wild-type LipA and the mutant LipA$_{F144E}$ are able to hydrolyse *p*NPB (blue and grey solid traces, respectively). Pre-incubation of the wild-type lipase in the absence of LipH (LipA$_{agg}$) leads to the partial inhibition of hydrolysis (blue dashed trace). LipA activity in the absence of LipH (red trace), and the autohydrolysis of the substrate (black trace) are indicated. **(D)** Quantification of the hydrolytic activity of LipA. The lipase activity was calculated based on the colorimetric signal after 15 min of *p*NPB hydrolysis (panel C). The assays were performed in technical triplicates, the mean values and the standard deviations (SD) are shown.

factors, i.e. the extracellular enzymes, such as exotoxins, lipases and elastases, which facilitate the bacterial infection and adaptation pathways (Strateva & Mitov, 2011). The lipase A (LipA; Figure 1A) belongs to the most ubiquitously secreted extracellular enzymes (Lazdunski et al., 1990; Jaeger et al., 1994; Nardini et al., 2000). Secreted LipA is able to hydrolyse long- and short-chain triacylglycerols and, in cooperation with the phospholipase C, it facilitates the release of inflammatory mediators from the host cells (König et al., 1996). LipA accumulates in the biofilm matrix of *P. aeruginosa* on infected tissues, where it interacts with the bacterial exopolysaccharide alginate (Tielen et al., 2013). Although the physiological role of this interaction is not yet clarified, the biofilm assembly contributes to the bacterial growth, differentiation, and communication within the infection cycle, so the abundant LipA is seen as an element of bacterial pathogenicity (Tielen et al., 2013).

Similar to other secretory proteins, LipA is synthesised as a precursor with an N-terminal signal peptide, a hydrophobic stretch of 26 amino acids, that targets the unfolded lipase to the general SecA:SecYEG translocation pathway (Tsirigotaki et al., 2017). After the accomplished translocation across the cytoplasmic membrane, the signal peptide is cleaved off to release LipA into the periplasm for folding and maturation, followed by export via the type II secretion system (T2SS) (Douzi et al., 2011). LipA spontaneously folds into a compact intermediate state that manifests secondary and tertiary structure, however it lacks enzymatic activity (El Khattabi et al., 2000; Pauwels et al., 2012). To achieve the functional conformation prior to T2SS-mediated export, LipA of *P. aeruginosa* requires interaction with a specific foldase LipH encoded in the same operon as LipA (Hobson et al., 1993; Rosenau et al., 2004). LipH is a membrane-anchored protein with its C-terminal chaperone domain protruding into the periplasm. The available crystal structure

of the homologous lipase:foldase complex from *Burkholderia glumae* (Pauwels et al., 2006) and extensive biochemical and bioinformatics analysis (El Khattabi et al., 2000; Pauwels et al., 2012; Verma et al., 2020; Viegas et al., 2020) suggest that LipH-bound LipA acquires a so-called "open state," where its α-helix 5 is displaced as a "lid" aside to provide access to the catalytic site. Thus, LipH has been described as a steric chaperone that ensures correct positioning of the LipA lid domain, being a distinct feature of the lipase maturation pathway.

In the absence of the chaperone LipH, the non-activated LipA is prone to aggregation in the crowded bacterial periplasm, which is followed by proteolytic degradation or accumulation in inclusion bodies (Frenken et al., 1993). Alike, aggregation and proteolysis challenge the biogenesis of ubiquitous outer membrane proteins (OMPs), which, once translocated from the cytoplasm, should cross the periplasm prior to the integration into the outer membrane (Rollauer et al., 2015; De Geyter et al., 2016). To facilitate their targeting and disaggregation, a range of ATP-independent chaperones is present in the periplasm at micromolar concentrations (Masuda et al., 2009; Tsirigotaki et al., 2017). Widely conserved proteins SurA, Skp, and FkpA are the best-studied chaperones, which serve as holdases and escort client proteins to the outer membrane, while preventing their premature folding or aggregation. Studies using the model Gram-negative bacterium *Escherichia coli* have shown that the concentration of these chaperones in the periplasm may reach tens and hundreds of μM (Schmidt et al., 2016; Tsirigotaki et al., 2017). The soluble chaperones are further complemented by less-abundant PpiD and YfgM proteins anchored at the inner membrane and associated with the SecYEG translocon (Götzke et al., 2014; Sachelaru et al., 2014). Next to OMPs, the periplasmic chaperones are also involved in biogenesis of several secretory proteins (Purdy et al., 2007; Jarchow et al., 2008; Narayanan et al., 2011; Entzminger et al., 2012), but the mechanism of these interactions has been barely investigated.

Here, we demonstrate that folding of LipA is challenged by the high aggregation propensity of its lid domain, while a mutation within this region as well as interactions with the foldase LipH greatly stabilize the protein. When examining interactions of LipA with the general periplasmic chaperones of *P. aeruginosa*, we discover a potent anti-aggregation effect of the chaperone Skp, while LipA:Skp interactions do not prevent LipH-mediated activation of the lipase. Notably, the lipase secretion in *P. aeruginosa* is nearly abolished when the *skp* gene is knocked-out. The structural analysis of Skp reveals a characteristic jellyfish-shaped trimeric assembly and suggests extensive conformational dynamics. The hydrophobic central cavity within the Skp trimer may expand to accommodate a LipA molecule, although two bound copies of Skp trimer are required to prevent LipA from aggregation. The results of *in vitro* and *in vivo* experiments suggest that Skp is a crucial chaperone in the LipA biogenesis pathway that ensures client's maturation and secretion under challenging environmental conditions.

Materials and methods

Molecular cloning

The genes of *P. aeruginosa* PAO1 strain were identified using *Pseudomonas* Genome database (www.pseudomonas.com). Those included PA2862 (*lipA*), PA2863 (*lipH*), PA3262 (*fkpA*), PA3801 (*yfgM*), PA 1805 (*ppiD*), PA0594 (*surA*) and PA3647 (*skp/ompH/hlpA*). The genomic DNA from *P. aeruginosa* PAO1 served as a template for the amplification of the genes of interest via PCR using the KOD Xtreme polymerase (Novagen/Merck) and cloning primers containing the restriction sites (Eurofins Genomics). The PCR products were isolated using the NucleoSpin Gel and PCR Clean-up kit (Macherey-Nagel). Standard molecular cloning techniques were further employed to insert the genes of interest into target vectors using restriction nucleases (New England Biolabs). The amplified genes encoding the full-length periplasmic chaperones were initially cloned into the pET21a vector to contain C-terminal hexa-histidine tags. The following combinations of the restriction sites were used for cloning: *BamHI/HindIII* for *skp and surA*, *EcoRI/HindIII* for *yfgM* and *ppiD*, and *EcoRI/SalI* for *fkpA*. The positions of signal peptides and membrane-anchoring domains within the chaperones were identified using SignalP-5.0 and TMHMM services, respectively (Krogh et al., 2001; Petersen et al., 2011). For overexpression of the soluble proteins, the regions encoding the N-terminal signal peptides and the membrane anchors were removed via PCR and the plasmids were re-ligated. *E. coli* strain DH5α (Thermo Fisher Scientific) served as a recipient strain for cloning and plasmid multiplication. Plasmid DNA was isolated using the NucleoSpin.Plasmid.kit (Macherey-Nagel) and analysed by Sanger sequencing (Eurofins Genomics).

Expression and purification of periplasmic chaperones

The soluble chaperones were heterologously expressed in *E. coli* BL21(DE3), and Skp was expressed in *E. coli* BL21(DE3) pLysS. Overnight cultures were grown at 37°C upon shaking at 180 rpm and used for inoculation of pre-warmed LB medium. Cells were grown at 37°C upon shaking at 180 rpm until reaching OD_{600} 0.6, and overexpression was induced with 0.5 mM isopropyl-β-D-thiogalactopyranoside (IPTG; Merck/Sigma-Aldrich). After 2 h of expression, the cells were harvested by centrifugation at 6,000 g for 15 min, 4°C (rotor SLC-6000, Sorvall/Thermo Fischer) and resuspended in 50 mM KCl, 1 mM DTT, 10% glycerol, 20 mM HEPES pH 7.4 supplemented with protease inhibitors (cOmplete

Protease Inhibitor Cocktail, Roche). The cells were lysed by shear force (M-110P cell disruptor, Microfluidics Inc.) and the debris and membranes were removed by ultracentrifugation at 205,000 g for 1 h at 4°C (rotor 45 Ti, Beckman Coulter). The supernatants were applied to IMAC with Ni^{2+}-NTA-agarose resin (Qiagen) in the presence of 5 mM imidazole. After binding and extensive wash with the resuspension buffer containing 10 mM imidazole to remove weakly and non-specifically bound proteins, the chaperones were eluted with the buffer supplemented with 300 mM imidazole. The elution fractions were concentrated and subjected to SEC using Superdex 200 Increase 10/300 GL column (Cytiva). Fractions containing the chaperones were identified by SDS-PAGE, and the protein concentrations were determined spectrophotometrically based on calculated extinction coefficients at 280 nm: SurA 30940 M^{-1} cm^{-1}, FkpA 8940 M^{-1} cm^{-1}, PpiD 24870 M^{-1} cm^{-1}, YfgM 8940 M^{-1} cm^{-1} and Skp 5960 M^{-1} cm^{-1}. Monomer protein concentrations were adjusted to 50 µM and the aliquoted proteins were flash frozen and stored at −80°C. Before the experiments, the samples were thawed, centrifuged at 100.000 g, 4°C for 1 h to remove occasional aggregates and applied for SEC to match buffering conditions required for the conducted assays.

The lipase-specific foldase LipH lacking the TMD and bearing the N-terminal hexa-histidine tag was expressed heterologously as a soluble protein in *E. coli* BL21(DE3) using plasmid pEHTHis19 (Hausmann et al., 2008). LipH was purified by IMAC and subsequent SEC in 100 mM NaCl, 200 µM TCEP, 10% glycerol and 50 mM Tris-HCl pH 8.0. Samples were flash-frozen and stored at −80°C. Directly before experiments LipH samples were thawed, centrifuged at 100.000 g, 4°C for 1 h and subject to SEC in 100 mM NaCl, 10% glycerol and 20 mM Tris-HCl pH 8.0 unless other buffers are specified.

Size exclusion chromatography combined with multi-angle light scattering

SEC-MALS was employed to probe the oligomeric states of the isolated chaperones of *P. aeruginosa*. The purified proteins were concentrated to 2 mg/ml using centrifugal filters with either 3 kDa or 30 kDa cut-off (Amicon Ultra-0.5, Merck/Millipore) and the samples were centrifuged at 100,000 g, 4°C for 1 h to remove occasional aggregates. Subsequently, 80–200 µL were injected on Superdex 200 Increase 10/300 GL column (Cytiva) connected to miniDAWN TREOS II light scattering device and Optilab-TrEX Ri-detector (Wyatt Technology Corp.). FkpA, SurA and PpiD were analysed in 50 mM KCl, 5 mM $MgCl_2$ and 20 mM HEPES-KOH pH 7.4; YfgM in 5 mM glycine, 20 mM NaCl and 5 mM Tris-HCl pH 8.5; Skp in 100 mM NaCl and 20 mM Tris-HCl pH 8.0, and LipH in 100 mM NaCl, 200 µM TCEP and 50 mM Tris-HCl pH 8.0. The data analysis was performed with ASTRA 7.3.2 software (Wyatt Technology Corp.).

Small-angle X-ray scattering

SAXS data on Skp chaperone was collected using Xeuss 2.0 Q-Xoom system from Xenocs, equipped with a PILATUS3 R 300K detector (Dectris) and a GENIX 3D CU Ultra Low Divergence X-ray beam delivery system. The chosen sample-to-detector distance for the experiment was 0.55 m, resulting in an achievable q-range of 0.05–6 nm^{-1}. The measurement was carried out at 15 °C with a protein concentration of 1.20 mg/ml. Skp samples were injected into the Low Noise Flow Cell (Xenocs) via autosampler. 24 frames were collected with an exposure time of 10 minutes per frame and the data was scaled to the absolute intensity against water.

All used programs for data processing were part of the ATSAS software package, version 3.0.3 (Manalastas-Cantos et al., 2021). Primary data reduction was performed with the program PRIMUS (Konarev et al., 2003). With the Guinier approximation, the forward scattering *I(0)* and the radius of gyration (R_g) were determined. The program GNOM (Svergun, 1992) was used to estimate the maximum particle dimension (D_{max}) with the pair-distribution function *p(r)*. The *ab initio* reconstitution of the protein structure by dummy residues with P3 symmetry was performed using the GASBOR program (Svergun et al., 2001). The Skp trimer model was built using the cloud-based AlphaFold 2 Multimer algorithm (Evans et al., 2021; Jumper et al., 2021) and compared against the SAXS scattering data using CRYSOL (Svergun et al., 1995). The conformation analysis was performed using Ensemble Optimisation Method (EOM) using the default parameters (10000 models in the initial ensemble, native-like models, constant subtraction allowed) (Bernadó et al., 2007; Tria et al., 2015).

Lipase isolation

The gene PA2862 encoding for the mature LipA was cloned into pET22b plasmid via *NdeI/BamHI* restriction sites (Hausmann et al., 2008) and the protein was expressed in *E. coli* BL21(DE3). Briefly, the overnight culture with LB ampicillin (100 µg/ml) grown at 37°C upon shaking at 180 rpm was used to inoculate 100 ml LB media. Cells were grown at 37°C upon shaking at 180 rpm till reaching OD_{600} 0.6. LipA expression was induced by addition of 0.5 mM IPTG to the culture and was conducted for 2 h at 37°C. Cells were harvested by centrifugation at 4,000 g, 4°C for 15 min and resuspended in 50 mM Tris-HCl pH 7.0, 5 mM EDTA, 1 mM TCEP, supplemented with 10 µg/ml DNAse I and 50 µg/ml lysozyme (buffer IB). The suspension was incubated at 20°C for 15 min and

vortexed briefly, and the cells were lysed via sonication (ultrasonic homogenizer UP100H equipped with MS7 tip). The inclusion bodies were sedimented by centrifugation at 15000 g, 4°C for 10 min and suspended in the buffer IB for washing, followed by centrifugation. After repeating the procedure twice, the pellet was washed with 50 mM Tris-HCl pH 7.0. The inclusion bodies were dissolved in 8 M urea and 20 mM Tris-HCl pH 7.25, and the insoluble material was removed via a centrifugation step (21000 g, 10 min, 4°C). The protein purity was assessed by SDS-PAGE and subsequent staining (Quick Coomassie stain, Serva). LipA concentration was determined spectrophotometrically (extinction coefficient at 280 nm, ε_{280} = 27515 M^{-1} cm^{-1}). LipA was aliquoted in reaction tubes (Low Protein Binding, Sarstedt), flash-frozen and stored at -80°C.

Optionally, LipA was fluorescently labelled to increase the detection efficiency in the sedimentation assay. LipA contains two endogenous cysteines in positions 183 and 235, which were targeted for site-specific fluorescent labelling. The urea-denatured LipA was incubated in 25-fold molar excess of fluorescein-5-maleimide (FM, Thermo Fisher Scientific) for 3 h at the ambient temperature. After the incubation, LipA was precipitated with 15% TCA for at least 1 h on ice. The precipitated proteins were sedimented via centrifugation at 21000 g, 4°C for 15 min, and the supernatant was removed. The pellets were washed with 0.5 ml ice-cold acetone, and then repeatedly sedimented via centrifugation at 21000 g, 4°C for 10 min. After drying at 37°C, LipA-FM pellet was solubilised in 8 M urea and 20 mM Tris-HCl pH 7.25. To remove the remaining free dye, TCA precipitation and washing steps were repeated twice. The labelling efficiency of ~150% was determined spectrophotometrically based on the absorbance at 280 and 495 nm and the molar extinction coefficients for LipA and FM, respectively. LipA-FM was visualised on SDS-PAGE via blue-light excitation and following Coomassie blue staining.

In vitro activity of the lipase

To measure the hydrolytic activity of LipA, equimolar concentrations of the foldase LipH in TGCG buffer (5 mM Tris pH 9, 5 mM glycine, 1 mM $CaCl_2$, 5% glycerol) and the urea-denatured LipA (8 M urea and 20 mM Tris-HCl pH 7.25) were mixed together at concentration 1 µM in TGCG buffer to form lipase:foldase complexes in reaction tubes (Low Protein Binding, Sarstedt). The complex formation was set for 15 min at 37°C. After the incubation, 10 µL of the sample were diluted 10-fold with the TGCG buffer in 96-well plates. For the substrate preparation, 10 mM *para*-nitrophenyl butyrate, ~1.76 µL, (*p*NPB, Merck/Sigma) were diluted from the stock solution in 1 ml acetonitrile. Immediately before starting the measurement, the substrate solution was diluted 10-fold with 50 mM triethanolamine pH 7.4 and mixed. Subsequently, 100 µL of the substrate solution was transferred to 96-well-plates with the pre-assembled LipA:LipH complex, so each well contained 0.5 mM *p*NPB and 50 nM LipA:LipH complex. For the negative control, LipA without LipH were treated the same as all other samples. To measure the autohydrolysis of the substrate, both LipA and LipH were omitted, but the corresponding buffers were added to *p*NPB. The hydrolysis of *p*NPB to *p*-nitrophenolate and butyric acid was determined by measuring the absorbance of the liberated p-nitrophenolate at 410 nm over 3.5 h at 37°C on a plate reader (Infinite 200 pro, TECAN). Samples were shaken for 5 s prior to each measurement. The hydrolytic activity of LipA was analysed by monitoring the hydrolysis based the *p*-nitrophenolate absorbance (as previously described) and by calculating the active LipA in U/mL in the linear range of the reaction (first 15 min), with the estimated molar extinction coefficient of p-nitrophenolate at 410 nm under the applied conditions of 12500 M^{-1} cm^{-1} (Filloux & Walker, 2014). The light path length in the well was experimentally determined and was of 0.53–0.55 cm upon applied conditions.

When indicated, the experiments were performed in the presence of NaCl and calcium upon LipA:LipH assembly and during the substrate hydrolysis measurements. Prior to the experiments, LipH was transferred into 100 mM NaCl, 10% glycerol and 20 mM Tris-HCl pH 8.0 by SEC, and the composition of the buffer for LipA:LipH assembly, as well as for hydrolysis measurements were adjusted. To study the effect of the periplasmic chaperones (Skp, YfgM, FkpA, SurA, PpiD) on the hydrolytic activity, the chaperones were transferred into either the TGCG buffer or 100 mM NaCl, 10% glycerol (v/v) and 20 mM Tris-HCl pH 8.0 by SEC. LipA and LipH were added in concentrations of 1 µM to form the complex, while the periplasmic chaperones were added in 5-fold molar excess. The complex formation and hydrolysis measurements were performed as described above. The activation of LipA by the periplasmic chaperones was also determined by adding LipA to the periplasmic chaperones at 1:5 M ratio in the absence of LipH. To probe the effect of the periplasmic chaperones on LipA aggregation prior to the activation, 1 µM LipA was incubated with individual periplasmic chaperones for 15 min at 37°C. Afterwards, 1 µM LipH was added to the mixtures and incubated for 15 min at 37°C. The measurements of *p*NBP hydrolysis were performed as described above.

Light scattering assay of LipA aggregation

For the assay, either urea, TGCG buffer or 20 mM Tris-HCl pH 8.0 supplemented with NaCl were filtered using 0.1 µm syringe filters. 68.8 µL of each buffer was loaded in 96-well plates with flat transparent bottom. The urea-denatured LipA was diluted with the TGCG buffer from 150 µM stock solution to 1.6 µM, and 31.2 µl were added to 96-well microtiter plates, so the final LipA concentration was 0.5 µM. The residual urea

concentration was approx. 25 mM. The samples were incubated for 1 h at 37°C, while recording the optical density at 320 nm with intervals of 30 s (Infinite M200 PRO plate reader, Tecan Trading AG). For each condition, three technical replicates were performed.

Sedimentation analysis of LipA aggregation

LipA aggregation at various conditions was probed by sedimentation assay. To improve the detection sensitivity and so facilitate the experiment at low lipase concentrations, site-specific fluorescent labelling of the lipase was introduced. The endogenous cysteines at positions 183 and 235 were conjugated with FM, as described above, so as little as 5 ng LipA-FM could be detected via in-gel fluorescence imaging. The urea-denatured LipA-FM was diluted with the TGCG buffer from 150 μM stock solution to 1.6 μM and kept on ice protein in reaction tubes (Low Protein Binding, Sarstedt). The chaperones were transferred to 1.5 ml polypropylene reaction tubes containing 20 mM Tris-HCl pH 8.0 and varying NaCl concentrations, to achieve the specific ionic strength indicated for each assay. The minimal ionic strength conditions were probed when using the TGCG buffer. 15.6 μL of LipA-FM were added to the tube and mixed by pipetting, so the reactions contained 0.5 μM LipA-FM and 5 μM of individual chaperones in the total volume of 50 μl. For the dimeric FkpA and trimeric Skp, the monomer concentrations were 10 and 15 μM, respectively. The LipA-specific foldase LipH was used in the equimolar ratio to the lipase (final concentration 0.5 μM). The reaction tubes were incubated at 37°C for 15 min to promote LipA aggregation and the samples were then centrifuged (21000 g, 15 min, 4°C) to sediment the aggregates. To avoid disturbing the pellets, 40 μl of each supernatant fraction were transferred to new 1.5 ml tubes. The remaining material contained the pelleted LipA and 10 μL of the supernatant fraction. Both samples were precipitated by adding 100 μl of 20% TCA and incubating for 15 min on ice. The precipitated proteins were pelleted upon centrifugation at 21000 g, 4°C for 10 min, TCA was removed, and the samples were washed, as described above. Further, 15 μl of the reducing SDS-PAGE sample buffer were used to wash the tube walls, 5 μL of the sample were loaded on SDS-PAGE and in-gel fluorescence was recorded. The signal was quantified by ImageQuant software (Cytiva). The background was subtracted using the local average algorithm. The signals of the supernatant (I_{sol}) represent the soluble fraction of LipA and correspond to 80% of the total soluble LipA. The value was used then to calculate the actual signal intensities of the soluble ($I_{sol,\ corr}$) and aggregated ($I_{agg,\ corr}$) LipA, as:

$$I_{sol,corr} = 1.25 * I_{sol}$$
$$I_{agg,corr} = I_{agg} - 0.25 * I_{so\,l}$$

where I_{agg} is the signal measured for the aggregated LipA and the remaining 10 μL of the supernatant. The soluble fraction of LipA was calculated as a ratio:

$$\frac{I_{sol,corr}}{I_{sol} - I_{agg}}$$

Each assay was carried out in triplicates.

Amyloid-specific ThT fluorescence

Thioflavin T (ThT, Merck/Sigma-Aldrich) was dissolved to the concentration of 100 μM in the buffer TGCG, and the solution was kept on ice. Immediately prior to the experiment, ThT was diluted with the TGCG buffer to 10 μM and mixed with 0.5 μM urea-denatured LipA and 5 μM chaperones. For the dimeric FkpA and trimeric Skp, the monomer concentrations were 10 and 15 μM, respectively. The total volume was set to 65 μl, where the residual urea concentration was approx. 60 mM, and the reaction was carried out at 20°C in reaction tubes (Low Protein Binding, Sarstedt). For the control experiments, containing either the chaperones or LipA, the reaction volume was adjusted to 65 μl with an appropriate buffer. After incubation at 37°C for 15 min, each reaction was transferred into a quartz cuvette for measuring ThT fluorescence at the fluorescence spectrophotometer (Fluorolog 3, Horiba Scientific). The excitation wavelength was set at 450 nm, and the emission spectra were recorded from 467 to 520 nm. ThT fluorescence intensity at 485 nm was used to evaluate and compare LipA aggregation between samples. Each measurement was carried out in independent triplicates.

Microscale thermophoresis

MST was used to monitor interactions of Skp from *P. aeruginosa* with FM-labelled $LipA_{F144E}$. $LipA_{F144E}$ was diluted to 100 nM in the TGCG buffer supplemented with 0.05% Tween 20 and kept on ice protected from light. For the MST measurement, 10 μl of 50 nM LipA were mixed with Skp ranging from 2.3 nM to 18.5 μM in a 0.5 ml reaction tube (Low Protein Binding, Sarstedt). LipA:Skp samples were incubated for 15 min at 22°C in the dark, then loaded into Premium-type capillaries and analysed in Monolith NT.115 instrument (NanoTemper Technologies, Munich, Germany). The MST power was set to 80% and the LED power in the blue channel was set to 60%. The thermophoresis was detected by the normalised fluorescence time traces for 30 s with 5 s delay and 5 s for recovery. The putative LipA aggregation at the capillary surface was controlled by recording the fluorescence intensity profiles of individual

capillaries before and after the experiment (time difference approx. 1 h). The data was evaluated by NT Analysis software (NanoTemper Technologies, Munich, Germany). Each sample was analysed twice, and the measurement were performed in independent triplicates.

Transmission electron microscopy

TEM was utilized to visualize the formation of LipA aggregates. All buffers were filtered with 0.1 µm syringe filters (Whatman Puradisc). Denatured LipA was diluted to 300–500 µM in 8 M urea and 20 mM Tris-HCl pH 7.25 and then further diluted to 3–5 µM in either 8 M urea and 20 mM Tris-HCl pH 7.25, TGCG buffer or in 150 mM NaCl, 10% glycerol and 20 mM Tris-HCl pH 8.0. Samples containing Skp or LipH were prepared in 150 mM NaCl, 10% glycerol and 20 mM Tris-HCl pH 8.0 to promote lipase aggregation and examine the anti-aggregating effect of the chaperones. LipA:LipH samples contained 5 µM LipA and 15 µM LipH (molar ratio 1:3) and LipA:Skp_3 samples contained 3 µM LipA and 15 µM Skp_3 (molar ratio 1:5). All samples were incubated for 15 min at 37°C and used for grid preparation on a carbon-coated copper grid. 3 µl of sample were added on top of the grid incubated for 1 min at the ambient temperature. Excess liquid was removed using filter paper. For negative staining, the grid was incubated in 2% uranyl acetate (solution in distilled water pH 4.3) for 1 min in the dark. Afterwards, excess liquid was removed. Grids were dried at the ambient temperature for at least 15 min prior TEM imaging. TEM images were acquired at the Zeiss EM902 operating at 80 keV using a slow-scan CCD-Camera (Typ 7899 inside) controlled by the imaging software ImageSP (SYSPROG, TRS) and prepared using the image processing software "Fiji" (Schindelin et al., 2012).

Analysis of LipA secretion *in vivo*

The genomic DNA of *P. aeruginosa* PAO1 isolated with the DNeasy blood and tissue kit (QIAGEN, Germany) was used as the PCR template to amplify the *lipA-lipH* operon using Phusion® DNA polymerase (Thermo Fisher Scientific, Darmstadt, Germany). The pGUF-lipAH plasmid for gene expression in *P. aeruginosa* was constructed by ligation of the PCR product into the pGUF vector (Babic, 2022) at AflII and SmaI restriction sites. Molecular cloning was conducted in *E. coli* DH5α, and the plasmid assembly was confirmed by Sanger sequencing (Eurofins Genomics). *P. aeruginosa* PA14 wild-type and Δ*skp* strains (Klein et al., 2019) transformed with pGUF (empty vector, EV) and pGUF-lipAH were cultivated in triplicates in Erlenmeyer flasks in 10 ml autoinduction medium (Terrific Broth medium containing 0.04% lactose (w/v) and 0.2% glucose (v/v)) supplemented with 100 µg/ml tetracycline. Plates were shaken at 600 rpm, volume 1.2 ml, for 24 h at 37°C. Cells were harvested by centrifugation at 4,000 g, 4°C for 10 min and the culture supernatants were filtered through 0.22 µm pore size cellulose acetate filter to remove the remaining cells. The cell pellets and the culture supernatants were kept on ice to prevent proteolysis. The supernatant concentrations were adjusted based on absorbance at 280 nm. 40 µl of the mupernatnts were diluted to final volume of 80 µl with TGCG buffer and further used for measuring the lipolytic activity of the secreted enzymes. The measurements were conducted in technical duplicates for all biological triplicates, thus 40 µl of sample were put in 96-well microtiter plates, and 40 uL of 1 mM of *p*NPB were added for measuring the esterase activity. The hydrolytic activity of the secreted elastase LasB was determined using Abz-Ala-Gly-Leu-Ala-*p*-nitro-benzyl-amide substrate (Echelon Biosciences) (Zhu et al., 2015). Supernatants were diluted 20-fold with 100 mM Tris-HCl pH 7.5 and 20 µl of each supernatant was loaded in 96-well microtiter plates. Prior to measurement, 250 mM substrate solution in 50 mM Tris-HCl pH 7.0, 2.5 mM $CaCl_2$, 1% DMSO (v/v) was added to the samples in volumes of 100 µl. The increase in fluorescence (λ_{ex} = 340 nm, λ_{em} = 415 nm) was monitored for 30 min at 37°C. As a positive control, the substrate was incubated with 0.3 units of proteinase K (Thermo Scientific, PCR grade). To measure the oxidase activity, the substrate solution (50 mM Tris-HCl pH 7.4, 0.12 mM NADH, 0.2 mM DTT) was added to the diluted supernatants in volumes of 100 µl per well prior to measurement. *E. coli* DH5α cells lysed via sonication (Sonotrode) were used as a positive control. The decrease in absorbance at 340 nm due to the enzymatic conversion of NADH to NAD^+ was measured for 2 h at 23°C.

For immunoblotting the secreted proteins from the supernatant fractions were 5-fold concentrated by precipitation with trichloroacetic acid and suspension with SDS-PAGE sample buffer (100 mM Tris-HCl pH 6.8, 4% (w/v) SDS, 0.02% (w/v) bromophenol blue, 200 mM DTT, 20% glycerol). Based on the absorbance measured at 280 nm, equal amounts of samples were loaded on 15% SDS-PAGE and then transferred to PVDF membrane (Cytiva) for 1 h at 4°C using a tank-blot system (Bio-Rad Laboratories). Afterwards, the membrane was washed three times with TBS buffer (20 mM Tris-HCl pH 8.0, 250 mM NaCl) upon shaking at 20°C for 5 min. Blocking was conducted in TBS-T buffer (20 mM Tris-HCl pH 8.0, 250 mM NaCl, 0.1% Tween-20) supplemented with 10% skimmed milk for 1 h at 20°C. The membrane was rinsed and washed three times at 20°C with TBS-T followed by washing in TBS. Rabbit serum with polyclonal antibodies raised against the purified LipA (Speedy 28-Day program, Kaneka Eurogentec S.A.) were added in 1:2,000 dilution in TBS-T with 2% BSA and incubated overnight at 4°C. Afterwards, the membrane was

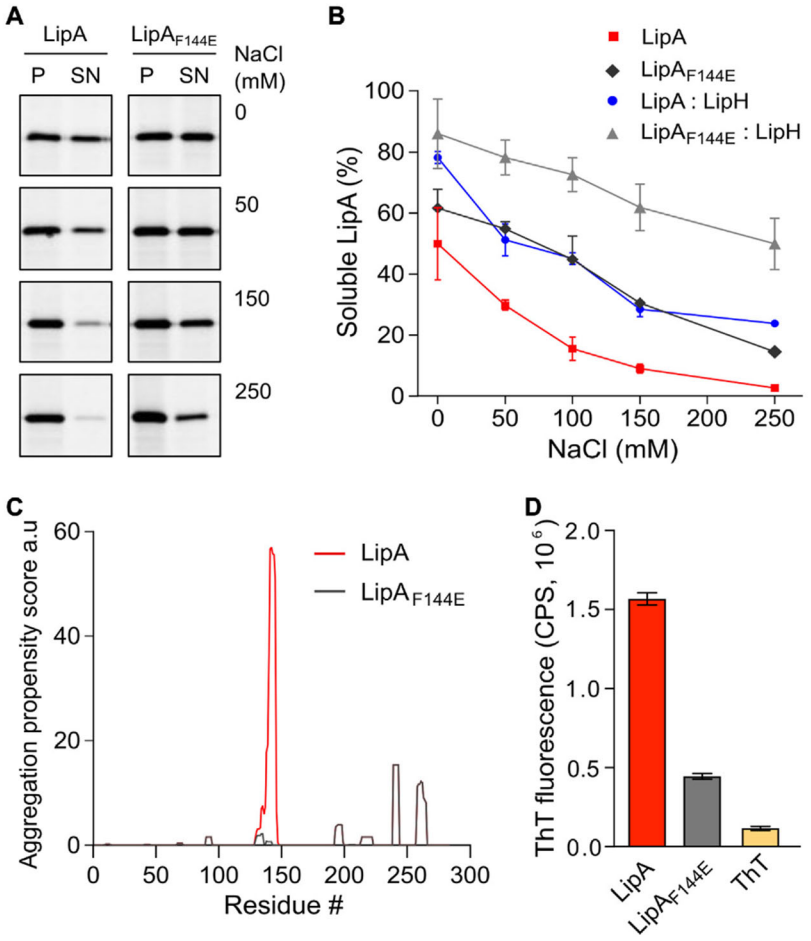

FIGURE 2
LipA aggregation propensity is sensitive to the environment and the structure of the lid domain. **(A)** SDS-PAGE of the aggregated and soluble LipA variants separated into the pellet (P) and the supernatant (SN) fractions, respectively, upon centrifugation. The concentrations of NaCl in the buffer are indicated. For the in-gel fluorescence detection, the lipases were labelled with fluorescein-5-maleimide. **(B)** Quantification of the soluble LipA at various conditions. The fraction of the soluble wild-type LipA and the mutant LipA$_{F144E}$ at various salt concentrations and, optionally, in presence of LipH was calculated from SDS-PAGE (panel A). The assays were performed in technical triplicates, the mean values and SD are shown. **(C)** Sequence-based prediction of LipA aggregation propensity by TANGO algorithm (Fernandez-Escamilla et al., 2004). Profiles for the β-aggregation propensity scores of the wild-type LipA (red) and the mutant LipA$_{F144E}$ (grey) indicate the aggregation-prone regions within the polypeptide chain. The aggregation propensity of the wild-type LipA is dominated by the α-helix 5 that forms the lid domain. **(D)** LipA aggregation is associated with the formation of β-structured amyloid-like aggregates. The intensity of the amyloid-sensitive ThT fluorescence at 485 nm was measured in the presence of either the wild-type LipA (red), the mutant LipA$_{F144E}$ (grey), or the dye alone (yellow). The assays were performed in technical triplicates, the mean values and SD are shown.

rinsed and washed three times at 20°C with TBS-T followed by washing in TBS. Secondary antibodies conjugated with horseradish peroxide (goat/anti-rabbit; Sigma A545) were added in 1:20,000 dilution in TBS-T with 2% BSA and incubated for 1 h at 20°C. The membrane was rinsed and washed three times at 20°C with TBS-T followed by washing in TBS. The blot was developed with Westar C Ultra 2.0 chemiluminescent substrate (Cyanagen) and imaged on Amersham Imager 680RGB (Cytiva).

Results

LipA aggregation is mediated by the lid domain

To investigate folding and activation of the lipase *in vitro*, LipA lacking the N-terminal signal peptide was heterologously overexpressed in *E. coli*. The overexpression resulted in formation of inclusion bodies consisting nearly exclusively of

LipA, and the protein was isolated in the urea-denatured state (Figure 1B). The denatured LipA is a relevant mimetic of the protein that enters the periplasm as an unfolded polypeptide chain, and it was used for the further analysis. To examine whether the recombinant protein may be refolded into its functional form, LipA was diluted into the urea-free low-salt TGCG buffer (5 mM Tris pH 9.0, 5 mM glycine, 1 mM $CaCl_2$ and 5% glycerol) and incubated in the presence of the foldase chaperone LipH. The enzymatic activity of LipA was assessed then via measuring the hydrolysis of a model substrate, *para*-nitrophenyl-butyrate (*p*NPB): Accumulation of the product, *p*-nitrophenolate, was followed colorimetrically until reaching the signal saturation, and the activity of the lipase A was quantified (Figures 1C,D). In the absence of LipH, the signal remained at the level of the autohydrolysis of *p*NPB, so the hydrolytic activity of LipA was not induced. Thus, the recombinant LipA could be folded *in vitro*, and LipH was required for activation of LipA.

Notably, if LipA was incubated in the urea-free buffer prior to adding the foldase LipH, its hydrolytic activity was substantially reduced, as the amount of *p*-nitrophenolate generated in the first 15 min of the reaction decreased three-fold (Figures 1C,D). We speculated that the lipase underwent aggregation/misfolding in the absence of the foldase LipH, causing the loss of activity. Indeed, we observed a rapid increase in light scattering once the lipase was incubated in absence of urea (Supplementary Figure S1A), and approx. 50% of LipA could be sedimented upon mild centrifugation at 21000 g (Figure 2A). The sedimentation was enhanced upon increasing the ionic strength of the solution, reaching 70% and 95% in the presence of 50 and 150 mM NaCl, respectively (Figure 2B) and abundant large particles were observed by negative-stain electron microscopy (Supplementary Figure S1B). The stoichiometric amount of LipH stabilised the lipase, although the efficiency decreased at elevated salt concentrations and the hydrolytic activity of the lipase reduced (Figure 2B and Supplementary Figure S1C). Since LipA:LipH binding is primarily driven by electrostatic interactions (El Khattabi et al., 2000; Pauwels et al., 2006, 2012), the affinity of the complex was likely reduced at the high ionic strength and LipA aggregation became a dominant pathway even in the presence of the chaperone.

Based on its amino acid sequence, the α-helix 5 known as the "lid domain" of LipA is predicted to be the primary aggregation-prone region within the protein, with a high propensity to misfold into β-strands (Figure 2C, red line) (Fernandez-Escamilla et al., 2004). Previous studies on a homologous lipase demonstrated that a point mutation Phe to Glu within the lid domain diminished the aggregation propensity and rendered an aggregation-resistant protein (Rashno et al., 2018). Based on the structure homology, we recognised an identically positioned phenylalanine residue within *P. aeruginosa* PAO1 LipA at position 144, where the point mutation to glutamate could suppress the lipase misfolding (Figure 2C, black line). To examine the effect of the mutation on the lipase folding and activity, the mutant $LipA_{F144E}$ was overexpressed and isolated in its urea-denatured state. In the presence of LipH, $LipA_{F144E}$ displayed the enzymatic activity, indicating that the mutation did not hinder the chaperone-mediated folding (Figures 1C,D). Indeed, the lid domain is not involved in LipA:LipH contacts (Pauwels et al., 2006), and the mutated residue is oriented toward the solvent and does not belong to the moiety of the catalytic site (Figure 1A).

To examine whether $LipA_{F144E}$ is indeed more resistant against aggregation than the wild-type lipase, its solubility was probed over a range of salt concentrations. The point mutation had a notable effect on the protein stability: Nearly 50% of $LipA_{F144E}$ remained soluble in the presence of 100 mM NaCl, where the soluble fraction of the wild-type LipA did not exceed 15% (Figure 2B), and the activity of the refolded lipase mutant was weakly affected by the ionic strength (Supplementary Figure S1C). As the aggregated lipase tends to form β-sheet-rich structures and amyloids (Rashno et al., 2018), we further examined this propensity for the wild-type LipA and $LipA_{F144E}$ mutant. To do so, we measured the fluorescence intensity of the dye thioflavin T (ThT), which fluorescence increases manifold upon binding to β-strands characteristic to amyloids (Biancalana & Koide, 2010). Once the dye was added to the wild-type lipase in the TGCG buffer supplemented with 20 mM NaCl, its fluorescence intensity increased 10-fold, suggesting that β-stranded structures were formed even at the low salt concentration (Figure 2D and Supplementary Figure 1D). In contrast, the ThT fluorescence was only modestly affected in the presence of $LipA_{F144E}$, increasing 3-fold above the signal of free ThT, in agreement with the reduced aggregation of the mutant.

As both the mutation within the lid domain of LipA and the LipA:LipH assembly favoured the soluble state of the lipase, we questioned whether both cases involve the same stabilisation mechanism. To address this, the solubility of the wild-type LipA and $LipA_{F144E}$ in the presence of the foldase was compared (Figure 2B). Strikingly, the solubility of the mutant $LipA_{F144E}$ was further enhanced by LipH: At elevated salt concentrations, the fraction of the soluble $LipA_{F144E}$ exceeded approx. two-fold that of the wild-type LipA, so even at 250 mM NaCl the major fraction of $LipA_{F144E}$:LipH remained soluble. Conclusively, the effects of the mutation within the lid domain and the lipase: foldase binding were additive, and distinct mechanisms must have contributed to the lipase stabilisation.

Characterisation of periplasmic chaperones of *P. aeruginosa*

The extensive aggregation of the wild-type LipA observed already at moderate salt concentrations is a potential challenge for its timely interactions with the stabilising foldase LipH,

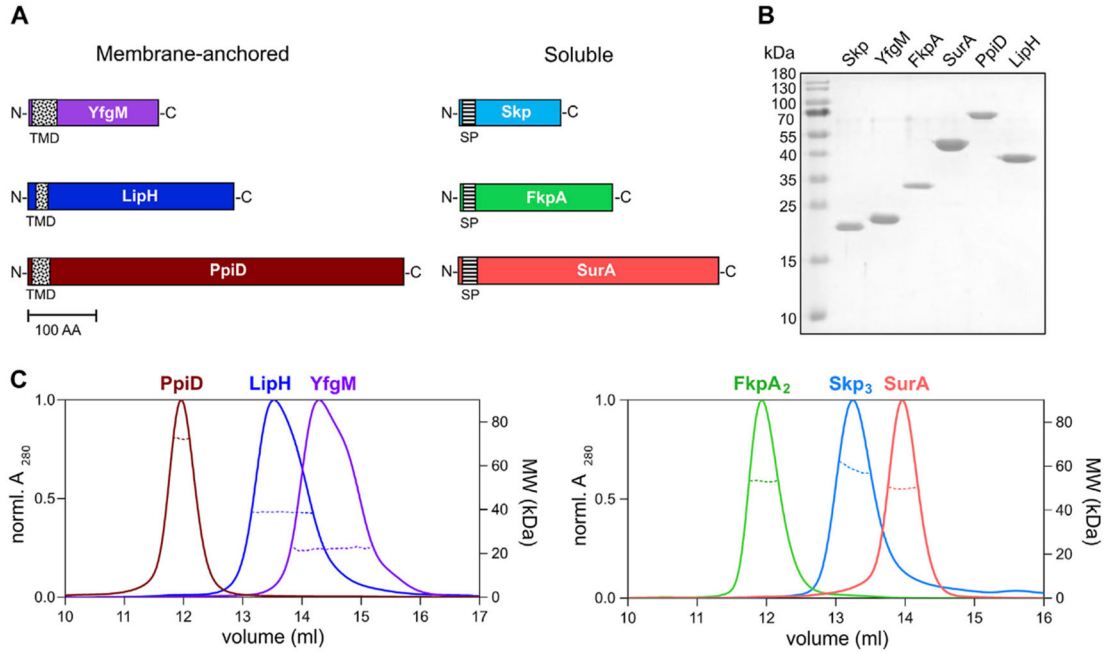

FIGURE 3
Periplasmic chaperones of *P. aeruginosa* PAO1. **(A)** Schematic overview of the periplasmic chaperones of *P. aeruginosa* PAO1. The predicted transmembrane domains (TMD, black-dotted) and the signal peptides (SP, black-ruled) were removed to express the soluble chaperones. Scale bar: 100 amino acid residues (AA). **(B)** SDS-PAGE of the isolated periplasmic chaperones of *P. aeruginosa*. **(C)** SEC-MALS analysis of the periplasmic chaperones to determine the oligomeric states in solution. Solid traces represent the absorbance at 280 nm, and dashed traces indicate the molecular weights (*y*-axis on the right) calculated from the light scattering. The analysis reveals dimers of FkpA ($FkpA_2$) and trimers of Skp (Skp_3), while SurA, YfgM, PpiD and LipH are monomeric in solution.

especially under high-salinity conditions within cystic fibrosis patients' sputum (Grandjean Lapierre et al., 2017). As highly abundant periplasmic chaperones may facilitate folding and secretion of several recombinant proteins, including a recombinantly expressed lipase of *Burkholderia* (Purdy et al., 2007; Jarchow et al., 2008; Narayanan et al., 2011; Entzminger et al., 2012; Dwyer et al., 2014), we speculated that the chaperones of *P. aeruginosa* may recognize LipA and protect it from aggregation prior interactions with the specific foldase LipH.

To characterize LipA:chaperone interactions in a well-defined *in vitro* system, the primary soluble chaperones Skp, FkpA and SurA lacking their signal peptides (Figure 3A), as well as the periplasmic domains of YfgM and PpiD of *P. aeruginosa* PAO1 were heterologously expressed and purified from *E. coli*. The apparent molecular weights of the chaperones observed in SDS-PAGE agreed with the values calculated for individual protomers (18 kDa for Skp, 20 kDa for YfgM, 27 kDa for FkpA, 47 kDa for SurA and 67 kDa for PpiD; Figure 3B). To scrutinise the oligomeric states of the isolated chaperones, their native masses were determined by size exclusion chromatography combined with multi-angle light scattering analysis (SEC-MALS, Figure 3C). The experiment revealed monomers of SurA (determined molecular weight of 49.6 ± 0.6 kDa), dimers of FkpA (53.2 ± 0.9 kDa; $FkpA_2$), and trimers of Skp (58.6 ± 0.7 kDa; Skp_3), in agreement with the known structures of homologs from *E. coli* (Bitto & McKay, 2002; Saul et al., 2004; Walton & Sousa, 2004). The periplasmic domains of both YfgM and PpiD were found to be monomers, with molecular masses of 22.2 ± 0.4 kDa and 72.2 ± 0.2 kDa, respectively. The periplasmic chaperone domain of LipH appears to be monomeric in solution (determined molecular weight 39.4 ± 0.3 kDa). The attempts to analyse the molecular mass of either wild-type LipA or $LipA_{F144E}$ were not successful, as the hydrophobic protein was possibly interacting with the column matrix and could not be eluted with aqueous buffers.

The chaperone Skp prevents LipA from aggregation

The propensity of the individual chaperones to prevent LipA aggregation was first evaluated by the sedimentation analysis. To mimic the natural abundance of SurA, $FkpA_2$ and Skp_3 in the

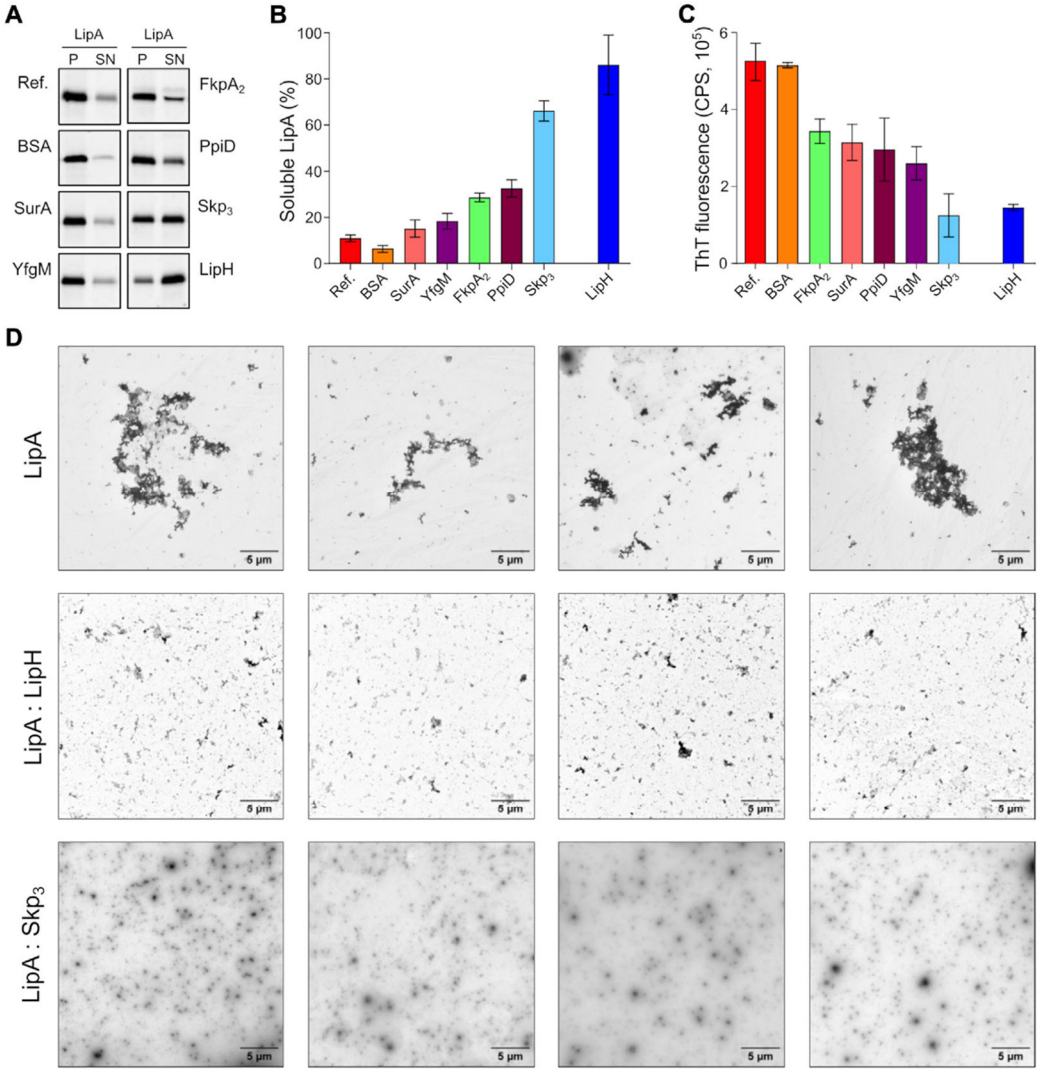

FIGURE 4
The periplasmic chaperone Skp rescues LipA from aggregation. **(A)** LipA solubility in the presence of the periplasmic chaperones. The aggregated and soluble LipA fractions are separated in pellet (P) and supernatant (SN) fractions in the sedimentation assay and visualized on SDS-PAGE via in-gel fluorescence. The supplemented chaperones are indicated. Bovine serum albumin (BSA) was used as a negative control. LipA in absence of chaperones is indicated as "Ref.". **(B)** Quantification of the soluble LipA in the presence of the periplasmic chaperones from SDS-PAGE (panel A). The assays were performed in technical triplicates, the mean values and SD are shown. **(C)** The periplasmic chaperones suppress formation of LipA β-structured aggregates. ThT fluorescence was recorded for the wild-type LipA in the presence of the periplasmic chaperones, and the fluorescence measured for the chaperones alone was subtracted. The assays were performed in technical triplicates, the mean values and SD are shown. **(D)** LipA aggregation in presence and absence of LipH (LipA:LipH) or Skp (LipA:Skp_3) visualized *via* negative-stain TEM. Scale bars are indicated. The relatively low contrast repeatedly observed in LipA:Skp_3 samples was attributed to the high concentration of the chaperone (45 µM of monomeric Skp).

bacterial periplasm, as described for the model organism *E. coli* (Schmidt et al., 2016; Tsirigotaki et al., 2017), and to ensure the uniform lipase:chaperone molar ratio of 1:10, 0.5 µM LipA and 5 µM of chaperones were used in the experiments, corresponding to 10 µM of FkpA and 15 µM Skp monomers. The salt concentration was set to 150 mM NaCl, which closely matches the salinity of the sputum environment (Grandjean Lapierre et al., 2017). In the absence of the chaperones, only 10% of LipA was found in the soluble form, and the value increased moderately in the presence of either SurA or $FkpA_2$ (solubility

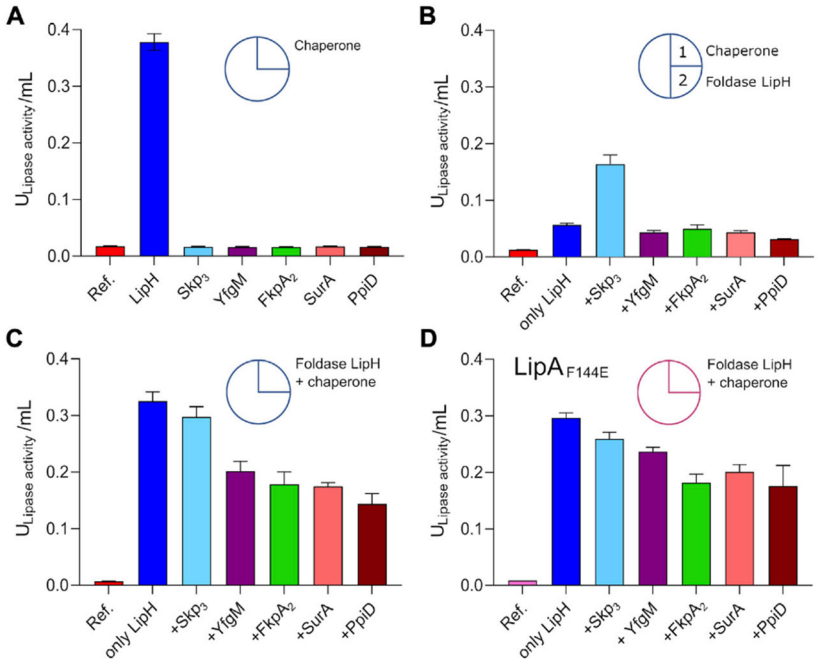

FIGURE 5
Interplay of periplasmic chaperones upon the lipase activation. The lipase activity against *p*NPB over the first 15 min of the hydrolysis reaction is shown in bars. Circle scheme describes the incubation steps. LipA activity in absence of chaperones is indicated as "Ref.". **(A)** Incubation of the wild-type LipA with either the foldase LipH or general periplasmic chaperones in the TGCG buffer. **(B)** Initial incubation of the wild-type LipA with general periplasmic chaperones at 100 mM NaCl (1) followed by incubation with LipH (2). **(C)** Simultaneous incubation of the wild-type LipA with LipH and periplasmic chaperones in 50 mM NaCl, 1 mM $CaCl_2$, 10% glycerol (v/v) and 20 mM Tris-HCl pH 8.0. **(D)** Simultaneous incubation of the mutant $LipA_{F144E}$ with LipH and periplasmic chaperones in 50 mM NaCl, 1 mM $CaCl_2$, 10% glycerol (v/v) and 20 mM Tris-HCl pH 8.0. The assays were performed in technical triplicates, the mean values and SD are shown.

of 15% and 29%, respectively; Figures 4A,B). In contrast, Skp_3 demonstrated prominent stabilisation of LipA, as the soluble fraction reached 66%. In the presence of the lipase-specific foldase LipH, more than 80% LipA was found soluble (LipA: LipH molar ratio 1:1).

The membrane-anchored proteins PpiD and YfgM are the recently described chaperones associated with the SecYEG translocon of *E. coli* (Matern et al., 2010; Götzke et al., 2014). Being proximal to the translocon, the peptidyl prolyl isomerase PpiD and the tetratricopeptide repeat-containing protein YfgM of *P. aeruginosa* may interact with LipA at the early stage of its translocation into the periplasm and mediate the handover to the membrane-anchored LipH. Similar to the soluble chaperones above, the potential effects of the periplasmic domains of PpiD and YfgM on LipA aggregation were investigated. YfgM did not stabilize LipA, as the soluble fraction remained below 20% (Figures 4A,B). This lack of the holdase activity is in agreement with earlier experiments, where luciferase and the precursor of OmpC were tested as putative YfgM clients (Götzke et al., 2014). In the presence of PpiD, the soluble fraction of LipA increased up to 34%, which matched closely the value measured for another peptidyl prolyl isomerase, $FkpA_2$. Overall, the sedimentation assay identified the non-specific soluble chaperone Skp as a potent stabilising factor of the lipase.

Next, we questioned whether the chaperones might be capable of preventing the assembly of β-sheet-rich aggregates of LipA. To probe this putative effect, ThT fluorescence was measured for LipA in the presence of individual chaperones and corrected to the values of the chaperones alone (Supplementary Figure S2). Although most of the chaperones had moderate to low effect on LipA solubility in the sedimentation assay (Figure 4B), they all could reduce the ThT fluorescence at least by 40%, as compared to LipA alone or LipA in the presence of bovine serum albumin (BSA) (Figure 4C). These values reflect the partial ability of chaperones to prevent formation of β-sheet-rich aggregates by LipA. Notably, the most prominent effect was observed again for Skp_3, as the β-sheet-specific ThT signal in the presence of the chaperone was reduced by approx. 75%. Similar low ThT fluorescence intensity was recorded in the presence of LipH.

Finally, negative-stain electron microscopy was used to visualize LipA aggregation. At the elevated ionic strength and

10.3389/fmolb.2022.1026724

in the absence of urea, LipA readily formed micrometer-sized aggregates, commonly assembled in larger clusters (Supplementary Figure S1B and Figure 4D). The sample morphology was altered when either LipH or Skp_3 were added at the molar ratios of 1:3 and 1:5, respectively, so only sub-micrometer featureless particles could be observed, suggesting reduced aggregation propensity. Thus, we concluded that both Skp and LipH offer protection from the assembly of aggregates, despite different mechanisms of interaction with the lipase.

The periplasmic chaperones modulate the activation of LipA

The interactions of the periplasmic chaperones with LipA and their anti-aggregation effects may affect the functionality of the lipase, e.g., by directly altering its folding pathways and/or by competing with the specific foldase LipH. None of the general periplasmic chaperones alone rendered the active lipase, as no enzymatic hydrolysis of *p*NPB was observed in the absence of LipH (Figure 5A). To examine the potential competition between the chaperones, we focused on the LipH-mediated activation of LipA in the presence of the general periplasmic chaperones, as it occurs in living cells. The wild-type LipA was pre-incubated either alone or in presence of 5-fold excess of Skp_3, YfgM, $FkpA_2$, SurA or PpiD under conditions of elevated ionic strength (100 mM NaCl, 1 mM $CaCl_2$ and 20 mM Tris-HCl pH 8.0) sufficient to induce the lipase aggregation. After the pre-incubation phase, the foldase LipH was added to activate LipA, and the resulting hydrolytic activity against *p*NPB was determined (Figure 5B). The conditions of the pre-incubation phase had an evident influence on LipA functionality: Once LipA was incubated without chaperones, its activity was suppressed to a large extent (blue bars in Figure 5A vs Figure 5B), in agreement with the documented aggregation of the lipase. The pre-incubation in the presence of SurA, $FkpA_2$, YfgM or PpiD chaperones either did not enhance or even further decreased LipA activity (Figure 5B). Differently though, pre-incubation of LipA with Skp_3 resulted in prominent stimulation of the substrate hydrolysis, in agreement with the anti-aggregation effect of the chaperone.

The reduced LipA activity in the presence of $FkpA_2$, SurA, YfgM or PpiD correlated with their poor propensity to prevent LipA aggregation, but also suggested the interference with the LipH-mediated activation, potentially by competing for the lipase binding. To examine this scenario, both, the general chaperones and LipH, were added to LipA simultaneously at the LipA:LipH:chaperone molar ratio of 1:1:5, so the lipase activity was dependent on the folding/aggregation balance and the competition between the chaperones for the lipase. In the presence of either SurA, $FkpA_2$, YfgM or PpiD, the activity of

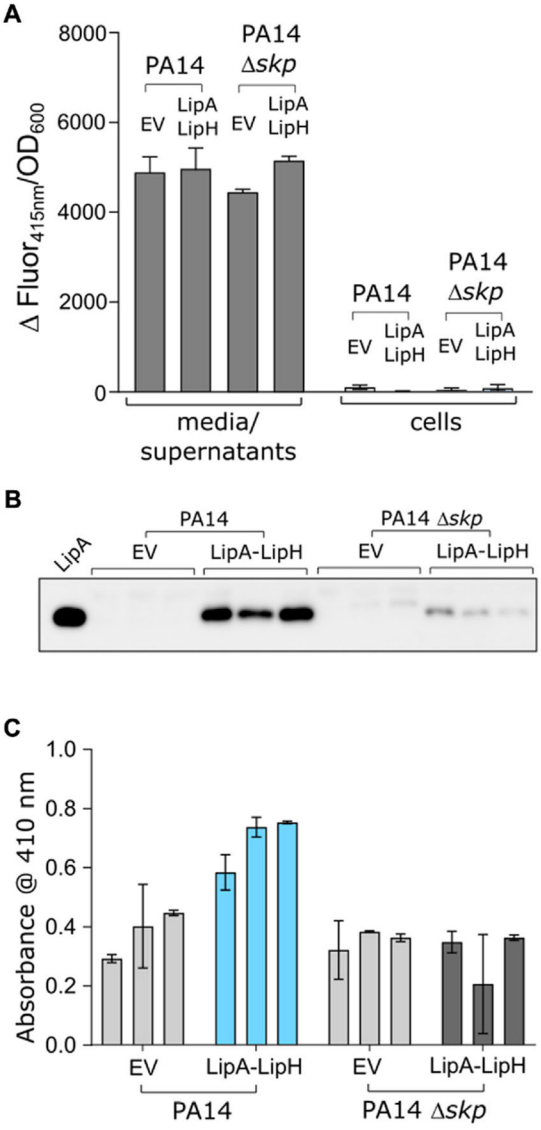

FIGURE 6
Deletion of *skp* gene in *P. aeruginosa* abolishes LipA secretion. **(A)** The functionality of *P. aeruginosa* T2SS is not affected by deletion of *skp* gene. Hydrolysis of Abz-Ala-Gly-Leu-Ala-*p*-nitro-benzyl-amide substrate by T2SS-dependent elastase was monitored as an increase in fluorescence at 415 nm in the cell-free media and in cells of *P. aeruginosa* strains PA14 and PA14 Δ*skp* carrying the empty vector (EV, pGUF) and LipA-LipH expression vector, as described. **(B)** Western blot against the secreted LipA in *P. aeruginosa*. Wild-type PA14 and *skp* null-mutant (PA14 Δ*skp*) strains were transformed with either an empty vector ("EV") or a plasmid encoding for lipA-lipH operon ("LipA-LipH"). Recombinantly expressed and purified LipA was used as a reference (left lane). The complete western blot is provided in Suppl. Figure 3A. **(C)** Lipolytic activity against *p*NPB measured in the extracellular media of *P. aeruginosa* PA14 strains described in the panel E.

LipA dropped by 30–50% (Figure 5C), while only minor, below 10% inhibition of substrate hydrolysis was observed for LipA:LipH:Skp_3 sample. Finally, to scrutinise the effect of the chaperone competition, the assay was conducted using the aggregation-resistant $LipA_{F144E}$ mutant (Figure 5D). When either SurA, $FkpA_2$, YfgM or PpiD were present in addition to LipH, the lipase activity reduced by 20–30%, so we concluded that the chaperones interfered with the LipH:LipA assembly. The effect of Skp_3 on LipH-mediated activation was minimal, so the chaperone allowed efficient LipH:LipA interactions, while being capable of preventing LipA aggregation.

We questioned then whether the observed favourable effect of Skp_3 on LipA solubility and activation also contributes to the lipase biogenesis *in vivo*. To examine this possibility, we analysed LipA secretion in the highly virulent *P. aeruginosa* strain PA14, where *skp/hlpA* gene was optionally knocked out (Klein et al., 2019). In contrast to the deletion of the essential *surA* gene, knock-out of *skp* does not have impact on the outer membrane integrity and so may have minor pleiotropic effect in cells (Klein et al., 2019). To verify that the *skp* deletion did not affect the T2SS assembly, we examined the activity of the elastase LasB, another secretory enzyme that utilizes the T2SS route. No significant change in hydrolysis of a model substrate was observed between various samples (Figure 6A), so we concluded that the absence of Skp chaperone was not detrimental for T2SS integrity and functionality. However, detection of the secreted lipase in the cell-free culture supernatant by immunoblotting revealed a drastic decrease in the amount of LipA upon deletion of Skp (Figure 6B and Supplementary Figure S3A). In agreement with the abolished secretion of LipA, the primary lipase of *P. aeruginosa* (Figure 6C), the total esterase activity measured for the cell-free media decreased approx. 2-fold, and the remaining activity could be related to other enzymes, such as the lipase LipC (Rosenau et al., 2010). Since only the mature form of LipA was detected in the western blot, and no oxidase activity was measured in the media for any of the samples (Supplementary Figure S3B), significant cell lysis could be excluded from consideration, so the differences in LipA abundance and the lipolytic activity must have originated from the altered secretion levels, likely dependent on LipA:Skp_3 interactions.

Trimeric Skp of *P. aeruginosa* acquires multiple conformations in solution

With the interest in the potent effect of Skp on LipA folding and secretion, we set out to shed more light on the functional mechanism of the chaperone. The well-studied Skp homolog from *E. coli* (*Ec*Skp_3) forms a "jellyfish"-like trimer that resembles the arrangement of prefoldin-type chaperones of mitochondria and archaea (Korndörfer et al., 2004; Walton & Sousa, 2004). Each protomer consists of the distinct "head" and "arm" domains. The "head" domain of *Ec*Skp_3 is predominantly formed by β-sheets which drive the oligomerization, and the "arm" domain is a helical section forming a hairpin extension. The client-binding pocket between the "arm" domains is constituted by all three protomers. The crystal structures and small-angle X-ray scattering (SAXS) experiments predicted a broad range of conformations for the *Ec*Skp trimer in its apo-state in solution, where three major states termed "closed", "intermediate" and "open" were described (Holdbrook et al., 2017).

Mature Skp of *P. aeruginosa* shares 22% sequence identity with *Ec*Skp and contains three unique proline residues per protomer, including two prolines in the predicted "head" domain and one in each helical "arm", which may alter the flexibility of the chaperone (Supplementary Figure S4). Thus, we employed SAXS to experimentally assess the conformational ensemble of *P. aeruginosa* Skp in solution (Figure 7A, Supplementary Figures S5A–D and Supplementary Table S1). In agreement with SEC-MALS data (Figure 3), Skp was found to be a trimer. The characteristic "jellyfish"-like shape with the "head" and "arm" domains of the trimer could be recognized in the *ab initio* reconstitution of the oligomer structure using the GASBOR program (Svergun et al., 2001) (χ^2 = 1.016) (Figures 7A,B). A structural model of *P. aeruginosa* Skp_3 built by AlphaFold 2 algorithm (Evans et al., 2021; Jumper et al., 2021) could be fitted into the experimental SAXS envelope (Figure 6B). However, the measured radius of gyration (R_g) of 3.50 nm for the averaged SAXS data is slightly higher than R_g of 3.32 nm calculated via CRYSOL for the modelled structure (χ^2 = 1.28) (Svergun et al., 1995), so Skp_3 of *P. aeruginosa* adopts a more open conformation.

The SAXS data also revealed some flexibility in Skp_3 of *P. aeruginosa*, as previously observed for the *Ec*Skp_3 homolog (Holdbrook et al., 2017). To characterize this conformational space, Ensemble Optimization Method (EOM) was applied (Bernadó et al., 2007; Tria et al., 2015). EOM generates a pool of sequence- and structure-based models (RANCH models; Figure 7C and Supplementary Figures S5E, S5F), and the implemented genetic algorithm GAJOE (Genetic Algorithm Judging Optimisation of Ensembles) selects an ensemble until an optimal fit to the experimental SAXS curve is reached. The selected models describe best the experimental SAXS data, and likely represent the most frequent conformations of the studied protein (Figure 7B). To model the Skp_3 dynamics by EOM, the "head" domain within the trimer was fixed and the helical "arms" were allowed moving to fit the SAXS data. As a result, the selected ensemble matched the experimental SAXS curves with χ^2 = 0.954 (Figure 6A, EOM models). The distribution of the models showed two primary states, resembling those reported for *Ec*Skp_3 (Holdbrook et al., 2017): The "compact" state with R_g of 3.42 nm and maximal dimensions (D_{max}) of 9.73 nm, which accounts up to 62% of the population, and the "open" state (R_g = 4.14 nm, D_{max} = 13.63 nm; 12% occupancy) (Figure 7D). While the dimensions of the open state were nearly identical for both Skp_3 homologs, the compact state of Skp_3 of *P. aeruginosa* was wider than the "intermediate" conformation of *Ec*Skp_3 (R_g of 3.42 vs. 3.2 nm), and no "closed" state was observed for Skp_3 of *P. aeruginosa*. Nevertheless, the ability of Skp_3 of both

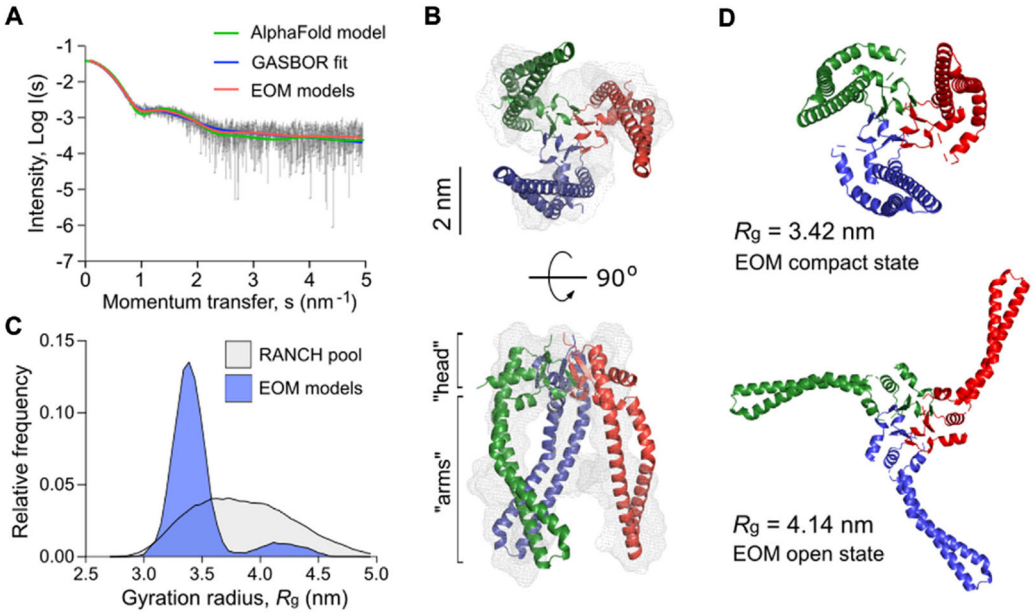

FIGURE 7
P. aeruginosa Skp forms a flexible trimer in solution. **(A)** Experimental SAXS data curve is shown in grey dots with error bars. The intensity (log *I*) is displayed as a function of the momentum transfer (s). The intensity patterns of Skp_3 models derived from GASBOR (blue), AlphaFold (green), and EOM (red) algorithms are overlaid. **(B)** The experimental SAXS envelope of *P. aeruginosa* Skp (grey mesh) calculated using GASBOR algorithm reflects the trimeric structure of the chaperone. The structural model of Skp_3 is superimposed with the SAXS envelope, with each protomer coloured individually (red, green, blue). The "head" and "arm" structural domains of Skp are indicated. The scale bar is shown on the side. **(C)** The distribution of Skp_3 conformations differing by their gyration radii (R_g) calculated by EOM (blue). The original RANCH pool based on 10000 random models is shown in grey. **(D)** Representative conformations of *P. aeruginosa* Skp_3 calculated by EOM in the compact (R_g of 3.42 nm, D_{max} of 9.73 nm; fraction ~0.62) and the open (R_g of 4.14 nm, D_{max} of 13.63 nm; fraction ~0.12) states.

E. coli and *P. aeruginosa* to undergo a large conformational change from a compact to a widely open state suggests that the proteins follow the same functional dynamics.

Two copies of Skp_3 are required to stabilize soluble LipA *via* apolar contacts

The documented clients of Skp in the bacterial periplasm span a broad range of molecular masses, from 19 to 89 kDa, and they belong to various classes, both membrane-associated and globular proteins (Qu et al., 2007; Schiffrin et al., 2016). Though the stimulatory effect of Skp_3 on secretion of a heterologous bacterial lipase has been previously demonstrated, it remained obscure whether the stimulation was indeed a result of direct client:chaperone interactions (Narayanan et al., 2011). Our biochemical and *in vivo* data substantiates the view that Skp_3 is a potent chaperone that prevents the lipase aggregation in *P. aeruginosa*, and here we set out to characterize LipA:Skp_3 interactions in detail.

Firstly, we questioned whether the interaction of *P. aeruginosa* Skp_3 with LipA is indeed of hydrophobic nature, as each of the "arms" within the Skp trimer has an apolar side (Figure 8A) that may bind unfolded and/or misfolded clients. As shown for the LipA:LipH complex, elevated ionic strength of the aqueous solution severely destabilizes the hydrophilic binding interface, so the released LipA irreversibly aggregates (Figure 2B). Hydrophobic interactions, in contrast, should be insensitive to the ionic strength and may facilitate the chaperoning at high salt concentrations. The solubility of the wild-type LipA in the presence of Skp_3 at the molar ratio 1:10 was examined over a range of NaCl concentrations via the sedimentation assay (Figure 8B). Different to LipA alone and LipA in the presence of LipH, no decay in the soluble fraction was observed when Skp_3 was present. At the highest examined concentration of 250 mM NaCl, Skp_3 ensured the lipase solubility of approx. 70%, while the chaperone-free LipA was nearly completely aggregated, and only 30% of LipA was found soluble in the presence of LipH. This observation implied that the lipase is recognized via non-polar contacts, likely associated with the unfolded state.

Next, we set out to determine the binding affinity of Skp to LipA. Earlier studies of Skp interactions with its most abundant clients, OMPs, provided the affinity estimates at low-nanomolar to low-micromolar scales for OMP:Skp_3 complexes formed at 1:

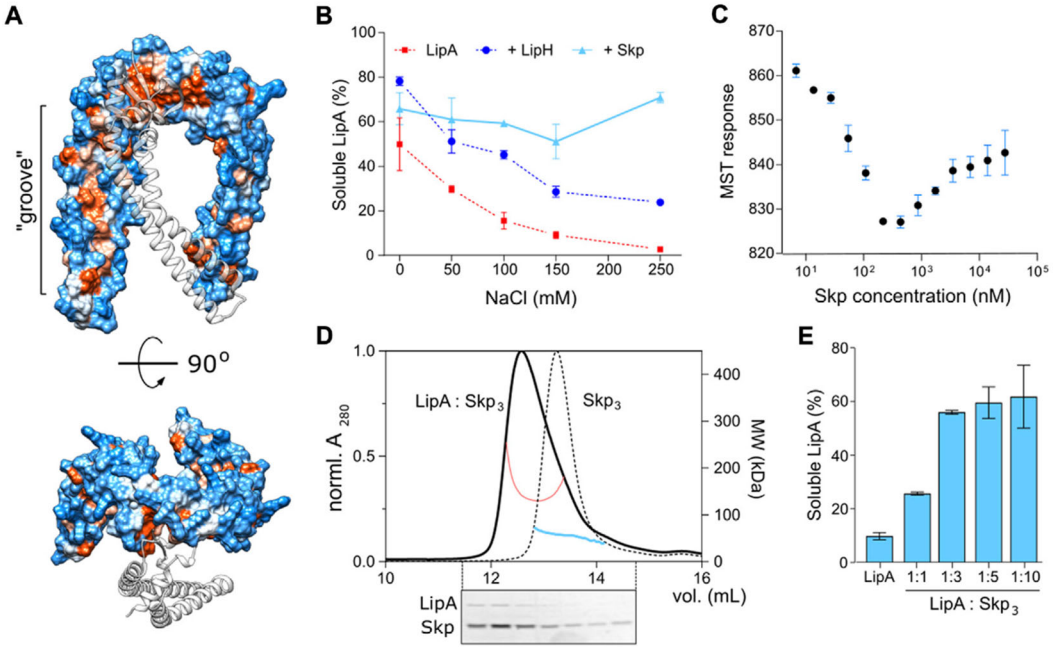

FIGURE 8
Characterisation of LipA:Skp_3 interactions. **(A)** Surface hydrophobicity plot of *P. aeruginosa* Skp_3. The hydrophobic groove along the "arm" domain is indicated. Polar/charged residues are shown in blue, apolar in orange. One subunit within the Skp trimer is shown as a transparent ribbon for clarity. **(B)** Skp supports the solubility of LipA over a broad range of ionic strength. The soluble fraction of the wild-type LipA in presence of Skp (light blue) was determined from SDS-PAGE after the sedimentation assay at various salt concentrations. The assays were performed in technical triplicates, the mean values and SD are shown. Salt-dependent aggregation of LipA alone and LipA in presence of LipH are indicated in red and dark blue, respectively, and correspond to those in Figure 2B. **(C)** LipA:Skp_3 interactions manifest biphasic behaviour. Microscale thermophoresis of $LipA_{F144E}$:Skp interactions was performed using fluorescently labelled $LipA_{F144E}$ and Skp titrations (monomers concentration indicated). The high-affinity interaction at 20 nM Skp may be assigned to LipA binding a single chaperone trimer, followed by recruitment of the second chaperone with a lower affinity. The assay was performed in technical triplicates, the mean values and SD are shown. **(D)** SEC-MALS of the $LipA_{F144E}$:Skp_3 complex and Skp_3 alone. Normalized UV absorbance of $LipA_{F144E}$:Skp_3 (solid black line) and Skp_3 (dotted black line), and the corresponding molecular weights are indicated. Below: SDS-PAGE of the $LipA_{F144E}$:Skp_3 eluate. **(E)** Solubility of the lipase is dependent of the LipA:Skp_3 ratio. The soluble fraction of the wild-type LipA was determined from SDS-PAGE after the sedimentation assay at various LipA:Skp_3 ratios. The assays were performed in technical triplicates, the mean values and SD are shown.

1 and 1:2 stoichiometry, respectively (Qu et al., 2007; Schiffrin et al., 2016; Mas et al., 2020; Pan et al., 2020), while the interactions with soluble proteins have not been addressed. For the analysis here, we employed microscale thermophoresis (MST) and used the aggregation-resistant mutant $LipA_{F144E}$ as the fluorescently labelled component. $LipA_{F144E}$-FM was mixed with Skp ranging from 4.5 nM to 37 μM (concentration of Skp monomers), and the MST response of $LipA_{F144E}$-FM, i.e., its mobility within the micrometer-sized temperature gradient, was analysed. Strikingly, $LipA_{F144E}$ manifested a bimodal MST response upon increasing the Skp concentration that appeared as a V-shaped plot with a transition at approx. 300 nM Skp_1 (100 nM Skp_3) (Figure 8C). The data suggested two distinct modes of binding to the chaperone, where individual K_D's were ~20 nM and 2 μM, and the values were in a good agreement with values measured for OMP:Skp_3 interactions where either one or two Skp timers were involved (Qu et al., 2007; Schiffrin et al., 2016; Pan et al., 2020). Thus, we proposed that once Skp is present at micro-molar concentration, LipA may bind two chaperones simultaneously.

The LipA:Skp affinity measured in the MST experiments suggested that two copies of Skp trimer were recruited to stabilize the soluble lipase in the assays, described above (Figures 4, 5; monomeric Skp of 15 μM). To test the stoichiometry of the complex experimentally, SEC-MALS analysis was performed on $LipA_{F144E}$:Skp mixture (molar ratio 1:3; Figure 8D). The elution peak demonstrated a prominent shift in comparison to Skp_3 alone, and the estimated molecular mass of 139 kDa approached closely the calculated mass of the complex LipA:2*Skp_3 (148 kDa). SDS-PAGE confirmed presence of both the chaperone and the lipase in the peak fractions, and the densitometry analysis of the corresponding bands suggested the excess of Skp (estimated LipA:Skp_3 ratio 1:3). The remaining free LipA fraction was likely bound to the column

resin, as we observed previously. Thus, we concluded that the relatively small protein LipA provided sufficient surface area for binding two copies of the trimeric Skp. To test, whether this stoichiometry was beneficial for the solubility of the lipase, we used the aggregation-prone wild-type LipA in the sedimentation assay where the LipA:Skp_3 ratio was varied (Figure 8E). At the molar ratios of 1:10 and 1:3, above 70% of LipA could be rescued from aggregation by Skp_3. Strikingly, the rescued fraction of LipA dropped dramatically when the ratio was reduced to 1:1 (monomeric Skp 1.5 μM), suggesting that a single Skp trimer was not capable of rescuing the client from aggregation/misfolding. An independent titration experiment was also performed to compare the anti-aggregase activity of Skp_3 with other periplasmic chaperones (Supplementary Figure S6). In all three examined ratios Skp_3 appeared as the most potent chaperone, although its propensity to rescue LipA was notably dependent on the concentration. Although the concentration of Skp_3 in *P. aeruginosa* is unknown to date, it seems plausible that it is sufficiently high to ensure binding of LipA within the consolidated cavity of two Skp trimers. Further folding and activation of the lipase should depend on the hand-over and high-affinity specific interactions with the foldase LipH.

Discussion

The protein fold is determined by its primary amino acid sequence, but the pathways followed by the polypeptide chain towards the functional structure commonly involve the assistance of chemical and proteinaceous chaperones. The chaperones steer their client dynamics along the energy landscape, facilitate the local and global folding/unfolding events, prevent off-pathway intermediates, and serve to disaggregate occasional misfolded structures (Hartl et al., 2011; Stull et al., 2018). The role of chaperones is of particular importance under stress factors, such as elevated temperature, or challenging environments, such as bacterial periplasm, where the protein folding should proceed under broadly varying conditions. Here, we demonstrate that the non-specific periplasmic chaperone Skp of the pathogenic bacterium *P. aeruginosa* efficiently protects the secretory lipase LipA from aggregation and suppresses its assembly into β-sheet-rich structures. The structural analysis of trimeric Skp in solution by SAXS reveals an ensemble of co-existing states. The interaction analysis of the LipA:Skp_3 complex suggests that either one and two copies of Skp trimers may bind the lipase via hydrophobic interactions, but two copies are required for stabilizing the aggregation-prone protein. As the deletion of the *skp* gene in *P. aeruginosa* correlates with the reduced LipA secretion, we suggest that Skp is a crucial factor in the lipase biogenesis pathway.

Folding of the lipase LipA takes place in the periplasm, where the protein is transiently localized and interacts with the specialized chaperone LipH. The chaperone serves for correct positioning of the lid domain of LipA, thus rendering the active enzyme prior its further secretion via T2SS (Rosenau et al., 2004; Pauwels et al., 2006). The non-activated lipase tends to acquire loosely folded intermediate states, which are accessible for proteases and prone to aggregation (Frenken et al., 1993; Rashno et al., 2017). The chaperone-dependent folding is not common among bacterial lipases, and it might be related to the particular structure of the lid domain (Khan et al., 2017). In agreement with the earlier findings of Chiti and co-workers (Rashno et al., 2017, 2018), our data show that the lid domain greatly contributes to LipA aggregation and misfolding into β-stranded structures, thus interfering with the protein biogenesis. As the assembly of the LipA:LipH complex rescues LipA from aggregation to a large extent, two distinct functions can be assigned to LipH, namely stabilization and activation of the client lipase. Speculatively, the chaperone might initially serve to stabilize the lipase in its folded state and hand it over to T2SS, and through the course of the evolution it has gained the propensity to activate the lipase via steric re-positioning of the lid domain.

Several challenges can be envisioned for productive LipA:LipH interactions in the living cell. Firstly, the expression levels of the foldase are substantially lower than those of LipA, so each LipH molecule should carry out multiple chaperoning cycles upon binding nascent lipases, refining the structure and releasing them for further secretion (Rosenau et al., 2004). Secondly, the accessibility of the membrane-anchored foldase for its client may be limited, especially in the crowded periplasmic environment. Finally, the high ionic strength encountered in the sputum of cystic fibrosis patients (Kirchner et al., 2012; Grandjean Lapierre et al., 2017) strongly promotes the aggregation of LipA and may also inhibit the electrostatic interactions at the LipA:LipH interface. Thus, accessory factors, such as non-specific but ubiquitous periplasmic chaperones may be beneficial for biogenesis of the intrinsically unstable lipase. Here, we elucidate that Skp_3, a conditionally essential protein in *P. aeruginosa* (Lee et al., 2015), is a potent holdase for LipA that efficiently maintains the soluble state of the lipase, blocks the assembly of β-structured aggregates, and ensures secretion of the functional lipase *in vivo*. Notably, even 10-fold excess of Skp_3 did not inhibit LipA activation and thus allowed LipA:LipH interactions, so we described the chaperone as a factor in LipA biogenesis that steers folding pathways by preventing aggregation events.

Up to date, the vast majority of insights on Skp functioning have been gained from studies on the chaperone from *E. coli*. Differently from other periplasmic chaperones, Skp targets its clients based on the hydrophobicity exposed in the unfolded/misfolded structures rather than a specific sequence motif or conformations of proline residues (Burmann et al., 2013; Schiffrin et al., 2016). The periplasmic concentration of *Ec*Skp may reach hundreds of μM (Tsirigotaki et al., 2017), and the chaperone extensively interacts with unfolded OMPs (Denoncin

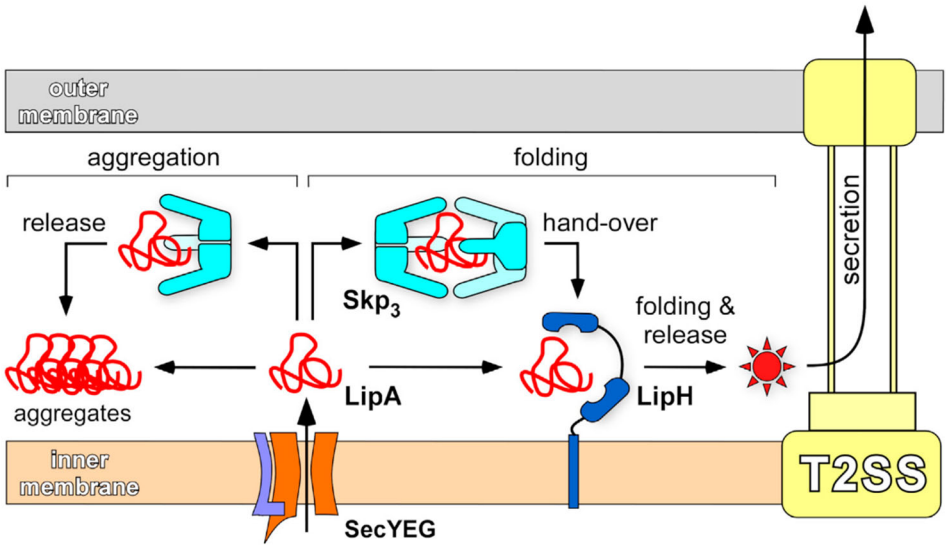

FIGURE 9
Chaperone-assisted folding of LipA in the periplasm. After the initial translocation *via* SecYEG complex into the periplasm, the aggregation-prone LipA may be directly picked up by the foldase LipH, acquire the native, enzymatically active structure (indicated as a red star) and be transferred to the type II secretion machinery (T2SS). Alternatively, LipA may interact with the abundant trimeric chaperone Skp_3 that prevents LipA from aggregation, when a complex at 1:2 stoichiometry is formed. Upon its release, LipA may bind LipH and proceed along the folding/secretion pathway. A single copy of Skp_3 does not ensure the holdase function and does not rescue LipA from aggregation.

et al., 2012; Schiffrin et al., 2016; Pan et al., 2020). Although no OMP essentially depends on Skp in the presence of SurA (Denoncin et al., 2012; He & Hiller, 2018), other moonlighting activities have been suggested exclusively for Skp. Recently, the chaperone has been described as an adaptor protein that delivers the misfolded OMP LamB to the periplasmic protease DegP (Combs & Silhavy, 2022). Skp is a potent disaggregase of OmpC and OmpX (Li et al., 2018; Chamachi et al., 2022) and it also demonstrates the holdase and disaggregase activity towards several soluble proteins (Purdy et al., 2007; Wagner et al., 2009; Entzminger et al., 2012). Heterologous expression and secretion of a lipase from *Burkholderia* in *E. coli* could be improved by 36% upon co-expression of Skp, but not SurA (Narayanan et al., 2011). The limited increase in the secretion efficiency may be related to the intrinsically high concentration of Skp in *E. coli* periplasm, while deletion of Skp abolishes LipA secretion, as it is presented in our work. Biochemical analysis suggests that Skp-mediated solubility of the lipase is a decisive factor for the efficient biogenesis of the enzyme.

While the functional insights on Skp of *P. aeruginosa* are sparse (Klein et al., 2019), the chaperone appears to be essential for the survival of bacteria in the sputum media, where the salt concentration exceeds 100 mM (Lee et al., 2015). The chaperone has been detected in multiple proteomics studies (Peng et al., 2005; Rao et al., 2011; Park et al., 2014, 2015; Carruthers et al., 2020), which revealed that the abundance of Skp changes upon switching from the planktonic to the biofilm state, and upon antibiotic treatment. Structural analysis on Skp_3 of *P. aeruginosa* presented here suggests that its architecture and dynamics resemble those of *Ec*Skp_3, despite the low sequence similarity and presence of multiple proline residues. *P. aeruginosa* Skp exists as an assembled trimer in solution, and its conformational plasticity and the hydrophobic interior fulfil the requirements for being a promiscuous non-specific holdase chaperone. The SAXS data describe the transient outward motion of the "arm" domains that ensures opening of the interior cavity of the Skp trimer. The aggregation-prone folding intermediates of LipA are likely to be recognized by Skp_3, kept in the protective hydrophobic cavity and then handed over to LipH for activation.

The biphasic LipA:Skp_3 binding with affinities of ~20 nM and 2 μM is in remarkable agreement with the chaperone interactions with OMPs, where binding of either one or two copies of Skp_3 has been described (Qu et al., 2007; Schiffrin et al., 2016; Mas et al., 2020; Pan et al., 2020). The close match between the Skp_3 affinities to different classes of clients is likely due to non-specific hydrophobicity-based interactions. Unexpectedly though, the relatively small protein LipA is able to recruit two trimers of Skp. The exposed hydrophobic areas must be sufficiently large to form the extensive binding interface; however, the relatively low affinity for the second Skp_3 suggests limited exposure of the lipase beyond the primary

LipA.Skp_3 complex. The high affinity of a single Skp_3 to LipA is comparable to that of the LipA:LipH complex (Pauwels et al., 2006; Viegas et al., 2020), raising a question about the interplay of these chaperones on the lipase activation pathway. We may speculate that interactions of unfolded LipA with Skp_3 are associated with rapid capture and release events, while the sterically and electrostatically tuned complex of LipA:LipH is characterized by a low dissociation rate (Viegas et al., 2020). At a large excess of Skp_3, likely present in the periplasm, a nascent LipA molecule experiences multiple rapid association/dissociation events with monomers and dimers of Skp_3 before acquiring its specific fold, required for binding to the foldase LipH. The release of the lipase from LipH may be triggered via interactions with components of T2SS. The putative model of LipA interactions and pathways in the periplasm, derived from *in vitro* and *in vivo* analysis, is illustrated by Figure 9.

Our data provide first evidence for interactions of *P. aeruginosa* LipA with the general and highly abundant periplasmic chaperone Skp that result in stabilization of the lipase. It remains to be shown at what stage along the biogenesis pathway LipA requires the involvement of Skp, and whether the chaperone:client interactions are beneficial under particular conditions, such as elevated ionic strengths. Future experiments in the native environment of *P. aeruginosa* combined with *in vitro* analysis will account for the membrane-anchored LipH and its putative competition with Skp for the nascent LipA, as well as the handover of LipA to the T2SS machinery and potential involvement of Skp at that stage.

Data availability statement

The datasets presented in this study can be found in online repositories. The names of the repository/repositories and accession number(s) can be found in the article/Supplementary Material.

Author contributions

AP and MBU carried out cloning, protein expression and isolation, and biochemical and fluorescence-based experiments; JR and SS carried out SAXS measurements and structural characterization of chaperones; EH carried out SEC-MALS analysis; MBA carried out TEM imaging; JB, FK and AP carried out *in vivo* experiments; LS, K-EJ, FK, SS and AK supervised the research. AP and AK wrote the manuscript with the help of all co-authors.

Funding

All sources of funding received for the research being submitted. This information includes the name of granting agencies and grant numbers, as well as a short description of each funder's role.

Acknowledgments

We would like to thank Erwin Bohn (Universitätsklinikum Tübingen) for providing PA14 Δ*skp* strain, Sajedeh Mirshahvalad (University of Düsseldorf) for help with *in vivo* experiments, and Jakub Kubiak (University of Düsseldorf) for valuable discussions. Our special thanks go to Jessica Hausmann and Stefanie Weidtkamp-Peters for their kind support on TEM. The research was supported by the German Research Foundation (Deutsche Forschungsgemeinschaft, DFG) *via* the Collaborative Research Centre 1208 "Identity and Dynamics of Membrane Systems—from Molecules to Cellular Functions" (project 267205415, sub-projects A1, A2, A10, and Z02). The Center for Structural Studies is funded by DFG, projects 417919780 and INST 208/761-1 FUGG. Center of Advanced imaging is funded by DFG, project 284074525.

Conflict of interest

The authors declare that the research was conducted in the absence of any commercial or financial relationships that could be construed as a potential conflict of interest.

Publisher's note

All claims expressed in this article are solely those of the authors and do not necessarily represent those of their affiliated organizations, or those of the publisher, the editors and the reviewers. Any product that may be evaluated in this article, or claim that may be made by its manufacturer, is not guaranteed or endorsed by the publisher.

Supplementary material

The Supplementary Material for this article can be found online at: https://www.frontiersin.org/articles/10.3389/fmolb.2022.1026724/full#supplementary-material

References

Babic, N. (2022). *Homology modeling-guided medium-throughput screening of novel hydrolases among* Pseudomonas aeruginosa *genes of unknown function*. PhD thesis. Düsseldorf (Germany): University of Düsseldorf.

Bernadó, P., Mylonas, E., Petoukhov, M. V., Blackledge, M., and Svergun, D. I. (2007). Structural characterization of flexible proteins using small-angle X-ray scattering. *J. Am. Chem. Soc.* 129, 5656–5664. doi:10.1021/ja069124n

Biancalana, M., and Koide, S. (2010). Molecular mechanism of Thioflavin-T binding to amyloid fibrils. *Biochim. Biophys. Acta* 1804, 1405–1412. doi:10.1016/j.bbapap.2010.04.001

Bitto, E., and McKay, D. B. (2002). Crystallographic structure of SurA, a molecular chaperone that facilitates folding of outer membrane porins. *Structure* 10, 1489–1498. doi:10.1016/s0969-2126(02)00877-8

Burmann, B. M., Wang, C., and Hiller, S. (2013). Conformation and dynamics of the periplasmic membrane-protein-chaperone complexes OmpX-Skp and tOmpA-Skp. *Nat. Struct. Mol. Biol.* 20, 1265–1272. doi:10.1038/nsmb.2677

Carruthers, N. J., McClellan, S. A., Somayajulu, M., Pitchaikannu, A., Bessert, D., Peng, X., et al. (2020). Effects of glycyrrhizin on multi-drug resistant pseudomonas aeruginosa. *Pathogens* 9, 7666–E814. doi:10.3390/pathogens9090766

Chamachi, N., Hartmann, A., Ma, M. Q., Krainer, G., and Schlierf, M. (2022). Chaperones Skp and SurA dynamically expand unfolded OmpX and synergistically disassemble oligomeric aggregates. *Proc. Natl. Acad. Sci. U. S. A.* 119, e2118919119. doi:10.1073/pnas.2118919119

Combs, A. N., and Silhavy, T. J. (2022). The sacrificial adaptor protein Skp functions to remove stalled substrates from the β-barrel assembly machine. *Proc. Natl. Acad. Sci. U. S. A.* 119, e2114997119. doi:10.1073/pnas.2114997119

De Geyter, J., Tsirigotaki, A., Orfanoudaki, G., Zorzini, V., Economou, A., and Karamanou, S. (2016). Protein folding in the cell envelope of *Escherichia coli*. *Nat. Microbiol.* 1, 16107. doi:10.1038/nmicrobiol.2016.107

Denoncin, K., Schwalm, J., Vertommen, D., Silhavy, T. J., and Collet, J. F. (2012). Dissecting the *Escherichia coli* periplasmic chaperone network using differential proteomics. *Proteomics* 12, 1391–1401. doi:10.1002/pmic.201100633

Douzi, B., Ball, G., Cambillau, C., Tegoni, M., and Voulhoux, R. (2011). Deciphering the Xcp *Pseudomonas aeruginosa* type II secretion machinery through multiple interactions with substrates. *J. Biol. Chem.* 286, 40792–40801. doi:10.1074/jbc.M111.294843

Driscoll, J. A., Brody, S. L., and Kollef, M. H. (2007). The epidemiology, pathogenesis and treatment of *Pseudomonas aeruginosa* infections. *Drugs* 67, 351–368. doi:10.2165/00003495-200767030-00003

Dwyer, R. S., Malinverni, J. C., Boyd, D., Beckwith, J., and Silhavy, J. (2014). Folding LacZ in the periplasm of *Escherichia coli*. *J. Bacteriol.* 196, 3343–3350. doi:10.1128/JB.01843-14

El Khattabi, M., Van Gelder, P., Bitter, W., and Tommassen, J. (2000). Role of the lipase-specific foldase of Burkholderia glumae as a steric chaperone. *J. Biol. Chem.* 275, 26885–26891. doi:10.1074/jbc.M003258200

Entzminger, K. C., Chang, C., Myhre, R. O., McCallum, K. C., and Maynard, J. A. (2012). The skp chaperone helps fold soluble proteins *in vitro* by inhibiting aggregation. *Biochemistry* 51, 4822–4834. doi:10.1021/bi300412y

Evans, R., O'Neill, M., Pritzel, A., Antropova, N., Senior, A., Green, T., et al. (2021). *Protein complex prediction with AlphaFold-Multimer*.

Fernandez-Escamilla, A. M., Rousseau, F., Schymkowitz, J., and Serrano, L. (2004). Prediction of sequence-dependent and mutational effects on the aggregation of peptides and proteins. *Nat. Biotechnol.* 22, 1302–1306. doi:10.1038/nbt1012

Filloux, A., and Walker, J. M. (2014) Pseudomonas methods and protocols. In, A. Filloux and J-L. Ramos (eds) pp 293–301. New York, NY: Springer New York.

Frenken, L. G. J., de Groot, A., Tommassen, J., Verrips, C. T., and de Groot, A. (1993). Role of the lipB gene product in the folding of the secreted lipase of Pseudomonas glumae. *Mol. Microbiol.* 9, 591–599. doi:10.1111/j.1365-2958.1993.tb01719.x

Götzke, H., Palombo, I., Muheim, C., Perrody, E., Genevaux, P., Kudva, R., et al. (2014). YfgM is an ancillary subunit of the SecYEG translocon in *Escherichia coli*. *J. Biol. Chem.* 289, 19089–19097. doi:10.1074/jbc.M113.541672

Grandjean Lapierre, S., Phelippeau, M., Hakimi, C., Didier, Q., Reynaud-Gaubert, M., Dubus, J-C., et al. (2017). Cystic fibrosis respiratory tract salt concentration: An Exploratory Cohort Study. *Med. Baltim.* 96, e8423. doi:10.1097/MD.0000000000008423

Hartl, F. U., Bracher, A., and Hayer-Hartl, M. (2011). Molecular chaperones in protein folding and proteostasis. *Nature* 475, 324–332. doi:10.1038/nature10317

Hausmann, S., Wilhelm, S., Jaeger, K-E., and Rosenau, F. (2008). Mutations towards enantioselectivity adversely affect secretion of *Pseudomonas aeruginosa* lipase. *FEMS Microbiol. Lett.* 282, 65–72. doi:10.1111/j.1574-6968.2008.01107.x

He, L., and Hiller, S. (2018). Common patterns in chaperone interactions with a native client protein. *Angew. Chem. Int. Ed. Engl.* 57, 5921–5924. doi:10.1002/anie.201713064

Hobson, A. H., Buckley, C. M., Aamand, J. L., Jorgensen, S. T., Diderichsen, B., and McConnell, D. J. (1993). Activation of a bacterial lipase by its chaperone. *Proc. Natl. Acad. Sci. U. S. A.* 90, 5682–5686. doi:10.1073/pnas.90.12.5682

Holdbrook, D. A., Burmann, M., Huber, R. G., Petoukhov, M. V., Svergun, D. I., Hiller, S., et al. (2017). A spring-loaded mechanism governs the clamp-like dynamics of the skp chaperone. *Structure* 25, 1079–1088. doi:10.1016/j.str.2017.05.018

Jaeger, K-E., Ransac, S., Dijkstra, B. W., Colson, C., van Heuvel, M., and Misset, O. (1994). Bacterial lipases. *FEMS Microbiol. Rev.* 15, 29–63. doi:10.1111/j.1574-6976.1994.tb00121.x

Jarchow, S., Lück, C., Görg, A., and Skerra, A. (2008). Identification of potential substrate proteins for the periplasmic *Escherichia coli* chaperone Skp. *Proteomics* 8, 4987–4994. doi:10.1002/pmic.200800288

Jumper, J., Evans, R., Pritzel, A., Green, T., Figurnov, M., Ronneberger, O., et al. (2021). Highly accurate protein structure prediction with AlphaFold. *Nature* 596, 583–589. doi:10.1038/s41586-021-03819-2

Khan, F. I., Lan, D., Durrani, R., Huan, W., Zhao, Z., and Wang, Y. (2017). The lid domain in lipases: Structural and functional determinant of enzymatic properties. *Front. Bioeng. Biotechnol.* 5, 16. doi:10.3389/fbioe.2017.00016

Kikhney, A. G., Borges, C. R., Molodenskiy, D. S., Jeffries, C. M., and Svergun, D. I. (2020). Sasbdb: Towards an automatically curated and validated repository for biological scattering data. *Protein Sci.* 29, 66–75. doi:10.1002/pro.3731

Kirchner, S., Fothergill, J. L., Wright, E. A., James, C. E., Mowat, E., and Winstanley, C. (2012). Use of artificial sputum medium to test antibiotic efficacy against *Pseudomonas aeruginosa* in conditions more relevant to the cystic fibrosis lung. *J. Vis. Exp.* 1–8, e3857. doi:10.3791/3857

Klein, K., Sonnabend, M. S., Frank, L., Leibiger, K., Franz-Wachtel, M., Macek, B., et al. (2019). Deprivation of the periplasmic chaperone SurA reduces virulence and restores antibiotic susceptibility of multidrug-resistant *Pseudomonas aeruginosa*. *Front. Microbiol.* 10, 100. doi:10.3389/fmicb.2019.00100

Konarev, P. V., Volkov, V. V., Sokolova, A. V., Koch, M. H. J., and Svergun, D. I. (2003). Primus: A Windows PC-based system for small-angle scattering data analysis. *J. Appl. Crystallogr.* 36, 1277–1282. doi:10.1107/s0021889803012779

König, B., Jaeger, K. E., Sage, A. E., Vasil, M. L., and König, W. (1996). Role of *Pseudomonas aeruginosa* lipase in inflammatory mediator release from human inflammatory effector cells (platelets, granulocytes, and monocytes). *Infect. Immun.* 64, 3252–3258. doi:10.1128/IAI.64.8.3252-3258.1996

Korndörfer, I. P., Dommel, M. K., and Skerra, A. (2004). Structure of the periplasmic chaperone Skp suggests functional similarity with cytosolic chaperones despite differing architecture. *Nat. Struct. Mol. Biol.* 11, 1015–1020. doi:10.1038/nsmb828

Krogh, A., Larsson, B., Von Heijne, G., and Sonnhammer, E. L. L. (2001). Predicting transmembrane protein topology with a hidden markov model : Application to complete genomes. *J. Mol. Biol.* 305, 567–580. doi:10.1006/jmbi.2000.4315

Lazdunski, A., Guzzo, J., Filloux, A., Bally, M., and Murgier, M. (1990). Secretion of extracellular proteins by *Pseudomonas aeruginosa*. *Biochimie* 72, 147–156. doi:10.1016/0300-9084(90)90140-c

Lee, S. A., Gallagher, L. A., Thongdee, M., Staudinger, B. J., Lippman, S., Singhc, P. K., et al. (2015). General and condition-specific essential functions of *Pseudomonas aeruginosa*. *Proc. Natl. Acad. Sci. U. S. A.* 112, 5189–5194. doi:10.1073/pnas.1422186112

Li, G., He, C., Bu, P., Bi, H., Pan, S., Sun, R., et al. (2018). Single-molecule detection reveals different roles of skp and SurA as chaperones. *ACS Chem. Biol.* 13, 1082–1089. doi:10.1021/acschembio.8b00097

Manalastas-Cantos, K., Konarev, P. V., Hajizadeh, N. R., Kikhney, A. G., Petoukhov, M. V., Molodenskiy, D. S., et al. (2021). Atsas 3.0: Expanded functionality and new tools for small-angle scattering data analysis. *J. Appl. Crystallogr.* 54, 343–355. doi:10.1107/S1600576720013412

Mas, G., Burmann, B. M., Sharpe, T., Claudi, B., Bumann, D., and Hiller, S. (2020). Regulation of chaperone function by coupled folding and oligomerization. *Sci. Adv.* 6, eabc5822. doi:10.1126/sciadv.abc5822

Masuda, T., Saito, N., Tomita, M., and Ishihama, Y. (2009). Unbiased quantitation of *Escherichia coli* membrane proteome using phase transfer surfactants. *Mol. Cell. Proteomics* 8, 2770–2777. doi:10.1074/mcp.M900240-MCP200

Matern, Y., Barion, B., and Behrens-Kneip, S. (2010). PpiD is a player in the network of periplasmic chaperones in *Escherichia coli*. *BMC Microbiol.* 10, 251. doi:10.1186/1471-2180-10-251

Narayanan, N., Khan, M., and Chou, C. P. (2011). Enhancing functional expression of heterologous Burkholderia lipase in *Escherichia coli*. *Mol. Biotechnol.* 47, 130–143. doi:10.1007/s12033-010-9320-3

Nardini, M., Lang, D. A., Liebeton, K., Jaeger, K-E., and Dijkstra, B. W. (2000). Crystal structure of *Pseudomonas aeruginosa* lipase in the open conformation. The prototype for family I.1 of bacterial lipases. *J. Biol. Chem.* 275, 31219–31225. doi:10.1074/jbc.M003903200

Pan, S., Yang, C., and Zhao, X. S. (2020). Affinity of Skp to OmpC revealed by single-molecule detection. *Sci. Rep.* 10, 14871. doi:10.1038/s41598-020-71608-4

Park, A. J., Murphy, K., Krieger, J. R., Brewer, D., Taylor, P., Habash, M., et al. (2014). A temporal examination of the planktonic and biofilm proteome of whole cell pseudomonas aeruginosa pao1 using quantitative mass spectrometry. *Mol. Cell. Proteomics* 13, 1095–1105. doi:10.1074/mcp.M113.033985

Park, A. J., Murphy, K., Surette, M. D., Bandoro, C., Krieger, J. R., Taylor, P., et al. (2015). *Tracking the dynamic relationship between cellular systems and extracellular subproteomes in* Pseudomonas aeruginosa *bio fi lms.*

Pauwels, K., Lustig, A., Wyns, L., Tommassen, J., Savvides, S. N., and Van Gelder, P. (2006). Structure of a membrane-based steric chaperone in complex with its lipase substrate. *Nat. Struct. Mol. Biol.* 13, 374–375. doi:10.1038/nsmb1065

Pauwels, K., Sanchez del Pino, M. M., Feller, G., and Van Gelder, P. (2012). Decoding the folding of Burkholderia glumae lipase: Folding intermediates en route to kinetic stability. *PLoS One* 7, e36999. doi:10.1371/journal.pone.0036999

Peng, X., Xu, C., Ren, H., Lin, X., Wu, L., and Wang, S. (2005). Proteomic analysis of the sarcosine-insoluble outer membrane fraction of *Pseudomonas aeruginosa* responding to ampicilin, kanamycin, and tetracycline resistance. *J. Proteome Res.* 4, 2257–2265. doi:10.1021/pr050159g

Petersen, T. N., Brunak, S., Von Heijne, G., and Nielsen, H. (2011). SignalP 4.0: Discriminating signal peptides from transmembrane regions. *Nat. Methods* 8, 785–786. doi:10.1038/nmeth.1701

Purdy, G. E., Fisher, C. R., and Payne, S. M. (2007). IcsA surface presentation in Shigella flexneri requires the periplasmic chaperones DegP, skp, and SurA. *J. Bacteriol.* 189, 5566–5573. doi:10.1128/JB.00483-07

Qu, J., Mayer, C., Behrens, S., Holst, O., and Kleinschmidt, J. H. (2007). The trimeric periplasmic chaperone skp of *Escherichia coli* forms 1:1 complexes with outer membrane proteins via hydrophobic and electrostatic interactions. *J. Mol. Biol.* 374, 91–105. doi:10.1016/j.jmb.2007.09.020

Rao, J., Damron, F. H., Basler, M., DiGiandomenico, A., Sherman, N. E., Fox, J. W., et al. (2011). Comparisons of two proteomic analyses of non-mucoid and mucoid *Pseudomonas aeruginosa* clinical isolates from a cystic fibrosis patient. *Front. Microbiol.* 2, 162–212. doi:10.3389/fmicb.2011.00162

Rashno, F., Khajeh, K., Capitini, C., Sajedi, R. H., Shokri, M. M., and Chiti, F. (2017). Very rapid amyloid fibril formation by a bacterial lipase in the absence of a detectable lag phase. *Biochim. Biophys. Acta. Proteins Proteom.* 1865, 652–663. doi:10.1016/j.bbapap.2017.03.004

Rashno, F., Khajeh, K., Dabirmanesh, B., Sajedi, R. H., and Chiti, F. (2018). Insight into the aggregation of lipase from Pseudomonas sp. using mutagenesis: Protection of aggregation prone region by adoption of α-helix structure. *Protein Eng. Des. Sel.* 31, 419–426. doi:10.1093/protein/gzz003

Rollauer, S. E., Sooreshjani, M. A., Noinaj, N., and Buchanan, S. K. (2015). Outer membrane protein biogenesis in Gram-negative bacteria. *Philos. Trans. R. Soc. Lond. B Biol. Sci.* 370, 20150023–20150110. doi:10.1098/rstb.2015.0023

Rosenau, F., Isenhardt, S., Gdynia, A., Tielker, D., Schmidt, E., Tielen, P., et al. (2010). Lipase LipC affects motility, biofilm formation and rhamnolipid production in *Pseudomonas aeruginosa*. *FEMS Microbiol. Lett.* 309, 25–34. doi:10.1111/j.1574-6968.2010.02017.x

Rosenau, F., Tommassen, J., and Jaeger, K-E. (2004). Lipase-specific foldases. *ChemBioChem* 5, 152–161. doi:10.1002/cbic.200300761

Sachelaru, I., Petriman, N. A., Kudva, R., and Koch, H. G. (2014). Dynamic interaction of the Sec translocon with the chaperone PpiD. *J. Biol. Chem.* 289, 21706–21715. doi:10.1074/jbc.M114.577916

Sadikot, R. T., Blackwell, T. S., Christman, J. W., and Prince, A. S. (2005). Pathogen–host interactions in *Pseudomonas aeruginosa* pneumonia. *Am. J. Respir. Crit. Care Med.* 171, 1209–1223. doi:10.1164/rccm.200408-1044SO

Saul, F. A., Arié, J. P., Vulliez-le Normand, B., Kahn, R., Betton, J. M., and Bentley, G. A. (2004). Structural and functional studies of FkpA from *Escherichia coli*, a cis/trans peptidyl-prolyl isomerase with chaperone activity. *J. Mol. Biol.* 335, 595–608. doi:10.1016/j.jmb.2003.10.056

Schiffrin, B., Calabrese, A. N., Devine, P. W. A., Harris, S. A., Ashcroft, A. E., Brockwell, D. J., et al. (2016). Skp is a multivalent chaperone of outer-membrane proteins. *Nat. Struct. Mol. Biol.* 23, 786–793. doi:10.1038/nsmb.3266

Schindelin, J., Arganda-Carreras, I., Frise, E., Kaynig, V., Longair, M., Pietzsch, T., et al. (2012). Fiji: An open-source platform for biological-image analysis. *Nat. Methods* 9, 676–682. doi:10.1038/nmeth.2019

Schmidt, A., Kochanowski, K., Vedelaar, S., Ahrné, E., Volkmer, B., Callipo, L., et al. (2016). The quantitative and condition-dependent *Escherichia coli* proteome. *Nat. Biotechnol.* 34, 104–110. doi:10.1038/nbt.3418

Strateva, T., and Mitov, I. (2011). Contribution of an arsenal of virulence factors to pathogenesis of *Pseudomonas aeruginosa* infections. *Ann. Microbiol.* 61, 717–732. doi:10.1007/s13213-011-0273-y

Stull, F., Betton, J-M., and Bardwell, J. C. A. (2018). Periplasmic chaperones and prolyl isomerases. *EcoSal Plus* 8, 1. doi:10.1128/ecosalplus.ESP-0005-2018

Svergun, D., Barberato, C., and Koch, M. H. (1995). Crysol - a program to evaluate X-ray solution scattering of biological macromolecules from atomic coordinates. *J. Appl. Crystallogr.* 28, 768–773. doi:10.1107/s0021889895007047

Svergun, D. I. (1992). Determination of the regularization parameter in indirect-transform methods using perceptual criteria. *J. Appl. Crystallogr.* 25, 495–503. doi:10.1107/s0021889892001663

Svergun, D. I., Petoukhov, M. V., and Koch, M. H. J. (2001). Determination of domain structure of proteins from x-ray solution scattering. *Biophys. J.* 80, 2946–2953. doi:10.1016/S0006-3495(01)76260-1

Tielen, P., Kuhn, H., Rosenau, F., Jaeger, K-E., Flemming, H. C., and Wingender, J. (2013). Interaction between extracellular lipase LipA and the polysaccharide alginate of *Pseudomonas aeruginosa*. *BMC Microbiol.* 13, 159. doi:10.1186/1471-2180-13-159

Tria, G., Mertens, H. D. T., Kachala, M., and Svergun, D. I. (2015). Advanced ensemble modelling of flexible macromolecules using X-ray solution scattering. *IUCrJ* 2, 207–217. doi:10.1107/S205225251500202X

Tsirigotaki, A., De Geyter, J., Šoštarić, N., Economou, A., and Karamanou, S. (2017). Protein export through the bacterial Sec pathway. *Nat. Rev. Microbiol.* 15, 21–36. doi:10.1038/nrmicro.2016.161

Verma, N., Dollinger, P., Kovacic, F., Jaeger, K-E., and Gohlke, H. (2020). The membrane-integrated steric chaperone lif facilitates active site opening of *Pseudomonas aeruginosa* lipase A. *J. Comput. Chem.* 41, 500–512. doi:10.1002/jcc.26085

Viegas, A., Dollinger, P., Verma, N., Kubiak, J., Viennet, T., Seidel, C. A. M., et al. (2020). Structural and dynamic insights revealing how lipase binding domain MD1 of *Pseudomonas aeruginosa* foldase affects lipase activation. *Sci. Rep.* 10, 3578. doi:10.1038/s41598-020-60093-4

Wagner, J. K., Heindl, J. E., Gray, A. N., Jain, S., and Goldberg, M. B. (2009). Contribution of the periplasmic chaperone skp to efficient presentation of the autotransporter IcsA on the surface of Shigella flexneri. *J. Bacteriol.* 191, 815–821. doi:10.1128/JB.00989-08

Walton, T. A., and Sousa, M. C. (2004). Crystal structure of skp, a prefoldin-like chaperone that protects soluble and membrane proteins from aggregation. *Mol. Cell* 15, 367–374. doi:10.1016/j.molcel.2004.07.023

Zhu, J., Cai, X., Harris, T. L., Gooyit, M., Wood, M., Lardy, M., et al. (2015). Disarming *Pseudomonas aeruginosa* virulence factor LasB by leveraging a *Caenorhabditis elegans* infection model. *Chem. Biol.* 22, 483–491. doi:10.1016/j.chembiol.2015.03.012

5.3.2 Structural characterization of prominent periplasmic chaperones

Since the periplasmic chaperones FkpA, SurA, Skp, YfgM and PpiD indicate interactions with the lipase A of *P. aeruginosa* PAO1, further investigations to characterize those proteins were aimed. The proteins were previously purified and characterized by biochemical and biophysical methods (Papadopoulos *et al.*, 2022). SAXS analysis of the periplasmic chaperones indicated the shape and oligomeric state of the proteins in solution (Figure 5.2), matching with recent data (Papadopoulos *et al.*, 2022). Additionally, the crystal structure of Skp of *P. aeruginosa* PAO1 was resolved at a resolution of 2.7 Å and represents the protomer of the natively trimeric protein (Figure 5.2, B). Superimposition of the homology model and the resolved crystal structure of Skp indicates a nearly perfect overlap with an RMSD value of 1.145, pointing to the a high accuracy of the structural prediction modeling that was utilized for previous investigations (Figure 5.2, C) and used in recent investigations (Papadopoulos *et al.*, 2022).

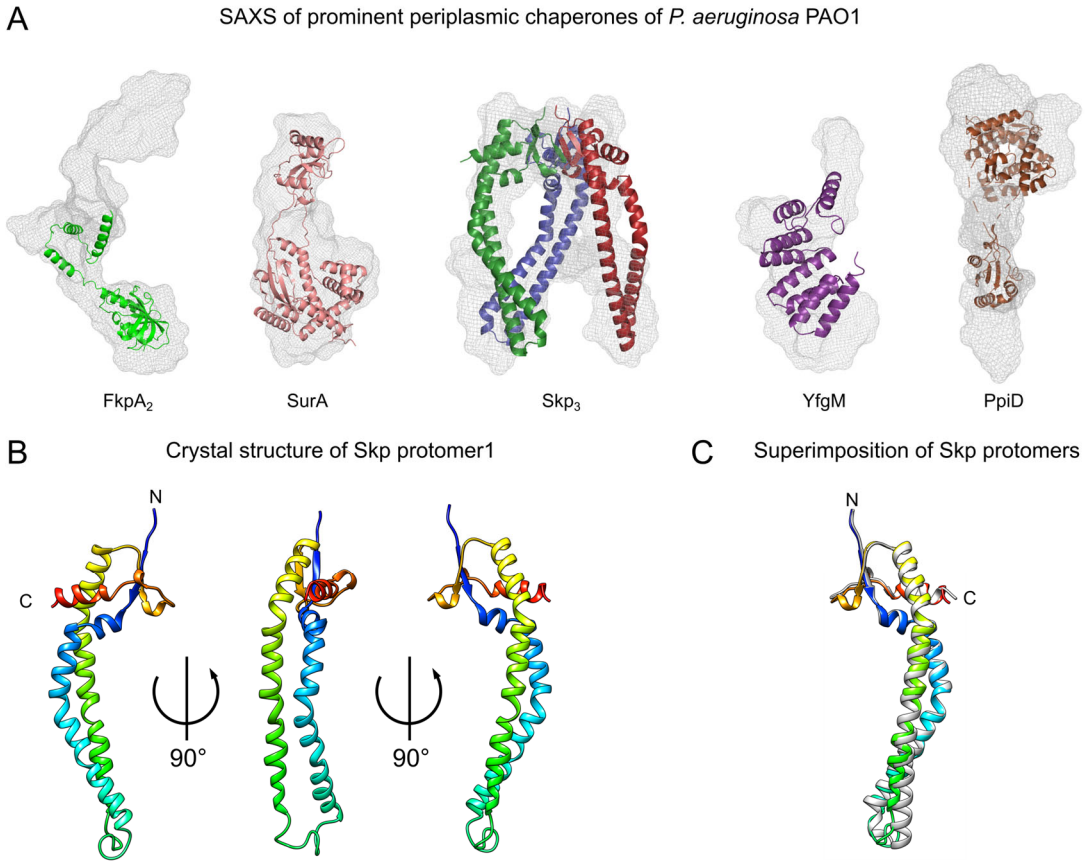

Figure 5. 2: Structural analysis of prominent periplasmic chaperones of *P. aeruginosa* PAO1

A: The SAXS envelope structure of the periplasmic chaperones $FkpA_2$ (dimer), SurA and Skp_3 (trimer), YfgM and PpiD. The data for Skp derives from recent research (Papadopoulos *et al.*, 2022). **B**: Crystal structure of Skp protomer at 2.7 Å resolution. **C**: Superimposition of crystal structure and homology model (grey) of Skp protomer. N- and C-terminus are indicated in the figure.

5.4 Discussion

Little is known about the periplasmic chaperones of *Pseudomonas aeruginosa*, thus a first attempt to investigate those proteins was their structural characterization. The present discussion focuses on structural features and biochemical aspects of the prominent periplasmic chaperones FkpA, SurA, YfgM and PpiD. The structural analysis by SAXS conducted on the periplasmic chaperones revealed their oligomeric state in solution and suggested high similarity to their homologs of *E. coli* (Stull, Betton and Bardwell, 2018). For FkpA, the determined dimeric structure matches the previously published structural information of *P. aeruginosa* FkpA (Huang *et al.*, 2021), this information could be used for further interaction studies with secretory proteins which promote the pathogenicity of *Pseudomonas*. So far, no structure is known for SurA of *P. aeruginosa*, but the AlphaFold prediction matches with the crystal structure of *E. coli* and fits well with the obtained SAXS structure (Bitto and McKay, 2002). The periplasmic chaperone SurA, as well as further peptidyl-prolyl isomerases are crucial for survival and/or virulence of bacterial pathogens (Stull, Betton and Bardwell, 2018; Figaj *et al.*, 2022). In *P. aeruginosa*, SurA is involved in virulence, while deprivation of SurA enhances the susceptibility to antibiotics (Klein *et al.*, 2019).

The membrane-bound chaperones YfgM and PpiD represent ancillary subunits of the bacterial translocon and are involved in protein translocation (Götzke *et al.*, 2014; Sachelaru *et al.*, 2014). It was proposed that YfgM mediates the handover of translocated clients to the periplasmic chaperone network (Götzke *et al.*, 2014, 2015). The lack of structural information on YfgM might be due to the highly flexible structure of the protein which consists of tetratricopeptide repeats (TPRs) that are to find in proteins with high potential for protein:protein interactions and can be related to bacterial virulence (Zeytuni and Zarivach, 2012; Cerveny *et al.*, 2013). The SAXS data acquired for the soluble YfgM, lacking its TMD, indeed imply a highly flexible protein. As mutational studies indicated that the physiological function of YfgM overlaps with those of SurA and Skp, it is of interest to track the interactions with further virulence-determinants as it was conducted with LipA (Götzke *et al.*, 2014; Papadopoulos *et al.*, 2022). Multiple proteins were down-regulated in *yfgM*-depletion *E. coli* strain as quantified by proteomics, including the stress-responsive periplasmic chaperone HdeB (Götzke *et al.*, 2015). Thus, YfgM represents a potent candidate for additional interaction studies with putative virulence and resistance determinative secretory proteins in gram-negative bacterial pathogens.

For PpiD similar observations were made by SAXS, whereby the data indicates a flexible behavior of the protein soluble domain. The protein contains three periplasmic domains and a TMD located close to the translocon SecYEG (Weininger *et al.*, 2010). So far, only the structure of the second periplasmic domain, which is a parvulin-like domain of PpiD, has been solved for the chaperone from *E. coli* (Weininger *et al.*, 2010). The parvulin-like domain of PpiD resembles a prolyl isomerase (PPIase) domain that is not active and is structurally related to a domain within SurA structure (Weininger *et al.*, 2010). The chaperone domains of the protein are mostly helical which could represent suitable sites for

protein:protein interactions. PpiD functions as a translocation mediator and can partially substitute for SurA or Skp function (Fürst *et al.*, 2018; Stull, Betton and Bardwell, 2018). Upon translocation it is suggested that PpiD promotes the clearance of the translocon from the transported substrate, thus increasing the translocation efficiency (Fürst *et al.*, 2018).

The interaction studies of LipA with the prominent periplasmic chaperones of *P. aeruginosa* PAO1 showed that Skp is capable of preventing the misfolding of the LipA *in vitro* and suggested its crucial role for lipase secretion (Papadopoulos *et al.*, 2022). The major discussion about the results obtained on LipA:Skp interactions is to find within the published research article (Papadopoulos *et al.*, 2022). Additional studies indicate that Skp-like proteins play an important role in bacterial virulence (Figaj *et al.*, 2022). The solved crystal structure of Skp protomer of *P. aeruginosa* PAO1 resembles the structural information known for Skp homolog of *E. coli* (Walton and Sousa, 2004), and the SAXS structure indicates the trimeric protein in solution and in its functional state (Papadopoulos *et al.*, 2022).

Periplasmic chaperones can substitute for each other function, thus further investigations with the set of already characterized prominent periplasmic chaperones of *P. aeruginosa* PAO1 and various secretory substrates would be of interest. Especially secretory proteins which are involved in promoting virulence and support pathogenicity of *Pseudomonas* are interesting for further interaction studies with periplasmic chaperones.

6 Conclusion

Life-threatening bacterial infections are a high risk for common human health. Identifying and determining the processes which convey the gain of bacterial pathogenicity is crucial to prevent and treat bacterial infections. Among other bacterial traits, the secretion of proteins which act as virulence factors and mediate pathogenicity is of major importance upon bacterial infection. Elucidating and understanding the processes which guide the biogenesis of a secretory virulence factor could help to develop novel therapeutic treatments against bacterial pathogens. The biogenesis of the major secretory lipase (LipA) of *Pseudomonas aeruginosa* can serve as an example in aim to elucidate the export pathways of virulence factors. LipA covers a stunning way from the place of its synthesis to the place of action. The lipase is synthesized and released into the cytoplasm, transported through the general secretory (Sec) pathway across the inner membrane to the periplasm where it gets folded by a lipase-specific foldase prior being secreted to the extracellular space by T2SS.

The Sec-dependent translocation of LipA is an important initial step upon the lipase biogenesis and crucial for understanding the export of the protein. As the preproteins are targeted to the Sec machinery for post-translational translocation in unfolded state, the isolated proLipA was unfolded by high molar concentration of urea and applied for *in vitro* transport analysis through the newly reconstituted Sec system of *P. aeruginosa* PAO1. Although tremendous efforts were made to enhance the transport efficiency of proLipA *in vitro*, the transport remained low and was not in a comparable range with the reference substrate proOmpA of *E. coli*. The high aggregation propensity of the lipase and an instant folding into intermediate folding states combined with less efficient targeting by SecB and other cytoplasmic chaperones suggestively cause the low transport efficiency of proLipA upon *in vitro* Sec transport. The creation of a more stable mutant of the lipase, as well as single-cysteine variant did not promote the transport efficiency. Additional efforts, including the exchange of the signal peptide for more efficient targeting as well as truncation of the protein did not increase the transport efficiency as well. Further substrates originating from *Pseudomonas* and utilized for Sec-dependent translocation *in vitro* also indicated low transport efficiencies, far off the efficiency observed for proOmpA. These results point out that more nuanced substrates are required to classify the Sec-dependent protein translocation *in vitro*. So far, preliminary observations indicated moderate transport for proFapC which is the only substrate so far reaching approximately 10 % of efficiency *in vitro* (in collaboration with M. Busch). Although the Sec system is highly conserved between gram-negative bacteria, especially when comparing *P. aeruginosa* and *E. coli*, the varying demands of the different species might correlate with the requirements for the setup of the *in vitro* Sec-transport of different *Pseudomonas* substrates. In addition, the Sec systems of both *P. aeruginosa* and *E. coli* showed equal transport efficiency for proOmpA when IMVs were utilized for the transport reaction, while the reconstituted translocons indicated varying efficiency in dependence to the lipid composition of the liposomes. These results highlight the varying requirements of the Sec system for each species and

should be investigated further in aim to find the most optimized conditions that are required for each system.

The second crucial step upon the lipase biogenesis is the protein folding and maturation in the bacterial periplasm. The lipase requires its cognate lipase-specific foldase for folding into its active state. Until yet, investigations of the foldase-mediated lipase folding have been conducted by using the soluble chaperone domain of the foldase. *In vivo* the full-length foldase is a membrane-anchored protein with its chaperone domain facing towards the periplasmic space. The isolation and reconstitution of the full-length foldase was achieved and indicated the functionality of the chaperone in membrane systems. The successful isolation of polymer-extracted near native nanodiscs (NDs) and the MSP-based assembly of NDs with the reconstituted foldase form the basis for investigations of the lipase:foldase interactions at the membrane interface. The detergent-solubilized and reconstituted foldase can be utilized to track lipase:foldase binding by further biophysical methods, e.g. surface plasmon resonance in presence of a model membrane. Furthermore, the co-expression of the foldase LipH and the translocon SecYEG, optionally followed by isolation of those proteins from the bacterial membrane by polymer-based extraction offers a great opportunity to conduct further biochemical and biophysical studies which may elucidate whether the foldase is involved upon lipase translocation and/or interacts with the translocon.

Release of the lipase from the foldase might require the recognition of emerging lipase from translocation step to displace the folded and maturated protein from LipH as well as further interactions with the T2SS. Indeed, interaction studies with the soluble domain of LipH and N- and C-terminal truncations of LipA indicate that the N-terminus is important for recognition by the foldase, while large truncation of the C-terminal part does not affect binding. These results indicate that the foldase might recognize the lipase at an early translocation step. Whether further proteins, besides the suggested T2SS components, are involved in releasing the folded substrate needs further to be investigated. Interaction studies of the lipase and prominent periplasmic chaperones indicated that the trimeric periplasmic chaperone Skp prevents misfolding of the lipase *in vitro* and plays a crucial role for the secretion of the lipase *in vivo* (Papadopoulos *et al.*, 2022). The further characterization of putative interaction partners of the lipase or *vice versa* of further virulence factors that likely interact with prominent periplasmic chaperones can help to elucidate the secretion process of such proteins. For the lipase, the current overexpression system and the observations made during the present investigations can serve as basis for further studies on the lipase transport, folding and maturation. The lipase:foldase system of *P. aeruginosa* PAO1 is a peculiar system that brings multiple pitfalls with it. The high aggregation potential of the lipase, the unknown targeting procedure, the suggested fast intermediate folding, the requirement for chaperone-mediated folding and the possibility to follow off-pathway routes when not timely secreted, make that system very challenging for experimental work. The creation of a stable lipase mutant that does not suffer from aggregation as much as the wild type allowed for investigations of the aggregational behavior of the lipase. The reconstitution of the *Pseudomonas* Sec system in its fully functional state allows for investigation of the Sec-dependent protein translocation of multiple substrates

and is of special interest for those which are involved in virulence. The isolation of functional full-length foldase allows to track the folding and maturation of the lipase in the membrane environment. And the determination of further periplasmic chaperones as putative interaction partners enables to identify possible routes of the lipase, as was shown for Skp which prevents misfolding and supports secretion of LipA. A great opportunity to study the process of lipase biogenesis might rely on the recent advantages of cryotomography on bacterial cells, although the limitation of resolution might be challenging.

Taken together, the presented research forms the basis for further detailed analysis on the lipase biogenesis, enabling i) to study its Sec-dependent transport *in vitro*, ii) to investigate folding and maturation by the full-length foldase in the membrane environment, and iii) to determine further putative interactions with periplasmic proteins which might be involved in prevention of off-pathway routes and secretion not only of the lipase, but also of other virulence factors.

7 Literature

Aboubi, R. (2008) 'Struktur und physiologische Funktion einer Lipase-spezifischen Foldase aus Pseudomonas aeruginosa', *Diploma Thesis, Heinrich Heine Universität*.

Allen, W. J. *et al.* (2016) 'Two-way communication between SecY and SecA suggests a brownian ratchet mechanism for protein translocation', *eLife*, 5(e15598). doi: 10.7554/eLife.15598.

Amann, E., Ochs, B. and Abel, K.-J. (1988) 'Tightly regulated tac promoter vectors useful for the expression of unfused and fused proteins in Escherichia coli', *Gene*, 69(2), pp. 301–315. doi: 10.1016/0378-1119(88)90440-4.

Anfinsen, C. B. *et al.* (1961) 'The kinetics of formation of native Ribonuclease during oxidation of the reduced polypeptide chain', *Proceedings of the National Academy of Sciences*, 47(9), pp. 1309–1314. doi: 10.1073/pnas.47.9.1309.

Anfinsen, C. B. (1973) 'Principles that Govern the Folding of Protein Chains', *Science*, 181(4096), pp. 223–230. doi: 10.1126/science.181.4096.223.

Angelini, S., Deitermann, S. and Koch, H. (2005) 'FtsY, the bacterial signal-recognition particle receptor, interacts functionally and physically with the SecYEG translocon', *EMBO reports*, 6(5), pp. 476–481. doi: 10.1038/sj.embor.7400385.

Arkowitz, R. A., Joly, J. C. and Wickner, W. (1993) 'Translocation can drive the unfolding of a preprotein domain.', *The EMBO Journal*, 12(1), pp. 243–253. doi: 10.1002/j.1460-2075.1993.tb05650.x.

Arkowitz, R. A. and Wickner, W. (1994) 'SecD and SecF are required for the proton electrochemical gradient stimulation of preprotein translocation.', *The EMBO Journal*, 13(4), pp. 954–963. doi: 10.1002/j.1460-2075.1994.tb06340.x.

Arpigny, J. L. and Jaeger, K. E. (1999) 'Bacterial lipolytic enzymes: classification and properties.', *The Biochemical journal*, 343 Pt 1(Pt 1), pp. 177–83. doi: 10.1042/0264-6021:3430177.

Auclair, S. M., Bhanu, M. K. and Kendall, D. A. (2012) 'Signal peptidase I: Cleaving the way to mature proteins', *Protein Science*, 21(1), pp. 13–25. doi: 10.1002/pro.757.

Babic, N. (2022) 'Homology modeling-guided medium-throughput screening of novel hydrolases among Pseudomonas aeruginosa genes of unknown function', *Doctoral Thesis, Heinrich Heine Universität*.

Balchin, D., Hayer-Hartl, M. and Hartl, F. U. (2020) 'Recent advances in understanding catalysis of protein folding by molecular chaperones', *FEBS Letters*, 594(17), pp. 2770–2781. doi: 10.1002/1873-3468.13844.

Ball, G. *et al.* (2002) 'A novel type II secretion system in Pseudomonas aeruginosa', *Molecular Microbiology*, 43(2), pp. 475–485. doi: 10.1046/j.1365-2958.2002.02759.x.

Bariya, P. and Randall, L. L. (2019) 'Coassembly of SecYEG and SecA Fully Restores the Properties of the Native Translocon', *Journal of Bacteriology*, 201(1). doi: 10.1128/JB.00493-18.

Bascos, N. A. D. and Landry, S. J. (2019) 'A History of Molecular Chaperone Structures in the Protein Data Bank', *International Journal of Molecular Sciences*, 20(24:6195). doi: 10.3390/ijms20246195.

Bechtluft, P. *et al.* (2010) 'SecB - A chaperone dedicated to protein translocation', *Molecular BioSystems*, 6(4), pp. 620–627. doi: 10.1039/b915435c.

Beckwith, J. (2013) 'The Sec-dependent pathway', *Research in Microbiology*, 164(6), pp. 497–504. doi: 10.1016/j.resmic.2013.03.007.

Belin, D. *et al.* (2015) 'Escherichia coli SecG Is Required for Residual Export Mediated by Mutant Signal Sequences and for SecY-SecE Complex Stability', *Journal of Bacteriology*, 197(3), pp. 542–552. doi: 10.1128/JB.02136-14.

Berg, B. van den *et al.* (2004) 'X-ray structure of a protein-conducting channel', *Nature*, 427, pp. 36–44. doi: 10.1038/nature02218.

Bessonneau, P. (2002) 'The SecYEG preprotein translocation channel is a conformationally dynamic and dimeric structure', *The EMBO Journal*, 21(5), pp. 995–1003. doi: 10.1093/emboj/21.5.995.

Bhagirath, A. Y. *et al.* (2016) 'Cystic fibrosis lung environment and Pseudomonas aeruginosa infection', *BMC Pulmonary Medicine*, 16(174). doi: 10.1186/s12890-016-0339-5.

Bhanu, M. K., Zhao, P. and Kendall, D. A. (2013) 'Mapping of the SecA Signal Peptide Binding Site and Dimeric Interface by Using the Substituted Cysteine Accessibility Method', *Journal of Bacteriology*, 195(20), pp. 4709–4715. doi: 10.1128/JB.00661-13.

Bieri, O. and Kiefhaber, T. (1999) 'Elementary Steps in Protein Folding', *Biological Chemistry*, 380(7–8), pp. 923–929. doi: 10.1515/BC.1999.114.

Bitto, E. and McKay, D. B. (2002) 'Crystallographic Structure of SurA, a Molecular Chaperone that Facilitates Folding of Outer Membrane Porins', *Structure*, 10(11), pp. 1489–1498. doi: 10.1016/S0969-2126(02)00877-8.

Blanchet, C. E. *et al.* (2015) 'Versatile sample environments and automation for biological solution X-ray scattering experiments at the P12 beamline (PETRA III, DESY)', *Journal of Applied Crystallography*, 48(2), pp. 431–443. doi: 10.1107/S160057671500254X.

Bleves, S. *et al.* (2010) 'Protein secretion systems in Pseudomonas aeruginosa: A wealth of pathogenic weapons', *International Journal of Medical Microbiology*, 300(8), pp. 534–543. doi: 10.1016/j.ijmm.2010.08.005.

Blow, D. M., Birktoft, J. J. and Hartley, B. S. (1969) 'Role of a buried acid group in the mechanism of action of chymotrypsin.', *Nature*, 221(5178), pp. 337–40. doi: 10.1038/221337a0.

Bolhuis, A. (2004) 'The archaeal Sec–dependent protein translocation pathway', *Philosophical Transactions of the Royal Society of London. Series B: Biological Sciences*, 359(1446), pp. 919–927. doi: 10.1098/rstb.2003.1461.

Buchner, J. (2019) 'Molecular chaperones and protein quality control: an introduction to the JBC Reviews thematic series', *Journal of Biological Chemistry*, 294(6), pp. 2074–2075. doi: 10.1074/jbc.REV118.006739.

Busch, M. (2021) 'Investigating the protein transport via SecYEG translocon of Pseudomonas aeruginosa', *Master Thesis, Heinrich Heine Universität*.

Cadoret, F. *et al.* (2014) 'Txc, a New Type II Secretion System of Pseudomonas aeruginosa Strain PA7, Is Regulated by the TtsS/TtsR Two-Component System and Directs Specific Secretion of the CbpE Chitin-Binding Protein', *Journal of Bacteriology*, 196(13), pp. 2376–2386. doi: 10.1128/JB.01563-14.

Casas-Godoy, L. *et al.* (2018) 'Lipases: An Overview', in Sandoval, G. (ed.) *Lipases and Phospholipases: Methods and Protocols*. New York, NY, pp. 3–38. doi: 10.1007/978-1-4939-8672-9_1.

Castanié-Cornet, M.-P., Bruel, N. and Genevaux, P. (2014) 'Chaperone networking facilitates protein targeting to the bacterial cytoplasmic membrane', *Biochimica et Biophysica Acta (BBA) - Molecular Cell Research*, 1843(8), pp. 1442–1456. doi: 10.1016/j.bbamcr.2013.11.007.

Catipovic, M. A. *et al.* (2019) 'Protein translocation by the SecA ATPase occurs by a power-stroke mechanism', *The EMBO Journal*, 38(9:e101140). doi: 10.15252/embj.2018101140.

Cendra, M. del M. and Torrents, E. (2021) 'Pseudomonas aeruginosa biofilms and their partners in crime', *Biotechnology Advances*, 49:107734. doi: 10.1016/j.biotechadv.2021.107734.

Cerveny, L. *et al.* (2013) 'Tetratricopeptide repeat motifs in the world of bacterial pathogens: Role in virulence mechanisms', *Infection and Immunity*, 81(3), pp. 629–635. doi: 10.1128/IAI.01035-12.

Chadha, J., Harjai, K. and Chhibber, S. (2022) 'Revisiting the virulence hallmarks of Pseudomonas aeruginosa: a chronicle through the perspective of quorum sensing.', *Environmental microbiology*, 24(6), pp. 2630–2656. doi: 10.1111/1462-2920.15784.

Chagnot, C. *et al.* (2013) 'Proteinaceous determinants of surface colonization in bacteria: bacterial adhesion and biofilm formation from a protein secretion perspective', *Frontiers in Microbiology*, 4, pp. 1–26. doi: 10.3389/fmicb.2013.00303.

Chatzi, K. E. *et al.* (2014) 'SecA-mediated targeting and translocation of secretory proteins', *Biochimica et Biophysica Acta (BBA) - Molecular Cell Research*, 1843(8), pp. 1466–1474. doi: 10.1016/j.bbamcr.2014.02.014.

Chatzi, K. E. *et al.* (2017) 'Preprotein mature domains contain translocase targeting signals that are essential for secretion', *Journal of Cell Biology*, 216(5), pp. 1357–1369. doi: 10.1083/jcb.201609022.

Chihara-Siomi, M. *et al.* (1992) 'Purification, molecular cloning, and expression of lipase from Pseudomonas aeruginosa', *Archives of Biochemistry and Biophysics*, 296(2), pp. 505–513. doi: 10.1016/0003-9861(92)90604-U.

Chum, A. P. *et al.* (2019) 'Plasticity and transient binding are key ingredients of the periplasmic chaperone network', *Protein Science*, 28(7), pp. 1340–1349. doi: 10.1002/pro.3641.

Ciofu, O. and Tolker-Nielsen, T. (2019) 'Tolerance and Resistance of Pseudomonas aeruginosa Biofilms to Antimicrobial Agents—How P. aeruginosa Can Escape Antibiotics', *Frontiers in Microbiology*, 10. doi: 10.3389/fmicb.2019.00913.

Collinson, I. (2019) 'The Dynamic ATP-Driven Mechanism of Bacterial Protein Translocation and the Critical Role of Phospholipids', *Frontiers in Microbiology*, 10. doi: 10.3389/fmicb.2019.01217.

Collinson, I., Corey, R. A. and Allen, W. J. (2015) 'Channel crossing: how are proteins shipped across the bacterial plasma membrane?', *Philosophical Transactions of the Royal Society B: Biological Sciences*, 370(1679), p. 20150025. doi: 10.1098/rstb.2015.0025.

Costa, T. R. D. *et al.* (2015) 'Secretion systems in Gram-negative bacteria: structural and mechanistic insights', *Nature Reviews Microbiology*, 13(6), pp. 343–359. doi: 10.1038/nrmicro3456.

Crane, J. M. and Randall, L. L. (2017) 'The Sec System: Protein Export in Escherichia coli', *EcoSal Plus*. Edited by S. T. Lovett and H. D. Bernstein, 7(2). doi: 10.1128/ecosalplus.ESP-0002-2017.

Cranford-Smith, T. *et al.* (2020) 'Iron is a ligand of SecA-like metal-binding domains in vivo', *Journal of Biological Chemistry*, 295(21), pp. 7516–7528. doi: 10.1074/jbc.RA120.012611.

Crone, S. *et al.* (2020) 'The environmental occurrence of Pseudomonas aeruginosa', *APMIS*, 128(3), pp. 220–231. doi: 10.1111/apm.13010.

Dalbey, R. E. *et al.* (2014) 'The membrane insertase YidC', *Biochimica et Biophysica Acta (BBA) - Molecular Cell Research*, 1843(8), pp. 1489–1496. doi: 10.1016/j.bbamcr.2013.12.022.

Dalbey, R. E. and Kuhn, A. (2012) 'Protein Traffic in Gram-negative bacteria - how exported and secreted proteins find their way', *FEMS Microbiology Reviews*, 36(6), pp. 1023–1045. doi: 10.1111/j.1574-6976.2012.00327.x.

Das, S. and Oliver, D. B. (2011) 'Mapping of the SecA·SecY and SecA·SecG Interfaces by Site-directed in Vivo Photocross-linking', *Journal of Biological Chemistry*, 286(14), pp. 12371–12380. doi:

10.1074/jbc.M110.182931.

Davane, M. (2014) 'Pseudomonas aeruginosa from hospital environment', *Journal of Microbiology and Infectious Diseases*, 4(1), pp. 42–43. doi: 10.5799/ahinjs.02.2014.01.0124.

Dekker, C., De Kruijff, B. and Gros, P. (2003) 'Crystal structure of SecB from Escherichia coli', *Journal of Structural Biology*, 144(3), pp. 313–319. doi: 10.1016/j.jsb.2003.09.012.

Denks, K. *et al.* (2014) 'The Sec translocon mediated protein transport in prokaryotes and eukaryotes', *Molecular Membrane Biology*, 31(2–3), pp. 58–84. doi: 10.3109/09687688.2014.907455.

Deuerling, E. *et al.* (1999) 'Trigger factor and DnaK cooperate in folding of newly synthesized proteins', *Nature*, 400(6745), pp. 693–696. doi: 10.1038/23301.

Deuerling, E. *et al.* (2003) 'Trigger factor and DnaK possess overlapping substrate pools and binding specificities', *Molecular Microbiology*, 47(5), pp. 1317–1328. doi: 10.1046/j.1365-2958.2003.03370.x.

Diggle, S. P. and Whiteley, M. (2020) 'Microbe Profile: Pseudomonas aeruginosa: opportunistic pathogen and lab rat', *Microbiology*, 166(1), pp. 30–33. doi: 10.1099/mic.0.000860.

Dill, K. A. and MacCallum, J. L. (2012) 'The Protein-Folding Problem, 50 Years On', *Science*, 338, pp. 1042–1046. doi: 10.1126/science.1219021.

Ding, H. *et al.* (2003) 'Bacillus subtilis SecA ATPase Exists as an Antiparallel Dimer in Solution', *Biochemistry*, 42(29), pp. 8729–8738. doi: 10.1021/bi0342057.

Dinner, A. R. *et al.* (2000) 'Understanding protein folding via free-energy surfaces from theory and experiment', *Trends in Biochemical Sciences*, 25(7), pp. 331–339. doi: 10.1016/S0968-0004(00)01610-8.

Dittrich, J. *et al.* (2023) 'Resolution of Maximum Entropy Method-Derived Posterior Conformational Ensembles of a Flexible System Probed by FRET and Molecular Dynamics Simulations', *Journal of Chemical Theory and Computation*, 19(8), pp. 2389–2409. doi: 10.1021/acs.jctc.2c01090.

Dobson, C. M. (2003) 'Protein folding and misfolding', *Nature*, 426(6968), pp. 884–890. doi: 10.1038/nature02261.

Dods, R. (2019) 'The Amino Acid Sequences of Proteins Determine Folding and Non-folding', in *Concepts in Bioscience Engineering*. Cham: Springer International Publishing, pp. 37–83. doi: 10.1007/978-3-030-28303-2_2.

van der Does, C. *et al.* (2000) 'Non-bilayer Lipids Stimulate the Activity of the Reconstituted Bacterial Protein Translocase', *Journal of Biological Chemistry*, 275(4), pp. 2472–2478. doi: 10.1074/jbc.275.4.2472.

Dollinger, P. (2018) 'Lipase - specific foldase - aided folding of Lipase A from Pseudomonas aeruginosa', *Doctoral Thesis, Heinrich Heine Universität*.

Dong, L. *et al.* (2023) 'Structural basis of SecA-mediated protein translocation', *Proceedings of the National Academy of Sciences*, 120(2:e2208070120). doi: 10.1073/pnas.2208070120.

Döring, G. *et al.* (1987) 'Virulence factors of Pseudomonas aeruginosa.', *Antibiotics and chemotherapy*, 39(Figure 1), pp. 136–48. doi: 10.1159/000414341.

Douzi, B. *et al.* (2011) 'Deciphering the Xcp Pseudomonas aeruginosa Type II Secretion Machinery through Multiple Interactions with Substrates', *Journal of Biological Chemistry*, 286(47), pp. 40792–40801. doi: 10.1074/jbc.M111.294843.

Driessen, A. J. M. and Nouwen, N. (2008) 'Protein Translocation Across the Bacterial Cytoplasmic Membrane', *Annual Review of Biochemistry*, 77(1), pp. 643–667. doi:

10.1146/annurev.biochem.77.061606.160747.

Driscoll, J. A., Brody, S. L. and Kollef, M. H. (2007) 'The epidemiology, pathogenesis and treatment of Pseudomonas aeruginosa infections', *Drugs*, 67(3), pp. 351–368. doi: 10.2165/00003495-200767030-00003.

Dudek, J. *et al.* (2015) 'Protein Transport into the Human Endoplasmic Reticulum', *Journal of Molecular Biology*, 427(6), pp. 1159–1175. doi: 10.1016/j.jmb.2014.06.011.

Durán, O. *et al.* (2022) 'Pyoverdine as an Important Virulence Factor in Pseudomonas aeruginosa Antibiotic Resistance', in *The Global Antimicrobial Resistance Epidemic - Innovative Approaches and Cutting-Edge Solutions*. IntechOpen, pp. 225–240. doi: 10.5772/intechopen.104222.

Economou, A. *et al.* (2006) 'Secretion by numbers: Protein traffic in prokaryotes', *Molecular Microbiology*, 62(2), pp. 308–319. doi: 10.1111/j.1365-2958.2006.05377.x.

Ellis, R. J. (1993) 'The general concept of molecular chaperones', *Philosophical Transactions of the Royal Society of London. Series B: Biological Sciences*, 339(1289), pp. 257–261. doi: 10.1098/rstb.1993.0023.

Ellis, R. J. (1998) 'Steric chaperones', *Trends in Biochemical Sciences*, 23(2), pp. 43–45. doi: 10.1016/S0968-0004(98)01175-X.

Englander, S. W. and Mayne, L. (2014) 'The nature of protein folding pathways', *Proceedings of the National Academy of Sciences of the United States of America*, 111(45), pp. 15873–15880. doi: 10.1073/pnas.1411798111.

Erlandson, K. J. *et al.* (2008) 'A role for the two-helix finger of the SecA ATPase in protein translocation', *Nature*, 455(7215), pp. 984–987. doi: 10.1038/nature07439.

Fekkes, P. *et al.* (1998) 'Preprotein transfer to the Escherichia coli translocase requires the co-operative binding of SecB and the signal sequence to SecA', *Molecular Microbiology*, 29(5), pp. 1179–1190. doi: 10.1046/j.1365-2958.1998.00997.x.

Fekkes, P. *et al.* (1999) 'Zinc Stabilizes the SecB Binding Site of SecA', *Biochemistry*, 38(16), pp. 5111–5116. doi: 10.1021/bi982818r.

Fersht, A. R. (2000) 'Transition-state structure as a unifying basis in protein-folding mechanisms: Contact order, chain topology, stability, and the extended nucleus mechanism', *Proceedings of the National Academy of Sciences*, 97(4), pp. 1525–1529. doi: 10.1073/pnas.97.4.1525.

Figaj, D. *et al.* (2022) 'SurA-like and Skp-like Proteins as Important Virulence Determinants of the Gram Negative Bacterial Pathogens', *International Journal of Molecular Sciences*, 24(1)(295). doi: 10.3390/ijms24010295.

Filloux, A. (1998) 'GSP-dependent protein secretion in Gram-negative bacteria: the Xcp system of Pseudomonas aeruginosa', *FEMS Microbiology Reviews*, 22(3), pp. 177–198. doi: 10.1016/S0168-6445(98)00013-8.

Filloux, A. (2004) 'The underlying mechanisms of type II protein secretion', *Biochimica et Biophysica Acta (BBA) - Molecular Cell Research*, 1694(1–3), pp. 163–179. doi: 10.1016/j.bbamcr.2004.05.003.

Filloux, A. (2011) 'Protein secretion systems in Pseudomonas aeruginosa: An essay on diversity, evolution, and function', *Frontiers in Microbiology*, 2(155). doi: 10.3389/fmicb.2011.00155.

Filloux, A. (2022) 'Bacterial protein secretion systems: Game of types', *Microbiology*, 168(5). doi: 10.1099/mic.0.001193.

Filloux, A. and Davies, J. C. (2019) 'Chronic infection by controlling inflammation', *Nature Microbiology*, 4(3), pp. 378–379. doi: 10.1038/s41564-019-0397-6.

Frenken, L. G. J. *et al.* (1993) 'Role of the lipB gene product in the folding of the secreted lipase of Pseudomonas glumae', *Molecular Microbiology*, 9(3), pp. 591–599. doi: 10.1111/j.1365-2958.1993.tb01719.x.

Freschi, L. *et al.* (2019) 'The Pseudomonas aeruginosa Pan-Genome Provides New Insights on Its Population Structure, Horizontal Gene Transfer, and Pathogenicity', *Genome Biology and Evolution*. Edited by B. Martin, 11(1), pp. 109–120. doi: 10.1093/gbe/evy259.

Freudl, R. (2018) 'Signal peptides for recombinant protein secretion in bacterial expression systems', *Microbial Cell Factories*, 17(1), pp. 1–10. doi: 10.1186/s12934-018-0901-3.

Funken, H. *et al.* (2011) 'The Lipase LipA (PA2862) but Not LipC (PA4813) from Pseudomonas aeruginosa Influences Regulation of Pyoverdine Production and Expression of the Sigma Factor PvdS', *Journal of Bacteriology*, 193(20), pp. 5858–5860. doi: 10.1128/JB.05765-11.

Fürst, M. *et al.* (2018) 'Involvement of PpiD in Sec-dependent protein translocation', *Biochimica et Biophysica Acta - Molecular Cell Research*, 1865(2), pp. 273–280. doi: 10.1016/j.bbamcr.2017.10.012.

Furukawa, A. *et al.* (2017) 'Tunnel Formation Inferred from the I-Form Structures of the Proton-Driven Protein Secretion Motor SecDF', *Cell Reports*, 19(5), pp. 895–901. doi: 10.1016/j.celrep.2017.04.030.

Gao, M., Nakajima An, D. and Skolnick, J. (2022) 'Deep learning-driven insights into super protein complexes for outer membrane protein biogenesis in bacteria', *eLife*, 11(e82885). doi: 10.7554/eLife.82885.

Gasteiger, E. *et al.* (2005) 'Protein Identification and Analysis Tools on the ExPASy Server', in *The Proteomics Protocols Handbook*. Totowa, NJ: Humana Press, pp. 571–607. doi: 10.1385/1-59259-890-0:571.

De Geyter, J. *et al.* (2016) 'Protein folding in the cell envelope of Escherichia coli', *Nature Microbiology*, 1(8)(e82885). doi: 10.1038/nmicrobiol.2016.107.

De Geyter, J. *et al.* (2020) 'Trigger factor is a bona fide secretory pathway chaperone that interacts with SecB and the translocase', *EMBO reports*, 21(e49054). doi: 10.15252/embr.201949054.

Gilbert, E. J. (1993) 'Pseudomonas lipases: Biochemical properties and molecular cloning', *Enzyme and Microbial Technology*, 15(8), pp. 634–645. doi: 10.1016/0141-0229(93)90062-7.

Goemans, C., Denoncin, K. and Collet, J.-F. (2014) 'Folding mechanisms of periplasmic proteins', *Biochimica et Biophysica Acta (BBA) - Molecular Cell Research*, 1843(8), pp. 1517–1528. doi: 10.1016/j.bbamcr.2013.10.014.

Gold, V. A. M. *et al.* (2010) 'The action of cardiolipin on the bacterial translocon', *Proceedings of the National Academy of Sciences*, 107(22), pp. 10044–10049. doi: 10.1073/pnas.0914680107.

Götzke, H. *et al.* (2014) 'YfgM Is an Ancillary Subunit of the SecYEG Translocon in Escherichia coli', *Journal of Biological Chemistry*, 289(27), pp. 19089–19097. doi: 10.1074/jbc.M113.541672.

Götzke, H. *et al.* (2015) 'Identification of putative substrates for the periplasmic chaperone YfgM in Escherichia coli using quantitative proteomics', *Molecular and Cellular Proteomics*, 14(1), pp. 216–226. doi: 10.1074/mcp.M114.043216.

Gouridis, G. *et al.* (2013) 'Quaternary Dynamics of the SecA Motor Drive Translocase Catalysis', *Molecular Cell*, 52(5), pp. 655–666. doi: 10.1016/j.molcel.2013.10.036.

Grady, L. M., Michtavy, J. and Oliver, D. B. (2012) 'Characterization of the Escherichia coli SecA Signal Peptide-Binding Site', *Journal of Bacteriology*, 194(2), pp. 307–316. doi: 10.1128/JB.06150-11.

Green, E. R. and Mecsas, J. (2016) 'Bacterial Secretion Systems: An Overview', *Microbiology Spectrum*. Edited by I. T. Kudva, 4(1). doi: 10.1128/microbiolspec.VMBF-0012-2015.

Guinier, A. (1939) ‘Small-angle X-ray diffraction: application to the study of ultramicroscopic phenomena’, *Ann. Phys.*, 12(1), pp. 161–237.

Guzman, L. M. *et al.* (1995) ‘Tight regulation, modulation, and high-level expression by vectors containing the arabinose PBAD promoter’, *Journal of Bacteriology*, 177(14), pp. 4121–4130. doi: 10.1128/jb.177.14.4121-4130.1995.

Hanahan, D. (1983) ‘Studies on transformation of Escherichia coli with plasmids’, *Journal of Molecular Biology*, 166(4), pp. 557–580. doi: 10.1016/S0022-2836(83)80284-8.

Hartl, F. U. *et al.* (1990) ‘The binding cascade of SecB to SecA to SecY E mediates preprotein targeting to the E. coli plasma membrane’, *Cell*, 63(2), pp. 269–279. doi: 10.1016/0092-8674(90)90160-G.

Hartl, F. U., Bracher, A. and Hayer-Hartl, M. (2011) ‘Molecular chaperones in protein folding and proteostasis’, *Nature*, 475(7356), pp. 324–332. doi: 10.1038/nature10317.

Hartl, F. U. and Hayer-Hartl, M. (2002) ‘Molecular Chaperones in the Cytosol: from Nascent Chain to Folded Protein’, *Science*, 295(5561), pp. 1852–1858. doi: 10.1126/science.1068408.

Hausmann, S. (2008) ‘Einfluss des Lipase-spezifischen Chaperons LipH auf die Faltung und Sekretion der Lipasen LipA und LipC aus Pseudomonas aeruginosa’, *Doctoral Thesis, Heinrich Heine Universität*, (April 2008).

Hausmann, S. *et al.* (2008) ‘Mutations towards enantioselectivity adversely affect secretion of Pseudomonas aeruginosa lipase’, *FEMS Microbiology Letters*, 282(1), pp. 65–72. doi: 10.1111/j.1574-6968.2008.01107.x.

Hausmann, S. and Jaeger, K. (2010) *Handbook of Hydrocarbon and Lipid Microbiology*, *Handbook of Hydrocarbon and Lipid Microbiology*. Edited by K. N. Timmis. Berlin, Heidelberg: Springer Berlin Heidelberg. doi: 10.1007/978-3-540-77587-4.

Hiller, S. (2019) ‘Chaperone-Bound Clients: The Importance of Being Dynamic’, *Trends in Biochemical Sciences*, 44(6), pp. 517–527. doi: 10.1016/j.tibs.2018.12.005.

Hobson, A. H. *et al.* (1993) ‘Activation of a bacterial lipase by its chaperone’, *Proceedings of the National Academy of Sciences of the United States of America*, 90(12), pp. 5682–5686. doi: 10.1073/pnas.90.12.5682.

Hoffmann, A., Bukau, B. and Kramer, G. (2010) ‘Structure and function of the molecular chaperone Trigger Factor’, *Biochimica et Biophysica Acta (BBA) - Molecular Cell Research*, 1803(6), pp. 650–661. doi: 10.1016/j.bbamcr.2010.01.017.

Holland, I. B. (2004) ‘Translocation of bacterial proteins—an overview’, *Biochimica et Biophysica Acta (BBA) - Molecular Cell Research*, 1694(1–3), pp. 5–16. doi: 10.1016/j.bbamcr.2004.02.007.

Holloway, B. W., Krishnapillai, V. and Morgan, A. F. (1979) ‘Chromosomal genetics of Pseudomonas.’, *Microbiological Reviews*, 43(1), pp. 73–102. doi: 10.1128/MMBR.43.1.73-102.1979.

Holmes, C. L. *et al.* (2021) ‘Pathogenesis of Gram-Negative Bacteremia’, *Clinical Microbiology Reviews*, 34(2)(e00234-20). doi: 10.1128/CMR.00234-20.

Hong, W. *et al.* (2012) ‘Chaperone-dependent mechanisms for acid resistance in enteric bacteria’, *Trends in Microbiology*, 20(7), pp. 328–335. doi: 10.1016/j.tim.2012.03.001.

Horowitz, S. *et al.* (2018) ‘Folding while bound to chaperones’, *Current Opinion in Structural Biology*, 48, pp. 1–5. doi: 10.1016/j.sbi.2017.06.009.

Houben, B., Rousseau, F. and Schymkowitz, J. (2022) ‘Protein structure and aggregation: a marriage of necessity ruled by aggregation gatekeepers’, *Trends in Biochemical Sciences*, 47(3), pp. 194–205. doi: 10.1016/j.tibs.2021.08.010.

Huang, C. *et al.* (2016) 'Structural basis for the antifolding activity of a molecular chaperone', *Nature*, 537(7619), pp. 202–206. doi: 10.1038/nature18965.

Huang, Q. *et al.* (2021) 'Structural characterization of PaFkbA: A periplasmic chaperone from Pseudomonas aeruginosa', *Computational and Structural Biotechnology Journal*, 19, pp. 2460–2467. doi: 10.1016/j.csbj.2021.04.045.

Hunt, J. F. *et al.* (2002) 'Nucleotide Control of Interdomain Interactions in the Conformational Reaction Cycle of SecA', *Science*, 297(5589), pp. 2018–2026. doi: 10.1126/science.1074424.

Irvine, G. B. *et al.* (2008) 'Protein Aggregation in the Brain: The Molecular Basis for Alzheimer's and Parkinson's Diseases', *Molecular Medicine*, 14(7–8), pp. 451–464. doi: 10.2119/2007-00100.Irvine.

Jaeger, K.-E., Dijkstra, B. W. and Reetz, M. T. (1999) 'Bacterial Biocatalysts: Molecular Biology, Three-Dimensional Structures, and Biotechnological Applications of Lipases', *Annual Review of Microbiology*, 53(1), pp. 315–351. doi: 10.1146/annurev.micro.53.1.315.

Jaeger, K.-E., Kharazmi, A. and Høiby, N. (1991) 'Extracellular lipase of Pseudomonas aeruginosa: biochemical characterization and effect on human neutrophil and monocyte function in vitro', *Microbial Pathogenesis*, 10(3), pp. 173–182. doi: 10.1016/0882-4010(91)90052-C.

Jaeger, K. E. *et al.* (1994) 'Bacterial lipases', *FEMS Microbiology Reviews*, 15(1), pp. 29–63. doi: 10.1016/0168-6445(94)90025-6.

Jaeger, K. E. and Reetz, M. T. (1998) 'Microbial lipases form versatile tools for biotechnology.', *Trends in biotechnology*, 16(9), pp. 396–403. doi: 10.1016/s0167-7799(98)01195-0.

Jarosińska, O. D. and Rüdiger, S. G. D. (2021) 'Molecular Strategies to Target Protein Aggregation in Huntington's Disease', *Frontiers in Molecular Biosciences*, 8(769184). doi: 10.3389/fmolb.2021.769184.

Jauss, B. *et al.* (2019) 'Noncompetitive binding of PpiD and YidC to the SecYEG translocon expands the global view on the SecYEG interactome in Escherichia coli', *Journal of Biological Chemistry*, 294(50), pp. 19167–19183. doi: 10.1074/jbc.RA119.010686.

Jiang, C., Wynne, M. and Huber, D. (2021) 'How Quality Control Systems AID Sec-Dependent Protein Translocation', *Frontiers in Molecular Biosciences*, 8(669376). doi: 10.3389/fmolb.2021.669376.

Jomaa, A. *et al.* (2017) 'Structure of the quaternary complex between SRP, SR, and translocon bound to the translating ribosome', *Nature Communications*, 8(15470). doi: 10.1038/ncomms15470.

Judy, E. and Kishore, N. (2019) 'A look back at the molten globule state of proteins: thermodynamic aspects', *Biophysical Reviews*, 11(3), pp. 365–375. doi: 10.1007/s12551-019-00527-0.

Jumper, J. *et al.* (2021) 'Highly accurate protein structure prediction with AlphaFold', *Nature*, 596(7873), pp. 583–589. doi: 10.1038/s41586-021-03819-2.

Jurado-Martín, I., Sainz-Mejías, M. and McClean, S. (2021) 'Pseudomonas aeruginosa: An Audacious Pathogen with an Adaptable Arsenal of Virulence Factors', *International Journal of Molecular Sciences*, 22(6)(3128). doi: 10.3390/ijms22063128.

Kamel, M. *et al.* (2022) 'Unsaturated fatty acids augment protein transport via the SecA:SecYEG translocon', *The FEBS Journal*, 289(1), pp. 140–162. doi: 10.1111/febs.16140.

Kanonenberg, K. *et al.* (2019) 'Shaping the lipid composition of bacterial membranes for membrane protein production', *Microbial Cell Factories*, 18(1)(131). doi: 10.1186/s12934-019-1182-1.

Kater, L. *et al.* (2019) 'Partially inserted nascent chain unzips the lateral gate of the Sec translocon', *EMBO reports*, 20(e48191). doi: 10.15252/embr.201948191.

Kaushik, S., He, H. and Dalbey, R. E. (2022) 'Bacterial Signal Peptides- Navigating the Journey of Proteins', *Frontiers in Physiology*, 13(933153). doi: 10.3389/fphys.2022.933153.

Kawagoe, S., Ishimori, K. and Saio, T. (2022) 'Structural and Kinetic Views of Molecular Chaperones in Multidomain Protein Folding', *International Journal of Molecular Sciences*, 23(5)(2485). doi: 10.3390/ijms23052485.

Kelley, L. A. *et al.* (2015) 'The Phyre2 web portal for protein modeling, prediction and analysis', *Nature Protocols*, 10(6), pp. 845–858. doi: 10.1038/nprot.2015.053.

de Keyzer, J. *et al.* (2002) 'The F286Y mutation of PrlA4 tempers the signal sequence suppressor phenotype by reducing the SecA binding affinity', *FEBS Letters*, 510(1–2), pp. 17–21. doi: 10.1016/S0014-5793(01)03213-6.

de Keyzer, J., van der Does, C. and Driessen, A. J. M. (2002) 'Kinetic Analysis of the Translocation of Fluorescent Precursor Proteins into Escherichia coli Membrane Vesicles', *Journal of Biological Chemistry*, 277(48), pp. 46059–46065. doi: 10.1074/jbc.M208449200.

Khan, F. I. *et al.* (2017) 'The lid domain in lipases: Structural and functional determinant of enzymatic properties', *Frontiers in Bioengineering and Biotechnology*, 5(16). doi: 10.3389/fbioe.2017.00016.

El Khattabi, M. *et al.* (1999) 'Specificity of the lipase-specific foldases of gram-negative bacteria and the role of the membrane anchor', *Molecular and General Genetics*, 261(4–5), pp. 770–776. doi: 10.1007/s004380050020.

El Khattabi, M. *et al.* (2000) 'Role of the lipase-specific foldase of Burkholderia glumae as a steric chaperone', *Journal of Biological Chemistry*, 275(35), pp. 26885–26891. doi: 10.1074/jbc.M003258200.

Kim, E. K. *et al.* (2001) 'Lipase and its modulator from Pseudomonas sp. strain KFCC 10818: Proline-to-glutamine substitution at position 112 induces formation of enzymatically active lipase in the absence of the modulator', *Journal of Bacteriology*, 183(20), pp. 5937–5941. doi: 10.1128/JB.183.20.5937-5941.2001.

Kim, H. *et al.* (2022) 'Cytoplasmic molecular chaperones in Pseudomonas species', *Journal of Microbiology*, 60(11), pp. 1049–1060. doi: 10.1007/s12275-022-2425-0.

Kim, H., Wu, K. and Lee, C. (2021) 'Stress-Responsive Periplasmic Chaperones in Bacteria', *Frontiers in Molecular Biosciences*, 8(678697). doi: 10.3389/fmolb.2021.678697.

Klein, K. *et al.* (2019) 'Deprivation of the Periplasmic Chaperone SurA Reduces Virulence and Restores Antibiotic Susceptibility of Multidrug-Resistant Pseudomonas aeruginosa', *Frontiers in Microbiology*, 10(100.). doi: 10.3389/fmicb.2019.00100.

Koch, S. *et al.* (2021) 'Single-molecule analysis of dynamics and interactions of the SecYEG translocon', *The FEBS Journal*, 288(7), pp. 2203–2221. doi: 10.1111/febs.15596.

Koldewey, P. *et al.* (2016) 'Forces Driving Chaperone Action', *Cell*, 166(2), pp. 369–379. doi: 10.1016/j.cell.2016.05.054.

Konarev, P. V *et al.* (2003) 'PRIMUS: a Windows PC-based system for small-angle scattering data analysis', *Journal of Applied Crystallography*, 36(5), pp. 1277–1282. doi: 10.1107/S0021889803012779.

König, B., Jaeger, K.-E. and König, W. (1994) 'Induction of Inflammatory Mediator Release (12-Hydroxyeicosatetraenoic Acid) from Human Platelets by *Pseudomonas aeruginosa*', *International Archives of Allergy and Immunology*, 104(1), pp. 33–41. doi: 10.1159/000236706.

Korotkov, K. V. and Sandkvist, M. (2019) 'Architecture, Function, and Substrates of the Type II Secretion System', *EcoSal Plus*. Edited by E. Cascales and P. J. Christie, 8(2). doi: 10.1128/ecosalplus.ESP-0034-2018.

Kovach, M. E. *et al.* (1995) 'Four new derivatives of the broad-host-range cloning vector pBBR1MCS, carrying different antibiotic-resistance cassettes', *Gene*, 166(1), pp. 175–176. doi: 10.1016/0378-1119(95)00584-1.

Kovacic, F. *et al.* (2019) 'Classification of Lipolytic Enzymes from Bacteria', in *Aerobic Utilization of Hydrocarbons, Oils, and Lipids*. Cham: Springer International Publishing, pp. 255–289. doi: 10.1007/978-3-319-50418-6_39.

Kozin, M. B. and Svergun, D. I. (2001) 'Automated matching of high- and low-resolution structural models', *Journal of Applied Crystallography*, 34(1), pp. 33–41. doi: 10.1107/S0021889800014126.

Krishnamurthy, S. *et al.* (2022) 'Preproteins couple the intrinsic dynamics of SecA to its ATPase cycle to translocate via a catch and release mechanism', *Cell Reports*, 38(6), p. 110346. doi: 10.1016/j.celrep.2022.110346.

Kuhn, P. *et al.* (2011) 'The Bacterial SRP Receptor, SecA and the Ribosome Use Overlapping Binding Sites on the SecY Translocon', *Traffic*, 12(5), pp. 563–578. doi: 10.1111/j.1600-0854.2011.01167.x.

Kusters, I. and Driessen, A. J. M. (2011) 'SecA, a remarkable nanomachine', *Cellular and Molecular Life Sciences*, 68(12), pp. 2053–2066. doi: 10.1007/s00018-011-0681-y.

Kuwajima, K. (1989) 'The molten globule state as a clue for understanding the folding and cooperativity of globular-protein structure', *Proteins: Structure, Function, and Genetics*, 6(2), pp. 87–103. doi: 10.1002/prot.340060202.

Lapidus, L. J. *et al.* (2007) 'Protein Hydrophobic Collapse and Early Folding Steps Observed in a Microfluidic Mixer', *Biophysical Journal*, 93(1), pp. 218–224. doi: 10.1529/biophysj.106.103077.

Lee, V. T. and Schneewind, O. (2001) 'Protein secretion and the pathogenesis of bacterial infections', *Genes & Development*, 15(14), pp. 1725–1752. doi: 10.1101/gad.896801.

Levinthal, C. (1969) 'How to fold graciously', *Mössbauer Spectroscopy in Biological Systems Proceedings*, 24(41), pp. 22–24. Available at: http://www.cc.gatech.edu/~turk/bio_sim/articles/proteins_levinthal_1969.pdf.

Liao, C. *et al.* (2022) 'Virulence Factors of Pseudomonas Aeruginosa and Antivirulence Strategies to Combat Its Drug Resistance', *Frontiers in Cellular and Infection Microbiology*, 12(926758). doi: 10.3389/fcimb.2022.926758.

Liebeton, K., Zacharias, A. and Jaeger, K. E. (2001) 'Disulfide bond in Pseudomonas aeraginosa lipase stabilizes the structure but is not required for interaction with its foldase', *Journal of Bacteriology*, 183(2), pp. 597–603. doi: 10.1128/JB.183.2.597-603.2001.

Linde, D. *et al.* (2003) 'Interaction of the Bacillus subtilis chaperone CsaA with the secretory protein YvaY', *FEMS Microbiology Letters*, 226(1), pp. 93–100. doi: 10.1016/S0378-1097(03)00578-0.

Lindič, N. *et al.* (2020) 'The structure of clostridioides difficile seca2 atpase exposes regions responsible for differential target recognition of the seca1 and seca2-dependent systems', *International Journal of Molecular Sciences*, 21(17)(6153). doi: 10.3390/ijms21176153.

Liu, W. *et al.* (2018) 'PmrA/PmrB two-component system regulation of lipA expression in Pseudomonas aeruginosa PAO1', *Frontiers in Microbiology*, 8(2690). doi: 10.3389/fmicb.2017.02690.

Liu, Y. *et al.* (2004) 'Periplasmic proteins of Escherichia coli are highly resistant to aggregation: reappraisal for roles of molecular chaperones in periplasm', *Biochemical and Biophysical Research Communications*, 316(3), pp. 795–801. doi: 10.1016/j.bbrc.2004.02.125.

Lycklama a Nijeholt, J. A. and Driessen, A. J. M. (2012) 'The bacterial Sec-translocase: structure and mechanism', *Philosophical Transactions of the Royal Society B: Biological Sciences*, 367(1592), pp.

1016–1028. doi: 10.1098/rstb.2011.0201.

Lycklama a Nijeholt, J. A., Wu, Z. C. and Driessen, A. J. M. (2011) 'Conformational Dynamics of the Plug Domain of the SecYEG Protein-conducting Channel', *Journal of Biological Chemistry*, 286(51), pp. 43881–43890. doi: 10.1074/jbc.M111.297507.

Ma, C. *et al.* (2019) 'Structure of the substrate-engaged SecA-SecY protein translocation machine', *Nature Communications*, 10(2872). doi: 10.1038/s41467-019-10918-2.

Maier, T. *et al.* (2005) 'A cradle for new proteins: Trigger factor at the ribosome', *Current Opinion in Structural Biology*, 15(2), pp. 204–212. doi: 10.1016/j.sbi.2005.03.005.

Manalastas-Cantos, K. *et al.* (2021) 'ATSAS 3.0: Expanded functionality and new tools for small-angle scattering data analysis', *Journal of Applied Crystallography*, 54, pp. 343–355. doi: 10.1107/S1600576720013412.

Martinez, A., Ostrovsky, P. and Nunn, D. N. (1999) 'LipC, a second lipase of Pseudomonas aeruginosa, is LipB and Xcp dependent and is transcriptionally regulated by pilus biogenesis components', *Molecular Microbiology*, 34(2), pp. 317–326. doi: 10.1046/j.1365-2958.1999.01601.x.

McKenney, D., Brown, K. E. and Allison, D. G. (1995) 'Influence of Pseudomonas aeruginosa exoproducts on virulence factor production in Burkholderia cepacia: evidence of interspecies communication', *Journal of Bacteriology*, 177(23), pp. 6989–6992. doi: 10.1128/jb.177.23.6989-6992.1995.

Miroux, B. and Walker, J. E. (1996) 'Over-production of Proteins inEscherichia coli: Mutant Hosts that Allow Synthesis of some Membrane Proteins and Globular Proteins at High Levels', *Journal of Molecular Biology*, 260(3), pp. 289–298. doi: 10.1006/jmbi.1996.0399.

Missiakas, D. and Raina, S. (1997) 'Protein folding in the bacterial periplasm', *Journal of Bacteriology*, 179(8), pp. 2465–2471. doi: 10.1128/jb.179.8.2465-2471.1997.

Mitra, R. *et al.* (2021) 'Mechanism of the small ATP-independent chaperone Spy is substrate specific', *Nature Communications*, 12(851). doi: 10.1038/s41467-021-21120-8.

Miyazaki, R. *et al.* (2022) 'Inner membrane YfgM–PpiD heterodimer acts as a functional unit that associates with the SecY/E/G translocon and promotes protein translocation', *Journal of Biological Chemistry*, 298(11)(102572). doi: 10.1016/j.jbc.2022.102572.

Mogk, A., Huber, D. and Bukau, B. (2011) 'Integrating protein homeostasis strategies in prokaryotes', *Cold Spring Harbor Perspectives in Biology*, 3(4)(a004366). doi: 10.1101/cshperspect.a004366.

Moradali, M. F., Ghods, S. and Rehm, B. H. A. (2017) 'Pseudomonas aeruginosa Lifestyle: A Paradigm for Adaptation, Survival, and Persistence', *Frontiers in Cellular and Infection Microbiology*, 7(39). doi: 10.3389/fcimb.2017.00039.

Mori, H. and Ito, K. (2006) 'Different modes of SecY–SecA interactions revealed by site-directed in vivo photo-cross-linking', *Proceedings of the National Academy of Sciences*, 103(44), pp. 16159–16164. doi: 10.1073/pnas.0606390103.

Morrison, L. and Zembower, T. R. (2020) 'Antimicrobial Resistance', *Gastrointestinal Endoscopy Clinics of North America*, 30(4), pp. 619–635. doi: 10.1016/j.giec.2020.06.004.

Müller, J. P. *et al.* (2000) 'Interaction of Bacillus subtilis CsaA with SecA and precursor proteins', *Biochemical Journal*, 348(2), p. 367. doi: 10.1042/0264-6021:3480367.

Nagradova, N. (2007) 'Enzymes Catalyzing Protein Folding and Their Cellular Functions', *Current Protein & Peptide Science*, 8(3), pp. 273–282. doi: 10.2174/138920307780831866.

Nardini, M. *et al.* (2000) 'Crystal Structure of Pseudomonas aeruginosa Lipase in the Open

Conformation', *Journal of Biological Chemistry*, 275(40), pp. 31219–31225. doi: 10.1074/jbc.M003903200.

Nishiyama, M. *et al.* (2005) 'Structural basis of chaperone–subunit complex recognition by the type 1 pilus assembly platform FimD', *The EMBO Journal*, 24(12), pp. 2075–2086. doi: 10.1038/sj.emboj.7600693.

Oliver, D. B. *et al.* (1990) 'Azide-resistant mutants of Escherichia coli alter the SecA protein, an azide-sensitive component of the protein export machinery.', *Proceedings of the National Academy of Sciences*, 87(21), pp. 8227–8231. doi: 10.1073/pnas.87.21.8227.

Oliver, D. B. and Beckwith, J. (1981) 'E. coli mutant pleiotropically defective in the export of secreted proteins', *Cell*, 25(3), pp. 765–772. doi: 10.1016/0092-8674(81)90184-7.

Ollis, D. L. *et al.* (1992) 'The α / β hydrolase fold', *'Protein Engineering, Design and Selection'*, 5(3), pp. 197–211. doi: 10.1093/protein/5.3.197.

Oswald, J. *et al.* (2021) 'The Dynamic SecYEG Translocon', *Frontiers in Molecular Biosciences*, 8(664241). doi: 10.3389/fmolb.2021.664241.

Owji, H. *et al.* (2018) 'A comprehensive review of signal peptides: Structure, roles, and applications', *European Journal of Cell Biology*, 97(6), pp. 422–441. doi: 10.1016/j.ejcb.2018.06.003.

Palmer, T. and Berks, B. C. (2012) 'The twin-arginine translocation (Tat) protein export pathway', *Nature Reviews Microbiology*, 10(7), pp. 483–496. doi: 10.1038/nrmicro2814.

Panjkovich, A. and Svergun, D. I. (2018) 'CHROMIXS: automatic and interactive analysis of chromatography-coupled small-angle X-ray scattering data', *Bioinformatics*. Edited by A. Valencia, 34(11), pp. 1944–1946. doi: 10.1093/bioinformatics/btx846.

Papadopoulos, A. *et al.* (2022) 'The periplasmic chaperone Skp prevents misfolding of the secretory lipase A from Pseudomonas aeruginosa', *Frontiers in Molecular Biosciences*, 9(1026724). doi: 10.3389/fmolb.2022.1026724.

Papanikolau, Y. *et al.* (2007) 'Structure of Dimeric SecA, the Escherichia coli Preprotein Translocase Motor', *Journal of Molecular Biology*, 366(5), pp. 1545–1557. doi: 10.1016/j.jmb.2006.12.049.

Papanikou, E., Karamanou, S. and Economou, A. (2007) 'Bacterial protein secretion through the translocase nanomachine', *Nature Reviews Microbiology*, 5(11), pp. 839–851. doi: 10.1038/nrmicro1771.

Park, E. and Rapoport, T. A. (2011) 'Preserving the membrane barrier for small molecules during bacterial protein translocation', *Nature*, 473(7346), pp. 239–242. doi: 10.1038/nature10014.

Pauwels, K. *et al.* (2006) 'Structure of a membrane-based steric chaperone in complex with its lipase substrate', *Nature Structural and Molecular Biology*, 13(4), pp. 374–375. doi: 10.1038/nsmb1065.

Pauwels, K. *et al.* (2007) 'Chaperoning Anfinsen: The steric foldases', *Molecular Microbiology*, 64(4), pp. 917–922. doi: 10.1111/j.1365-2958.2007.05718.x.

Pendleton, J. N., Gorman, S. P. and Gilmore, B. F. (2013) 'Clinical relevance of the ESKAPE pathogens', *Expert Review of Anti-infective Therapy*, 11(3), pp. 297–308. doi: 10.1586/eri.13.12.

Pernot, P. *et al.* (2010) 'New beamline dedicated to solution scattering from biological macromolecules at the ESRF', *Journal of Physics: Conference Series*, 247. doi: 10.1088/1742-6596/247/1/012009.

Pernot, P. *et al.* (2013) 'Upgraded ESRF BM29 beamline for SAXS on macromolecules in solution', *Journal of Synchrotron Radiation*, 20(4), pp. 660–664. doi: 10.1107/S0909049513010431.

Petersen, T. N. *et al.* (2011) 'SignalP 4.0: discriminating signal peptides from transmembrane regions',

Nature Methods, 8(10), pp. 785–786. doi: 10.1038/nmeth.1701.

Petoukhov, M. V. *et al.* (2012) 'New developments in the ATSAS program package for small-angle scattering data analysis', *Journal of Applied Crystallography*, 45(2), pp. 342–350. doi: 10.1107/S0021889812007662.

Petoukhov, M. V. and Svergun, D. I. (2005) 'Global rigid body modeling of macromolecular complexes against small-angle scattering data', *Biophysical Journal*, 89(2), pp. 1237–1250. doi: 10.1529/biophysj.105.064154.

Petriman, N.-A. *et al.* (2018) 'The interaction network of the YidC insertase with the SecYEG translocon, SRP and the SRP receptor FtsY', *Scientific Reports*, 8(1)(578). doi: 10.1038/s41598-017-19019-w.

Du Plessis, D. J. F., Nouwen, N. and Driessen, A. J. M. (2011) 'The Sec translocase', *Biochimica et Biophysica Acta - Biomembranes*, 1808(3), pp. 851–865. doi: 10.1016/j.bbamem.2010.08.016.

Plotkin, S. S. and Onuchic, J. N. (2002) 'Understanding protein folding with energy landscape theory Part I: Basic concepts', *Quarterly Reviews of Biophysics*, 35(2), pp. 111–167. doi: 10.1017/S0033583502003761.

Potvin, E. *et al.* (2003) 'In vivo functional genomics of Pseudomonas aeruginosa for high-throughput screening of new virulence factors and antibacterial targets', *Environmental Microbiology*, 5(12), pp. 1294–1308. doi: 10.1046/j.1462-2920.2003.00542.x.

Power, P. M. *et al.* (2004) 'Whole genome analysis reveals a high incidence of non-optimal codons in secretory signal sequences of Escherichia coli', *Biochemical and Biophysical Research Communications*, 322(3), pp. 1038–1044. doi: 10.1016/j.bbrc.2004.08.022.

Pugsley, A. P. (1993) 'The complete general secretory pathway in gram-negative bacteria', *Microbiological Reviews*, 57(1), pp. 50–108. doi: 10.1128/mr.57.1.50-108.1993.

Pugsley, A. P. and Schwartz, M. (1985) 'Export and secretion of proteins by bacteria', *FEMS Microbiology Letters*, 32(1), pp. 3–38. doi: 10.1016/0378-1097(85)90024-2.

Qin, S. *et al.* (2022) 'Pseudomonas aeruginosa: pathogenesis, virulence factors, antibiotic resistance, interaction with host, technology advances and emerging therapeutics', *Signal Transduction and Targeted Therapy*, 7(1)(199). doi: 10.1038/s41392-022-01056-1.

Randall, L. L. and Henzl, M. T. (2010) 'Direct identification of the site of binding on the chaperone SecB for the amino terminus of the translocon motor SecA', *Protein Science*, 19(6), pp. 1173–1179. doi: 10.1002/pro.392.

Rashno, F. *et al.* (2018) 'Insight into the aggregation of lipase from Pseudomonas sp. using mutagenesis: Protection of aggregation prone region by adoption of α-helix structure', *Protein Engineering, Design and Selection*, 31(11), pp. 419–426. doi: 10.1093/protein/gzz003.

Reading, E. *et al.* (2015) 'The Effect of Detergent, Temperature, and Lipid on the Oligomeric State of MscL Constructs: Insights from Mass Spectrometry', *Chemistry & Biology*, 22(5), pp. 593–603. doi: 10.1016/j.chembiol.2015.04.016.

Reimmann, C. *et al.* (1997) 'The global activator GacA of Pseudomonas aeruginosa PAO positively controls the production of the autoinducer N -butyryl-homoserine lactone and the formation of the virulence factors pyocyanin, cyanide, and lipase', *Molecular Microbiology*, 24(2), pp. 309–319. doi: 10.1046/j.1365-2958.1997.3291701.x.

Ribeiro, B. D. *et al.* (2011) 'Production and Use of Lipases in Bioenergy: A Review from the Feedstocks to Biodiesel Production', *Enzyme Research*, 2011(1), pp. 1–16. doi: 10.4061/2011/615803.

Rice, L. B. (2008) 'Federal funding for the study of antimicrobial resistance in nosocomial pathogens:

No ESKAPE', *Journal of Infectious Diseases*, 197(8), pp. 1079–1081. doi: 10.1086/533452.

Rios, N. S. *et al.* (2018) 'Biotechnological potential of lipases from Pseudomonas: Sources, properties and applications', *Process Biochemistry*, 75(July), pp. 99–120. doi: 10.1016/j.procbio.2018.09.003.

Rocha, A. J. *et al.* (2019) 'Pseudomonas Aeruginosa: Virulence Factors and Antibiotic Resistance Genes', *Brazilian Archives of Biology and Technology*, 62, pp. 1–15. doi: 10.1590/1678-4324-2019180503.

Rosenau, F. and Jaeger, K. E. (2000) 'Bacterial lipases from Pseudomonas: Regulation of gene expression and mechanisms of secretion', *Biochimie*, 82(11), pp. 1023–1032. doi: 10.1016/S0300-9084(00)01182-2.

Rosenau, F., Tommassen, J. and Jaeger, K.-E. (2004) 'Lipase-Specific Foldases', *ChemBioChem*, 5(2), pp. 152–161. doi: 10.1002/cbic.200300761.

Rusch, S. L. and Kendall, D. A. (2007) 'Interactions That Drive Sec-Dependent Bacterial Protein Transport', *Biochemistry*, 46(34), pp. 9665–9673. doi: 10.1021/bi7010064.

Sachelaru, I. *et al.* (2014) 'Dynamic Interaction of the Sec Translocon with the Chaperone PpiD', *Journal of Biological Chemistry*, 289(31), pp. 21706–21715. doi: 10.1074/jbc.M114.577916.

Sadikot, R. T. *et al.* (2005) 'Pathogen–Host Interactions in Pseudomonas aeruginosa Pneumonia', *American Journal of Respiratory and Critical Care Medicine*, 171(11), pp. 1209–1223. doi: 10.1164/rccm.200408-1044SO.

Saibil, H. (2013) 'Chaperone machines for protein folding, unfolding and disaggregation', *Nature Reviews Molecular Cell Biology*, 14(10), pp. 630–642. doi: 10.1038/nrm3658.

Salvi, G., De Los Rios, P. and Vendruscolo, M. (2005) 'Effective interactions between chaotropic agents and proteins', *Proteins: Structure, Function, and Bioinformatics*, 61(3), pp. 492–499. doi: 10.1002/prot.20626.

Sandkvist, M. (2001) 'Biology of type II secretion', *Molecular Microbiology*, 40(2), pp. 271–283. doi: 10.1046/j.1365-2958.2001.02403.x.

Sardis, M. F. *et al.* (2017) 'Preprotein Conformational Dynamics Drive Bivalent Translocase Docking and Secretion', *Structure*, 25(7), pp. 1056-1067.e6. doi: 10.1016/j.str.2017.05.012.

Sardis, M. F. and Economou, A. (2010) 'SecA: a tale of two protomers', *Molecular Microbiology*, 76(5), pp. 1070–1081. doi: 10.1111/j.1365-2958.2010.07176.x.

Schiffrin, B. *et al.* (2022) 'Dynamic interplay between the periplasmic chaperone SurA and the BAM complex in outer membrane protein folding', *Communications Biology*, 5(1)(560). doi: 10.1038/s42003-022-03502-w.

Schneewind, O. and Missiakas, D. (2014) 'Sec-secretion and sortase-mediated anchoring of proteins in Gram-positive bacteria', *Biochimica et Biophysica Acta (BBA) - Molecular Cell Research*, 1843(8), pp. 1687–1697. doi: 10.1016/j.bbamcr.2013.11.009.

Sharma, A., Kumari, S. and Goel, M. (2021) 'Uncovering the structure-function aspects of an archaeal CsaA protein', *Biochimica et Biophysica Acta - Proteins and Proteomics*, 1869(5)(140615). doi: 10.1016/j.bbapap.2021.140615.

Sharma, A., Rani, S. and Goel, M. (2018) 'Navigating the structure–function–evolutionary relationship of CsaA chaperone in archaea', *Critical Reviews in Microbiology*, 44(3), pp. 274–289. doi: 10.1080/1040841X.2017.1357535.

Sharma, V. *et al.* (2003) 'Crystal structure of Mycobacterium tuberculosis SecA, a preprotein translocating ATPase', *Proceedings of the National Academy of Sciences*, 100(5), pp. 2243–2248. doi: 10.1073/pnas.0538077100.

Shibata, H., Kato, H. and Oda, J. (1998a) 'Calcium Ion-Dependent Reactivation of a Pseudomonas Lipase by Its Specific Modulating Protein, LipB', *Journal of Biochemistry*, 123(1), pp. 136–141. doi: 10.1093/oxfordjournals.jbchem.a021900.

Shibata, H., Kato, H. and Oda, J. (1998b) 'Molecular Properties and Activity of Amino-Terminal Truncated Forms of Lipase Activator Protein', *Bioscience, Biotechnology, and Biochemistry*, 62(2), pp. 354–357. doi: 10.1271/bbb.62.354.

Shibata, H., Kato, H. and Oda, J. (1998c) 'Random mutagenesis on the Pseudomonas lipase activator protein, LipB: exploring amino acid residues required for its function', *Protein Engineering Design and Selection*, 11(6), pp. 467–472. doi: 10.1093/protein/11.6.467.

Shingler, V. (1996) 'Signal sensing by σ 54 -dependent regulators: derepression as a control mechanism', *Molecular Microbiology*, 19(3), pp. 409–416. doi: 10.1046/j.1365-2958.1996.388920.x.

Singh, A. *et al.* (2015) 'Protein recovery from inclusion bodies of Escherichia coli using mild solubilization process', *Microbial Cell Factories*, 14(1), p. 41. doi: 10.1186/s12934-015-0222-8.

Smets, D. *et al.* (2022) 'Signal Peptide-rheostat Dynamics Delay Secretory Preprotein Folding', *Journal of Molecular Biology*, 434(19)(167790). doi: 10.1016/j.jmb.2022.167790.

Smith, W. D. *et al.* (2017) 'Current and future therapies for Pseudomonas aeruginosa infection in patients with cystic fibrosis', *FEMS Microbiology Letters*, 364(14). doi: 10.1093/femsle/fnx121.

Sneath, P. H. A., McGowan, V. and Skerman, V. B. D. (1980) 'Approved Lists of Bacterial Names', *International Journal of Systematic and Evolutionary Microbiology*, 30(1), pp. 225–420. doi: 10.1099/00207713-30-1-225.

Sockolosky, J. T. and Szoka, F. C. (2013) 'Periplasmic production via the pET expression system of soluble, bioactive human growth hormone', *Protein Expression and Purification*, 87(2), pp. 129–135. doi: 10.1016/j.pep.2012.11.002.

Sohl, J. L., Jaswal, S. S. and Agard, D. A. (1998) 'Unfolded conformations of α-lytic protease are more stable than its native state', *Nature*, 395(6704), pp. 817–819. doi: 10.1038/27470.

Stathopoulos, C. *et al.* (2000) 'Secretion of virulence determinants by the general secretory pathway in Gram-negative pathogens: an evolving story', *Microbes and Infection*, 2(9), pp. 1061–1072. doi: 10.1016/S1286-4579(00)01260-0.

Stehr, F. *et al.* (2003) 'Microbial lipases as virulence factors', *Journal of Molecular Catalysis B: Enzymatic*, 22(5–6), pp. 347–355. doi: 10.1016/S1381-1177(03)00049-3.

Steinberg, R. *et al.* (2018) 'Co-translational protein targeting in bacteria', *FEMS Microbiology Letters*, 365(11). doi: 10.1093/femsle/fny095.

Steinberg, R. *et al.* (2020) 'Posttranslational insertion of small membrane proteins by the bacterial signal recognition particle', *PLOS Biology*, 18(9)(e3000874). doi: 10.1371/journal.pbio.3000874.

Stetsenko, A. and Guskov, A. (2017) 'An Overview of the Top Ten Detergents Used for Membrane Protein Crystallization', *Crystals*, 7(7). doi: 10.3390/cryst7070197.

Stover, C. K. *et al.* (2000) 'Complete genome sequence of Pseudomonas aeruginosa PAO1, an opportunistic pathogen', *Nature*, 406(6799), pp. 959–964. doi: 10.1038/35023079.

Strateva, T. and Mitov, I. (2011) 'Contribution of an arsenal of virulence factors to pathogenesis of Pseudomonas aeruginosa infections', *Annals of Microbiology*, 61(4), pp. 717–732. doi: 10.1007/s13213-011-0273-y.

Studier, F. W. and Moffatt, B. A. (1986) 'Use of bacteriophage T7 RNA polymerase to direct selective high-level expression of cloned genes', *Journal of Molecular Biology*, 189(1), pp. 113–130. doi:

10.1016/0022-2836(86)90385-2.

Stull, F., Betton, J.-M. and Bardwell, J. C. A. (2018) 'Periplasmic Chaperones and Prolyl Isomerases', *EcoSal Plus*. Edited by J. M. Slauch and M. Ehrmann, 8(1). doi: 10.1128/ecosalplus.ESP-0005-2018.

Svergun, D. I. (1992) 'Determination of the regularization parameter in indirect-transform methods using perceptual criteria', *Journal of Applied Crystallography*, 25(4), pp. 495–503. doi: 10.1107/S0021889892001663.

Svergun, D. I., Petoukhov, M. V. and Koch, M. H. J. (2001) 'Determination of Domain Structure of Proteins from X-Ray Solution Scattering', *Biophysical Journal*, 80(6), pp. 2946–2953. doi: 10.1016/S0006-3495(01)76260-1.

Swift, S. *et al.* (2001) *Quorum sensing as a population-density-dependent determinant of bacterial physiology*, *Advances in Microbial Physiology*. doi: 10.1016/S0065-2911(01)45005-3.

Tacconelli, E. *et al.* (2018) 'Discovery, research, and development of new antibiotics: the WHO priority list of antibiotic-resistant bacteria and tuberculosis', *The Lancet Infectious Diseases*, 18(3), pp. 318–327. doi: 10.1016/S1473-3099(17)30753-3.

Tanaka, Y. *et al.* (2015) 'Crystal Structures of SecYEG in Lipidic Cubic Phase Elucidate a Precise Resting and a Peptide-Bound State', *Cell Reports*, 13(8), pp. 1561–1568. doi: 10.1016/j.celrep.2015.10.025.

Thomassin, J. L. *et al.* (2017) 'The trans-envelope architecture and function of the type 2 secretion system: new insights raising new questions', *Molecular Microbiology*, 105(2), pp. 211–226. doi: 10.1111/mmi.13704.

Tielen, P. *et al.* (2013) 'Interaction between extracellular lipase LipA and the polysaccharide alginate of Pseudomonas aeruginosa', *BMC Microbiology*, 13(1). doi: 10.1186/1471-2180-13-159.

Tommassen, J. *et al.* (1992) 'Protein secretion in Pseudomonas aeruginosa.', *FEMS microbiology reviews*, 9(1), pp. 73–90. doi: 10.1016/0378-1097(92)90336-m.

Tsirigotaki, A. *et al.* (2017) 'Protein export through the bacterial Sec pathway', *Nature Reviews Microbiology*, 15(1), pp. 21–36. doi: 10.1038/nrmicro.2016.161.

Tsirigotaki, A. *et al.* (2018) 'Long-Lived Folding Intermediates Predominate the Targeting-Competent Secretome', *Structure*, 26(5), pp. 695-707.e5. doi: 10.1016/j.str.2018.03.006.

Tsukazaki, T. (2018) 'Structure-based working model of SecDF, a proton-driven bacterial protein translocation factor', *FEMS Microbiology Letters*, 365(12)(fny112). doi: 10.1093/femsle/fny112.

Tsukazaki, T. and Nureki, O. (2011) 'The mechanism of protein export enhancement by the SecDF membrane component', *Biophysics*, 7, pp. 129–133. doi: 10.2142/biophysics.7.129.

Tuon, F. F. *et al.* (2022) 'Pathogenesis of the Pseudomonas aeruginosa Biofilm: A Review', *Pathogens*, 11(3)(300). doi: 10.3390/pathogens11030300.

Urusova, D. V. *et al.* (2019) 'The structure of Acinetobacter-secreted protease CpaA complexed with its chaperone CpaB reveals a novel mode of a T2SS chaperone–substrate interaction', *Journal of Biological Chemistry*, 294(36), pp. 13344–13354. doi: 10.1074/jbc.RA119.009805.

Valentini, M. *et al.* (2018) 'Lifestyle transitions and adaptive pathogenesis of Pseudomonas aeruginosa', *Current Opinion in Microbiology*, 41, pp. 15–20. doi: 10.1016/j.mib.2017.11.006.

Veenendaal, A. K. J., Van Der Does, C. and Driessen, A. J. M. (2004) 'The protein-conducting channel SecYEG', *Biochimica et Biophysica Acta - Molecular Cell Research*, 1694(1-3 SPEC.ISS.), pp. 81–95. doi: 10.1016/j.bbamcr.2004.02.009.

Verma, N. *et al.* (2020) 'The Membrane-Integrated Steric Chaperone Lif Facilitates Active Site Opening

of Pseudomonas aeruginosa Lipase A', *Journal of Computational Chemistry*, 41(6), pp. 500–512. doi: 10.1002/jcc.26085.

Vetsch, M. *et al.* (2004) 'Pilus chaperones represent a new type of protein-folding catalyst', *Nature*, 431(7006), pp. 329–333. doi: 10.1038/nature02891.

Viegas, A. *et al.* (2020) 'Structural and dynamic insights revealing how lipase binding domain MD1 of Pseudomonas aeruginosa foldase affects lipase activation', *Scientific Reports*, 10(3578). doi: 10.1038/s41598-020-60093-4.

Voth, W. and Jakob, U. (2017) 'Stress-Activated Chaperones: A First Line of Defense', *Trends in Biochemical Sciences*, 42(11), pp. 899–913. doi: 10.1016/j.tibs.2017.08.006.

Vrontou, E. and Economou, A. (2004) 'Structure and function of SecA, the preprotein translocase nanomotor', *Biochimica et Biophysica Acta - Molecular Cell Research*, 1694(1–3), pp. 67–80. doi: 10.1016/j.bbamcr.2004.06.003.

Walton, T. A. and Sousa, M. C. (2004) 'Crystal structure of Skp, a prefoldin-like chaperone that protects soluble and membrane proteins from aggregation', *Molecular Cell*, 15(3), pp. 367–374. doi: 10.1016/j.molcel.2004.07.023.

Waterhouse, A. M. *et al.* (2009) 'Jalview Version 2—a multiple sequence alignment editor and analysis workbench', *Bioinformatics*, 25(9), pp. 1189–1191. doi: 10.1093/bioinformatics/btp033.

Weininger, U. *et al.* (2010) 'The prolyl isomerase domain of PpiD from Escherichia coli shows a parvulin fold but is devoid of catalytic activity', *Protein Science*, 19(1), pp. 6–18. doi: 10.1002/pro.277.

Wild, J. *et al.* (1992) 'DnaK and DnaJ heat shock proteins participate in protein export in Escherichia coli.', *Genes & Development*, 6(7), pp. 1165–1172. doi: 10.1101/gad.6.7.1165.

Winsor, G. L. *et al.* (2016) 'Enhanced annotations and features for comparing thousands of Pseudomonas genomes in the Pseudomonas genome database', *Nucleic Acids Research*, 44(D1), pp. D646–D653. doi: 10.1093/nar/gkv1227.

Wohlfarth, S. and Winkler, U. K. (1988) 'Chromosomal mapping and cloning of the lipase gene of Pseudomonas aeruginosa.', *Journal of general microbiology*, 134(2), pp. 433–40. doi: 10.1099/00221287-134-2-433.

Van Der Wolk, J. P. W. *et al.* (1998) 'PrlA4 prevents the rejection of signal sequence defective preproteins by stabilizing the SecA-SecY interaction during the initiation of translocation', *EMBO Journal*, 17(13), pp. 3631–3639. doi: 10.1093/emboj/17.13.3631.

Xu, C. *et al.* (2022) 'A Review of Current Bacterial Resistance to Antibiotics in Food Animals', *Frontiers in Microbiology*, 13(822689). doi: 10.3389/fmicb.2022.822689.

Xu, Z., Knafels, J. D. and Yoshino, K. (2000) 'Crystal structure of the bacterial protein export chaperone SecB', *Nature Structural Biology*, 7(12), pp. 1172–1177. doi: 10.1038/82040.

Yuan, J. *et al.* (2010) 'Protein transport across and into cell membranes in bacteria and archaea', *Cellular and Molecular Life Sciences*, 67(2), pp. 179–199. doi: 10.1007/s00018-009-0160-x.

Zalucki, Y. M., Beacham, I. R. and Jennings, M. P. (2009) 'Biased codon usage in signal peptides: a role in protein export', *Trends in Microbiology*, 17(4), pp. 146–150. doi: 10.1016/j.tim.2009.01.005.

Zeytuni, N. and Zarivach, R. (2012) 'Structural and Functional Discussion of the Tetra-Trico-Peptide Repeat, a Protein Interaction Module', *Structure*, 20(3), pp. 397–405. doi: 10.1016/j.str.2012.01.006.

Zimmer, J., Nam, Y. and Rapoport, T. A. (2008) 'Structure of a complex of the ATPase SecA and the protein-translocation channel', *Nature*, 455(7215), pp. 936–943. doi: 10.1038/nature07335.

Zimmer, J. and Rapoport, T. A. (2009) 'Conformational Flexibility and Peptide Interaction of the Translocation ATPase SecA', *Journal of Molecular Biology*, 394(4), pp. 606–612. doi: 10.1016/j.jmb.2009.10.024.

8 Appendix

8.1 List of Abbreviations

Abbreviation	Definition
A	
Å	Angstrom
A	Absorbance
ATP	Adenosine triphosphate
ADP	Adenosine diphosphate
B	
BAM	β-barrel assembly machinery
Bp	Base pair
B. glumae	*Burkholderia glumae*
C	
$CaCl_2$	Calcium chloride
CDS	Coding sequence
CL	Cardiolipin
CMC	Critical micellar concentration
Cryo-EM	Cryo electron microscopy
CV	Column volume
Cy6	Cymal-6
C4-HSL	*N*-butyryl-L-homoserine lactone
D	
DDM	n-Dodecyl-β-D-maltopyranoside
DIBMA	diisobutylene-maleic acid
DM	n-Decyl-β-D-maltopyranoside
DMSO	Dimethyl sulfoxide
DNA	Deoxyribonucleic acid
DTT	1,4-dithiothreitol
DOPC	1,2-dioleoyl-sn-glycero-3-phosphocholine
DOPE	1,2-dioleoyl-sn-glycero-3-phosphoethanolamine

DOPG	1,2-dioleoyl-sn-glycero-3-phospho-(1'-rac-glycerol)

E

E. coli	*Escherichia coli*
EDTA	Ethylenediaminetetraacetic acid
e. g	*"exempli gratia" – for example*
EHD	Extended helical domain
EK	Bovine enterokinase light chain
EM	Electron microscopy

F

Fc14	Fos-Choline-14

G

g	g-force, gravitational force equivalent: ~9.8 m/s^2
g	gram, unit of mass
GSP	"General Secretory pathway"
gDNA	Genomic DNA
GdnHCl	Guanidine hydrochloride

H

Hepes	4-(2-hydroxyethyl)-1-piperazineethanesulfonic acid

I

IM	Inner membrane
IMAC	Immobilized metal ion affinity chromatography
IMVs	Inner membrane vesicles
IPTG	Isopropyl β-D-1-thiogalactopyranoside

K

KCl	Potassium chloride
K_D	Dissociation constant
kDa	kilo Dalton (= 1000 Dalton), Dalton (Da or u) is unified atomic mass unit, 1 Da = ~1.66×10^{-27} kg
KOH	Potassium hydroxide

L

LB	Lysogeny broth
Ligase	T4 DNA Ligase
LMNG	Lauryl Maltose Neopentyl Glycol
LPS	Lipopolysaccharides

M

MALS	Multi angle light scattering
Mbp	Million base pairs
MCS	Multiple cloning site
MD	Mini domain
µg	microgram
mg	milligram
$MgCl_2$	Magnesium chloride
$Mg(OAc)_2$	Magnesium acetate
min	min
µl	microliter
ml	milliliter
µM	micromolar
mM	millimolar
µm	micrometer
MQ	“Milli-Q”, deionized water

N

n.d.	Not determined
NaCl	Sodium chloride
NaOH	Sodium hydroxide
Ni^{2+}-NTA resin	nickel-nitrilotriacetic acid agarose resin
nm	nanometer

O

OD	Optical density
OG	n-Octyl-β-D-glucopyranoside
OM	Outer membrane
OMP	Outer membrane protein

P

P. aeruginosa	*Pseudomonas aeruginosa*
PAGE	Polyacrylamide gel electrophoresis
PelB	Periplasmic pectate lyase
PG	Phosphatidyl-glycerol
PMF	Proton motive force
PMSF	Phenylmethylsulfonyl fluoride
PNK	T4 Polynucleotide kinase
PP	Periplasm
PCR	Polymerase chain reaction
PDB	Protein database
Phyre	Protein homology/analogy recognition engine
PPIase	Peptidyl-prolyl isomerase
PQS	2-heptyl-3-hydroxy-4-quinolone
p-NPB	p-Nitrophenyl butyrate

R

RNC	Ribosome nascent chain
RT	“Room temperature”, ambient temperature of the laboratory

S

SAXS	Small angle X-ray scattering
SB	Sample loading Buffer for SDS-PAGE
SDS	Sodium dodecyl sulfate
SEC	Size exclusion chromatography
Sec	Secretory pathway
SN	Supernatant
SP	Signal peptide
SPR	Surface plasmon resonance
SRP	Signal recognition particle

T

Tat	Twin arginine translocation pathway
TBS	Tris buffered saline
TBS-T	Tris buffered saline with Tween 20

TCEP	Tris-(2-carboxymethyl)-phosphine
TEV Protease	Tobacco etch virus protease
TF	Trigger factor
Tris	Tris (hydroxymethyl)aminoethane
TOCL	Tetraoleoyl cardiolipin, 18:1 Cardiolipin, 1',3'-bis[1,2-dioleoyl-sn-glycero-3-phospho]-glycerol
T1SS	Type I secretion system
T2SS	Type II secretion system
T3SS	Type III secretion system
T4SS	Type IV secretion system
T5SS	Type V secretion system
T6SS	Type VI secretion system
T7SS	Type VII secretion system
T8SS	Type VIII secretion system
SecYEG	Translocon

U

Unified atomic mass unit	u (or Da), 1 u = ~1.66×10^{-24} g

V

VD	Variable domain

W

w/v	weight per volume

#

2HF	Two helix finger
3C Protease	Human Rhinovirus Typ14 Protease (HRV-3C)
3-oxo-C12-HSL	*N*-3-oxo-dodecanyl-L-homoserine lactone
°C	Degree Celsius, unit of temperature

Commonly known abbreviations have not been included to the list of abbreviations.

Amino Acid	Three letter code	One letter code
Alanine	Ala	A
Arginine	Arg	R
Asparagine	Asn	N
Aspartic acid	Asp	D
Cysteine	Cys	C
Glutamic acid	Glu	E
Glutamine	Gln	Q
Glycine	Gly	G
Histidine	His	H
Isoleucine	Ile	I
Leucine	Leu	L
Lysine	Lys	K
Methionine	Met	M
Phenylalanine	Phe	F
Proline	Pro	P
Serine	Ser	S
Threonine	Thr	T
Tryptophane	Trp	W
Tyrosine	Tyr	Y
Valine	Val	V

8.2 List of Publications

Peer-reviewed articles:

Papadopoulos A, Busch M, Reiners J, Hachani E, Baeumers M, Berger J, Schmitt L, Jaeger K-E, Kovacic F, Smits SHJ and Kedrov A (2022), The periplasmic chaperone Skp prevents misfolding of the secretory lipase A from Pseudomonas aeruginosa. Front. Mol. Biosci. 9:1026724. doi: 10.3389/fmolb.2022.1026724

Others:

Löwe M, Papadopoulos A, Kamel M, Kedrov A, (2019), Membranproteinfaltung — Kernwissen aus (nicht zu) vereinfachten Systemen. *Biospektrum* **25**, 385–387. doi: 10.1007/s12268-019-1066-2

8.3 List of Tables

8.4 List of Figures

8.5 List of Supervisions

Thesis:

Ronja Knöfel, 2018: Cloning and overexpression the bacterial translocon.
Bachelor Thesis, Heinrich Heine University, Duesseldorf.

Max Busch, 2019: LipA interactions with periplasmic and cytoplasmic chaperones.
Bachelor Thesis, Heinrich Heine University, Duesseldorf.

Susanna Makarski, 2020: Outer membrane protein insertion under near-native conditions.
Bachelor Thesis, Heinrich Heine University, Duesseldorf.

Sven Cygan, 2021: Biophysical analysis of outer membrane protein insertion *in vitro*.
Bachelor Thesis, Heinrich Heine University, Duesseldorf.

Pascal Convent, 2021: Studying the role of XcpP in maturation of the lipase A of *Pseudomonas aeruginosa*. Bachelor Thesis, Heinrich Heine University, Duesseldorf.

Max Busch, 2021: Investigating the protein transport via SecYEG translocon of *Pseudomonas aeruginosa*. Master thesis, Heinrich Heine University, Duesseldorf.

Internships:

Sven Cygan; 2021: Studying membrane protein insertion *in vitro*

Vanessa Valencia, 2021: Studies of the outer membrane protein OprG of *P. aeruginosa* PAO1

Zoë Vande Kieft, 2021: Enzymatic Lipase Activity in the Presence of Crowding Agents

Pascal Convent, 2021: Expression studies of XcpP from *P. aeruginosa* PAO1

Claudia Strzelczyk, 2021: Molecular works on the translocon SecYEG of *P. aeruginosa* PAO1

Additional Supervision:

iGEM 2019, Scientific Advisor of SynMylk, Gold award, Boston, MA, USA

8.6 Bacterial strains and plasmids

Table 1: List of bacterial strains

Strain	Genotype	Reference
E. coli DH5α	F⁻ Φ80*lac*ZΔM15 Δ (*lac*ZYA-argF) U169 recA1 endA1 hsdR17 (rK–, mK+) phoA supE44 λ– thi-1 gyrA96 relA1	(Hanahan, 1983)
E. coli BL21 (DE3)	*E. coli* str. B F⁻ *ompT gal dcm lon hsdS*$_B$ ($r_B^-m_B^-$) λ (DE3) [*lacI lacUV5-T7p07 ind1 sam7 nin5*]) [*malB*$^+$]$_{K\text{-}12}$ (λ^S)	(Studier and Moffatt, 1986)
Rosetta™ (DE3) pLysS	*E. coli* str. F⁻ *ompT gal dcm lon hsdS*$_B$ ($r_B^-m_B^-$) λ (DE3) [*lacI lacUV5-T7p07 ind1 sam7 nin5*]) [*malB*$^+$]$_{K\text{-}12}$ (λ^S) pLysSRARE[*T7p20 ileX argU thrU tyrU glyT thrT argW metT leuW proL ori*$_{p15A}$] (Cm^R)	Novagen
E. coli C41 (DE3)	*E. coli* str. F⁻ *ompT gal dcm hsdS*$_B$ ($r_B^-m_B^-$) λ (DE3) [*lacI lacUV5-T7p07 ind1 sam7 nin5*]) [*malB*$^+$]$_{K\text{-}12}$ (λ^S)	(Miroux and Walker, 1996)
P. aeruginosa PAO1	wild type	(Holloway, Krishnapillai and Morgan, 1979)
P. aeruginosa PA14	wild type, DSM No.: 19882	DSMZ Braunschweig
P. aeruginosa PA14 Δ*skp* (PA14_17170)	In-frame *hlpA* (*skp*)-deletion mutant of PA14	(Klein *et al.*, 2019)

Table 2: Lists of Plasmids

The following plasmids were utilized for the research purposes of the present thesis. Commercially available, obtained by reference, and de novo created constructs are listed.

Name	Genotype	Reference
pBBR1MCS3	Tc^r rep mob lacZα P_{lac} P_{T7} pBBR1 oriV	(Kovach *et al.*, 1995)
pET19b	Amp^r $lacI^q$ P_{T7} ColE1	Novagen
pET21a	Amp^r $lacI^q$ P_{T7} ColE1	Novagen
pET22b	Amp^r $lacI^q$ P_{T7} ColE1	Novagen
pET24	Amp^r $lacI^q$ P_{T7} ColE1, no RBS	Novagen
pET24a	Amp^r $lacI^q$ P_{T7} ColE1	Novagen
pET28b	Kan^r $lacI^q$ P_{T7} ColE1	Novagen
pETDuet1	Amp^r $lacI^q$ P_{T7} ColE1	Novagen
pGUF	Tc^r $lacI^q$ rep mob lacZα P_{T7} P_{lac} pBBR1 oriV Afl II His_6 $Term_{T7}$	(Babic, 2022)
pTrc99a	Amp^r $lacI^q$ P_{trc} pBR322	Pharmacia
pRSET A	Amp^r P_{T7} ColE1	Invitrogen
pRSF1b	Kan^r $lacI^q$ P_{T7} RSF1030	Novagen

pEM268	pTrc99a (Amp^r lacI^q P_{trc} pBR322), *E. coli secY, secE, secG*, encoding for His_{10}-3C upstream *secY*	A. Kedrov
pAT1	pTrc99a, N-terminal His_{10}-3C, PA4243 (*secY*), *E. coli secEG*	This work
pAT2	pTrc99a His10-PaSecYE-EcSecG	This work
pAT3	pTrc99a_His10_PaSecYEG	This work
pAT4	pTrc99a_PaSecA	This work
pAT5	pTrc99a_PaSecA-His	This work
pAT6	pRSFDuet1_PaSecB	This work
pAT7	pRSFDuet1_His8-PaSecB	This work
pAT8	pTrc99a His10_LipH-FL	This work
pAT9	pET19b pET19b_His10_LipHΔTMD (pEHTHis19)	S. Hausmann (Hausmann *et al.*, 2008)
pAT10	pBBR1 His10_LipH-FL	This work
pAT11	pTrc99a His10_LipH-FL_S48A	This work
pAT12	pTrc99a His10_LipH-FL_S48P	This work
pAT13	pET21a_T7_pLipAΔ251_His6	This work
pAT14	pET21a_T7_pLipAΔ251	This work
pAT15	pBAD_pLipAΔ251	A. Kedrov
pAT16	pTrc99a_pLipAΔ251	This work
pAT17	pTrc99a_pLipA_His6	This work
pAT18	pBBR1_pLipA_His6	This work
pAT19	pBBR1_OmpA-SS-LipAΔ251	This work
pAT20	pRSET_A_pLipA_His6	This work
pAT21	pET21a_T7_PaTIG	This work
pAT22	pET21a_PaFkpA_His6	This work
pAT23	pET21a_PaFkpA-SS_His6	This work
pAT24	pET21a_PaSkp_His6	This work
pAT25	pET21a_PaSkp-SS_His6	This work
pAT26	pET21a_PaSurA_His6	This work
pAT27	pET21a_PaSurA-SS_His6	This work
pAT28	pET21a_PaYfgM_His6	This work
pAT29	pET21a_PaYfgMΔTMD_His6	This work
pAT30	pET21a_PaYfgMΔTMD_C2_His6	This work
pAT31	pET21a_PaYfgMΔTMD_C179_His6	This work
pAT32	pET21a_PaPpiD-His6	This work

pAT33	pBBR1_His10_PaSecYEG	This work
pAT34	pET21a_PaPpiDΔTMD-His6	This work
pAT35	pET21a_pLipA_CO	This work
pAT36	pETDuet1_His10_PaSecYEG	This work
pAT37	pET21a_T7_PaSecA_His6	This work
pAT38	pTrc99a_mixSS1_LipAΔ251	This work
pAT39	pTrc99a_mixSS2_LipAΔ251	This work
pAT40	pTrc99a_mixSS3_LipAΔ251	This work
pAT41	pRSF_His8_PaSecB_W69A	This work
pAT42	pET21a_PaPpiDΔTMD-His6	This work
pAT43	pET21a_His6_PaTIG_His6_G364C	This work
pAT44	pRSF_LipH-FL_S48P	This work
pAT45	pRSF_His8_PaSecB_W69Y	This work
pAT46	pET19b_His10_LipHΔTMDΔVD	This work
pAT47	pET19b_His10_LipHΔTMDΔMD2	This work
pAT48	pET21a_OmpA-His6	This work
pAT49	pET21a_His6_PaSkp-SS_His6	This work
pAT50	pET21a_His6_OprG-SS	This work
pAT51	pET21a_ΔT7_OprG-SS	This work
pAT52	pET21a_OprF-SS_His6	This work
pAT53	pET21a_OprF-SS	This work
pAT54	pET21a_ΔT7_OprF-SS	This work
pAT55	pRSFDuet1_His8_LipH-FL_S48P	This work
pAT56	pRSFDuet1_His8_LipH-FL	This work
pAT57	pRSFDuet1_LipH-FL	This work
pAT58	pRSFDuet1_His8_LipH_FL_S48A	This work
pAT59	pRSFDuet1_LipH-FL_S48A	This work
pAT60	pET21a_OmpA	This work
pAT61	pET21a_ΔT7_OmpA	This work
pAT62	pET21a_NdeI_TIG_XhoI	This work
pAT63	pET21a_pLipA_CO_LipA50	This work
pAT64	pUC18_pLipC	This work
pAT65	pET21a_PaSecA-His6	This work
pAT66	pTrc99a_His10_3C_PaYEG_His10_3C_LipH-FL (GA)	This work
pAT67	pET21a_PaTIG-His6_T149C	This work
pAT68	pET21a_PaTIG-His6_T216C	This work

pAT69	pGUF_PaFkpA	This work
pAT70	pTrc99a_pOprG_C210	This work
pAT71	pTrc99A_pOprG_T144I_C210	This work
pAT72	pET22b_LipA-SS_S1M	S. Hausmann (Hausmann, 2008)
pAT73	pTrc99a_pOprG_C210_COSS	This work
pAT74	pET21a_PaSkp-SS	This work
pAT75	pET21a_His6_PaSkp-SS	This work
pAT76	pET21a_ΔT7_PaSecA-3C_His	This work
pAT77	pET21a_ΔT7_pLipA_CO_LipA50	This work
pAT78	pET21a_pLipC	This work
pAT79	pET21a_pLipA_CO_6xHis	This work
pAT80	pET21a_ΔT7_pLipA_CO_6xHis	This work
pAT81	pET22b_LipA-SS_S1M_F144E	This work
pAT82	pET21a_ΔT7_pLipA_CO_6xHis_space	This work
pAT83	pET21a_ΔT7_pLipA_CO	This work
pAT84	pET21a_ΔT7_pLipA_CO_6xHis_F144E	This work
pAT85	pET21a_ΔT7_pLipA_CO_F144E	This work
pAT86	pET21a_ΔT7_pLipC	This work
pAT87	pET21a_LipC	This work
pAT88	pET21a_pOprG_COSS	This work
pAT89	pTrc99a_PaSecYEG	This work
pAT90	pTrc99a_His6_EK_PaSecYEG	This work
pAT91	pET21a_XcpP-FL_His6	This work
pAT92	pET21a_ΔT7_XcpP-FL_His6	This work
pAT93	pET21a_XcpPΔTMDΔNterm_His6	This work
pAT94	pGUF_PaSkp	This work
pAT95	pET28b_His6-XcpPΔTMDΔNterm	This work
pAT96	pET28b_His6_3C_XcpPΔTMDΔNterm	This work
pAT97	pET24 LipH-FL_3C_His6	This work
pAT98	pET21a_ΔT7_pLipA_CO_C209S, equals C183S in mature lipase	This work
pAT99	pET21a_ΔT7_pLipA_CO_C209S_F144E, equals C183S in mature lipase	This work
pAT100	pET21a_ΔT7_pLipC_C209S, equals C183S in mature lipase	This work
pAT101	pET24a_LipH-FL_3C_His6	This work
pAT102	pBAD_His_3C_CsaA	This work
pAT103	pET28a_His_Tb_CsaA	This work
pAT104	pET28a_His_Tb_ΔT7_CsaA	This work

pAT105	pET21a_PaSkp-SS_S54C	This work
pAT106	pET21a_PaSkp-SS_S57C	This work
pAT107	pET21a_PaSkp-SS_S60C	This work
pAT108	pTrc99a_His6_EK_PaSecYEG_His10_3C_LipH-FL	This work
pAT109	pTrc99a_His6_EK_PaSecYEG_SecE_S118C	This work
pAT110	pTrc99a_His6_EK_PaSecYEG_SecY_Q299C	This work
pAT111	pTrc99a_His6_EK_PaSecYEG_SecY_S146C	This work
pAT112	pTrc99a_His6_EK_PaSecYEG_F281Y	This work
pAT113	pTrc99a_His6_EK_PaSecYEG_F281Y_I403N	This work
pAT114	pBAD_His_3C_Skp-SS	This work
pAT115	pET28b_His6_TK_Skp-SS	This work
pAT116	pET22_pelBSS_LipA	This work
pAT117	pET22_pelBSS_LipA_F144E	This work
pAT118	pET21a_ΔT7_pFapC_A251T-His	This work
pAT119	pET28b_pFapC_G2_A252T	This work
pAT120	pET21a_ΔT7_t-g-pFapC	This work
pAT121	pET28b_pFapC_mixSS-1_A253T	This work
pAT122	pET21a_pPhoA_PAO1	This work
pAT123	pET21a_pPhoA_PAO1_T240I-His	This work
pAT124	pETtg_pPhoA_PAO1	This work
pAT125	pETtg_pPhoA_PAO1_R245C-His	This work
pAT126	pET21a_ΔT7_pLipA_CO_d6xHis_d251	This work
pAT127	pET21a_ΔT7_pLipA_CO_F144E_d6xHis_d251	This work
pAT128	pET21a_ΔT7_pLipA_CO_d6xHis_d31-64_F144E_L201P	This work
pAT129	pET22_pelBSS_LipA_F144E_d251	This work
pAT130	pET22_pelBSS_LipA_F144E_d232	This work
pAT131	pET22b_pelBSS_Skp_Cys_His6	This work
pAT132	pET21a_ΔT7_PaSkp-His6	This work
pAT133	pET21a_ΔT7_pOprF	This work
pAT134	pET21a_pOprF	This work
pAT135	pET21_ΔT7_OmpA-SS_PaSkp_Cys_D139V	This work
pAT136	pET21a_PapPhoA_COSS_GAP	This work
pAT137	pET21a_PapPhoA_COSS	This work
pAT138	pET21a_PapPhoA_COSS_A166S	This work
pAT139	pET21a_ΔT7_PapPhoA	This work
pAT140	pET28b_pFapC_mixSS1_A253T_C329S	This work

pAT141	pTrc99a_OmpASS_LipAΔ251_ (pKAD162)	A. Kedrov
pAT142	pTrc99a_His10_3C_PaSecYEG_SecYcysless_ (pKAD165)	A. Kedrov
pAT143	pET28b_pFapC_mixSS1_A253T_His6	This work
pAT144	pET24a_pFapC_Stag2	This work
pAT145	pET22b_LipA-SS_S1M_F144E_Cterm_Del1	This work
pAT146	pET22b_LipA-SS_S1M_F144E_Cterm_Del2	This work
pAT147	pET22b_LipA-SS_S1M_A126T_F144E_Cterm_Del3	This work
pAT148	pET22b_LipA-SS_S1M_F144E_Cterm_Del4	This work
pAT149	pET22b_LipA-SS_S1M_F144E_Cterm_Del5	This work
pAT150	pET22b_LipA-SS_S1M_F144E_Cterm_Del6	This work
pAT151	pGUF_His6_EK_PaSecYEG	This work
pAT152	pET22b_LipA-SS_S1M_F144E_ΔY8	This work
pAT153	pET22b_LipA-SS_S1M_F144E_ΔM16	This work
pAT154	pET22b_LipA-SS_S1M_F144E_ΔF29	This work
pAT155	pET22b_LipA-SS_S1M_F144E_ΔD38	This work
pAT156	pET21a_ΔT7_OmpASS-LipAF144E	This work
pAT157	pGUF_LipA	Collaboration with S. Mirshahvalad
pAT158	pGUF_LipAH	Collaboration with S. Mirshahvalad

9 Curriculum Vitae

Personal Data

Name	Papadopoulos, Athanasios
Date of Birth	13.03.1989
Nationality	Greek and German

Education and Training

Since 01/2023	Postdoctoral researcher Center for Structural Sciences, Faculty of Mathematics and Natural Sciences, Heinrich Heine University, Duesseldorf, Germany
04/2018 – 11/2022	Doctoral candidate, Biochemistry Faculty of Mathematics and Natural Sciences, Synthetic Membrane Systems, Heinrich Heine University, Duesseldorf, Germany
04/2015 – 04/2018	Graduate Student Master of Science, Biology Thesis: Tolerance of lichen associated bacteria to astrobiological relevant conditions Department of Biology, Institute of Botany, Symbiotic Interactions, Heinrich Heine University, Duesseldorf, Germany In close collaboration with the German Aerospace Center (DLR), Cologne, Germany
10/2010 – 04/2015	Undergraduate Student Bachelor of Science, Biology Thesis: Isolation and characterization of culturable lichen associated bacteria from the astrobiological model organism *Xanthoria elegans* Department of Biology, Institute of Botany, Symbiotic Interactions, Heinrich Heine University, Duesseldorf, Germany
07/2000 – 04/2009	Primary and secondary school Examination for college entrance (Abitur): Major subjects: Biology and history Minor subjects: German and physical education High-school diploma Municipal Hulda – Pankok Schule, Duesseldorf, Germany

Work Experience

2018 – 2023	Research associate Faculty of Mathematics and Natural Sciences, Synthetic Membrane Systems, Heinrich Heine University, Duesseldorf, Germany
2014 – 2018	Laboratory assistant

Attendances, Projects, and Fellowships

Conferences

Annual meeting of German Society for Biochemistry and Molecular Biology (GBM), 2022,
Heinrich Heine University, Duesseldorf, Germany:
Interactions guiding the folding and maturation processes of the lipase A
of *Pseudomonas aeruginosa* PAO1

International Conference of the Collaborative Research Center 1208, 2022, Duesseldorf, Germany:
Membrane translocation and chaperone dependent folding of lipase A
from *Pseudomonas aeruginosa* PAO1.

Jahrestagung der Vereinigung für Allgemeine und Angewandte Mikrobiologie (VAAM), 2022,
Heinrich Heine University, Duesseldorf, Germany:
The periplasmic chaperone Skp is a potent mediator of lipase A of *Pseudomonas aeruginosa*

EMBO Workshop:
Current Advances in Protein Translocation and across Membranes", 2019,
Sant Feliu de Guíxols, Girona, Spain:
Sec-dependent translocation of the virulence factor lipase A from *Pseudomonas aeruginosa* PAO1

International Conference of the Collaborative Research Center 1208, 2019, Duesseldorf, Germany:
Membrane translocation and chaperone dependent folding of lipase A
from *Pseudomonas aeruginosa* PAO1.

Moon Village Workshop 2016, ESA, ESTEC, Noordwijk, Netherlands:
Mohac-Modular Habitable Complex.

EANA 2016, Athens Planetarium, Athens, Greece:
Lichen associated bacteria as putative candidates for astrobiological research.

First Astrobiology and Space Medicine Workshop 2015,
Medical University of Graz:
The lichen *Xanthoria elegans* and its impact on present day Astrobiology.

AbGradE Symposium & Workshop 2015,
ESA, ESTEC, Katwijk, Netherlands:
HOLE Observation of former life on mars.

Projects

Biogenesis of virulence factors of *Pseudomonas aeruginosa* PAO1
Project A10,
Collaborative Research Council 1208,
Heinrich-Heine University, Duesseldorf, Germany

The Periplasmic Chaperone Network of *Pseudomonas aeruginosa* PAO1 (Project A10, CRC1208)
Collaborative Research Council 1208,
Heinrich-Heine University, Duesseldorf and Juelich Research Center, Juelich, Germany

Hitchhiker: Research on lichen associated bacteria in astrobiological and symbiotic context.
European Space Agency & German Aerospace Center. Heinrich-Heine University, Duesseldorf.

SynMylk: Project to create animal-free synthetic milk. International Genetically Engineered Machine (iGEM) 2019. Heinrich-Heine University, Duesseldorf.

Memberships

2019 – 2022	Member of the steering board, Collaborative Research Center 1208, Heinrich-Heine University Duesseldorf, Germany
2019 – 2022	Elected representative of the doctoral students and Postdocs, Collaborative Research Center 1208, Heinrich-Heine University Duesseldorf, Germany
2018 – 2022	Research associate of the Synthetic Membrane Systems work group, Collaborative Research Center 1208, Faculty of Mathematics and Natural Sciences, Heinrich-Heine University Duesseldorf, Germany
2015 – 2019	Member of the European Astrobiological Network Association (EANA)
2017 – 2023	Member of the German Astrobiological Society (DabG)
2018 – present	Member of the German Society for Biochemistry and Molecular Biology (GBM)
2018 – present	Member of the German Biophysical Society (DgfB)

Fellowships

2023 – present	Postdoctoral fellow in MibiNet (Project Z01) Collaborative Research Center 1535, Faculty of Mathematics and Natural Sciences, Heinrich-Heine University Duesseldorf, Germany
2019	Heine Research Academies (HERA); Heinrich Heine University, Duesseldorf, Germany

Awards

2019	Grant for research associated traveling to Boston, MA, USA Heine Research Academies (HERA), Heinrich Heine University, Duesseldorf, Germany

Publications

The periplasmic chaperone Skp prevents misfolding of the secretory lipase A from *Pseudomonas aeruginosa*
Athanasios Papadopoulos, Max Busch, Jens Reiners, Eymen Hachani, Miriam Baeumers, Julia Berger, Lutz Schmitt, Karl-Erich Jaeger, Filip Kovacic, Sander H.J. Smits and Alexej Kedrov
Frontiers in Molecular Biosciences, Volume 9,1026724, 2022
DOI=10.3389/fmolb.2022.1026724

10 Acknowledgements

First of all I would like to emphasize my precious thanks to Prof. Dr. Alexej Kedrov who created the outstanding project and allowed me to conduct my doctoral research within that. It had been a very thoughtful and demanding time, for both of us. I think that we both faced challenges which were not always easy and straightforward to overcome, especially when being the first doctoral candidate in a newly established work group within such a great collaborative research center as represented in 1208. But as a good old saying brings to the point "what does not kill you, makes you strong". Now, at the end writing these few words, I can recognize the personal developmental steps that I pursued, and it is also your achievement since you put me on that track. I learned so much during that time, and not everything can be mentioned within this short paragraph. Considering of what I learned about research is not simple to be summarized in just one sentence but let me tell you one thing: the work we did is so interdisciplinary that it expanded my expectations of becoming a true researcher. Therefore, I truly thank you!

I would like to thank my second supervisor Prof. Dr. Karl Erich Jäger. As an "grandmaster" on the field of lipase research, the discussions we had and the opportunities for collaboration were always supportive and gained the value of the present project.

I would also like to thank Prof. Dr. Lutz Schmitt who was always there for discussions and greatly supportive on all topics related to the CRC1208 and the success of my doctoral research. Lutz you are the source of experience that every young scientist should be able to have access to, and from you I learned a lot about "our daily business" that goes far beyond our research activity.

I would like to stress my grateful thanks to Prof. Dr. Sander Smits for the unrestricted support in every topic that popped up in the past years. You are always there, listening to my thoughts and advising me in such a generous way that simple words cannot reflect how. I thank you for your trust in me, and I promise to you that it will pay off that you gave me the opportunity to conduct my postdoctoral research in the Center for Structural Studies.

My special thanks go to Dr. Cordula Kruse. You were always there with helpful advises and fruitful suggestions, not only taking care about the organization of the CRC1208 but also thinking of the wealth of the doctoral candidates. It was a pleasure working with you. Thank you!

Further I would like to thank my friend and colleague Dr. Jens Reiners for his support and the fruitful discussions. Without your straight advise, the field of structural studies on proteins would remain still widely elusive for me. You showed me how powerful structural determination can be in aim to elucidate the workwise of a protein.

At this place I would like to thank my colleagues, Maryna Löwe and Michael Kamel of the synthetic membrane systems group for the productive time and the lively atmosphere in the laboratory. I am pretty sure that we will get the opportunity again to chat, drink a beer and laugh together about the experiences

we shared upon pursuing our doctoral research. I would also like to thank Max Busch for his contributions to the project, especially as an additional pair of working hands. It is nice to see you "growing up" in the field of research and I think you will do a great job as my successor.

My further thanks belong to my friends and colleagues, Eymen Hachani and Cigdem Günes. I had a great time with you. I thank you for your support and the honest words we shared. You both are outstanding persons and candidates. At this point, please remember this saying "Wenn der Löwe brüllt, so zittert der Wald".

A special thanks goes to my long-time friend and colleague Julia Gottstein. You always brought the "sunshine" into the institute, and I must admit that this was really necessary during so many "cloudy" days. Thank you little amiga!

I would also like to thank Dr. Olivia Spitz for her advice and straight treatment! Oli, you took me as a friend by the first time we met, therefore I thank you!

I would like to thank our laboratory technicians, Martina Wesemann and Silke Mavaro for their kind support and nice working atmosphere.

The "old" generation of doctoral candidates, Dr. Marcel Lagedorste, Dr. Manuel Wagner, Dr. Tim Kroll and all the others, I would like to thank for the nice welcome and introduction to the laboratories as well as the nice working atmosphere.

I would also like to mention my special thanks to Dr. Marten Exterkate, Dr. Sakshi Khosa, Jun.-Prof. Dr. Miriam Kutsch for their kind support and fruitful discussions.

In general, I would like to emphasize my thanks for the whole Institute of Biochemistry, the department Biochemistry I, the work group Synthetic Membrane Systems, and especially the Center for Structural Studies of the Heinrich Heine University. You all enabled in certain different ways the successful path of my doctoral work.

My special thanks go to my long-term mentor Dr. Sabine Etges and my advisor Dr. Hans-Peter Schmitt-Wrede, who supported me from my first semester of undergraduate studies. You both are great personalities. I learned much from you. You accompany me through-out various developmental steps during whole of my studies. Thank you!

A great thanks goes to the team of the botanical garden of Düsseldorf, and especially to Andreas Fischbach. Thank you Andreas for the nice working atmosphere and insights into botanical work.

The further part of acknowledgments is dedicated to my family and beloved persons; therefore it is written in Hellenic language.

Θα ήθελα να ξεκινήσω με μια πρώτη αναφορά στους γονείς μου και να εκφράσω την βαθιά ευγνωμοσύνη μου. Έκαναν θυσίες και παραιτήθηκαν απο προσωπικές τους ανάγκες, για να με

στηρίξουν σε όλη αυτή την προσπάθεια. Προτεραιότητα τους ήταν πάντα η προσπάθεια μου για την επίτευξη αυτού του στόχου. Χωρίς την δική τους στήριξη τίποτα από ολα αυτά δεν θα ήταν εφικτό.

Επίσης θέλω να ευχαριστήσω θερμά την γιαγιά και τον παππού μου, τους οποίους νιώθω σαν δεύτερους γονείς μου. Θεωρώ, πως ότι κατάφερα μέχρι τώρα, οφείλεται κατα ενα μεγάλο μέρος και σε αυτούς. Μεγάλο ρόλο στη διαμόρφωση του χαρακτήρα μου, έπαιξε και η ανατροφή, που έλαβα τα πρώτα χρόνια της ζωής μου. Πέρα απο την επίμονη προσπάθεια μου και το εντατικό διάβασμα υπήρχαν πάντα στο νού μου οι συμβουλές τους. Ως εκ τούτου, ένα μεγάλο μέρος της επίμονης προσπάθειάς μου να ολοκληρώσω το διδακτορικό μου ανάγεται στο παρελθόν μου. Θα ήθελα να ευχαριστήσω όλους τους ανθρώπους γύρω μου που ήταν πάντα δίπλα μου και με στήριξαν τόσο στις δύσκολες όσο και στις εύκολες στιγμές.

Οι δυσκολίες που πέρασα κατά τη διάρκεια του διδακτορικού μου είχαν πολύ μεγάλο αντίκτυπο σε όλους τους ανθρώπους γύρω μου. Δεν είναι αυτονόητο ότι οι άνθρωποι αυτοί παρέμειναν στο πλευρό μου χωρίς δισταγμό. Συχνά οι συμβουλές και οι ενέργειές τους ήταν πιο σημαντικές για μένα από οτιδήποτε άλλο.

Επιπλέον, η διδακτορική διατριβή ήταν ταυτόχρονα μια περίοδος αμφιβολιών, φόβου και χαράς. Δεν αποτελεί έκπληξη το γεγονός ότι αυτή η κατάσταση μπορεί να στερήσει πολλά από ένα άτομο. Αυτό κάνει την υποστήριξη που μου δώσετε ακόμη πιο πολύτιμη. Γιατί στο τέλος, χάρη σε εσάς, δεν έχασα τον εαυτό μου, και δεν χρειάστηκε να ξαναβρώ τον εαυτό μου. Ετσι μπόρεσα να αναπτύξω τη δημιουργικότητά μου. Αυτό είναι πολύ συγκινητικό για μένα. Με αυτές τις λίγες προτάσεις που προέρχονται από την πιο αγνή καρδιά, θα ήθελα να σας ευχαριστήσω θερμά. Παρόλο που είμαι πολύ λογικός άνθρωπος, μπορώ ωστόσο να πω με ταπεινότητα ότι χωρίς εσάς δεν θα ήταν δυνατόν να περάσω αυτό το διάστημα και να φύγω με επιτυχία από τον χώρο ως "νικητής". Ευχαριστώ θερμά, όλους τους δικούς μου ανθρώπους, που με αγαπούν και με στηρίζουν.

Θα ήθελα να ευχαριστήσω ειλικρινά την σύντροφό μου. Ήσουν εκεί από την πρώτη μέρα του πανεπιστημίου. Έτσι, αυτή η ιστορία εδώ είναι και η προσωπική σου ιστορία. Ποτέ δεν με αμφισβήτησες και σε ευχαριστώ πολύ γι' αυτό. Το γέλιο και η αισιοδοξία σου μου έδιναν πάντα αυτοπεποίθηση και χαρά. Δεν ήταν σύμπτωση αλλά μοίρα ότι συναντηθήκαμε την πρώτη μέρα του πανεπιστημίου. Σε ευχαριστώ που είσαι πάντα στο πλευρό μου.

Σε αυτούς αφιερώνω αυτό το υπάρχων έργο.

Τελευταίο αλλά όχι λιγότερο σημαντικό, δεν πρέπει να ξεχάσω να ευχαριστήσω τον εαυτό μου! Χωρίς τον ακούραστο αγώνα μου, τίποτα από όλα αυτά δεν θα είχε γίνει. Είμαι περήφανος που δεν έχασα ποτέ τον εαυτό μου, παρόλο που η διδακτορική διατριβή προσπάθησε να μου υποδείξει τα όριά μου.

Η πίστη μου, η υπομονή μου και η επιμονή μου είναι αρετές που δεν θέλω ποτέ να χάσω. Με τη βοήθεια του Θεού, την πίστη και τη δύναμη της διάνοιας, δεν υπάρχει πρόβλημα που δεν θα μπορούσα να λύσω. Αυτή η διδακτορική διατριβή είναι ένα εξαιρετικό παράδειγμα γι' αυτό. Ακριβώς όπως το όνομα του προστάτη μου Αγίου Αθανασίου σκοπεύει στην αθανασία, έτσι και το πνεύμα μου θα είναι διαρκές. Μετά από αυτή τη σταδιοδρομία, υπάρχει μόνο ένα συμπέρασμα για μένα, προσπαθήστε να βρείτε την εσωτερική ειρήνη για τον εαυτό σας και μην ορίζετε την επιτυχία και την ευτυχία σας και τις φιλοδοξίες σας με βάση τις φιλοδοξίες που δημιουργούν οι άλλοι γύρω σας. Ο Θεός μας έχει δώσει την ευλογία του για να μπορούμε να είμαστε αγνοί με τον εαυτό μας. Αυτή πρέπει να είναι η συνεχής προσπάθειά μας.

11 Declaration

Eidesstattliche Versicherung

Ich versichere an Eides statt, dass die Dissertation mit dem Thema „Membrane translocation and chaperone-dependent folding of the lipase A of *Pseudomonas aeruginosa*" von mir selbständig und ohne unzulässige fremde Hilfe unter Beachtung der „Grundsätze zur Sicherung guter wissenschaftlicher Praxis an der Heinrich-Heine-Universität Düsseldorf" erstellt worden ist. Die Dissertation wurde bei keiner anderen Fakultät eingereicht und ich habe bisher keine erfolglosen Promotionsversuche unternommen. Es handelt sich bei allen von mir eingereichten Dissertationsschriften um in Wort und Bild völlig übereinstimmende Exemplare.
Weiterhin erkläre ich, dass digitale Abbildungen nur die originalen Daten enthalten und in keinem Fall inhaltsverändernde Bildbearbeitungen vorgenommen wurden.

Düsseldorf, den

_____
Athanasios Papadopoulos